Plant Aquaporins That Facilitate Cation Transport and Their Regulation by Phosphorylation

Samantha McGaughey

October 2019

This thesis is submitted for the degree of
Doctor of Philosophy
to the School of Agriculture, Food and Wine,
The University of Adelaide.

THE UNIVERSITY of ADELAIDE

Table of Contents

Abstract

Plants respond to osmotic stresses by adjusting the regulation of water and ion transport mechanisms. A subset of aquaporins are candidates for being involved in these mechanisms. For example, two Arabidopsis Plasma membrane Intrinsic Proteins (PIPs), AtPIP2;1 and AtPIP2;2, were previously reported to be water and ion transporting aquaporins. Here, the ion and water transport properties of sets of aquaporins from different plant species were investigated using the heterologous expression systems *Xenopus laevis* oocytes and yeast (*Saccharomyces cerevisiae*). These sets included PIP isoforms from the model dicot Arabidopsis, the model monocot *Setaria* (*Setaria viridis*) and the agricultural crop barley (*Hordeum vulgare*); and a candidate Tonoplast Intrinsic Protein (TIP) aquaporin from barley, HvTIP2;2. One or more aquaporins from each different plant species was found to facilitate ion transport in heterologous systems.

The identification of ion transporting aquaporins in a range of plant species, including dicot and monocot species, indicates that this feature could have had an early evolutionary origin that preceded monocot-dicot divergence 140-170 million years ago. To further test the hypothesis of an early evolutionary origin for ion transporting aquaporins a PIP-like aquaporin from a filamentous terrestrial alga was tested and confirmed to facilitate water and ion transport.

AtPIP2;1-associated permeability properties are similar to previously reported features associated with non-selective cation channels (NSCCs), and AtPIP2;1 has been proposed as an NSCC molecular candidate. Testing of AtPIP2;1 permeability revealed that it can facilitate the transport of a range of monovalent cations, such as sodium (Na^+), potassium (K^+), cesium (Cs^+) and rubidium (Rb^+), and AtPIP2;1 permeability is influenced by changes in calcium, pH and treatments involving addition of cyclic nucleotides (cNMPs). Ion transporting PIP2;1 homologs in cereals may also be candidates for NSCCs. The PIPs from *Setaria* were tested for boric acid and hydrogen peroxide (H_2O_2) transport and it was observed that in general the transport of H_2O_2 and ions occurred for different sets of PIP isoforms.

The influence of post-translational modifications on AtPIP2;1 ion transport was investigated using site directed mutagenesis to mimic different phosphorylation states. Previously, the phosphorylation status of several serine (S) residues on the C-terminal domain (S280 and S283) and the intracellular loop B (S121) and loop D (S194) of AtPIP2;1, were linked to salt

stress responses and monomeric pore gating, respectively. The phosphorylation state of these sites regulated AtPIP2;1 water and ion channel function when expressed in heterologous systems and influenced whether AtPIP2;1 functioned primarily as a water channel or an ion channel. Candidate upstream kinases OST1 (Snrk2.6), and CDPKs CPK3 and CPK21 were investigated for their capacity to influence AtPIP2;1-associated water and ion transport in *X. laevis* oocytes. Co-expression with OST1 and CPK3 reduced both the water and ion transport of AtPIP2;1, whereas CPK21 co-expression only influenced AtPIP2;1 water channel activity.

Ion transporting plant aquaporins are candidates for NSCC and ion and water co-transport mechanisms, and they may contribute to osmotic stress tolerance mechanisms. The potential physiological roles of plant ion transporting aquaporins and options for future experiments are discussed.

Thesis declaration

I certify that this work contains no material which has been accepted for the award of any other degree or diploma in my name, in any university or other tertiary institution and, to the best of my knowledge and belief, contains no material previously published or written by another person, except where due reference has been made in the text. In addition, I certify that no part of this work will, in the future, be used in a submission in my name, for any other degree or diploma in any university or other tertiary institution without the prior approval of the University of Adelaide and where applicable, any partner institution responsible for the joint-award of this degree.

I acknowledge that copyright of published works contained within this thesis resides with the copyright holder(s) of those works.

I also give permission for the digital version of my thesis to be made available on the web, via the University's digital research repository, the Library Search and also through web search engines, unless permission has been granted by the University to restrict access for a period of time.

I acknowledge the support I have received for my research through the provision of an Australian Government Research Training Program Scholarship. I also acknowledge the support I have received for my research from the Australian Research Council Centre of Excellent in Plant Energy Biology and from the Grains Research Development Council through the provision of a GRS supplemental scholarship.

Samantha McGaughey

October 2019

Acknowledgments

This research was carried out at the University of Adelaide and the Australian National University and supported by the Australian Government Research Training Program in collaboration with the Australian Research Council Centre of Excellence in Plant Energy Biology and the Grains Research Development Council.

I would first like to thank my supervisors, Dr. Caitlin Byrt and Professor Steve Tyerman for their support. To Caitlin; thank you for being an amazing mentor, advocate and friend. Your passion and excitement for science is infectious and I have been very lucky to share that with you. To Steve; thank you for your encouragement, enthusiastic discussion and brilliant ideas.

I would like to acknowledge the help and support given to me by Dr. Jiaen Qiu throughout my PhD. Thank you for your friendship and for being a wonderful collaborator and sounding board. I hope we continue to work together for many years into the future. I would also like to specially thank Wendy Sullivan for her excellent technical support, particularly in the provision of oocytes – so many oocytes – which were fundamental for the work contained herein. Thanks to my lab-mates in Adelaide for your kindness and help over the years.

I would also like to thank Dr. Michael Groszmann for his assistance, advice and support, particularly with the yeast assays and willingness to share his ideas and resources.

Finally, I would like to thank my friends and family. To my friends; thank you all so much (particularly my PhD-mates Bianca and Lily), you have been an amazing support. To my family, especially my Dad and my partner Joe; thank you for always picking me up when I've been down.

List of publications

List of publications arising from PhD candidature:

McGaughey, S. A., Osborn, H. L., Chen, L., Pegler, J. L., Tyerman, S. D., Furbank, R. T., Byrt, C. S. and Grof, C. P. L. (2016). Roles of Aquaporins in *Setaria viridis* Stem Development and Sugar Storage. *Frontiers in plant science,* 7, 1815. doi: 10.3389/fpls.2016.01815

Kourghi, M., Nourmohammadi, S., Pei, J., Qiu, J., **McGaughey, S.**, Tyerman, S., Byrt, C. and Yool, A. (2017). Divalent Cations Regulate the Ion Conductance Properties of Diverse Classes of Aquaporins. *International Journal of Molecular Science*. 18, 2323. doi: 10.3390/ijms18112323.

McGaughey, S. A., Qiu, J., Tyerman, S. D. and Byrt, C. S. (2018). Regulating Root Aquaporin Function in Response to Changes in Salinity. *Annual Plant Reviews* 1, 1–36. doi: 10.1002/9781119312994.APR0626

Hoai, P. T. T, Tyerman, S. D., Schnell, N., Tucker, M. R., **McGaughey, S. A.**, Qiu, J., Groszmann, M. R., and Byrt, C. S. (2019). Roles for aquaporins in seed water relations. *Journal of Experimental Botany* (accepted).

Chapter 1: General introduction

1.1 Aquaporins are implicated in plant osmotic stress responses

Osmotic stress limits plant productivity. The two major causes of plant osmotic stress include drought and soil salinity. Increasing incidence of drought and salinity are inevitable features of the future global agricultural landscape due to climate change (Dai, 2013; Trenberth *et al.,* 2014). United Nations projections indicate that the global population will reach 9.73 billion by the year 2050 and to meet food demands our current agricultural productivity will need to increase by 50% (Source: FAO The Future of Food and Agriculture, 2017). Generating crops with enhanced tolerance to drought and salt stress could increase productivity. To achieve this we need to progress our understanding of how plants cope with these stresses.

Plants exposed to drought or saline conditions experience osmotic stress (from the reduced availability or capacity to take up water from the soil), and soil salinity may additionally induce ionic stress (from the accumulation of ions to toxic levels such that the metabolic activity of the cell is disrupted) (Bartels and Sunkar, 2005; Munns, 2002). Osmotic stress has immediate effects on the vegetative growth and development of the plant. Cellular dehydration or loss of cell turgor reduces rates of cell division and expansion, leading to decreases in leaf size, stem elongation and root proliferation (Farooq *et al.,* 2009). Osmotic stress also induces stomatal closure to limit transpiration (Farooq *et al.,* 2012). Although this mechanism prevents water loss, it lowers CO_2 uptake leading to decreased photosynthesis (Chaves *et al.,* 2009; Osakabe *et al.,* 2014). Ionic stress occurs when excess ions accumulate in plant tissues and disrupt metabolic processes, such as when excess salt ions accumulate in the shoot to an extent that the capacity of the vacuole to sequester the salt ions is exceeded (Munns and Tester, 2008). While saline soils may contain a variety of salts at high concentrations, NaCl typically predominates and for most plant species it is an excess of sodium ions (Na^+) that has a toxic effect (Tester and Davenport, 2003). However, for some plant species, such as grapevine and soybean, excess chloride ions (Cl^-) has a toxic effect (White and Broadley, 2001). The accumulation of Na^+ or Cl^- ions to excessive levels disrupts the metabolic activity of the cell, including disruption to the function of essential organelles the chloroplast and mitochondria (Bose *et al.,* 2017; Che-Othman *et al.,* 2017).

As sessile organisms, plants are continuously exposed to a changing environment and they require physiological plasticity to adapt to new and challenging conditions. Plant water and ion transport mechanisms are increasingly becoming targets of drought and salt tolerance studies due to their roles in osmotic and ionic stress responses (Groszmann *et al.,* 2017; Hrmova and Gilliham, 2018; Munns *et al.,* 2019; Schroeder *et al.,* 2013). For example, expression of an ancestral sodium transporter in commercial wheat varieties increased yield by up to 25% under saline conditions (James *et al.,* 2012; Munns *et al.,* 2012). Plant aquaporins are membrane integral channel proteins that can generally facilitate the passive transport of water and sometimes other solutes, including ions. As water channels, aquaporins are intrinsically linked to plant water relations (Chaumont and Tyerman, 2014). The hydraulic conductivity of plant tissues, particularly roots, has been demonstrated to be mediated by aquaporins, and aquaporins are heavily regulated in response to osmotic stress (for example: Boursiac *et al.,* 2005; Tournaire-Roux *et al.,* 2002; Vandeleur *et al.,* 2014; or see any number of reviews including: Chaumont and Tyerman, 2014; Maurel *et al.,* 2008; Tyerman *et al.,* 1999).

1.2 Review: Regulating root aquaporin function in response to changes in salinity

Aquaporins have many integral roles in plant growth, development, micronutrient uptake, transpiration and photosynthesis as well as in plant interaction and responses to biotic and abiotic stress. There has been much interest in how aquaporins function, particularly in relation to their water channel roles, and how they are regulated by plants in response to osmotic stresses, such as drought and salinity. Since the discovery that the highly abundant Arabidopsis plasma membrane aquaporins AtPIP2;1 and AtPIP2;2 facilitate ion transport (Byrt *et al.,* 2017; Kourghi *et al.,* 2017), PIP regulation under osmotic stresses, particularly salinity, must now be considered in a new context.

The following section is a published review:

McGaughey, S. A., Qiu, J., Tyerman, S. D. and Byrt, C. S. (2018). Regulating Root Aquaporin Function in Response to Changes in Salinity. *Annual Plant Reviews* 1, 1–36. doi: 10.1002/9781119312994.APR0626

This review provides a summary of the literature on PIP regulation in response to salinity, and suggests where this regulation may be influenced by PIP ion channel function. To improve the presentation of the thesis the review appears as it was published in Appendix 9.1 or the review can also be found online via the following link: https://onlinelibrary.wiley.com/doi/abs/10.1002/9781119312994.apr0626

1.3 Precedence for ion transport through aquaporins

1.3.1 Animal aquaporins that facilitate ion transport

Several ion permeable aquaporins have been identified in the animal kingdom. For instance, of the fifteen mammalian aquaporins (AQP0-AQP14), three of them (AQP0, AQP1 and AQP6) have ion channel function (Anthony *et al.,* 2000; Hazama *et al.,* 2002; Shen *et al.,* 1991). Another aquaporin found in Drosophila, called Big-Brain (BIB), also has demonstrated ion channel function (Yanochko and Yool, 2002). The concept of ion conducting aquaporins has been established for more than two decades in the animal field since ion channel activity was reported for the human aquaporin 1 (HsAQP1) (Yool *et al.,* 1996). The abnormal functioning of animal aquaporins has been implicated in a number of human diseases, for example kidney disease, inflammatory bowel disease, cataract formation and cancer metastasis (Bedford *et al.,* 2003; De Ieso and Yool, 2018; Kumari *et al.,* 2013; Ricanek *et al.,* 2015; Soveral *et al.,* 2018). There has therefore been a focus in animal aquaporin research to identify the regulatory mechanisms influencing aquaporin function. The water and ion channel permeability of animal ion conducting aquaporins have been demonstrated to be regulated by changes to pH and calcium (Ca^{2+}) concentration, and phosphorylation (for example: Campbell *et al.,* 2012; Németh-Cahalan and Hall, 2000; Yasui *et al.,* 1999b; for review also see: Törnroth-Horsefield *et al.,* 2010).

The most comprehensive study of aquaporin ionic conductance, including testing of regulatory mechanisms and physiological relevance, has been focussed on HsAQP1. HsAQP1 is a functional water and non-selective monovalent cation channel where ionic conductance through HsAQP1 is regulated in a cyclic GMP (cGMP) dependent manner. Injection of 8-Br-cGMP into HsAQP1 expressing *Xenopus laevis* oocytes resulted in increased ionic conductance (Anthony *et al.,* 2000). Truncation of the HsAQP1 C-terminal

domain (CTD) prevented ion channel activation but did not prevent water permeation indicating that there is a putative cGMP binding site on the HsAQP1 CTD (Saparov *et al.*, 2001). Further studies show that the ion channel activity of HsAQP1 is also regulated by the phosphorylation state of tyrosine residues on the CTD (Campbell *et al.*, 2012) and potential cGMP binding to arginine rich regions of the intracellular loop D (Yu *et al.*, 2006). The phosphorylation of Y253 in the CTD was found to increase cGMP-dependent ion channel activity of HsAQP1 whereas dephosphorylation prevented ionic conductance (Campbell *et al.*, 2012). The site directed mutagenesis of two arginine residues to alanine at positions 159 and 160 in loop D of HsAQP1 resulted in a large decrease in the response of ionic conductance to intracellular cGMP supplementation with no significant effect on water permeability (Yu *et al.*, 2006). It was proposed that cGMP binding, involving these phosphorylatable sites on both the CTD and loop D, results in a conformational change to the cytoplasmic opening of the tetrameric pore (Figure 1.1).

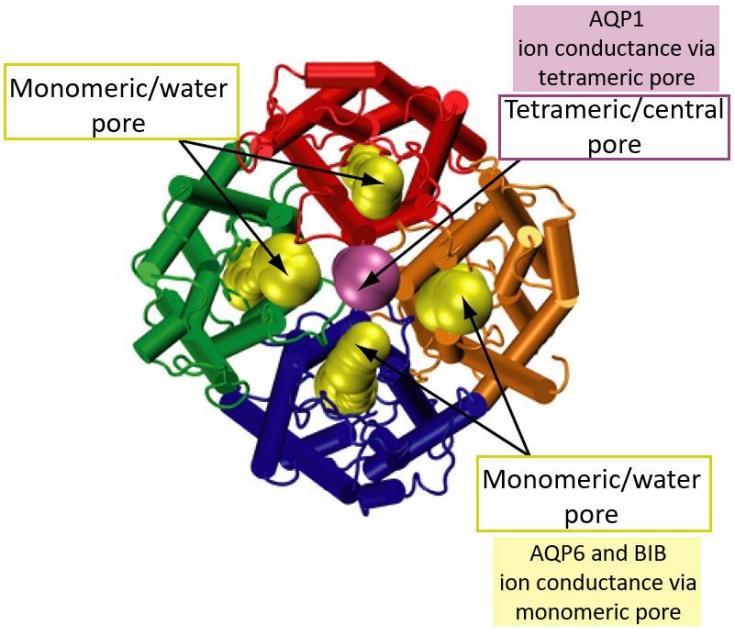

Figure 1.1: Tetrameric structure of HsAQP1 indicating the monomeric water pores and the proposed tetrameric or central pore. The tetrameric or central pore of HsAQP1 formed by the interaction of four HsAQP1 monomers. Each monomeric pore has water channel activity. The tetrameric pore of HsAQP1 is the proposed channel for ionic conductance. Figure adapted from Yu *et al.*, (2006).

Comparatively less is known of the other ion permeable animal aquaporins, AQP0 and AQP6, and the Drosophila BIB (for recent review see Kourghi *et al.*, 2018). AQP0, also

called lens MIP or MIP26, is a functional water channel (though with approximately 1/40th the water permeability of HsAQP1) (Chandy *et al.,* 1997; Kushmerick *et al.,* 1995) and when reconstituted in lipid bilayers had voltage dependent and anion selective ion channel activity (Ehring *et al.,* 1990; Shen *et al.,* 1991). AQP0 water and ion channel activity are pH and Ca^{+} sensitive (Németh-Cahalan and Hall, 2000). The AQP6 is an anion selective ion channel activated by $HgCl_2$ and low pH (< 5.5) (Hazama *et al.*, 2002; Ikeda *et al.*, 2002; Yasui *et al.,* 1999a). The anion permeability of AQP6 was abolished while water permeability was increased by a single point mutation of a residue N60G located in the second transmembrane domain (Liu *et al.,* 2005). Drosophila BIB is a monovalent cation channel, similar to HsAQP1, but does not have appreciable water permeability when expressed in *X. laevis* oocytes (Yanochko and Yool, 2002; Yanochko *et al.,* 2000). BIB is activated by tyrosine signalling pathways, most likely involving CTD tyrosine phosphorylation (Yanochko and Yool, 2002). As with AQP0 and AQP6, BIB is gated by Ca^{2+} (Yanochko and Yool, 2004).

The tetrameric pore has been suggested to function as the ion channel for HsAQP1 (Figure 1.1) (Yu *et al.,* 2006), whereas studies for both AQP6 and BIB indicate that the intrasubunit or monomeric pores are mediating ionic conductance (Yasui *et al.,* 1999b; Yool, 2006). Several studies propose that the tetrameric arrangement of HsAQP1 monomers possesses marked similarities in overall structure to other ion channels and features a central gated ion permeable pore similar to potassium (K^{+}) and cyclic nucleotide gated channels (Liu *et al.,* 2005; Yasui *et al.,* 1999b; Yu *et al.,* 2006). The exact properties allowing for permeation through either the monomeric or tetrameric pore of animal aquaporins remains to be determined, and is similarly a source of controversy for plant aquaporins that also facilitate ion transport (Ozu *et al.,* 2018).

1.3.2 Plant aquaporins that facilitate ion transport

The first report of a plant aquaporin possessing ion channel function was in 1994; when reconstituted in planar lipid bilayers, the soybean (*Glycine max*) NIP Nodulin-26 (GmNOD-26) elicited voltage-sensitive ion currents (Weaver *et al.,* 1994). The next reports on ion conducting plant aquaporins were that of AtPIP2;1 and AtPIP2;2 by Byrt *et al.,* in 2017 and Kourghi *et al.,* in 2017 respectively.

As was briefly described in Chapter 1.2, both AtPIP2;1 and AtPIP2;2 are functional water and non-selective monovalent cation channels (Byrt *et al.,* 2017; Kourghi *et al.,* 2017) and will now be covered in greater detail.

AtPIP2;1 and AtPIP2;2 function was characterised in the heterologous expression systems *X. laevis* oocytes and yeast (*Saccharomyces cerevisiae*). In *X. laevis* oocytes, AtPIP2;1 was a functional water channel that also induced an Na^+-associated non-selective cation current and both oocytes and yeast expressing AtPIP2;1 accumulated more Na^+ when incubated in a high Na^+ solution than controls (Byrt *et al.,* 2017). AtPIP2;2 was similarly characterised in oocytes and was permeable to Na^+ (Kourghi *et al.,* 2017). Importantly, expression of the plant aquaporins AtPIP1;2 and AtPIP2;7 in the oocyte system did not elicit ionic conductances (Byrt *et al.,* 2017; Kourghi *et al.,* 2017). Furthermore, the co-expression of AtPIP2;1 with AtPIP1;2 decreased ionic currents but increased oocyte water permeability greater than that of AtPIP2;1 when expressed alone (Byrt *et al.,* 2017). These data indicate that not all plant aquaporins have the ability to conduct ions.

The ion channel activity of AtPIP2;1 and AtPIP2;2 was gated by pH and divalent cations as has been previously reported for plant aquaporin water channel activity (Frick *et al.,* 2013; Törnroth-Horsefield *et al.,* 2006; Verdoucq *et al.,* 2008). Divalent cations, particularly Ca^{2+}, in conjunction with cellular pH, have important roles as signalling molecules (for review see: Behera *et al.,* 2018). Exogenous application of $CaCl_2$ in the bath solution decreased the ionic conductance of AtPIP2;1 and AtPIP2;2 expressing oocytes (Byrt *et al.,* 2017; Kourghi *et al.,* 2017). Ionic conductance through AtPIP2;1 and AtPIP2;2 was also gated by other divalent cations magnesium (Mg^{2+}), barium (Ba^{2+}) and cadmium (Cd^{2+}) (Kourghi *et al.,* 2017). The inhibition of AtPIP2;1 conductance by Ca^{2+} followed a biphasic dose-response curve similar to that observed for the water permeability of *Beta vulgaris* aquaporins (Alleva *et al.,* 2006; Byrt *et al.,* 2017). Inhibition of aquaporin water channel activity by low pH (pH 6) has been demonstrated (Frick *et al.,* 2013; Tournaire-Roux *et al.,* 2002) and AtPIP2;1 mediated ionic conductance was also reduced by exposure to low pH (IC_{50} pH 6.8) (Byrt *et al.,* 2017). Non-selective cation channels (NSCCs) are similarly regulated by Ca^{2+} and pH; the voltage independent Na^+ currents that were observed in Arabidopsis root protoplasts mediated by NSCCs were blocked by low pH (pH 6) and Ca^{2+} (Demidchik and Tester, 2002). The ion permeability along with Ca^{2+} and pH mediated regulatory similarities between the dual water and ion channel AtPIP2;1 and NSCCs prompted the authors of Byrt *et al.,* (2017) to suggest AtPIP2;1 as a molecular candidate for the thus far unidentified NSCCs.

It is not yet clear whether ions permeate through the monomeric or tetrameric pore of AtPIP2;1 or AtPIP2;2 (Figure 1.1). Crystallographic analyses and molecular dynamics simulations have indicated that ion permeation through the monomeric pore of aquaporins is prohibited by the NPA motifs which act to block the passage of charged molecules (ions or protons) (for review see: Luang and Hrmova, 2017). In this case it is suggested that the tetrameric pore of ion-permeable plant aquaporins may be conducting ionic species, as is the case for HsAQP1 (Yu *et al.,* 2006). Permeation of CO_2 through AtPIP2;1 is also proposed to occur through the tetrameric (or "fifth") pore (Otto *et al.,* 2010; Wang *et al.,* 2016). In contrast to the suggestions of impossibility by molecular simulation, experimental data indicates that ions may be conducted through the monomeric pore of AtPIP2;1 (for review see Ozu *et al.,* 2018). Ion conductance through AtPIP2;1 was regulated similarly by the pH and Ca^{2+} as has been demonstrated for water conductance through the monomeric pore (Alleva *et al.,* 2006; Byrt *et al.,* 2017; Frick *et al.,* 2013; Tournaire-Roux *et al.,* 2002). Furthermore, single-point mutation of AtPIP2;1 G103W, located in the monomeric pore, abolished both water and ion conductivity when expressed in *X. laevis* oocytes, but it did not hinder AtPIP2;1 trafficking to the plasma membrane (Byrt *et al.,* 2017; Wang *et al.,* 2016). Although it cannot be discounted that the G103W mutation in the monomeric pore would not also affect the structure of the tetrameric pore. The pathway for ion permeation of ion conducting plant aquaporins remains to be determined.

Due to the early evolution of aquaporins and their functional and regulatory conservation throughout the taxonomic kingdoms of life, and considering that ion channel function has now been identified in both the plant and animal kingdoms, it may be that the properties allowing for ion permeation, while currently unknown, are similarly conserved. Interestingly, the AtPIP2;1 has the highest sequence similarity to the HsAQP1 among all Arabidopsis aquaporins and also shares this ion channel feature (Appendix 9.2; Figure S1). It then follows that other plant species would also have aquaporins capable of functioning as ion channels and that these aquaporins are unlikely to be isolated to a single plant aquaporin sub-family, as indicated by those initial reports on GmNOD-26 (Lee *et al.,* 1995; Weaver *et al.,* 1994).

1.4 Ion uptake and transport via non-selective cation channels

Ion transport and homeostasis is an essential component of plant function. For plants, the transport of ions into and out of its tissues is integral to survival. Ion transport is entwined with major physiological processes including water and nutrient uptake and their long-distance transport, organ movement, growth, and reproduction (for review see: Ward *et al.,* 2009). For example, most mineral nitrogen, phosphate and sulphate are taken up from the soil in their ionic forms as necessary components for synthesis of protein and nucleic acids (Hedrich and Roelfsema, 2001). Indeed, with the exception of carbon, most essential nutrients are taken up by plant roots as ions (Hedrich and Roelfsema, 2001). Despite the importance of these ion transport mechanisms, the molecular identity of many of the ion channels and/or transporters involved are unknown. This includes some major transport pathways for the primary toxic ionic species of saline soils Na^+, and the essential micronutrient and osmolyte K^+.

There are two major pathways for Na^+ and K^+ movement; one mediated largely by selective ion transporters, and the other mediated largely by ion channels (Britto and Kronzucker, 2008). The latter transport pathway is proposed to be in part mediated by non-selective cation channels (NSCCs). NSCCs is the umbrella term describing transmembrane channel proteins found in both animal and plant cells that are generally permeable to a wide range of cations (Demidchik and Maathuis, 2007; Estacion *et al.,* 2006; Guinamard *et al.,* 2006; Nilius, 1990). Although the heterogeneity of NSCC characteristics (Table 1.1) preclude a detailed and specific definition, Demidchik *et al*., (2002) state that in general NSCCs are (i) highly selective for cations over anions and, (ii) under a range of physiological conditions have low or similar selectivity between monovalent cations. Some NSCC classes may discriminate between some monovalent cations like K^+ and Na^+, but they will poorly discriminate between other monovalent cation species typically not permeable by K^+ and Na^+ selective channels (Demidchik *et al*., 2002).

In plant cells NSCCs are found on the plasma and vacuolar membranes (Table 1.1). NSCCs are proposed to have significant roles in plants experiencing salinity stress and have been implicated in both plasma membrane Na^+ and K^+ flux in roots but the complement of molecular mechanisms conferring NSCC currents are not yet known (Benito *et al.,* 2014; Demidchik and Maathuis, 2007; Pottosin and Dobrovinskaya, 2014).

Sodium (Na^+) is the primary ionic species that causes salinity related toxic effects in plants. Under typical physiological conditions Na^+ uptake from the external medium is generally a passive process that occurs across root hair and root epidermal cell plasma membranes (Apse and Blumwald, 2007). Cytosolic levels of Na^+ are maintained at relatively low concentrations (around 1-30 mM), particularly compared to cytosolic K^+ levels (100-200 mM; Higinbotham, 1973). K^+ is among the most abundant inorganic cations found in plant cells. It is also one of the most important inorganic nutrients for plants, having many biophysical and biochemical roles. Examples of these roles include: being an enzymatic co-factor for more than 70 different enzymes such as those involved in essential functions like protein and starch synthesis; being one of the primary solutes used to generate and adjust turgor pressure for plant growth and organ movement; and responses to biotic and abiotic stresses (Ahmad and Maathuis, 2014; Anschütz *et al.*, 2014).

It has been suggested, based largely on electrophysiological studies, that NSCCs facilitate the majority of Na^+ influx in saline conditions (for review see Kronzucker and Britto, 2011). However, because as yet no definitive molecular candidates for the NSCCs that catalyse this Na^+ flux have been identified, it is difficult to resolve exactly what proportion of Na^+ influx occurs through cation channels that are non-selective. Many of the ion channels and transporters involved in K^+ transport processes have been identified and characterised; genome wide surveys identified 7 major cation transporter protein families (consisting of a total of 75 genes) that facilitate K^+ movement across plant cell membranes (Anschütz *et al.*, 2014; Maser *et al.*, 2001; Sharma *et al.*, 2013; Véry and Sentenac, 2002). However, the molecular identity of proteins facilitating some aspects of K^+ uptake and efflux remain unknown (and are often grouped by the umbrella term of NSCCs) (Pottosin and Dobrovinskaya, 2014).

While there are a number of different sub-classes of NSCCs (Table 1.1), voltage-independent NSCCs (VI-NSCCs) are thought to be primarily responsible for Na^+ flux across the plasma membrane (PM) in plant root cells (Kronzucker and Britto, 2011). A number of electrophysiological studies on root cell protoplasts from Arabidopsis, wheat, maize, and barley reported Na^+ flux through VI-NSCCs (Davenport and Tester, 2000a; Demidchik and Tester, 2002; Maathuis, 2006; Maathuis and Sanders, 2001; Roberts and Tester, 1997; Shabala *et al.*, 2006; Tester and Davenport, 2003; Tyerman *et al.*, 1997; White and Davenport, 2002). VI-NSCCs conduct both inward and outward currents and therefore may constitute influx and efflux pathways (Shabala *et al.*, 2006; Volkov and Amtmann, 2006). Some VI-NSCCs also possess distinct pharmacological responses (compared to other known

Na^+ and K^+ channels) (for reviews see Demidchik and Maathuis, 2007; Demidchik *et al.*, 2002). Na^+ currents through VI-NSCCs were blocked by Ca^{2+} and application of Ca^{2+} significantly reduced Na^+ uptake (Essah *et al.*, 2003; Tyerman *et al.*, 1997). The partial block of VI-NSCC, and therefore of Na^+ uptake, by Ca^{2+} is proposed to be the mechanism responsible for the ameliorative effect observed from Ca^{2+} application in salt stressed plants (Greenway and Munns, 1980; Shabala *et al.*, 2006). In addition, some VI-NSCCs show pH sensitivity, specifically current activation at high pH and inhibition at low pH. (Demidchik and Tester, 2002). Interestingly, the influence of Ca^{2+} and pH on VI-NSCC regulation bears similarity to the influence of Ca^{2+} and pH on aquaporin regulation (see Chapter 1.3.2: Plant aquaporins that facilitate ion transport).

VI-NSCCs, like all NSCCs, are largely non-selective for cations. Despite this, permeation studies have determined minor ion preferences for VI-NSCCs in Arabidopsis, rye, and wheat (Davenport and Tester, 2000b; Demidchik and Tester, 2002; White and Tester, 1992). The examination of these selectivity series revealed that K^+ was typically preferentially transported over Na^+ (and other monovalent cations). Many NSCCs have a K^+:Na^+ selectivity ratio of 0.3 to 3 (Table 1.1; Demidchik and Maathuis, 2007). When growing in normal, non-stress conditions, NSCCs may be functioning in K^+ transport (including K^+ uptake) pathways. However, in saline soils where the external Na^+ concentration is greater, NSCCs may then be the primary contributors to Na^+ influx. In addition K^+ efflux from roots is commonly triggered in response to a range of biotic and abiotic stresses, including salinity (for review see Demidchik, 2014). K^+ efflux from roots was induced by exposure to salt stress and can be inhibited by the exogenous application of Ca^{2+} (Shabala *et al.*, 2005; Shabala *et al.*, 2006). Root exposure to high external Na^+ rapidly depolarises the PM resulting in K^+ leakage primarily through outward rectifying K^+ permeable channels (Pottosin and Dobrovinskaya, 2014). NSCCs have also been proposed to be contributing to K^+ efflux in saline conditions (Pottosin and Dobrovinskaya, 2014). Although Na^+ accumulation in plants is often described as undesirable, it is important to note that when not in excess, Na^+ can be used as a low-cost solute for osmoregulation (Shabala and Shabala, 2011). AtPIP2;1 and AtPIP2;2 have been shown to be permeable to Na^+ and suggested as molecular candidates for the elusive NSCCs (McGaughey *et al.*, 2018).

Table 1.1: Summary of types of non-selective cation channels (NSCCs) identified in plants. VI: voltage-insensitive; ROS; reactive oxygen species; DA: depolarisation activated; HA: hyperpolarisation activated; CNGC: cyclic-nucleotide gated channel; AA: amino acid; GLR: glutamate-receptor-like; SV: slow vacuolar channel; FV: fast vacuolar channel; PM: plasma membrane.

Name	Brief description and voltage characteristics	Species	Membrane location	Selectivity profile	Regulatory mechanisms	Molecular Candidates	Proposed Physiological Role	References
VI-NSCC	Voltage insensitive; instantaneously activated; weakly selective; conduct outward and inward currents equally. Two types: Type I - partially blocked by divalent cations; Type II - permeable to divalent cations	Arabidopsis - predominately root cells; Pea (*Pisum sativa*); maize; Green algae *Nitella flexilis*	PM	$K^+ > NH_4^+ > Rb^+ \sim Cs^+ \sim Na^+ > Li^+ >$ tetraethylammonium (TEA^+)	Current inhibited by di- and tri-valent cations (e.g. Ca^{2+}, Ba^{2+}, Zn^{2+}, lantanides; not inhibited by organic antagonists of Ca^{2+} channels (e.g. nifedipine and verapamil); not inhibited by conventional K^+ channel blockers (e.g. TEA^+, TTX, Cs^+, Li^+ and Na^+); inhibited by polyamines	?	Type I: uptake of cations Na^+, NH_4^+ and K^+; mediate K^+ influx under conditions where other members of the low-affinity uptake pathway is inhibited Type II: uptake of divalent cations Ca^{2+} and Mg^{2+}, Mn^{2+}(?) and Zn^{2+}(?)	(Demidchik and Tester, 2002; Demidchik *et al.*, 2002b; Elzenga and Van Volkenburgh, 1994; Essah *et al.*, 2003; Maathuis, 2006; Maathuis and Sanders, 2001; Roberts and Tester, 1997; Shabala *et al.*, 2006; Shabala *et al.*, 2007; Tyerman *et al.*, 1997; Velarde-Buendía *et al.*, 2012; Very *et al.*, 1998; Volkov *et al.*, 2004; White, 1997; White and Davenport, 2002; Zhao *et al.*, 2007)
ROS-NSCC	Activated by ROS; voltage-independent, instantaneous non-selective cation current	Green algae *Nitella flexilis*; Arabidopsis; wheat mesophyll?	PM	K^+ (1.00) ≈ NH_4^+ (0.91) ≈ Na^+ (0.71) ≈ Cs^+ (0.67) > Ba^{2+} (0.32) ≈ Ca^{2+} (0.24) >TEA^+ (0.09)	Sensitive to: divalent cations, protons, Ca^{2+} channel blocker nifedipine; activated by Cu^{2+}(?)	?	Cell expansion/elongation; H_2O_2 induces inward Ca^{2+} currents in protoplasts from the epidermal elongation zone	(Demidchik *et al.*, 1997; Demidchik *et al.*, 2003; Demidchik *et al.*, 2007; Foreman *et al.*, 2003; Wu *et al.*, 2015)

Name	Brief description and voltage characteristics	Species	Membrane location	Selectivity profile	Regulatory mechanisms	Molecular Candidates	Proposed Physiological Role	References
DA-NSCC	Activated by membrane depolarisation; activation kinetics and voltage-dependence similar for outwardly rectifying K^+ channels	Arabidopsis; Barley; Green bean (*Phaseolus vulgaris*)	PM	A comparative study on Arabidopsis and its halophytic relative *Thellungiella halophila* showed an approximately four-fold higher P_K/P_{Na} of DA-NSCC-like channels in roots of *T. halophila* compared with Arabidopsis	Stimulated by cytosolic Ca^{2+}; blocked by extracellular Ca^{2+}; insensitive to extracellular/intracellular Na^+ block (unlike outwardly rectifying K^+ channels)	?	Influx of divalent cations; Ca^{2+} influx?; Zn^{2+} influx?; K^+ xylem loading; K^+ redistribution in seeds; Na^+ uptake and translocation; may be responsible for some K^+ loss and Na^+ influx under salt stress	(Cerana and Colombo, 1992; de Boer and Wegner, 1997; Piñeros and Kochian, 2003; Shabala *et al.*, 2006; Spalding *et al.*, 1992; Stoeckel and Takeda, 1989; Wegner and Raschke, 1994; Zhang *et al.*, 2002; Zhang *et al.*, 2004)
HA-NSCC	Activated by membrane hyperpolarisation	Arabidopsis; Rye (*Secale cereal*) roots; wheat (*Triticum aestivum*) roots	PM; guard cell PM; peribacteroid membrane	Ca^{2+}; NH_4^+; permeable to mono- and di-valent cations	In symbiosomes: require cytosolic Mg^{2+} for their inward rectification; inhibited by polyamines and Ca^{2+} in the symbiosome lumen In peribacteroid membrane: mediate NH_4^+ flux?	Plant annexins?	Ca^{2+} signalling and nutrition; Catalyse large Ca^{2+} influx required for cell elongation e.g. root hairs; mediate nitrogen flux in legumes?	(Clark and Roux, 1995; Demidchik *et al.*, 2002b; Gelli and Blumwald, 1997; Hamilton *et al.*, 2000; Kiegle *et al.*, 2000; Roberts and Tyerman, 2002; Tyerman *et al.*, 1995; Véry and Davies, 2000)
CNGC	Gated by cyclic nucleotides (cAMP,	Arabidopsis	PM	Non-selective to monovalent	Blocked by Cs^+ and external Mg^{2+}	AtCNGC1; AtCNGC2;	Plant pathogen interaction – role in	(Balagué *et al.*, 2003; Clough *et al.*, 2000;

Name	Brief description and voltage characteristics	Species	Membrane location	Selectivity profile	Regulatory mechanisms	Molecular Candidates	Proposed Physiological Role	References
	cGMP); may also be gated by calmodulin; some CNGCs are voltage-dependent with strong inward rectification			cations; limited Ca^{2+} permeability **AtCNGC2 has much greater selectivity for K^+ than Na^+		AtCNGC4; NtCBP4	signalling during pathogen attack; cation nutrition and homeostasis – Ca^{2+} uptake, K^+ uptake	Gobert *et al.*, 2006; Hua *et al.*, 2003; Leng *et al.*, 2002; Li *et al.*, 2005)
AA-NSCC/ GLR-NSCC	Gated/activated by amino acids (specifically glutamate and glycine); glutamate activated currents are voltage-independent	Arabidopsis	PM	Ca^{2+} permeable; glutamate activated conductance was non-selective for monovalent cations	Inhibited by lanthanides; sensitive to quinine	AtGLRs	Ca^{2+} uptake and signalling	(Davenport, 2002; Demidchik *et al.*, 2004; Dennison and Spalding, 2000; Dubos *et al.*, 2003; Lam *et al.*, 1998; Qi *et al.*, 2006)
SV	Slow vacuolar channel; voltage dependent - activated by tonoplast depolarisation; slow kinetics	Arabidopsis, rice, tobacco (*Nicotiana tabacum*)	Tonoplast; possibly PM depending on plant species (e.g. rice and tobacco)	K^+/Na^+ and K^+/Ca^{2+}selectivity ratios of around 1 and 4	Requires high cytoplasmic $[Ca^{2+}]$; blocked by luminal Ca^{2+}; regulated by phosphorylation, 14-3-3 proteins, organic cations and redox potential	AtTPC1	In guard cells: facilitate Ca^{2+} release from the vacuole	(Allen and Sanders, 1997; Bethke and Jones, 1997; Peiter *et al.*, 2005; Van den Wijngaard *et al.*, 2001)
FV	Fast vacuolar channel; in barley – moderate outward rectification and	Red beet (*Beta vulgaris*); barley	Tonoplast	Similar to SV	Inhibited by high cytoplasmic $[Ca^{2+}]$ (> 200nM); cytoplasmic and luminal $[K^+]$	?	K^+ homeostasis; osmoregulation; regulation of tonoplast potential	(Allen and Sanders, 1997; Hedrich and Neher, 1987; Pottosin and Martínez-Estévez,

Name	Brief description and voltage characteristics	Species	Membrane location	Selectivity profile	Regulatory mechanisms	Molecular Candidates	Proposed Physiological Role	References
	biphasic voltage dependence				influence FV open probability			2003; Tikhonova *et al.*, 1997)
Mechano-sensitive NSCCs	Activated by membrane stretch (also called stretch activated channels)	Broad bean (*Vicia faba*) guard cells	PM	Anion and cation permeability; mediates rapid Ca^{2+} influx	Blocked by trivalent cations (e.g. Gd^{3+} and Al^{3+})	AtMSLs	Ca^{2+} signalling/signal transduction of mechanical stimuli	(Cosgrove and Hedrich, 1991; Dutta and Robinson, 2004; Haswell and Meyerowitz, 2006; Pickard and Ding, 1993; Qi *et al.*, 2004)

1.5 Contextual statement and project aims

The threat to agricultural productivity by extreme weather linked to climate change and the increasing prevalence of drought and salinity give new urgency to uncovering plant mechanisms for adaptation and tolerance to these stresses. The discovery of a subset of ion permeable plant aquaporins alters our understanding of plant water relations and ion transport, because it opens up the possibility that ion permeable aquaporins have a greater diversity of roles in plant responses to drought and salinity stress. The next steps in revealing these roles require us to progress our understanding of the functional properties and regulation of plant ion channel aquaporins.

Towards advancing this understanding, the aims of this thesis are:

1. Characterise the regulatory influence of salt-stress-induced phosphorylation on the water and non-selective cation channel function of AtPIP2;1.
2. Determine if other potential phosphorylation sites of AtPIP2;1 influence the water and ion channel function of AtPIP2;1 and investigate candidate upstream plant kinases.
3. Determine if monocots also possess PIP aquaporins that facilitate ion transport by testing candidates from the model grass species *Setaria viridis* and the agricultural crop barley (*Hordeum vulgare*).
4. Test a barley TIP isoform for ion channel function.
5. Investigate other channel properties of ion-transporting aquaporins including permeability to other monovalent cations and if ion transport is osmo-sensitive.
6. Investigate whether aquaporin-facilitated ion transport is evolutionarily conserved using a PIP-like aquaporin from the filamentous alga *Klebsormidium nitens* as a case study.

Chapter 2: Materials and methods

2.1 Cloning and construct generation

All components for solutions and media used in gene cloning and plasmid propagation steps were molecular biology grade. General solutions and growth media used for *Escherichia coli* cloning and propagation steps are described in Table 2.1. Chemically competent *E.coli* One shot® TOP10 cells (Invitrogen, Carlsbad, CA, USA) were used for bacterial transformation steps. Bacterial transformation was achieved via the heat-shock method. A full list of constructs generated for use in the *X. laevis* oocyte and yeast expression systems is located in Appendix 9.3, Tables S1 and S2.

Table 2.1: General media and solutions used in gene cloning and plasmid propagation steps

Media/Solution	Components	Constructs used for
LB	1% (w/v) tryptone, 1% (w/v) NaCl, 0.5% (w/v) yeast extract (add 1.5% (w/v) agar for plates); pH 7 with NaOH	-
Low Salt LB	1% (w/v) tryptone, 0.5% (w/v) NaCl, 0.5% (w/v) yeast extract (add 1.5% (w/v) agar for plates); pH 7.5 with NaOH	-
LB + Kan	LB + 50 μg mL^{-1} of kanamycin	pENTR1A/pUC-57
LB + Amp	LB + 100 μg mL^{-1} of ampicillin	pGEMHE-DEST/ pRS423-GPD-ccdB
Low Salt LB + Zeo	LB + 25 μg mL^{-1} of Zeocin™	pDONR-Zeo

2.1.1 Generation of constructs for *Xenopus laevis* oocyte expression system

2.1.1.1 Arabidopsis *PIPs*

The *AtPIP2;1* (At3g53420) coding sequence (CDS) was originally cloned by Dr Jiaen Qiu (University of Adelaide) using high-fidelity Phusion® polymerase (New England Biolabs, USA) from Arabidopsis root cDNA into a Gateway-enabled pCR8/GW/TOPO entry vector (Invitrogen) before being transferred into the pGEMHE (DEST) oocyte expression vector

using LR clonase II (Invitrogen). The pGEMHE::AtPIP2;1 vector was subsequently used as the template to generate *AtPIP2;1* phopsho-mutant constructs.

All *AtPIP2;1* phospho-mutants constructs that were designed and generated for use in the *X. laevis* oocyte expression system was in collaboration with Dr. Jiaen Qiu (UoA). Site-directed mutagenesis was achieved via high-fidelity PCR where primers were designed to introduce single or double point mutations (Table 2.2). Primer design and PCR reaction set-up and cycling conditions for site-directed mutagenesis were based on the QuickChange® Site-Directed Mutagenesis Kit (Agilent Technologies). Mutations were confirmed by sequencing.

Table 2.2: Primer sequences used in site-directed mutagenesis PCR to generate single and double point mutations in pGEMHE::AtPIP2;1

pGEMHE::AtPIP2;1	Forward primer (5' – 3')	Reverse primer (5' – 3')
S121A	CTTGGCACGTAAAGTGGCGTTACCTAGG	CAATAGGGCCCTAGGTAACGCCACTTTAC
S121D	CTTGGCACGTAAAGTGGATTTACCTAGGG	CAATAGGGCCCTAGGTAAATCCACTTTACG
S194A	CACTGACCCCAAACGTGCTGCCAGA	GTGGGAGTCTCTGGCAGCACGTTTG
S194E	ACTGACCCCAAACGTGAAGCCAGAGACT	ACGTGGGAGTCTCTGGCTTCACGTTTG
S194D	CCACTGACCCCAAACGTGATGCCAGA	CGTGGGAGTCTCTGGCATCACGTTTG
S280A	GGTTCTAAGTCTCTTGGAGCATTCAGAAGTG	GTTGGCAGCACTTCTGAATGCTCCAAG
S280D	GGTTCTAAGTCTCTTGGAGACTTCAGAAGTGC	GTTGGCAGCACTTCTGAAGTCTCCAAG
S283A	CTAAGTCTCTTGGATCATTCAGAGCTGCTGC	TTAGACGTTGGCAGCAGCTCTGAATGATC
S283D	CTCTTGGATCATTCAGAGATGCTGCCAA	TAGACGTTGGCAGCATCTCTGAATGATC
S280A/S283A	CTTGGAGCATTCAGAGCTGCTGCCAACGTCT	GCAGCAGCTCTGAATGCTCCAAGAGACTTAGAAC
S280A/S283D	CTTGGAGCATTCAGAGATGCTGCCAACGTCT	GCAGCATCTCTGAATGCTCCAAGAGACTTAGAAC
S280D/S283A	CTTGGAGACTTCAGAGCTGCTGCCAACGTCT	GCAGCAGCTCTGAAGTCTCCAAGAGACTTAGAAC
S280D/S283D	CTTGGAGACTTCAGAGATGCTGCCAACGTCT	GCAGCATCTCTGAAGTCTCCAAGAGACTTAGAAC

2.1.1.2 Setaria viridis *PIPs*

The CDS of the *Setaria viridis PIPs* (accession numbers used from McGaughey *et al.,* 2016; Appendix 9.3, Table S3) were obtained from Phytozome (https://phytozome.jgi.doe.gov; last accessed January 2017) and synthesised commercially (Genscript, NJ, USA) into a standard pUC-57 vector. Constructs commercially synthesised were designed to be flanked by Gateway enabled border sequences. *SvPIP* genes were then sub-cloned into the pGEMHE (DEST) oocyte expression vector using LR clonase II (Invitrogen) according to manufacturer's instruction. All pGEMHE::SvPIP constructs were confirmed by sequencing.

2.1.1.3 Barley PIPs and TIP2;2

The pXBG-ev1 oocyte expression vectors containing the candidate barley *PIP* CDS were generously provided by Professors Maki Katsuhara and Keitaro Tanoi and Associate Professors Tomoaki Horie and Natsuko Kobayashi from Okayama University (M.K), Shinshu University (T.H) and University of Tokyo (K.T and N.K). The pXBG-ev1::HvPIP constructs were confirmed by sequencing.

The CDS of two alleles of the barley *TIP2;2* from two culitvars, Sloop and SloopSA, were synthesised with gateway enabled borders and inserted into a pUC-57 vector (Genscript). Gene sequences were kindly provided by Professor Diane Mather (UoA). The barley *TIPs* were then sub-cloned into the pGEMHE (DEST) oocyte expression vector using LR clonase II (Invitrogen) and confirmed by sequencing.

2.1.1.4 Klebsormidium nitens *PIP-like aquaporin*

The *K. nitens* PIP-like aquaporin was identified as described in Section 2.4.2 of this chapter. The CDS of the *K. nitens* PIP-like (accession number: kfl00044_0280) was obtained from the publicly available *K. nitens* genome ((http://www.plantmorphogenesis.bio.titech.ac.jp/~algae_genome_project/klebsormidium/index.html; last accessed September 2019) and synthesised commercially (GenScript) into a standard pUC-57 vector. Constructs commercially synthesised were designed to be flanked

by Gateway enabled border sequences. The *K. nitens PIP-like* sequence was then sub-cloned into the pGEMHE (DEST) oocyte expression vector using LR clonase II (Invitrogen) according to manufacturer's instruction and confirmed by sequencing.

2.1.2 Generation of constructs for yeast expression system

2.1.2.1 Arabidopsis PIPs for use in yeast expression system

The *AtPIP2;1* CDS was cloned from the pGEMHE::AtPIP2;1 construct using forward and reverse primers that contained BamHI and XhoI restriction sites respectively. The *AtPIP2;1* PCR product and pENTR1A entry vector were then digested with BamHI and XhoI restriction enzymes (NEB). The pENTR1A backbone was isolated from an agarose gel using a gel purification kit (illustra GFX PCR DNA and Gel Band Purification Kit; GE Healthcare) and the *AtPIP2;1* PCR product and pENTR1A backbone were then ligated using T4 ligase (NEB). pENTR1A::AtPIP2;1 was subsequently used as the template to generate single and double point mutants via site-directed mutagenesis primers and high fidelity PCR (Table 2.2). *AtPIP2;1* mutants in pENTR1A were sub-cloned into the gateway enabled constitutive yeast expression vector pRS423-GPD-ccdB (kindly provided by Dr Michael Groszmann, Australian National University) using LR clonase II (Invitrogen). All constructs were confirmed by sequencing. Constructs containing *AtPIP2;1* and *AtPIP2;1* mutants that were generated for use in the yeast expression system were made in collaboration with Dr. Jiaen Qiu (UoA).

2.1.2.2 Setaria viridis *PIPs for use in yeast expression system*

The CDS of *S. viridis PIPs*, with the exception of *SvPIP2;2*, *SvPIP2;3* and *SvPIP2;6*, were yeast codon-optimised and kindly provided by Dr. Hannah Osborn (ANU) in the yeast vector pSF-TPI1-URA3 (Osborn, 2017). Full-length *SvPIPs* were cloned out of the pSF-TPI1-URA3 vector by high fidelity PCR using primers that contained attB Gateway sites (Table 2.3). These PCR products were then sub-cloned into the Gateway enabled Donor vector pDONR-Zeo using BP clonase II (Invitrogen).

Table 2.3: Primers for cloning full length *SvPIPs*. Primers contain attB flanking sites (attB1 and attB2) for subsequent sub-cloning steps. Forward primers contain kozak sequence (K) for enhanced translation in yeast expression systems and Reverse primers contain stop codon (S).

Primer	Sequence (5'-3')
SiPIP1;1 K Fwd – attB1	GGGGACAAGTTTGTACAAAAAAGCAGGCTTATCGAAGGAGATAGAACCATGTCTGAGGGCAAAGAGGAAGA
SiPIP1;1 S Rev – attB2	GGGGACCACTTTGTACAAGAAAGCTGGGTATCAAGAACGTGATTTGAATGGTATAGC
SiPIP1;2 K Fwd – attB1	GGGGACAAGTTTGTACAAAAAAGCAGGCTTATCGAAGGAGATAGAACCATGTCTGAAGGGAAAGAAGAAGATGT
SiPIP1;2 S Rev – attB2	GGGGACCACTTTGTACAAGAAAGCTGGGTATCAAGATCTTGACTTGAAAGGGATCG
SiPIP1;5 K Fwd – attB1	GGGGACAAGTTTGTACAAAAAAGCAGGCTTATCGAAGGAGATAGAACCATGTCTGAGGGCAAAGAAGAAGAC
SiPIP1;5 S Rev – attB2	GGGGACCACTTTGTACAAGAAAGCTGGGTATCAATCTCTTGATTTAAAGGGAATTGCTC
SiPIP1;6 K Fwd – attB1	GGGGACAAGTTTGTACAAAAAAGCAGGCTTATCGAAGGAGATAGAACCATGTCTGCCGGGGGTAAATTAC
SiPIP1;6 S Rev – attB2	GGGGACCACTTTGTACAAGAAAGCTGGGTATCAATAGTGGGCAGAACTCTTAAATGG
SiPIP2;1 K Fwd – attB1	GGGGACAAGTTTGTACAAAAAAGCAGGCTTATCGAAGGAGATAGAACCATGTCTGGGAAGGATGATGTTATAGAATC
SiPIP2;1 S Rev – attB2	GGGGACCACTTTGTACAAGAAAGCTGGGTATCAAGCGTTACTTCTAAAAGAGCCC
SiPIP2;5 K Fwd – attB1	GGGGACAAGTTTGTACAAAAAAGCAGGCTTATCGAAGGAGATAGAACCATGTCTGCTAAAGATATCGAGGCAG
SiPIP2;5 S Rev – attB2	GGGGACCACTTTGTACAAGAAAGCTGGGTATCAACGAGAGAAAGACGCAGAAG
SiPIP2;8 K Fwd – attB1	GGGGACAAGTTTGTACAAAAAAGCAGGCTTATCGAAGGAGATAGAACCATGTCTCCCATAGAGGATGTGAGC
SiPIP2;8 S Rev – attB2	GGGGACCACTTTGTACAAGAAAGCTGGGTATCAGACCGTTGCTGAAGTTGACCTG

The *S. viridis* PIPs *SvPIP2;2*, *SvPIP2;3* and *SvPIP2;6* were yeast codon-optimised by Dr Michael Groszmann (ANU) and commercially synthesised with gateway enabled borders and inserted into a pUC-57 vector (GenScript). *SvPIP* genes in both the pUC-57 and pDONR-Zeo vectors were sub-cloned into the gateway enabled constitutive yeast expression

vector pRS423-GPD-ccdB using LR clonase II (Invitrogen) for use in functional assays. All constructs were confirmed by sequencing.

2.2 Oocyte expression system

2.2.1 Preparation of cRNA

To synthesise cRNA the pGEMHE and pXBG-ev1 constructs were first linearised using NheI-HF and BamHI-HF restriction enzymes respectively (NEB). cRNA from linearised pGEMHE and pXBG-ev1 was then synthesised using mMESSAGE mMACHINE® T7 Transcription and mMESSAGE mMACHINE® T3 Transcription kits (Thermo Fisher Scientific, Australia) respectively, as per manufacturer's instruction. cRNA isolation and clean-up was performed by phenol-chloroform precipitation as follows: 15 µL Ammonium acetate stop solution (provided in mMESSAGE mMACHINE® Transcription kits, Thermo Fisher Scientific) and 115 µL nuclease free water was added to the completed cRNA reaction and mixed gently by inversion before centrifugation at 14 000 x g for 1 min. Next, 151 µL phenol/chloroform was added, mixed by inversion and centrifuged at 16 000 x g for 5 min. As much of the top-phase as possible was removed into a new microfuge tube and 150 µL chloroform was added, mixed by inversion and centrifuged at 16 000 x g for 5 min. As much of the top-phase as possible was removed into a new microfuge tube and 15 µL sodium acetate (NaOAc) and 750 µL 100% isopropanol was added. The tube was placed in a -80°C freezer for a minimum of 2 h to help precipitate the cRNA. The tube was then centrifuged at 12 000 x g for 20 min at 4°C and the supernatant was removed. The remaining pellet was washed with ice cold 80% ethanol and centrifuged at 12 000 x g for 5 min at 4°C and the supernatant removed. The pellet was resuspended in 22 µL of nuclease free water. The concentration and quality of the cRNA was determined by both NanoDrop and gel electrophoresis.

All AtPIP cRNA synthesised for use in the *X. laevis* oocyte expression system was made in collaboration with Dr. Jiaen Qiu (UoA). AtPIP2;2 (At2g37170) cRNA was synthesised from a pGEMHE::AtPIP2;2 vector made previously (Manchun, 2013). The cRNA for the plant kinases OST1 (Snrk2.6; At4g33950), CPK3 (At4g23650) and CPK21 (At4g04720) were kindly provided by Dr Jiaen Qiu and Professor Matthew Gilliham (UoA).

2.2.2 Preparation of solutions

All components for solutions used in experiments involving *X. laevis* oocytes were molecular biology grade. General solutions used for *X. laevis* oocyte experiments are described in Table 2.4. If any solutions used in experiments deviate from the composition described in Table 2.4 the alterations will be specified in the figure legend where the data from that experiment appears. Solutions used in electrophysiology experiments were typically pH 8.5 with low (50 µM) CaCl concentrations based on data shown in Byrt *et al*., (2017) and Kourghi *et al*., (2017) reporting gating sensitivity of ion currents to low pH and high Ca^{2+}.

Table 2.4: General solutions used for experiments in the *X. laevis* oocyte expression system. The composition and use of experimental solutions are as described below unless otherwise specified in the figure legend.

Solution Name	Components	Use
Ringers	96 mM NaCl, 2 mM KCl, 5 mM $MgCl_2$, 0.6 mM $CaCl_2$, 5 mM HEPES, 5% (v/v) horse serum and antibiotics (0.05mg.mL^{-1} tetracycline, 100 units.mL^{-1} penicillin, 0.1 mg.mL^{-1} streptomycin), pH 7.6	Oocyte incubation
Low Na^+ Ringers	62 mM NaCl, 36 mM KCl, 5 mM $MgCl_2$, 0.6 mM $CaCl_2$, 5 mM HEPES, 5% (v/v) horse serum and antibiotics (0.05mg.mL^{-1} tetracycline, 100 units.mL^{-1} penicillin/0.1 mg.mL^{-1} streptomycin)), pH 7.6	Oocyte incubation
Na100	100 mM NaCl, 2 mM KCl, 1 mM $MgCl_2$, 5 mM HEPES, 50 µM $CaCl_2$, pH 8.5 with TRIS-base, adjusted to ~240 mOsm.kg^{-1} as needed with D-mannitol	TEVC/oocyte ion content
Na50	50 mM NaCl, 2 mM KCl, 1 mM $MgCl_2$, 5 mM HEPES, 50 µM $CaCl_2$, pH 8.5 with TRIS-base, adjusted to ~240 mOsm.kg^{-1} as needed with D-mannitol	TEVC
K100	100 mM KCl, 1 mM $MgCl_2$, 5 mM HEPES, 50 µM $CaCl_2$, pH 8.5 with TRIS-base, adjusted to ~240 mOsm.kg^{-1} as needed with D-mannitol	TEVC
Rb50	50 mM RbCl, 2 mM KCl, 1 mM $MgCl_2$, 5 mM HEPES, 50 µM $CaCl_2$, pH 8.5 with TRIS-base, adjusted to ~240 mOsm.kg^{-1} as needed with D-mannitol	TEVC

Cs100	100 mM CsCl, 2 mM KCl, 1 mM $MgCl_2$, 5 mM HEPES, 50 µM $CaCl_2$, pH 8.5 with TRIS-base, adjusted to ~240 $mOsm.kg^{-1}$ as needed with D-mannitol	TEVC
Isotonic swelling solution	5 mM NaCl, 2 mM KCl, 1 mM $MgCl_2$, 5 mM HEPES, 50 µM $CaCl_2$, pH 8.5 with TRIS-base, adjusted to ~240 $mOsm.kg^{-1}$ as needed with D-mannitol	Photometric swelling assay
Hypotonic swelling solution	5 mM NaCl, 2 mM KCl, 1 mM $MgCl_2$, 5 mM HEPES, 50 µM $CaCl_2$, pH 8.5 with TRIS-base, adjusted to ~45 $mOsm.kg^{-1}$ as needed with D-mannitol	Photometric swelling assay

2.2.3 Oocyte preparation, injection and storage

Unfertilised oocytes were harvested from *X. laevis* frogs. Oocytes were defolliculated by incubation in the following solution for 1-1.5 h: collagenase (type 1A, 2 $mg.mL^{-1}$) and trypsin inhibitor (1 $mg.mL^{-1}$) in 96 mM NaCl, 2mM KCl, 5 mM $MgCl_2$ and 5 mM HEPES, pH 7.6. The oocytes were then stored in Ringers solution that was replaced daily.

Oocytes were injected using a micro-injector (Nanoinject II, automatic nanolitre injector, Drummond Scientific). All oocytes were injected with 46 nL of water that contained either no cRNA or 23 ng cRNA, unless otherwise specified in the figure legend. Post injection and prior to experiments oocytes were stored at 18°C in Ringers or Low Na^+ Ringers solution for 24-36 h. Oocytes of each injection type were stored in individual petri dishes. The oocytes were checked periodically (at least every 12-16 h) and dead or dying oocytes were removed from the petri dishes. The Ringers or Low Na^+ Ringers solution was also changed every 12-16 h or as needed.

2.2.4 Two-Electrode Voltage Clamp

Two-electrode voltage clamp (TEVC) recordings were performed on oocytes 24-48 h post injection. Borosilicate glass pipettes (Warner Instruments, G150TF-4, 1.5 mm OD x 1.17 mm ID) used for voltage and current electrodes were pulled to have 0.5-1 MΩ resistance in Na100 solution. The electrodes were filled with 3 M KCl and a bath clamp system was used. The bath current and voltage sensing electrodes were silver-silver chloride electrodes that were connected to the bath by silver wire when the chloride concentration was equivalent in

the solutions used or otherwise by 2% agar/3 M KCl bridges. The silver wire or 2% agar/3 M KCl bridges were placed as near to the oocyte as possible. The TEVC experiments were performed with an Oocyte Clamp OC-725C (Warner Instruments, Hamden, CT, USA) and a Digidata 1440A data acquisition system interface (Axon Instruments, Foster City, CA, USA). The outer membrane of injected oocytes were carefully pierced with the voltage and current electrodes, and the oocyte bath was continuously perfused with solution while the oocytes membrane potential stabilised in each solution. TEVC measurements were recorded in the TEVC solutions described in Table 2.4 or as otherwise specified in the figure legend. Steady–state currents were recorded starting from −40 mV holding potential for 0.5 s and ranging from 40 mV to −120 mV with 20 mV decrements for 0.5 s before following a −40 mV pulse for another 0.5 s. Ionic conductance was calculated by taking the slope of a regression of the linear region across the reversal potential (−60 mV to +40 mV). TEVC recordings were analysed using the CLAMPEX 9.0 software (pClamp 9.0 Molecular Devices, CA, USA).

To ensure that the data and trends observed were not artefacts of the specific equipment used or due to handler technique, some of the controls for electrophysiology measurements that appear in Chapters 3, 4 and 7 were performed in parallel on two independent electrophysiology rigs, by both myself and a colleague, Dr Jiaen Qiu. Where this data appears in the thesis this collaborative work will be mentioned in each relevant figure legend. The data generated by the candidate along with the parallel data generated by Dr Qiu was analysed by the candidate.

2.2.5 Photometric swelling assay

The osmotic permeability (P_{os}) of oocytes injected with water or cRNA was determined via the photometric swelling assay. Oocytes were either incubated in Na100 or the Isotonic swelling solution before being transferred to a 1:5 dilution of Na100 or the Hypotonic swelling solution for the assay. Images were captured every 1 s over 60-100 s with a Nikon SMZ800 light microscope (Nikon, Japan) with a 1.5x objective lens WD45 and a Vicam colour camera (Pacific Communications, Australia) at 2x magnification using IC Capture 2.0 software (The Imagine Source). Image J software (National Institute of Health, USA) was used to analyse images and calculate the total area change of each oocyte. The osmotic permeability was calculated using the following formula:

$$P_{os} = \frac{V_0\left(\frac{d\left(\frac{V}{V_0}\right)}{dt}\right)}{S \times V_w(Osm_{in} - Osm_{out})}$$

where V_0 is the initial oocyte volume (mm^3) assuming they are perfect spheres; $d(V/V_0)/dt$ is the rate of initial relative cell volume change ($mm^3.s^{-1}$); S is the initial surface area (mm^3); V_w is the partial molar volume of water (18 $cm^3.mol^{-1}$); Osm_{in} - Osm_{out} is the change in osmolarity between the incubation and assay solutions.

2.2.6 Oocyte ion content

Water control and cRNA injected oocytes were incubated for 24 h in Na100. Oocytes were removed to individual 1.5 mL microfuge tubes and washed briefly with double distilled H_2O. All solution was removed from the tube and oocytes were stored at −20°C. Oocytes were thawed at room temperature before being homogenised in 0.1 M analytic nitric acid and digested at 42°C for 2 h. Nitric acid digested homogenates were diluted 1:10 with double distilled H_2O, vortexed briefly and centrifuged at 16 000 x g (Beckman Coulter Microfuge® 16) to pellet cell debris. An aliquot of the supernatant was removed for dilution and ion analysis was performed using an Atomic Absorption Spectrophotometer (AAS; Shimadzu AA-7000) according to manufacturer's instructions. The sodium standard used for AAS analysis was from Sigma-Aldrich (# 05201).

2.3 Yeast expression system

All components for solutions and media used in yeast culturing and experiments were from Sigma-Aldrich. General solutions and growth media used for yeast work are described in Table 2.5. A full list of yeast transformants generated for this thesis is located in Appendix 9.3, Table S2.

Table 2.5: Solutions and media used in yeast culturing and experiments. SD: Synthetic drop-out medium; HIS: histidine.

Solution	Components	Use
SD -HIS (liquid)	0.67% (w/v) Yeast Nitrogen Base without amino acids, 0.139% (w/v) Yeast Synthetic Drop-out Medium – HLTU, 2% v/v glucose, with added amino acids (v/v): Leucine: 0.133% Tryptophan:0.026% Uracil: 0.026%	Yeast propagation and transformation, yeast culture, yeast assays
SD -HIS (solid)	SD -HIS (liquid) + 2% bacteriological agar	Yeast propagation and transformation

2.3.1 Yeast strains and transformation

The *Saccharomyces cerevisiae* mutant strains *aqy1/aqy2* (Matα; leu2::hisG; trp1::hisG, his3::hisG; ura352 aqy1D::KanMX aqy2D::KanMX) and *skn7* (MATαade2-1 can1-100 his3-11,15 leu2-3,112 trp1 ura3-1 suc2 skn7Δ::HIS3) were used to test SvPIP permeability to water and boric acid, and hydrogen peroxide respectively. These strains were kindly provided by Dr Michael Groszmann (ANU). Competent yeast cells of *aqy1/aqy2* and *skn7* were made using the Frozen-EZ yeast transformation II kit (Zymo Research). The pRS423::SvPIP yeast vectors were transformed into both *aqy1/aqy2* and *skn7* yeast strains. Yeast transformations were performed using the Frozen-EZ yeast transformation II kit (Zymo research) as per manufacturer's instruction. Yeast transformations were plated onto solid SD -HIS and incubated at 30°C for 2-4 days where selection of transformants was based on amino acid complementation.

2.3.2 Yeast boric acid and hydrogen peroxide permeability assays

The yeast boric acid and hydrogen peroxide permeability assay methods that I used were created by Annamaria De Rosa and Dr Michael Groszmann (ANU).

SvPIP permeability to boric acid (BA) and hydrogen peroxide (H_2O_2) was determined via growth-based assays performed in 96-well plates where enhanced permeability of the yeast

to the substrate (BA or H_2O_2) by expression of the plant aquaporin is associated with growth inhibition. In 14 mL culture tubes, 1.5 mL SD -HIS media was inoculated with transformant yeast and these master cultures were grown for 24 h at 30°C and shaken at 200 rpm. The master cultures were then diluted 1:4 in SD -HIS and the OD_{660} was determined using the cuvette spectrophotometer of the BMG Spectrostar NANO plate-reader (BMG Labtech). Dilutions were made of the master cultures in new 1.5 mL microfuge tubes to 0.65 x 10^7 cells.mL^{-1}. Each microfuge tube was vortexed to resuspend the yeast cells, and aliquots transferred to wells of a Nunc-96 400 µL flat bottom plate to a total volume of 200 µL (Thermo Scientific Cat#243656). In the BA assays, BA was added to final concentrations of 0 mM, 10 mM, 20 mM and 30 mM to the 96-well plate, where each yeast transformant was exposed to each BA treatment. In the H_2O_2 assays, H_2O_2 was added to final concentrations of 0 mM, 5 mM, 10 mM, and 20 mM to the 96-well plate, where each yeast transformant was exposed to each H_2O_2 treatment. To capture the growth curve of the yeast transformants exposed to each treatment a growth analysis protocol was run over 41 h on a BMG Spectrostar NANO plate-reader where the OD_{660} of each well was measured every 10 min using 4 mm well scanning orbital averaging. Double orbital shaking at 400rpm was performed before each measurement. The plate was incubated at 30°C.

Raw OD_{660} measurements from the BMG Spectrostar NANO plate-reader was used to generate yeast growth curves. These yeast growth curves were processed individually for each yeast transformant under each treatment for each experimental replicate. Yeast growth curves were first blank corrected (where the blank consisted of wells containing only SD -HIS growth media) and then curve smoothed using cubic polynomial fitting on a 40-point sliding time-scale. Yeast growth curves were then corrected to remove any negative growth that occurred as a result of measurement variation from the plate-reader. Each OD_{660} measurement was than normalised to the initial OD_{660} (OD_{660i}) and the natural log of this value was taken:

$$Ln\left(\frac{OD_{660}}{OD_{660\mathrm{i}}}\right)$$

Area under the curve (AUC) was determined from the growth curve generated from normalisation to OD_{660i}. AUC percentage (AUC %) for each treatment was calculated relative to its untreated control (0 mM BA or H_2O_2) from time zero up until the untreated control culture reached stationary phase. Examples of growth curves are shown in Appendix 9.5.

2.3.3 Yeast freeze-thaw assay

Master cultures for the yeast freeze-thaw (FT) assay were inoculated and grown as in Section 2.3.2 for the BA and H_2O_2 assays with the exception they were grown for 26 h. The OD_{660} of the master cultures was determined and their subsequent dilution to 0.65 x 10^7 cells.mL^{-1} was performed as described in Section 2.3.2. The diluted cultures were then separated into two treatment sets of 1.5 mL tubes, a 0-FT and a 3-FT. The 0-FT cultures were placed on ice while the FT treatments were performed. One FT cycle consists of a 30 s incubation in liquid nitrogen (freeze) followed by a 20 min incubation in a 30°C water bath (thaw). After each thaw the tubes were shaken briefly by hand to avoid yeast settling. After 3-FT cycles the tubes were placed on ice. An aliquot for each yeast transformant from the 0-FT and 3-FT treatment were included in the 96-well plate. The growth analysis protocol for the 96-well plate run on a BMG Spectrostar NANO plate-reader was as described in Section 2.3.2.

Raw data from the BMG Spectrostar NANO plate-reader was processed and analysed as described for Chapter 2.3.2 with the exception that non-treated was 0-FT samples.

2.4 Bioinformatics and statistics

2.4.1 *Setaria viridis* and *Setaria italica* gene expression

Gene expression data for *Setaria viridis* and *Setaria italica* was obtained from the Phytomine database (https://phytozome.jgi.doe.gov/phytomine/begin.do; last accessed July 2019) for all available tissues and treatment types. RNA-seq datasets that are publicly available on Phytomine were next-generation sequencing reads that were aligned to reference genomes, and gene- and transcript-level expression values were determined using Cufflinks. Raw expression data from Phytomine was mined for *SvPIP* and *SiPIP* transcripts (gene accession numbers used can be found in Appendix 9.3, Table S3) and this data was used to generate gene expression heatmaps.

2.4.2 Identification and phylogeny of *Klebsormidium nitens* MIPs

The genome of *Klebsormidium nitens* (formerly *Klebsormidium flaccidum*) (http://www.plantmorphogenesis.bio.titech.ac.jp/~algae_genome_project/klebsormidium/index.html; last accessed September 2019) was mined for MIPs via BLAST searches using the protein sequences of algal MIPs identified in Anderberg *et al.*, (2011) and MIPs from the moss *Physcomitrella patens* and model dicot Arabidopsis (Danielson and Johanson, 2008; Johanson *et al.*, 2001). From these BLAST searches, 14 possible MIP orthologs were identified (for accession numbers see Figure 7.4a). The TMHMM v.2.0 online tool (http://www.cbs.dtu.dk/services/TMHMM/) was used to predict the transmembrane helices of putative *K. nitens* MIPs. A protein sequence alignment of algal and plant MIPs used in Anderberg *et al.*, (2011) (provided in their online supplementary materials) was used to align the *K. nitens* protein sequences. From this alignment NPA motifs were identified and the N and C termini of *K. nitens* MIPs excluded based on their alignment with truncated sequences used in Anderberg *et al.*, (2011). A phylogenetic tree was generated using protein sequences of the KnMIPs and the algal MIPs and the MIPs from the moss *P. patens* used by Anderberg *et al.*, (2011) with Geneious Tree Builder (Jukes-Cantor and Neighnour-Joining method) (Genieous 8.1.3; https://www.geneious.com).

2.4.3 Graphing and statistical analysis

All data were graphed using GraphPad Prism version 8.0.0 for Windows (GraphPad Software, La Jolla California USA, www.graphpad.com). Statistical analysis was performed using GraphPad Prism. In general, the statistical tests applied were unpaired t-test when comparing two sets of data or one-way ANOVA (fishers post-test) when comparing more than two sets of data. Significant differences ($p < 0.05$) are indicated by asterisks for t-tests and different lower-case letters for one-way ANOVAs. Data is shown as mean ± SEM. Number of experimental replicates are as stated in each respective figure legend.

Chapter 3: Manuscript - Phosphorylation influences water and ion channel function of AtPIP2;1

The following chapter is presented as a manuscript (*in preparation*). Research on the influence of phosphorylation of AtPIP2;1 C-terminal domain residues S280 and S283 on AtPIP2;1 facilitated water and ion transport is reported. Changes in the phosphorylation state of S280 and S283 have previously been reported to be induced by salt stress. Further experiments investigating the effects of S280 and S283 phosphorylation on AtPIP2;1 ion transport function are currently being undertaken in a yeast expression system.

This research was a collaborative effort between multiple authors as outlined in the Statement of Authorship.

Statement of Authorship

Title of Paper	Phosphorylation influences water and ion channel function of AtPIP2;1
Publication Status	☐ Published ☐ Accepted for Publication ☒ Unpublished and Unsubmitted work written in manuscript style ☐ Submitted for Publication
Publication Details	Title: Phosphorylation influences water and ion channel function of AtPIP2;1 List of authors: Jiaen Qiu, Samantha McGaughey, Michael Groszmann, Stephen Tyerman, Caitlin Byrt. This manuscript is an original research article in preparation for submission.

Principal Author

Name of Principal Author (Candidate)	Samantha McGaughey		
Contribution to the Paper	Performed gene cloning and prepared materials for oocyte experiments. Performed gene cloning for yeast experiments. Conducted TEVC and oocyte swelling experiments. Conducted oocyte ion content experiments. Drafted and revised the manuscript. Interpreted data. Plotted and designed figures and tables with Jiaen Qiu		
Overall percentage (%)	40 %		
Certification:	This paper reports on original research I conducted during the period of my Higher Degree by Research candidature and is not subject to any obligations or contractual agreements with a third party that would constrain its inclusion in this thesis. I am the primary author of this paper.		
Signature		Date	24-10-19

Co-Author Contributions

By signing the Statement of Authorship, each author certifies that:

i. the candidate's stated contribution to the publication is accurate (as detailed above);

ii. permission is granted for the candidate in include the publication in the thesis; and

iii. the sum of all co-author contributions is equal to 100% less the candidate's stated contribution.

Name of Co-Author	Jiaen Qiu		
Contribution to the Paper	Designed the C-terminal mutation experiments. Performed single/double C-terminal mutation cloning into yeast and oocyte expression vectors. Performed oocytes TEVC and swelling experiments. Plotted and designed figures with Samantha McGaughey.		
Signature		Date	28-10-19

Name of Co-Author	Michael Groszmann		
Contribution to the Paper	Prepared some of the GFP fusion constructs for AtPIP2;1 (WT and S280/S283 phospho-mutants). Performed all work related to Figure 4. 'Subcellular localisation of AtPIP2;1 wild-type (S280/S283) and 280/283 phospho-mutants in yeast'. Contributed to writing and revision of the manuscript.		
Signature		Date	28/10/2019

Name of Co-Author	Stephen Tyerman		
Contribution to the Paper	Co-conceived project and suggested experiments, interpreted data, contributed to writing and revision of the manuscript.		
Signature		Date	28/10/2019

Name of Co-Author	Caitlin Byrt		
Contribution to the Paper	Conceived project and designed experiments, interpreted data, contributed to writing and revision of the manuscript.		
Signature		Date	25/10/2019

Title: Phosphorylation influences water and ion channel function of AtPIP2;1

Running title: Phosphorylation influences aquaporin ion channel

Jiaen Qiu[1]*, Samantha A. McGaughey[1]*ǂ, Michael Groszmann[2], Stephen D. Tyerman[1], Caitlin S. Byrt[1,2]

*Joint first author

ǂ Corresponding author: samantha.mcgaughey@adelaide.edu.au

[1]ARC Centre of Excellence in Plant Energy Biology, School of Agriculture, Food and Wine, The University of Adelaide, South Australia, 5005.

[2]ARC Centre of Excellence for Translational Photosynthesis, Division of Plant Sciences, Research School of Biology, Australian National University, Acton, Australian Capital Territory, 0200.

Abstract

Salt and drought stress triggers changes in the phosphorylation state of aquaporins, such as AtPIP2;1. The phosphorylation of two serine residues within the C-terminal domain (S280 and S283) are associated with regulation of trafficking and plasma membrane localisation of AtPIP2;1 in Arabidopsis root cells in response to salt and osmotic stress. Phosphorylation also influences the water transport capacity of AtPIP2;1. We investigated whether changes in S280 and S283 phosphorylation influence AtPIP2;1 facilitated ion transport. A series of single and double S280 and S283 phospho-mimic and deficient mutant AtPIP2;1 proteins were heterologously expressed in *Xenopus laevis* oocytes and their ion and water transport capacity measured. The single and double phospho-mimic mutants AtPIP2;1 S280D, AtPIP2;1 S283D and AtPIP2;1 S280D/S283D had significantly greater ion conductance for Na^+ and K^+ whereas the single and double phospho-deficient mutants AtPIP2;1 S280A and AtPIP2;1 S280A/S283A had greater water permeability. A phosphorylation-dependent inverse relationship between AtPIP2;1 mediated water and ion transport with approximately a 10-fold change in both was observed indicating that phosphorylation of S280 and S283 may be regulating whether AtPIP2;1 proteins preferentially facilitate ion transport or water transport.

Introduction

Aquaporins are membrane bound channel proteins that facilitate the passive bidirectional movement of water and other small molecules across biological membranes. Substrates currently known to be transported by aquaporins include gases (O_2; Zwiazek *et al.,* 2017, CO_2; Rodrigues *et al.,* 2017; Uehlein *et al.,* 2003), metalloids (silicon; Ma *et al.,* 2006, boron; Takano *et al.,* 2006, arsenic; Li *et al.,* 2009), reactive oxygen species (H_2O_2; Bienert *et al.,* 2007; Dynowski *et al.,* 2008; Hooijmaijers *et al.,* 2012), monovalent cations (Na^+; Byrt *et al.,* 2017; Kourghi *et al.,* 2017; Weaver *et al.,* 1994) and other neutral substrates (urea; Dynowski *et al.,* 2008b, glycerol; Gerbeau *et al.,* 1999, ammonia; Loqué *et al.,* 2005). As facilitators of transmembrane water transport, members of the Plasma membrane Intrinsic Protein (PIP) sub-family have roles in mediating water uptake at the root-soil interface, in transcellular water flow, and in regulating hydraulic conductivity in response to abiotic stresses (for recent reviews see: Chaumont & Tyerman, 2014; Maurel *et al.,* 2015; Gambetta *et al.,* 2017). More recently, and similar to their mammalian counter-parts, a subset of plant PIPs (Arabidopsis PIP2;1 and PIP2;2) were found to facilitate the transport of monovalent cations such as Na^+, more evident at low external calcium and high pH (Byrt *et al.,* 2017; Kourghi *et al.,* 2017). The ability of some plant aquaporins to facilitate Na^+ transport has implications in plant salinity stress responses and tolerance.

At the physiological level, water uptake from soil to roots and changes to root hydraulic conductivity in response to stress are mediated by PIPs (Tournaire-Roux *et al.,* 2002). In Arabidopsis, root hydraulic conductance correlated positively with both protein abundance of PIP2 aquaporins and the abundance of phosphorylated PIP2 proteins (di Pietro *et al.,* 2013). Exogenous treatment of barley plants with the kinase inhibitor staurosporine significantly reduced root hydraulic conductance (Horie *et al.,* 2011). The phosphorylation state of several conserved serine residues in the cytoplasmic regions of PIPs, including those in the CTD, have been implicated in phospho-regulation directly influencing water permeation through the pore (Table 1; Johansson *et al.,* 1998; Törnroth-Horsefield *et al.,* 2006; Nyblom *et al.,* 2009; Yaneff *et al.,* 2016) and have been demonstrated to change in response to salt or osmotic stress, influencing PIP trafficking and localisation (Boursiac *et al.,* 2005; Boursiac *et al.,* 2008; Li *et al.,* 2011; Prak *et al.,* 2008). The phosphorylation state of two serine residues on the CTD of AtPIP2;1, S280 and S283, has been reported to change in plant roots exposed to salt treatments and the phosphorylation of S283 has been associated with the salt-induced internalisation of AtPIP2;1 in Arabidopsis roots (Prak *et al.,* 2008).

Extensive studies on aquaporin regulation in animals has also identified phosphorylation as a key regulator of animal aquaporin channel function (both water and ion), protein cycling, trafficking, and membrane localisation (Table 1). The water and ion channel function of soybean (*Glycine max*) NOD-26 (GmNOD-26), the first plant aquaporin to be identified as permeable to both water and ions, was shown to be regulated by the phosphorylation of a CTD residue S262 (Guenther *et al.,* 2003; Lee *et al.,* 1995; Weaver *et al.,* 1994). Phosphorylation of S262 altered the voltage sensitivity of GmNOD-26 ion channel activity (Lee *et al.,* 1995) and increased its water permeability (Guenther *et al.,* 2003). GmNOD-26 phosphorylation was also reported to increase in plants exposed to osmotic stress (Guenther *et al.,* 2003). It is therefore conceivable that phosphorylation could augment the ability of PIPs to facilitate water and Na^+ transport in isoforms capable of such activity. In which case, changes in phosphorylation states would not only regulate PIP protein trafficking and localisation in response to salt and osmotic stresses but also water and Na^+ transport capacity (Byrt *et al.,* 2017; McGaughey *et al.,* 2018).

In this study the phosphorylation state of the two conserved CTD serine residues (S280 and S283) in AtPIP2;1 was investigated in *X. laevis* oocytes in the context of the concurrent regulation of ion (Na^+ and K^+) and water transport. The influence of phosphorylation of these sites on AtPIP2;1 localisation was also probed in yeast. It is important to determine the relationships between PIP protein regulation by phosphorylation and water and ion transport capacity because these features influence plant tolerance to drought and NaCl stresses (McGaughey et al. 2018). Our results indicate that phosphorylation has a key role to play in AtPIP2;1 regulation of transport selectivity and capacity. Given existing information about the regulation of animal aquaporins, and how precisely channel activity, trafficking and localisation are co-ordinately controlled (Table 1), it is expected that there is similar complexity in the regulation of plant aquaporin function that are yet to be fully explored.

Table 1: Examples of regulation of aquaporins by phosphorylation.

AQP isoform	P site	P state (+/-)	Influence on protein				Experimental methods		Expression system	References
			W	**I**	T	L	SDM	Pharm.		
AQP2	Ser-256*	+	↑		✓	✓	✓	✓	PL, KC, LLC	1, 2, 3, 4
	Ser-269*	+			✓	✓	✓	✓	KC	5, 6, 7
	Ser-264*	+			✓	✓		✓	IN (rat, mouse)	8
AQP4	Ser-180	+	↓				✓	✓	LLC	9
	Ser-111[ǂ]	+	↑				✓	✓	AC	10
AQP1	Thr-157[Φ]	+	↑	↑				✓	O	11
	Thr-239*	+	↑	↑				✓		
	Tyr-253*	+		↑			✓	✓	O	12
BIB	Tyr-?	+		↑				✓	O	13
PpAQY1	Ser-107[ǂ]	+	↑				✓		SP	14
α-TIP	Ser-7[Ψ]	-	↓				✓		O	15
	Ser-23[Ψ]	-	↓				✓			
	Ser-99[ǂ]	-	↓				✓			
AtPIP2;1	Ser-121[ǂ]	+	↑				✓	✓	O, PP	16
	Ser-280*	+	?		✓		✓		IP (transgenics), PP	17, 18, 19
	Ser-283*	+	?		✓	✓	✓			
GmNodulin-26	Ser-262*	+		↑			✓		PLB	20, 21
	Ser-262*	+	↑				✓		O	22
SoPIP2;1 (PM28A)	Ser-115[ǂ]	+	↑				✓	✓	O	23
	Ser-274*	+	↑				✓	✓		
ZmPIP2;1	Ser-126[ǂ]	-	↓				✓		O	24
	Ser-203[Φ]	-	↓				✓			
	Ser-285*	+/-	NE				✓			
CsPIP2;1	Ser-121[ǂ]	-	↓				✓		O	25
	Ser-273*	-	↓				✓			

P: phosphorylation, [Ψ]: residue located on NTD, [ǂ]: residue located on intracellular loop B, [Φ]: residue located on intracellular loop D, *: residue located on CTD, P state +/-: phosphorylated or phospho-mimic and dephosphorylated or phospho-deficient respectively, W: water conductance, I: ion conductance, T: trafficking and/or protein cycling, L: protein localisation, SDM: phosphorylation or dephosphorylation mimic by site-directed mutagenesis, Pharm.: phosphorylation changes by application of pharmacological agents (kinase inhibitors or kinase activators). A ↑ or ↓ in the water or ion conductance column indicates if there was an increase or decreased observed; NE: No effect on function reported. In the expression systems column, O: *Xenopus laevis* oocytes; PL: proteoliposomes; PLB: planar lipid bilayers; KC: kidney cells; LLC: LLC-PK1 cells; AC: astrocyte cells; SP: spheroplasts; PP: protoplasts; IN: *in vivo*, IP: *in planta*. A blank box indicates it has not been reported on/tested. [1]Eto *et al.*, 2010; [2]Lu *et al.*, 2008**;** [3]Moeller *et al.*, 2010**;** [4]Van Balkom *et al.*, 2002**;** [5]Hoffert *et al.*, 2006**;** [6]Hoffert *et al.*, 2008**;** [7]Moeller *et al.*, 2010 [8]Fenton *et al.*, 2008; [9]Zelenina *et al.*, 2002; [10]Gunnarson *et al.*, 2005; [11]Zhang *et al.*, 2007; [12]Campbell *et al.*, 2012; [13]Yanochko and Yool, 2002; [14]Fischer *et al.*, 2009; [15]Maurel *et al.*, 1995; [16]Grondin *et al.*, 2015; [17]Prado and Maurel, 2013; [18]Prak *et al.*, 2008; [19]Qing *et al.*, 2016; [20]Lee *et al.*, 1995; [21]Weaver *et al.*, 1994; [22]Guenther *et al.*, 2003; [23]Johansson *et al.*, 1998; [24]Van Wilder *et al.*, 2008; [25]Jang *et al.*, 2014.

Materials and methods

Cloning, preparation of oocyte constructs and cRNA synthesis

The AtPIP2;1 (At3g53420) coding sequence was cloned using high-fidelity Phusion® polymerase (New England Biolabs, USA) from Arabidopsis root cDNA into a Gateway-enabled pCR8/GW/TOPO entry vector (Life Technologies) before being transferred into the pGEMHE (DEST) vector using LR clonase II (Invitrogen). Primers were designed to generate site-directed single and double point phosphomimetic mutations in AtPIP2;1 (Table S1) using AtPIP2;1 in pGEMHE as a template. All the constructs in pGEMHE were linearized using restriction enzyme NheI-HF (New England Biolabs, USA) before cRNA was synthesized using mMESSAGE mMACHINE® T7 Transcription kit (Thermo Fisher Scientific, Australia) as previously described Qiu *et al.,* (2016). The concentration and quality of cRNA was determined by NanoDrop and gel electrophoresis.

Preparation of *Xenopus laevis* oocytes

X. laevis oocytes were harvested and stored following Byrt *et al.,* (2017). Oocytes were injected with 46 nL of RNAse-free water using a micro-injector (Nanoinject II, automatic nanolitre injector, Drummond Scientific) with either no cRNA or 23 ng cRNA. Post injection and prior to experiments oocytes were stored at 18 °C in a Low Na^+ Ringer's solution (62 mM NaCl, 36 mM KCl, 5 mM $MgCl_2$, 0.6 mM $CaCl_2$, 5 mM Hepes, 5% (v/v) horse serum and antibiotics (0.05mg mL^{-1} tetracycline, 100 units mL^{-1} penicillin/0.1 mg mL^{-1} streptomycin)), pH 7.6 for 24-36 h. Expression of AtPIP2;1 within each oocyte batch was confirmed via burst test following Byrt *et al.,* (2017).

Oocyte water permeability

Water permeability (P_{os}) of oocytes injected with water or cRNA was determined following Byrt *et al.,* (2017) with the following important exception based on the previous finding of rapid Na^+ efflux when the external Na^+ concentration is reduced related to PIP2;1 expression (Byrt *et al*., 2017): oocytes were pre-incubated in 3 mL iso-osmotic solution (5 mM NaCl, 2 mM KCl, 1 mM $MgCl_2$, 50 µM $CaCl_2$, pH 8.5) with an osmolarity of 240 $mOsmol.kg^{-1}$ (adjusted with D-mannitol) for 1 h prior to being transferred to a solution with the same ionic composition (5 mM NaCl, 2 mM KCl, 1 mM $MgCl_2$, 50 µM $CaCl_2$, pH 8.5) with an osmolarity of 45 $mOsmol.kg^{-1}$ for the photometric swelling assay.

Electrophysiology

Two-electrode voltage clamp (TEVC) recordings were performed on *X. laevis* oocytes 24h-36h post injection. Preparation of glass pipettes was as described in Byrt *et al.,* (2017). TEVC experiments were performed using an Oocyte Clamp OC-725C (Warner Instruments, Hamden, CT, USA) with a Digidata 1440A data acquisition system interface (Axon Instruments, Foster City, CA, USA). Injected oocytes were continuously perfused with solution after being pierced with the voltage and current electrodes and allowed to stabilise. TEVC was performed in solutions consisting of 50 mM NaCl (Na50), 100 mM NaCl (Na100) or 100 mM KCl (K100) in a basal solution (2 mM KCl, 1 mM $MgCl_2$ and 5 mM HEPES, osmolarity was adjusted to 240 mOsmol.kg^{-1} with D-mannitol) with 50 µM $CaCl_2$ and pH 8.5. For experiments involving endogenous oocyte kinase stimulation or inhibition, injected oocytes were incubated prior to TEVC in Low Na^+ Ringers (described previously) supplemented with 1 mM 8-Br-cAMP (Sigma (St Louis, MO, USA), #B5386), or 1 mM 8-Br-cGMP (Sigma, #B1381) or 10 µM H7 dihydrochloride (Sigma, #17016) from concentrated stocks dissolved in water. Steady–state currents were recorded starting from -40 mV holding potential for 0.5 s and ranging from 40 mV to -120 mV with 20 mV decrements for 0.5 s before following a -40 mV pulse for another 0.5 s. Ionic conductance was calculated by taking the slope of a regression of the linear region across the reversal potential (-60 mV to +40 mV). TEVC recordings were analysed with CLAMPEX 9.0 software (pClamp 9.0 Molecular Devices, CA, USA).

Oocyte Na^+ Content

Water control and cRNA injected oocytes were incubated for 24 h in the Na100 solution as was used for as used for electrophysiology recordings. Oocytes were removed to individual 1.5 mL microfuge tubes and washed briefly with double distilled H_2O. All solution was removed from the tube and oocytes were stored at -20°C. Oocytes were thawed at room temperature before being homogenised in 0.1 M analytic nitric acid and digested at 42°C for 2 h. Nitric acid digested homogenates were diluted 1:10 with double distilled H_2O, vortexed briefly and centrifuged at 16 000 x g (Beckman Coulter Microfuge® 16) to pellet cell debris. An aliquot of the supernatant was removed for dilution and ion analysis was performed using an Atomic Absorption Spectrophotometer (AAS; Shimadzu AA-7000) according to manufacturer's instructions.

Yeast vector cloning and yeast localisation

Gateway compatible entry clone containing *AtPIP2;1* was generated in pENTR1a and used as a template to generate site-directed single and double point phosphomimetic mutations in AtPIP2;1 (Table S1). Additional non-stop codon versions of these genes were PCR amplified from the pENTR1a clones with primers containing attB sites and inserted into pZeo using BP clonase (Invitrogen). The pZeo non-stop-codon gene versions were shuttled into pAG426-GPD-eGFP by LR clonase II reaction (Invitrogen) to create C-terminal GFP fusion for sub-cellular protein localisation. The pAG426-GPD-GFP vector which confers strong constitutive transgene expression in yeast, were obtained from Addgene (plasmid #14150) and originally deposited by Susan Lindquist (Alberti *et al.,* 2007). The pAG426-GPD-GFP AtPIP2;1 wild-type and the single and double AtPIP2;1 S280 and S283 phosphorylation mutant constructs were transformed into the Saccharomyces cerevisiae *aqy1/aqy2* double mutant yeast strain (Matα; leu2::hisG; trp1::hisG, his3::hisG; ura352 aqy1D::KanMX aqy2D::KanMX) using Frozen-EZ Yeast Transformation II kit (Zymo Research). The *aqy1/aqy2* double mutant yeast strain was gifted by Peter Dahl (Hohmann Lab) (Tanghe *et al.,* 2002).

Sub-cellular GFP signal was visualised on a Zeiss LSM780 confocal laser-scanning microscope (Carl Zeiss) operated by Zen Black software and a DIC x40 oil immersion lens. eGFP was excited at 488nm and emission was captured at 495-570nm and RFP was excited at 561nm and emission captured at 580-735, with 24 µm pinhole and master and digital gains identically set for all images and analysis. Between 30 to 160 cells for each of the AtPIP2;1 wild-type and mutant proteins were scored across 3-4 independent experiments with differences in the localisation patterns between the genotypes consistent across sessions. pSM1959 was obtained through Addgene (Susan Michaelis - Addgene plasmid #41837; Metzger *et al.,* 2008).

Results

Cyclic nucleotide and kinase inhibitor treatments influence AtPIP2;1 mediated ionic conductance in *X. laevis* oocytes

AtPIP2;1 expression in *X. laevis* oocytes elicits Na^+-inducible currents (Byrt *et al.,* 2017). We investigated whether AtPIP2;1-facilitated ion transport may be altered by its phosphorylation state. The activity of endogenous kinases in *X. laevis* oocytes, and hence phosphorylation state of expressed proteins, were manipulated by the exogenous application of membrane permeable cyclic nucleotide (cNMP) analogues 8-Br-cAMP and 8-Br-cGMP as kinase stimulators and the kinase inhibitor H7 (Figure 1). These pharmacological agents have been used previously in this heterologous system to study functional regulation of mammalian aquaporins by phosphorylation (Campbell *et al.,* 2012; Han and Patil, 2000; Hoffert *et al.,* 2008; Yool *et al.,* 1996).

Oocytes were injected with water or AtPIP2;1 cRNA and either untreated, incubated in 1 mM 8-Br-cAMP (cAMP) or 8-Br-cGMP (cGMP) for 10 min, incubated in 10 µM H7 for 2 h, or incubated in H7 prior to a cNMP incubation. The ionic conductance of these oocytes was measured by TEVC (Figure 1). Data was collected from multiple independent oocyte batches; therefore, to remove batch to batch variation in native ionic conductance and examine only the response to the treatments the data for water injected oocytes were normalised to untreated water injected oocytes and treated AtPIP2;1 injected oocytes were normalised to untreated AtPIP2;1 injected oocytes within each batch.

Water injected oocytes did not respond to any treatment type (Figure 1a). Incubation of AtPIP2;1 injected oocytes in solutions containing H7 and cGMP resulted in a significant decrease in ionic conductance relative to untreated (Figure 1b). In contrast, incubation in cAMP increased the ionic conductance of AtPIP2;1 injected oocytes (Figure 1b). AtPIP2;1 injected oocytes that were first incubated in H7 followed by a cAMP incubation had increased ionic conductance compared to those incubated only in H7. This indicates that AtPIP2;1 facilitated Na^+ transport in oocytes is influenced by protein phosphorylation state and could involve multiple phosphorylation sites.

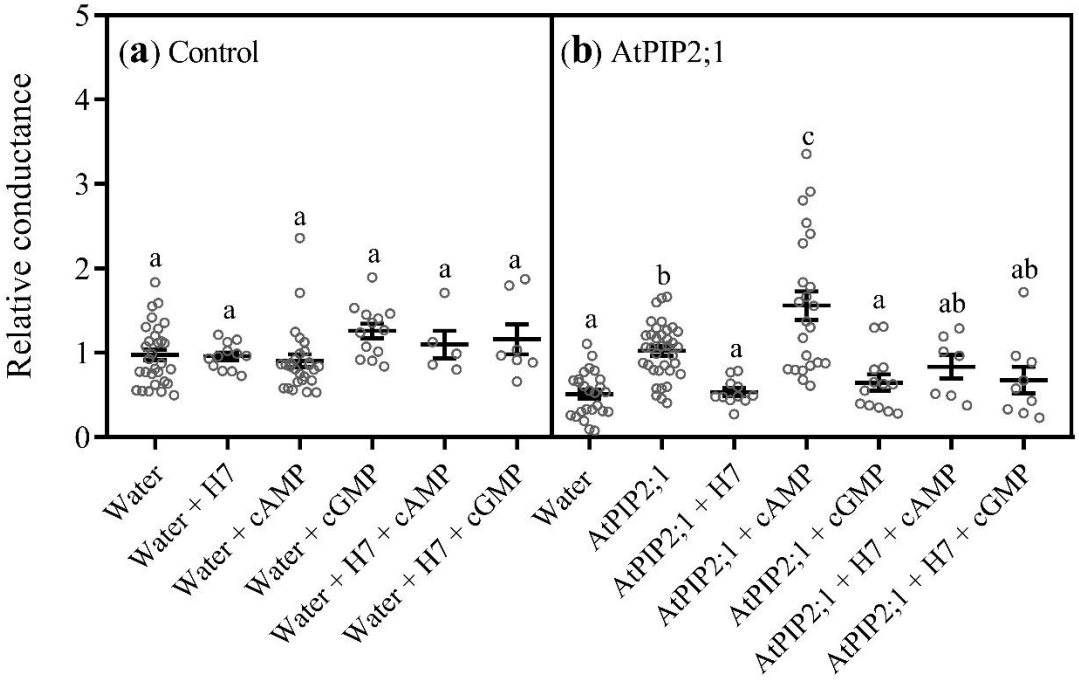

Figure 1: Exogenous application of membrane permeable cAMP and cGMP analogues as kinase stimulators and the kinase inhibitor H7 influence ionic conductance of AtPIP2;1 injected oocytes. Oocytes were either untreated or were pre-treated in Low Na^+ Ringers solution that contained 1 mM 8-Br-cAMP (cAMP), 1 mM 8-Br-cGMP (cGMP) or 10 µM H7 dihydrochloride (H7). TEVC was performed in a Na50 solution. The ionic conductance of treated water injected and AtPIP2;1 cRNA injected oocytes were normalised to untreated water injected and AtPIP2;1 cRNA injected oocytes respectively. **(a)** Relative ionic conductance of control oocytes. **(b)** Relative ionic conductance of AtPIP2;1 injected oocytes. Data was compiled from at least two independent oocytes batches with the exception of H7 + cNMP treatment where it is one batch. Data is represented as mean relative conductance ± SEM. Significant differences ($P < 0.05$) are indicated by different letters using one-way ANOVA, Fishers post-test.

Phospho-mimic and deficient AtPIP2;1 mutants had altered ionic conductance and Na^+ accumulation in *X. laevis* oocytes

The phosphorylation state of AtPIP2;1 CTD residues S280 and S283 is altered by salt treatment (Prak *et al.*, 2008). To explore potential regulatory roles of S280 and S283 phosphorylation on AtPIP2;1-facilitated ion transport several single and double S280 and S283 phospho-mimic (S > D) and phospho-deficient (S > A) versions of AtPIP2;1 were generated. The ionic conductance of oocytes expressing AtPIP2;1 wild-type (WT) or AtPIP2;1 phospho-mimic (S280D, S283D) and phospho-deficient (S280A, S283A) single and double mutants in the presences of Na^+ and K^+ were measured by TEVC (Figure 2, Figure S1).

In Na100 solution the single and double phospho-deficient mutants AtPIP2;1 S280A, AtPIP2;1 S283A and AtPIP2;1 S280A/S283A induced currents and had ionic conductance of similar magnitude to that of AtPIP2;1 WT (Figure 2a-d). Comparatively, the expression of the single phosphorylation mutants AtPIP2;1 S280D and AtPIP2;1 S283D and the double phosphorylation mutants AtPIP2;1 S280D/S283A, AtPIP2;1 S280A/S283D and AtPIP2;1 S280D/S283D induced greater currents and ionic conductance than WT or the phospho-deficient mutants (Figure 2a-d).

AtPIP2;1 WT was capable of functioning as a K^+ permeable ion channel when expressed in *X. laevis* oocytes (Figure 2a,c). The phosphorylation mutants had similar effects on conductance in a K100 solution to that observed in the Na100 solution. The phospho-mimics AtPIP2;1 S280D and AtPIP2;1 S283D had greater ionic conductance than either AtPIP2;1 WT or the phospho-deficient mutants (Figure 2c). However, the magnitude of conductances were larger in K100 than what was observed in Na100 by approximately 20-30% (Figure 2c).

We also investigated how expression of AtPIP2;1 and AtPIP2;1 phosphorylation mutants would influence the total Na^+ content of oocytes. The total Na^+ content of AtPIP2;1 WT and phospho-mutant expressing oocytes after 24 h incubation in Na100 solution was determined by analysis with an atomic absorption spectrophotometer (Figure 2e). Similar to the trends observed for ionic conductance in the same solution (Na100; Figure 2e) the phospho-mimic single and double mutants accumulated greater total Na^+ per oocyte than WT or the phospho-deficient mutants.

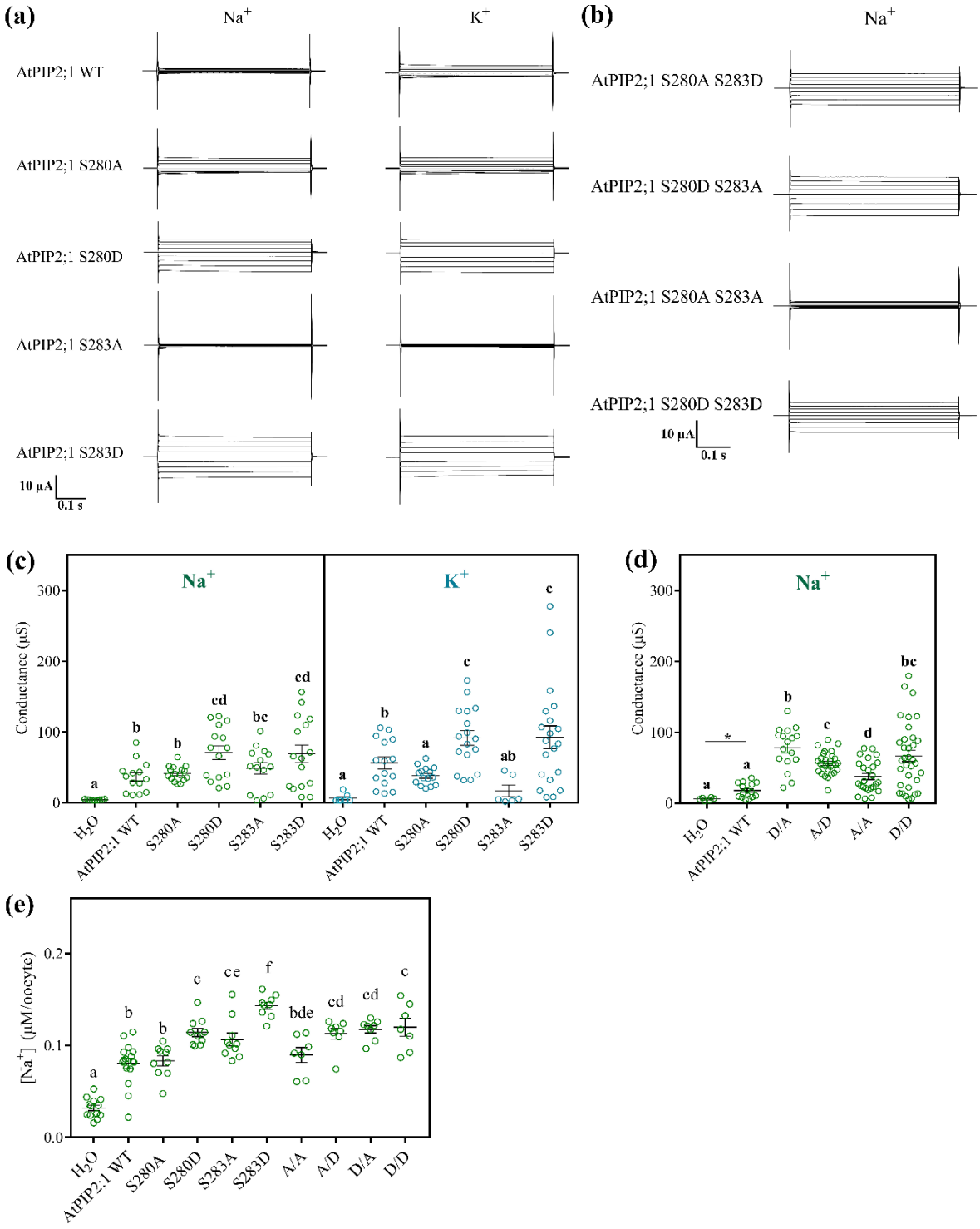

Figure 2: Influence of phosphorylation of CTD residues S280 and S283 on AtPIP2;1 facilitated ion transport. Oocytes were injected with 46 nL water (H_2O) or with 46 nL water containing 23 ng AtPIP2;1 WT (WT) or AtPIP2;1 S280A (S280A), AtPIP2;1 S280D (S280D), AtPIP2;1 S283A (S283A), AtPIP2;1 S283D (S283D), AtPIP2;1 S280A/S283A (A/A), AtPIP2;1 S280D/S283A (D/A), AtPIP2;1 S280A/S283D (A/D) or AtPIP2;1 S280D/S283D (D/D) cRNA. Oocytes were incubated for 24hrs in Low Na^+ Ringers. Representative superimposed currents as a function of time of **(a)** AtPIP2;1 single phosphorylation mutants in Na100 (Na^+) and K100 (K^+), and **(b)** AtPIP2;1

double phosphorylation mutants in Na100 (Na^+). Ionic conductance of oocytes expressing **(c)** AtPIP2;1 single phosphorylation mutants in Na100 (Na^+) and K100 (K^+), and **(d)** AtPIP2;1 double phosphorylation mutants in Na100 (Na^+). **(e)** Na^+ content of oocytes incubated in Na100 for 24 h. Data in (c-e) is compiled from 3 independent oocyte batches and is shown as mean ± SEM where each data point represents an individual oocyte. Significant differences ($P<0.05$) are indicated by different letters (one-way ANOVA, Fishers post-test), or by an * (un-paired t-test).

Relationship between phosphorylation, osmotic permeability and ionic conductance of AtPIP2;1

The phosphorylation state of AtPIP2;1 CTD sites S280 and S283 influenced AtPIP2;1 facilitated ionic conductance when expressed in oocytes (Figure 2, Figure S1). We then investigated the effect of phosphorylation of these sites on water permeation and whether a relationship exists between osmotic permeability and ion conductance in oocytes expressing AtPIP2;1 WT and phosphorylation state mutants (Figure 3).

The water permeability (P_{os}) of oocytes expressing AtPIP2;1 WT, and AtPIP2;1 S280 and S283 single and double phospho-mimic and -deficient mutants was determined via the photometric swelling assay (Figure 3a). Oocytes were first acclimatised to an iso-osmotic solution before being transferred to a hypo-osmotic solution during the assay. The single and double phospho-deficient mutants AtPIP2;1 S280A and AtPIP2;1 S280A/S283A had greater osmotic permeability compared to AtPIP2;1 WT (Figure 3a). Comparatively, the single and double phospho-mimic mutants AtPIP2;1 S280D, AtPIP2;1 S283D, AtPIP2;1 S280D/S283A, AtPIP2;1 S280A/S283D and AtPIP2;1 S280D/S283D all had lower osmotic permeability compared to AtPIP2;1 WT (Figure 3a). The lower osmotic permeability for the AtPIP2;1 S280D/S283A and AtPIP2;1 S280A/S283D mutants indicates that when either the S280 or S283 site is phosphorylated this has a dominant effect on function over the dephosphorylated state of the other site.

To test for a relationship between water permeability, ionic conductance and phosphorylation, TEVC and photo-metric swelling assays were performed consecutively on the same oocytes expressing AtPIP2;1 WT and double phosphorylation mutants after a 2 h recovery incubation (Figure 3b). A negative correlation between osmotic permeability and ionic conductance was observed (Pearson's correlation coefficient (r) = -0.560, $p < 0.0005$) (Figure 3b), demonstrating an approximately ten-fold increase in ion conductance corresponding to a ten-fold decrease in water permeability (note log-log scale). Furthermore, the phosphorylation state of the two AtPIP2;1 CTD sites S280 and S283 influences AtPIP2;1 tendency to facilitate water or ion transport; the AtPIP2;1 double phosphorylation mutants with at least one phospho-mimic residue (AtPIP2;1 S280A/S283D, S280D/S283A and S280D/S283D) had greater ion transport function than that of AtPIP2;1 WT or the double phospho-deficient mutant AtPIP2;1 S280A/S283A. AtPIP2;1 S280D/S283D exhibited large variation, whereas the other phosphorylation mutants tested did not (Figure 3b).

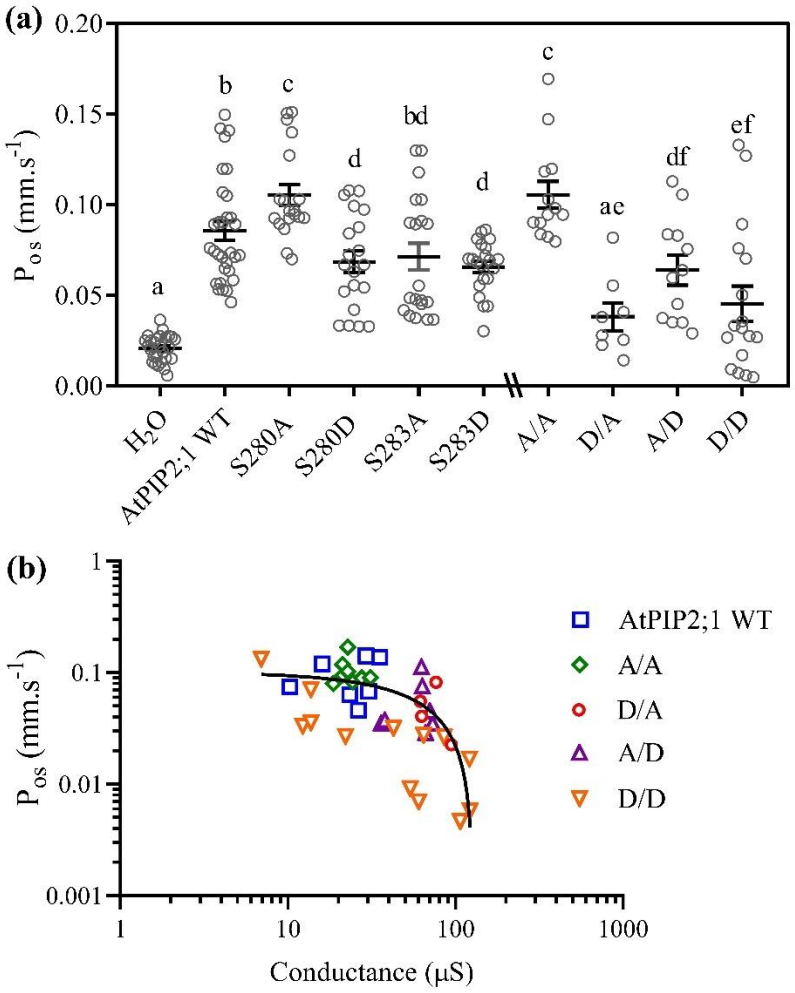

Figure 3: Phosphorylation state of AtPIP2;1 S280 and S283 residues influences its osmotic permeability and the relationship between water and ion transport. Osmotic permeability (P_{os}) and ionic conductance of water injected and AtPIP2;1 Wild-type (WT), AtPIP2;1 S280D (S280D), AtPIP2;1 S280A (S280A), AtPIP2;1 S283D (S283D), AtPIP2;1 S283A (S283A), AtPIP2;1 S280A/S283A (A/A), AtPIP2;1 S280D/S283A (D/A), AtPIP2;1 S280A/S283D (A/D) or AtPIP2;1 S280D/S283D (D/D) cRNA injected oocytes was determined via the photometric swelling assay and TEVC, respectively. **(a)** P_{os} of injected oocytes. Data for P_{os} was compiled from three representative oocyte batches. The dash in the x-axis indicates data was collected from different batches. Data is mean P_{os} ± SEM; significant differences ($P < 0.05$) are indicated by different letters using one way ANOVA, Fishers post-test. **(b)** Relationship between P_{os} and ionic conductance from one representative oocyte batch (log log scale). The negative correlation determined by Pearson's correlation was significant (r = -0.560, $P < 0.0005$).

Phosphorylation state of S280 and S283 influences AtPIP2;1 localisation in yeast

Sub-cellular localisation tendencies of the *AtPIP2;1* phospho-mutants were monitored in yeast using both N- or C-terminal GFP fusions. Fusion of AtPIP2;1 wild-type or AtPIP2;1 phospho-mutants to GFP, redirected GFP from a diffuse cytosolic pattern (Figure 4A) to a predominantly sharp ring around the cell perimeter coinciding with the PM (Figure 4C-I). Weaker GFP labelling associated with the tonoplast of the vacuole was also frequently observed. In addition, a proportion of cells showed internal and patchy perimeter GFP labelling, matching the localisation pattern of the SEC63::RFP endoplasmic reticulum (ER) marker (Figure 4B). The detectable frequency and intensity of the ER co-localisation differed between the AtPIP2;1 wild-type (S280/S283; S/S) and some of the AtPIP2;1 280/283 phospho-mimic mutants (Figure 4J). The most striking difference was observed with the AtPIP2;1 S280D (D/S) mutant which had frequently occurring intense GFP signal co-localising to the ER (Figures 5D, E and J). The AtPIP2;1 S283D (S/D) and AtPIP2;1 S280D/S283D (D/D) mutants showed an opposite pattern with a constant sharp GFP signal around the perimeter consistent with PM localisation, and a low intensity and frequency of ER co-localisation (Figures 5F, G, H and J). The AtPIP2;1 S280A (A/S) and AtPIP2;1 S280A/S283D (A/D) mutants showed a slightly more frequent tendency to co-localise to the ER than wild-type (Figures 5I and J). GFP localisation patterns for the phospho-deficient AtPIP2;1 S283A (S/A) and AtPIP2;1 S280A/S283A (A/A) mutants along with the AtPIP2;1 S280D/S283A (D/A) mutant were equivalent to that of wild-type AtPIP2;1 (Figure 4J). There was no discernible difference in the localisation patterning between the N- or C-terminal fusions (data not shown).

Comparisons between the phospho-mutants reveal co-ordinated effects of positions S280 and S283 in determining sub-cellular localisation. The more prominent PM targeting of the AtPIP2;1 D/D mutant in comparison to the A/A, D/A, or A/D mutants, implies that phosphorylation of both S280 and S283 are required to promote optimal PM localisation (Figure 4J). The fact that AtPIP2;1 S/D sub-cellular localisation is reminiscent of the D/D mutant (Figure 4J), suggests that S280 maybe innately phosphorylated by the yeast, possibly in response to position 283 being a phospho-mimic residue. The strong ER co-localisation of AtPIP2;1 D/S was not observed in either of the two other S280D phospho-mimic mutants (D/A or D/D) (Figure 4J), indicating that a serine at position 283 is specifically required in combination with the phospho-mimic aspartic acid at position 280 to achieve the strong ER co-localisation.

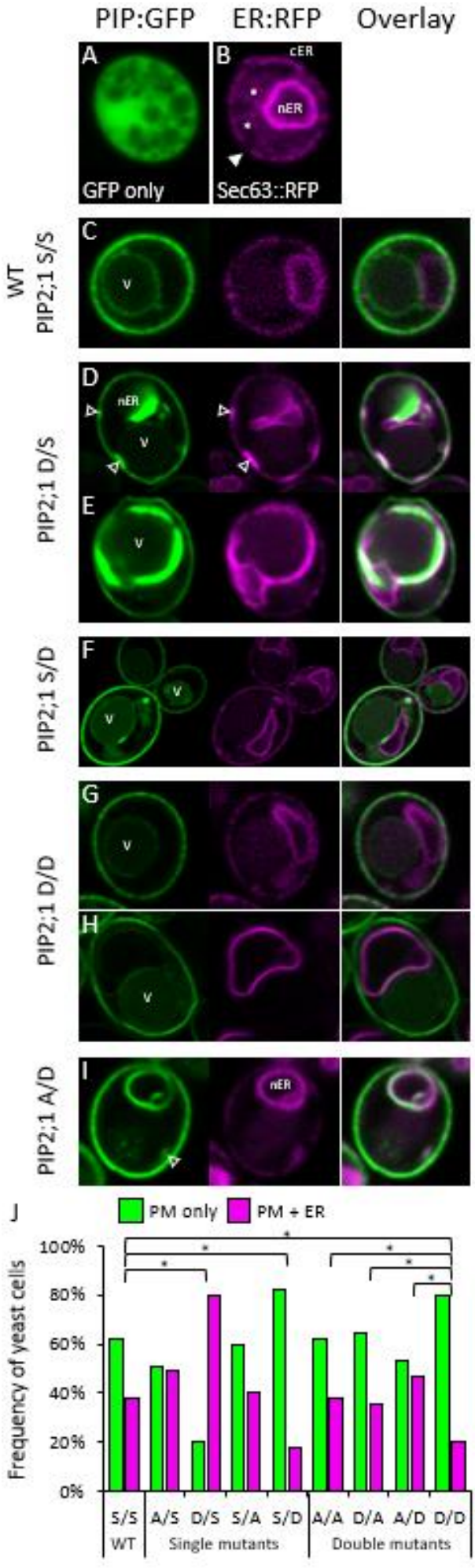

Figure 4: Subcellular localisation of AtPIP2;1 wild-type (S280/S283) and 280/283 phospho-mutants in yeast. (A) A control showing that GFP alone results in a diffuse cytosolic localised signal. **(B)** SEC63::RFP endoplasmic reticulum marker. The yeast ER network consists of the prominent nuclear envelope ER domain (nER) and a peripheral or cortical ER domain (cER). The cER lies just beneath the plasma membrane but is not continuous around the perimeter with gaps distinguishing it from plasma membrane localisation (solid triangle). Cytoplasmic tubules link the two ER domains (*). **(C)** Wild-type AtPIP2;1 S/S::eGFP localises to a distinct continuous ring of expression around the cell perimeter coinciding with the plasma membrane (PM). GFP signal is also weakly present in the tonoplast of the vacuole (V). In this example, no expression is detected in the nER. **(D-E)** The single phospho-mimetic PIP2;1 D/S mutant commonly shows a continuous ring of PM localisation along with a substantially stronger GFP signal co-localised with the ER marker in both the peripheral (open arrow heads) and internal ER networks (nER). **(F)** The single phospho-mimetic PIP2;1 S/D mutant shows a clean sharp localisation around the PM with little to no ER co-localisation. Weak GFP signal is occasionally observed in the periphery of the vacuoles (V). **(G-H)** The localisation of the double phosphorylated mimetic PIP2;1 D/D mutant occurs almost exclusively in the PM with comparably weak signal detectable in the tonoplast of the vacuole (V) and little to no signal in the ER. **(I)** The double PIP2;1 A/D mutant localises to the PM. Approximately half the yeast cells examined also exhibit strong co-localisation to the ER. **(J)** The frequency of yeast cells with GFP signal detected in the PM only versus co-localisation in both the PM and ER. Asterisks (*) denote statistically significant difference (Fisher's exact test $p \leq 0.05$). N = S/S(53), A/S(57), D/S(161), S/A(32), S/D(94), A/A(117), D/A(54), A/D(139) D/D(83).

Discussion

AtPIP2;1 facilitated water and monovalent cation transport activity *in vivo* is influenced by the phosphorylation state of CTD residues S280 and S283 (Figures 1-3). Phosphorylation altered the preferential transport capacity of AtPIP2;1, increasing water transport when un-phosphorylated and ion transport when phosphorylated. A phosphorylation-dependent inverse relationship between AtPIP2;1 facilitated water and ion transport was observed with approximately ten-fold changes in both permeabilities.

AtPIP2;1 facilitated ion transport is influenced by activity of endogenous oocyte kinases

Stimulation or inhibition of endogenous kinase activity of *X. laevis* oocytes expressing wild-type (WT) AtPIP2;1 by treatment with cNMPs or H7 resulted in changes to ionic conductances when compared to untreated AtPIP2;1 or water injected control oocytes (Figure 1). Both cAMP and cGMP stimulate oocyte endogenous kinase activity to alter protein phosphorylation (Glass and Krebs, 1980; Kuwahara *et al.,* 1995); different kinases respond to cAMP and cGMP signalling, and the kinases responding to these different signals have different target sites (Conti *et al.,* 2012). Endogenous oocyte kinases have been previously shown to alter plant aquaporin phosphorylation state and influence their water channel activity by treatments with kinase stimulators and inhibitors (Maurel *et al.,* 1995; Van Wilder *et al.,* 2008). Treatment of AtPIP2;1 expressing oocytes with cAMP or cGMP increased and decreased their measured ionic conductance, respectively (Figure 1). Treatment of AtPIP2;1 expressing oocytes with the kinase inhibitor H7 decreased ionic conductance (Figure 1b). H7 treatment similarly reduced ionic conductance for HsAQP1 expressing oocytes by inhibiting the influence of cAMP on endogenous kinases (Yool *et al.,* 1996). These data indicate that multiple phosphorylation sites may be involved in regulating AtPIP2;1-facilitated ion transport and that this capacity can be altered by the activity of endogenous oocyte kinases. However, a direct effect of cNMPs on AtPIP2;1 should also be considered; HsAQP1 ion channel function is activated by direct cGMP binding to its loop D in a phosphorylation-dependent manner (Anthony *et al.,* 2000; Campbell *et al.,* 2012). Although AtPIP2;1 does not possess the putative cGMP binding site identified in the loop D of HsAQP1, it could be interacting at another unknown site.

Phosphorylation of C-terminal S280 and S283 sites reciprocally regulates AtPIP2;1 facilitated water and ion transport

Phospho-mimic and phospho-deficient mutations of CTD residues S280 and S283 were found to influence AtPIP2;1 facilitated water and ion transport in oocytes (Figures 2-3). Oocytes expressing the single phospho-mimic versions of AtPIP2;1, S280D and S283D or the phospho-mimic double mutants AtPIP2;1 S280A/S283D, S280D/S283A and S280D/S283D had increased ionic conductance in solutions containing Na^+ and K^+ and increased Na^+ content compared to oocytes expressing either AtPIP2;1 WT or the single phospho-deficient variants AtPIP2;1 S280A and AtPIP2;1 S283A or double phospho-deficient mutant AtPIP2;1 S280A/S283A (Figure 2). Comparatively, oocytes expressing the single mutant AtPIP2;1 S280A and double mutant AtPIP2;1 S280A/S283A had increased water permeability (Figure 3). When the phosphorylation status of both CTD sites were controlled for the functional effect of the phospho-mimicked residue was dominant; both the AtPIP2;1 S280D/S283A and AtPIP2;1 S280A/S283D phospho-mutants had water and ion transport activity more consistent with the AtPIP2;1 S280D/S283D than the AtPIP2;1 S280A/283A (Figure 2 and 3). Of multiple phosphorylation events on the AQP2 CTD that occur in renal epithelial cells in response to vasopressin, the effect of phosphorylation of one site was was dominant with respect to its function and trafficking (Lu *et al.,* 2008). AQP2 CTD phosphorylation also exhibits a hierarchy where the phosphorylation of particular residues does not occur unless the phosphorylation of another site has preceded it (Hoffert *et al.,* 2008).

AtPIP2;1 facilitated the transport of K^+ and the single phospho-mimic mutants increased K^+ associated conductance similar to what was observed for Na^+ (Figure 2). AtPIP2;1 (and AtPIP2;2) have been proposed as the thus far elusive molecular candidates contributing to non-selective cation channel currents (Byrt *et al.,* 2017; McGaughey *et al.,* 2018; Munns *et al.,* 2019) that have been observed *in planta* (Demidchik and Tester, 2002; Essah *et al.,* 2003; Roberts and Tester, 1997). That AtPIP2;1 can facilitate K^+ transport i*n vivo* adds support to this hypothesis. Furthermore, the NSCCs observed by Demidchik and Tester, (2002), were more conductive to K^+ than Na^+ (with a selectivity ratio of 1.49:1.00), similar to that observed for AtPIP2;1 in *X. laevis* oocytes (Figure 2c). The regulation of AtPIP2;1 ion transport by cGMP (Figure 1) should also be noted; exogenous application of cGMP was previously shown to inhibit NSCCs *in planta* (Essah *et al.,* 2003; Maathuis and Sanders, 2001), and intracellular cGMP concentrations increase in response to salinity/osmotic stress (Donaldson *et al.,* 2004; Rubio *et al.,* 2003). Interestingly, a recent review proposed that Na^+

influx via AtPIP2;1 was inhibited by cGMP under salt stress (Isayenkov and Maathuis, 2019). AtPIP2;1 facilitated transport of the physiologically important K^+, and possibly NH_4^+, suggests a role in nutrient acquisition under normal conditions.

The negative correlation between AtPIP2;1 facilitated water and ion transport was phosphorylation dependent (Figure 3b). The AtPIP2;1 phospho-mimic mutants (AtPIP2;1 S280A/S283D, S280D/S283A and S280D/S283D) had greater tendency to facilitate the transport of ions over water compared to that of the phosphorylation deficient mutant AtPIP2;1 S280A/S283A. The variance seen for the S280D/S283D in this correlation suggests that there are likely other additional regulatory sites that were not controlled for and that these unknown sites may be dependent on a diphosphorylated CTD. It was recently reported that several General Regulatory Factors (GRFs; also known as 14-3-3 proteins) interacted preferentially with AtPIP2;1 when the S280 and S283 sites were phosphorylated, and co-expression of AtPIP2;1 S280D/S283D mutant with GRFs 3,4 and 10 in oocytes increased their osmotic permeability compared to AtPIP2;1 S280A/S283A (Prado *et al.*, 2019). Although it cannot be excluded, it is unlikely that a possible interaction with an endogenous oocyte GRF protein could account for differences in transport capacity reported here. For instance, in Arabidopsis AtPIP2;1, AtPIP2;2, AtPIP2;3, AtPIP2;4 and AtPIP2;7 were found to be unphosphorylated, singly phosphorylated at S280 or diphosphorylated at S280 and S283 (Prak *et al.*, 2008), but AtPIP2;7 did not facilitate ion transport when expressed in oocytes (Kourghi *et al.*, 2017). Another plant aquaporin, the soybean (*Glycine max*) Gm-NOD26, demonstrated ion channel activity when reconstituted in lipid bilayers (Weaver *et al.*, 1994). The water and ion channel function of Gm-NOD26 was also found to be regulated by the phosphorylation of a CTD residue S262 (Guenther *et al.*, 2003; Lee *et al.*, 1995).

The exact physiological role of dual water and ion transporting aquaporins in plants remains unknown and may differ in different tissues (McGaughey *et al.*, 2018). When exposed to a NaCl treatment, the phosphorylation states of AtPIP2;1 S280 and S283 residues was altered (Prak *et al.*, 2008); specifically, when plants were treated with 100 mM NaCl the abundance of the S280/S283 disphosphorylated form decreased. Since phosphorylation of S280 and S283 increase AtPIP2;1 ion channel function, this suggests reduction in S280/S283 diphosphorylated AtPIP2;1 may be a mechanism to reduce Na^+ influx (and possibly K^+ efflux) under salt stress. Salt treatment has also been reported to increase AtPIP2;1 location-cycling (Li *et al.*, 2011; Luu *et al.*, 2012), and induce AtPIP2;1 internalisation from the plasma-membrane into intra-cellular vesicles in root cells (Boursiac *et al.*, 2005; Prak *et al.*,

2008; Ueda *et al.,* 2016) where internalisation was reported to be dependent on S283 phosphorylation state (Prak *et al.*, 2008). By manipulating the phosphorylated state of the AtPIP2;1 CTD serine residues, we were able to alter trafficking and abundance of the AtPIP2;1 protein between the PM and ER (Figure 4). Firstly, we found that the phospho-mimic S280D mutation resulted in a substantial localisation of AtPIP2;1 to the ER over trafficking to the PM. This specifically required the presence of a serine residue at position 283 and could not be replicated by mimicking a phospho-deficient state using alanine. Secondly, we found that optimal PM targeting is not only dependent on S283 phosphorylation, but rather requires dual phosphorylation of both S280 and S283, with the presence of a phospho-mimic residue at position 283 potentially influencing the phosphorylation state of S280. Interestingly the localisation of the double phospho-deficient mutant AtPIP2;1 S280A/S283A was similar to other phospho-mimic mutants, such as AtPIP2;1 S280D/S280A and AtPIP2;1 S280A/S280D (Figure 4), that exhibited significantly greater ionic conductance than AtPIP2;1 S280A/S283A when expressed in *X. laevis* oocytes (Figure 2). These data, alongside the increased water permeability of AtPIP2;1 S280A/S283A (Figure 3), suggests that a mis-localisation of the AtPIP2;1 S280A/S283A, and therefore less protein abundance in the PM, in oocytes is not likely to be the cause of its lower ionic conductance. Furthermore, the fact we could make these observations in yeast using an aquaporin from the distant taxa of plants, implies an evolutionary early origin for CTD phosphorylation in regulating aquaporin trafficking.

The seemingly complex interaction between AtPIP2;1 phosphorylation state and AtPIP2;1 trafficking, localisation, and water and ion transport function may be a mechanism for rapidly, reversibly and co-ordinately adjusting water and Na^+ or K^+ flux into or out of the cell. This mechanism would be even more important for osmo-regulation in osmotically stressful conditions.

Conclusions

Data presented here provides a first glimpse into a new paradigm of plant water and ion channel aquaporin function and regulation. Mimicking a phosphorylated state of AtPIP2;1 S280 and S283 sites results in Na^+ and or K^+ ion conductance of a magnitude similar to that observed for other plant ion channels expressed in *X. laevis* oocytes, indicating that phosphorylation-dependent ion flux through AtPIP2;1 would be significant *in planta* (McGaughey *et al.,* 2018). Plant aquaporins capable of facilitating ion transport may be the

elusive non-selective cation channels responsible for a large proportion of Na^+ and K^+ flux across the PM (Demidchik and Tester, 2002; Rubio *et al.*, 2010). The *in planta* physiological influence of phosphorylation at S280 and S283 water and ion transport that are demonstrated here is yet to be resolved. Discovering how these features intersect and are regulated in plants, and their relationship with osmotic stress tolerance mechanisms, holds great potential for improving plant productivity in dry and saline environments.

Supplementary materials

Table S1: Single point mutagenesis primers to generate pGEMHE and pENTR1a AtPIP2;1 phospho-mutant constructs.

Mutation	FOR primer	REV primer
AtPIP2;1 S280A	GGTTCTAAGTCTCTTGGAGCATTC AGAAGTG	GTTGGCAGCACTTCTGAATGCTCC AAG
AtPIP2;1 S280D	GGTTCTAAGTCTCTTGGAGACTTC AGAAGTGC	GTTGGCAGCACTTCTGAAGTCTCC AAG
AtPIP2;1 S283A	CTAAGTCTCTTGGATCATTCAGAG CTGCTGC	TTAGACGTTGGCAGCAGCTCTGA ATGATC
AtPIP2;1 S283D	CTCTTGGATCATTCAGAGATGCTG CCAA	TAGACGTTGGCAGCATCTCTGAAT GATC\
AtPIP2;1 S280A/S283A	CTTGGAGCATTCAGAGCTGCTGCC AACGTCT	GCAGCAGCTCTGAATGCTCCAAG AGACTTAGAAC
AtPIP2;1 S280A/S283D	CTTGGAGCATTCAGAGATGCTGCC AACGTCT	GCAGCATCTCTGAATGCTCCAAG AGACTTAGAAC
AtPIP2;1 S280D/S283A	CTTGGAGACTTCAGAGCTGCTGCC AACGTCT	GCAGCAGCTCTGAAGTCTCCAAG AGACTTAGAAC
AtPIP2;1 S280D/S283D	CTTGGAGACTTCAGAGATGCTGCC AACGTCT	GCAGCATCTCTGAAGTCTCCAAG AGACTTAGAAC

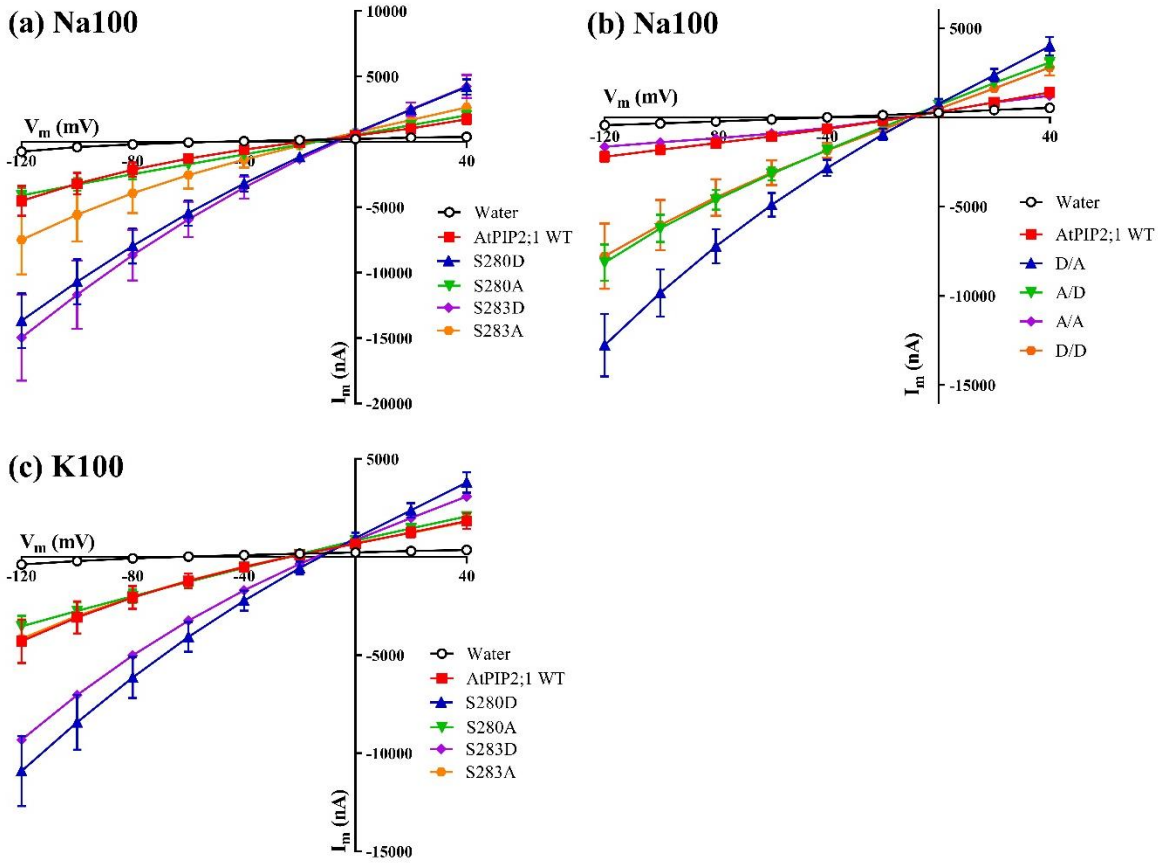

Figure S1: IV curves of AtPIP2;1 WT and AtPIP2;1 phosphorylation mutants. Oocytes were injected with 46 nL water (water) or with 46 nL water containing 23 ng AtPIP2;1 WT (WT) or AtPIP2;1 S280A (S280A), AtPIP2;1 S280D (S280D), AtPIP2;1 S283A (S283A), AtPIP2;1 S283D (S283D), AtPIP2;1 S280A/S283A (A/A), AtPIP2;1 S280D/S283A (D/A), AtPIP2;1 S280A/S283D (A/D) or AtPIP2;1 S280D/S283D (D/D) cRNA. Oocytes were incubated for 24hrs in Low Na^+ Ringers before TEVC was performed. TEVC measurements were taken when oocytes were perfused with **(a-b)** Na100, or **(c)** K100. IV data is of one representative batch where n = 3 for water injected and n = 6-14 for cRNA injected.

References

Alberti, S., Gitler, A. D. and Lindquist, S. (2007). A suite of Gateway® cloning vectors for high-throughput genetic analysis in Saccharomyces cerevisiae. *Yeast* **24**, 913–919.

Anthony, T. L., Brooks, H. L., Boassa, D., Leonov, S., Yanochko, G. M., Regan, J. W. and Yool, A. J. (2000). Cloned human aquaporin-1 Is a cyclic GMP-gated ion channel. *Mol. Pharmacol.* **57**, 576–588.

Bienert, G. P., Moller, A. L. B., Kristiansen, K. A., Schulz, A., Moller, I. M., Schjoerring, J. K. and Jahn, T. P. (2007). Specific aquaporins facilitate the diffusion of hydrogen peroxide across membranes. *J. Biol. Chem.* **282**, 1183–1192.

Boursiac, Y., Chen, S., Luu, D.-T. T., Sorieul, M., van den Dries, N. and Maurel, C. (2005). Early effects of salinity on water transport in Arabidopsis roots. Molecular and cellular features of aquaporin expression. *Plant Physiol.* **139**, 790–805.

Boursiac, Y., Boudet, J., Postaire, O., Luu, D.-T. T., Tournaire-Roux, C. and Maurel, C. (2008). Stimulus-induced downregulation of root water transport involves reactive oxygen species-activated cell signalling and plasma membrane intrinsic protein internalization. *Plant J.* **56**, 207–218.

Byrt, C. S., Zhao, M., Kourghi, M., Bose, J., Henderson, S. W., Qiu, J., Gilliham, M., Schultz, C., Schwarz, M., Ramesh, S. A., et al. (2017). Non-selective cation channel activity of aquaporin AtPIP2;1 regulated by Ca^{2+} and pH. *Plant Cell Environ.* **40**, 802–815.

Campbell, E. M., Birdsell, D. N. and Yool, A. J. (2012). The activity of human aquaporin 1 as a cGMP-gated cation channel is regulated by tyrosine phosphorylation in the carboxyl-terminal domain. *Mol. Pharmacol.* **81**, 97–105.

Chaumont, F. and Tyerman, S. D. (2014). Aquaporins: Highly regulated channels controlling plant water relations. *Plant Physiol.* **164**, 1600–1618.

Conti, M., Hsieh, M., Musa Zamah, A. and Oh, J. S. (2012). Novel signaling mechanisms in the ovary during oocyte maturation and ovulation. *Mol. Cell. Endocrinol.* **356**, 65–73.

Demidchik, V. and Tester, M. (2002). Sodium fluxes through nonselective cation channels in the plasma membrane of protoplasts from Arabidopsis roots. *Plant Physiol*. **128**, 379–387.

di Pietro, M., Vialaret, J., Li, G.-W., Hem, S., Prado, K., Rossignol, M., Maurel, C. and Santoni, V. (2013). Coordinated post-translational responses of aquaporins to abiotic and nutritional stimuli in Arabidopsis roots. *Mol. Cell. Proteomics* **12**, 3886–3897.

Donaldson, L., Ludidi, N., Knight, M. R., Gehring, C. and Denby, K. (2004). Salt and osmotic stress cause rapid increases in *Arabidopsis thaliana* cGMP levels. *FEBS Lett.* **569**, 317–320.

Dynowski, M., Schaaf, G., Loque, D., Moran, O. and Ludewig, U. (2008a). Plant plasma membrane water channels conduct the signalling molecule H_2O_2. *Biochem. J.* **414**, 53–61.

Dynowski, M., Mayer, M., Moran, O. and Ludewig, U. (2008b). Molecular determinants of ammonia and urea conductance in plant aquaporin homologs. *Febs Lett*. **582**, 2458–2462.

Essah, P. A., Davenport, R. and Tester, M. (2003). Sodium influx and accumulation in Arabidopsis. *Plant Physiol*. **133**, 307–318.

E**to, K., Noda, Y., Horikawa, S., Uchida, S. and Sasaki, S.** (2010). Phosphorylation of aquaporin-2 regulates its water permeability. *J. Biol. Chem*. **285**, 40777–40784.

Fenton, R. A., Moeller, H. B., Hoffert, J. D., Yu, M.-J., Nielsen, S. and Knepper, M. A. (2008). Acute regulation of aquaporin-2 phosphorylation at Ser-264 by vasopressin. *Proc. Natl. Acad. Sci.* **105**, 3134–3139.

Fischer, G., Kosinska-Eriksson, U., Aponte-Santamaría, C., Palmgren, M., Geijer, C., Hedfalk, K., Hohmann, S., De Groot, B. L., Neutze, R. and Lindkvist-Petersson, K. (2009). Crystal structure of a yeast aquaporin at 1.15 Å reveals a novel gating mechanism. *PLoS Biol*. **7**,.

Gambetta, G. A., Knipfer, T., Fricke, W. and McElrone, A. J. (2017). Aquaporins and root water uptake. In *Plant Aquaporins*, pp. 133–153. Springer.

Gerbeau, P., Guclu, J., Ripoche, P. and Maurel, C. (1999). Aquaporin Nt-TIPα can account for the high permeability of tobacco cell vacuolar membrane to small neutral solutes. *Plant J*. **18**, 577–587.

Glass, D. and Krebs, E. (1980). Protein phosphorylation catalyzed by cyclic AMP-dependent and cyclic GMP-dependent protein kinases. *Annu. Rev. Pharmacol. Toxicol*. **20**, 363–388.

Grondin, A., Rodrigues, O., Verdoucq, L., Merlot, S., Leonhardt, N. and Maurel, C. (2015). Aquaporins contribute to ABA-triggered stomatal closure through OST1-mediated phosphorylation. *Plant Cell* **27**, 1945–1954.

Guenther, J. F., Chanmanivone, N., Galetovic, M. P., Wallace, I. S., Cobb, J. A. and Roberts, D. M. (2003). Phosphorylation of soybean nodulin 26 on serine 262 enhances water permeability and is regulated developmentally and by osmotic signals. *Plant Cell* **15**, 981–991.

Gunnarson, E., Axehult, G., Baturina, G., Zelenin, S., Zelenina, M. and Aperia, A. (2005). Lead induces increased water permeability in astrocytes expressing aquaporin 4. *Neuroscience* **136**, 105–114.

Han, Z. and Patil, R. V. (2000). Protein kinase A-dependent phosphorylation of aquaporin-1. *Biochem. Biophys. Res. Commun*. **273**, 328–332.

Hoffert, J. D., Pisitkun, T., Wang, G., Shen, R.-F. and Knepper, M. A. (2006). Quantitative phosphoproteomics of vasopressin-sensitive renal cells: Regulation of aquaporin-2 phosphorylation at two sites. *Proc. Natl. Acad. Sci*. **103**, 7159–7164.

Hoffert, J. D., Fenton, R. A., Moeller, H. B., Simons, B., Tchapyjnikov, D., McDill, B. W., Yu, M. J., Pisitkun, T., Chen, F. and Knepper, M. A. (2008). Vasopressin-stimulated increase in phosphorylation at Ser269 potentiates plasma membrane retention of aquaporin-2. J. *Biol. Chem*. **283**, 24617–24627.

Hooijmaijers, C., Rhee, J. Y., Kwak, K. J., Chung, G. C., Horie, T., Katsuhara, M. and Kang, H. (2012). Hydrogen peroxide permeability of plasma membrane aquaporins of *Arabidopsis thaliana*. *J. Plant Res*. **125**, 147–153.

Horie, T., Kaneko, T., Sugimoto, G., Sasano, S., Panda, S. K., Shibasaka, M. and Katsuhara, M. (2011). Mechanisms of water transport mediated by PIP aquaporins

and their regulation via phosphorylation events under salinity stress in Barley roots. *Plant Cell Physiol*. **52**, 663–675.

Isayenkov, S. V. and Maathuis, F. J. M. (2019). Plant salinity stress: Many unanswered questions remain. *Front. Plant Sci*. **10**,.

Jang, H. Y., Rhee, J., Carlson, J. E. and Ahn, S. J. (2014). The Camelina aquaporin CsPIP2;1 is regulated by phosphorylation at Ser273, but not at Ser277, of the C-terminus and is involved in salt- and drought-stress responses. *J. Plant Physiol*. **171**, 1401–1412.

Johansson, I., Karlsson, M., Shukla, V. K., Chrispeels, M. J., Larsson, C. and Kjellbom, P. (1998). Water transport activity of the plasma membrane aquaporin PM28A is regulated by phosphorylation. *Plant Cell* **10**, 451–459.

Kourghi, M., Nourmohammadi, S., Pei, J., Qiu, J., McGaughey, S., Tyerman, S., Byrt, C. and Yool, A. (2017). Divalent cations regulate the ion conductance properties of diverse classes of aquaporins. *Int. J. Mol. Sci*. **18.**

Kuwahara, M., Fushimi, K., Terada, Y., Liqun, B., Marumo, F. and Sasaki, S. (1995). cAMP-dependent phosphorylation stimulates water permeability of aquaporin-collecting duct water channel protein expressed in *Xenopus* oocytes. J. *Biol. Chem.* **270**, 10384–10387.

Lee, J. W., Zhang, Y., Weaver, C. D., Shomer, N. H., Louis, C. F. and Roberts, D. M. (1995). Phosphorylation of Nodulin 26 on Serine 262 affects its voltage-sensitive channel activity in planar lipid bilayers. *J. Biol. Chem*. **270**, 27051–27057.

Li, R. Y., Ago, Y., Liu, W. J., Mitani, N., Feldmann, J., McGrath, S. P., Ma, J. F. and Zhao, F. J. (2009). The rice aquaporin Lsi1 mediates uptake of methylated arsenic species. *Plant Physiol*. **150**, 2071–2080.

Li, X., Wang, X., Yang, Y., Li, R., He, Q., Fang, X., Luu, D.-T., Maurel, C. and Lin, J. (2011). Single-molecule analysis of PIP2;1 dynamics and partitioning reveals multiple modes of Arabidopsis plasma membrane aquaporin regulation. *Plant Cell* **23**, 3780–3797.

Loqué, D., Ludewig, U., Yuan, L. and von Wirén, N. (2005). Tonoplast intrinsic proteins AtTIP2;1 and AtTIP2;3 facilitate NH_3 transport into the vacuole. *Plant Physiol*. **137**, 671–680.

Lu, H. J., Matsuzaki, T., Bouley, R., Hasler, U., Qin, Q. H. and Brown, D. (2008). The phosphorylation state of serine 256 is dominant over that of serine 261 in the regulation of AQP2 trafficking in renal epithelial cells. *Am J Physiol Ren. Physiol* **295**.

Luu, D. T., Martiniãre, A., Sorieul, M., Runions, J., Maurel, C., Martiniere, A., Sorieul, M., Runions, J. and Maurel, C. (2012). Fluorescence recovery after photobleaching reveals high cycling dynamics of plasma membrane aquaporins in Arabidopsis roots under salt stress. *Plant J.* **69**, 894–905.

Ma, J. F., Tamai, K., Yamaji, N., Mitani, N., Konishi, S., Katsuhara, M., Ishiguro, M., Murata, Y. and Yano, M. (2006). A silicon transporter in rice. *Nature* **440**, 688–691.

Maathuis, F. J. and Sanders, D. (2001). Sodium uptake in Arabidopsis roots is regulated by cyclic nucleotides. *Plant Physiol*. **127**, 1617–25.

Maurel, C., Kado, R. T., Guern, J. and Chrispeels, M. J. (1995). Phosphorylation regulates the water channel activity of the seed-specific aquaporin alpha-TIP. *Embo J*. **14**, 3028–3035.

Maurel, C., Boursiac, Y., Luu, D. D.-T. T., Santoni, V., Shahzad, Z. and Verdoucq, L. (2015). Aquaporins in plants. *Physiol. Rev*. **95**, 1321–1358.

McGaughey, S. A., Qiu, J., Tyerman, S. D. and Byrt, C. S. (2018). Regulating root aquaporin function in response to changes in salinity. *Annu. Plant Rev*. **1**, 1–36.

Metzger, M. B., Maurer, M. J., Dancy, B. M. and Michaelis, S. (2008). Degradation of a cytosolic protein requires endoplasmic reticulum-associated degradation machinery. *J. Biol. Chem*. **283**, 32302–32316.

Moeller, H. B., Praetorius, J., Rutzler, M. R. and Fenton, R. A. (2010). Phosphorylation of aquaporin-2 regulates its endocytosis and protein-protein interactions. *Proc. Natl. Acad. Sci*. **107**, 424–429.

Munns, R., Day, D. A., Fricke, W., Watt, M., Arsova, B., Barkla, B. J., Bose, J., Byrt, C. S., Chen, Z., Foster, K. J., et al. (2019). Energy costs of salt tolerance in crop plants. *New Phytol*.

Nyblom, M., Frick, A., Wang, Y., Ekvall, M., Hallgren, K., Hedfalk, K., Neutze, R., Tajkhorshid, E. and Törnroth-Horsefield, S. (2009). Structural and functional analysis of SoPIP2;1 mutants adds insight into plant aquaporin gating. *J. Mol. Biol.* **387**, 653–668.

Prado, K. and Maurel, C. (2013). Regulation of leaf hydraulics: from molecular to whole plant levels. *Front. Plant Sci*. **4**.

Prado, K., Cotelle, V., Li, G., Bellati, J., Tang, N., Tournaire-Roux, C., Martiniere, A., Santoni, V., Maurel, C., Martiniere, A., et al. (2019). Oscillating aquaporin phosphorylations and 14-3-3 proteins mediate circadian regulation of leaf hydraulics. *Plant Cell* **4**, tpc.00804.2018.

Prak, S., Hem, S., Boudet, J., Viennois, G., Sommerer, N., Rossignol, M., Maurel, C. and Santoni, V. (2008). Multiple phosphorylations in the C-terminal tail of plant plasma membrane aquaporins. *Mol. Cell. Proteomics* **7**, 1019–1030.

Qing, D., Yang, Z., Li, M., Wong, W. S., Guo, G., Liu, S., Guo, H. and Li, N. (2016). Quantitative and functional phosphoproteomic analysis reveals that ethylene regulates water transport via the C-Terminal phosphorylation of aquaporin PIP2;1 in Arabidopsis. *Mol. Plant* **9**, 158–174.

Qiu, J., Henderson, S. W., Tester, M., Roy, S. J. and Gilliham, M. (2016). SLAH1, a homologue of the slow type anion channel SLAC1, modulates shoot Cl- accumulation and salt tolerance in *Arabidopsis thaliana*. *J. Exp. Bot*. **67**, 4495–4505.

Roberts, S. K. and Tester, M. (1997). A patch clamp study of Na^+ transport in maize roots. *J. Exp. Bot.* **48**, 431–440.

Rodrigues, O., Reshetnyak, G., Grondin, A., Saijo, Y., Leonhardt, N., Maurel, C. and Verdoucq, L. (2017). Aquaporins facilitate hydrogen peroxide entry into guard cells to mediate ABA- and pathogen-triggered stomatal closure. *Proc. Natl. Acad. Sci.* **114**, 9200–9205.

Rubio, F., Flores, P., Navarro, J. M. and Martínez, V. (2003). Effects of Ca^{2+}, K^+ and cGMP on Na^+ uptake in pepper plants. *Plant Sci.* **165**, 1043–1049.

Rubio, F., Alemán, F., Nieves-Cordones, M. and Martínez, V. (2010). Studies on Arabidopsis athak5, atakt1 double mutants disclose the range of concentrations at which AtHAK5, AtAKT1 and unknown systems mediate K^+ uptake. *Physiol. Plant.* **139**, 220–228.

Takano, J., Wada, M., Ludewig, U., Schaaf, G., Von Wirén, N. and Fujiwara, T. (2006). The Arabidopsis major intrinsic protein NIP5;1 is essential for efficient boron uptake and plant development under boron limitation. *Plant Cell* **18**, 1498–1509.

Tanghe, A., Van Dijck, P., Dumortier, F., Teunissen, A., Hohmann, S. and Thevelein, J. M. (2002). Aquaporin expression correlates with freeze tolerance in baker's yeast, and overexpression improves freeze tolerance in industrial strains. *Appl. Environ. Microbiol*. **68**, 5981–5989.

Törnroth-Horsefield, S., Wang, Y., Hedfalk, K., Johanson, U., Karlsson, M., Tajkhorshid, E., Neutze, R. and Kjellbom, P. (2006). Structural mechanism of plant aquaporin gating. *Nature* **439**, 688–694.

Tournaire-Roux, C., Sutka, M., Javot, H. H., Gout, E. E., Gerbeau, P., Luu, D.-T. T., Bligny, R. and Maurel, C. (2002). Cytosolic pH regulates root water transport during anoxic stress through gating of aquaporins. *Nature* **425**, 187–194.

Ueda, M., Tsutsumi, N. and Fujimoto, M. (2016). Salt stress induces internalization of plasma membrane aquaporin into the vacuole in *Arabidopsis thaliana*. *Biochem. Biophys. Res. Commun.* **474**, 742–746.

Uehlein, N., Lovisolo, C., Siefritz, F. and Kaldenhoff, R. (2003). The tobacco aquaporin NtAQP1 is a membrane CO_2 pore with physiological functions. *Nature* **425**, 734–737.

Van Balkom, B. W. M., Savelkoul, P. J. M., Markovich, D., Hofman, E., Nielsen, S., Van Der Sluijs, P. and Deen, P. M. T. (2002). The role of putative phosphorylation sites in the targeting and shuttling of the aquaporin-2 water channel. *J. Biol. Chem.* **277**, 41473–41479.

Van Wilder, V. V. V., Miecielica, U., Degand, H. H. H., Derua, R., Waelkens, E. and Chaumont, F. F. (2008). Maize plasma membrane aquaporins belonging to the PIP1 and PIP2 subgroups are in vivo phosphorylated. *Plant Cell Physiol*. **49**, 1364–1377.

Weaver, C. D., Shomer, N. H., Louis, C. F. and Roberts, D. M. (1994). Nodulin 26, a nodule-specific symbiosome membrane protein from Soybean, is an ion channel. *J. Biol. Chem.* **269**, 17858–17862.

Yaneff, A., Sigaut, L., Gómez, N., Aliaga Fandiño, C., Alleva, K., Pietrasanta, L. I. and Amodeo, G. (2016). Loop B serine of a plasma membrane aquaporin type PIP2 but not PIP1 plays a key role in pH sensing. *Biochim. Biophys. Acta - Biomembr*. **1858**, 2778–2787.

Yanochko, G. M. and Yool, A. J. (2002). Regulated cationic channel function in *Xenopus* oocytes expressing *Drosophila* Big Brain. *J. Neurosci*. **22**, 2530–2540.

Yool, A. J., Stamer, W. D. and Regan, J. W. (1996). Forskolin stimulation of water and cation permeability in aquaporin1 water channels. *Science*. **273**, 1216–1218.

Zelenina, M., Zelenin, S., Bondar, A. A., Brismar, H. and Aperia, A. (2002). Water permeability of aquaporin-4 is decreased by protein kinase C and dopamine. *Am. J. Physiol. Physiol.* **283**, F309–F318.

Zhang, W., Zitron, E., Hö, M., Kihm, L., Morath, C., Scherer, D., Hegge, S., Thomas, D., Schmitt, C. P., Zeier, M., et al. (2007). Aquaporin-1 channel function is positively regulated by protein kinase C. *J. Biol. Chem*. **282**, 20933–20940.

Zwiazek, J. J., Xu, H., Tan, X., Navarro-Ródenas, A., Morte, A., Benga, G., Popescu, O., Pop, V. I., Holmes, R., Agre, P., et al. (2017). Significance of oxygen transport through aquaporins. *Sci. Rep*. **7**.

Chapter 4: Phosphorylation sites in the cytosolic loops and potential kinases involved in the regulation of cation transport through AtPIP2;1

4.1 Introduction

Protein phosphorylation is a key post-translational modification (PTM) that influences plant aquaporin function. For example, to date more than 70 influential phosphorylation sites have been identified across plant aquaporin sub-families and plant species (Santoni, 2017). There are likely somewhere in the order of 10-15 phosphorylation sites on PIP proteins based on experimental data (for review see Santoni, 2017). In addition to the C-terminal S280 and S283 sites described previously in this thesis (see Chapter 3), serine residues located on the cytoplasmic facing N-terminal and loops B and D of PIP proteins may also be differentially phosphorylated to regulate PIP function.

Phosphorylation of conserved serine residues in loop B and D of PIP proteins, corresponding to S121 and S194 sites within AtPIP2;1, respectively, have been previously reported (Chapter 1.2, Figure 4; located in published review in appendix 9.1). The phosphorylation of the loop B residue S121 has been described in a number of studies (Azad *et al.,* 2008; Johansson *et al.,* 1998; Temmei *et al.,* 2005; Van Wilder *et al.,* 2008) and has been implicated in the gating mechanism for PIP mediated water transport (Grondin *et al.,* 2015; Johansson *et al.,* 1998; Yaneff *et al.,* 2016) and in ABA-dependent stomatal closure (Grondin *et al.,* 2015; Rodrigues *et al.,* 2017). The significance of the phosphorylated loop D residue was identified for the maize aquaporin ZmPIP2;1 (Van Wilder *et al.,* 2008). ZmPIP2;1 S203 (corresponding to AtPIP2;1 S194) was found to be phosphorylated *in vivo* and a phospho-deficient mutant ZmPIP2;1 S203A had reduced water permeability when expressed in *X. laevis* oocytes. Molecular dynamics simulations and computational modelling of PIP gating via phosphorylation of the loop B S121 and loop D S194 revealed that phosphorylation of these residues promotes an open monomeric channel state whereas dephosphorylation promotes a closed or gated conformation to reduce water permeation (Nyblom *et al.,* 2009; Tornroth-Horsefield *et al.,* 2006). However, the influence of phosphorylation of both S121 and S194 on PIP facilitated ion transport remains unknown.

The specific kinases, and their associated regulatory pathways, which control phosphorylation of PIP proteins *in planta* is increasingly becoming an area of interest in plant aquaporin research. Members from two plant kinase families involved in signal transduction in plant osmotic stress responses, SnRK2 and CDPKs, have been found to phosphorylate PIPs. SnRK2s, consisting of 10 members in Arabidopsis, are serine/threonine plant kinases that are involved in ABA-dependent plant development processes and abiotic stress responses (for review see: Kulik *et al.,* 2011). The Open stomata 1 (OST1), also called Snf1-related protein kinase 2.6 (Snrk2.6), is a protein kinase identified in ABA related guard cell signalling pathways and was found to phosphorylate AtPIP2;1 at S121 *in vitro* (Grondin *et al.,* 2015). Calcium-dependent protein kinases (CDPKs) are a plant protein kinase family containing a large number of isoforms with 34 CDPKs being identified in Arabidopsis (Asano *et al.,* 2012; Hamel *et al.,* 2014; Hrabak *et al.,* 2003). This multiplicity enables CDPKs to be involved in many crucial physiological processes from plant growth and development to responses to biotic and abiotic stress (Schulz *et al.,* 2013). CDPKs perceive alterations in cellular calcium (Ca^{2+}) levels and translate these signals into phosphorylation events to alter protein function and/or localisation or to initiate further signalling pathways (Schulz *et al.,* 2013). Ca^{2+}-dependent kinases were found to target PIP CTD phosphorylation sites in spinach and maize (Sjövall-Larsen *et al.,* 2006; Van Wilder *et al.,* 2008). The rice CDPK OsCPK17 was found to phosphorylate PIP2 protein *in vivo,* and this feature was suggested to be involved in cold tolerance mechanisms (Almadanim *et al.,* 2017).

Although many aspects of PIP regulation by phosphorylation, including phosphorylation sites and the upstream kinases involved in these regulatory pathways, remain to be determined it is clear that they are crucial to the regulation of PIP function. This chapter investigates the role of phosphorylation of two serine residues, S121 and S194, located on cytosolic facing loops B and D respectively in the regulation of AtPIP2;1 ion and water permeation. Phospho-mimic and deficient AtPIP2;1 S121 and S194 mutants were generated and tested in *X. laevis* oocytes. The effect of co-expression of selected plant protein kinases with AtPIP2;1 was also investigated. Co-expression of transporters with candidate kinases in the oocyte system is often used to determine whether the transporter is targeted by the kinase of interest and to study the effect of the kinase-mediated phosphorylation events on transporter function (for example: Corratgé-Faillie *et al.,* 2017; Geiger *et al.,* 2010; Sato *et al.,* 2010). Two plant CDPKs, CPK3 and CPK21, and OST1 were examined in relation to the influence of their co-expression with AtPIP2;1 in *X. laevis* oocytes.

4.2 Results

4.2.1 OST1 influences AtPIP2;1 ion channel function *in vivo*

Previous literature reported that AtPIP2;1 is phosphorylated *in vivo* by OST1 at the loop B residue S121 (Grondin *et al.*, 2015). Functional co-expression of AtPIP2;1 with OST1 in *X. laevis* oocytes was also reported to increase oocyte water permeability compared with those expressing AtPIP2;1 alone (Grondin *et al.*, 2015). To determine if OST1 influenced the ionic conductivity of AtPIP2;1, AtPIP2;1 and OST1 were co-expressed in the oocyte system and ionic conductance determined by TEVC. Photometric swelling assays were also performed to determine osmotic permeability.

As reported by Byrt *et al.*, (2017), and shown in the previous chapter (Chapter 3), AtPIP2;1 increased ionic conductance when expressed in *X. laevis* oocytes (Figure 4.1). However, when AtPIP2;1 was co-expressed with OST1 this ionic conductance was reduced; the currents of AtPIP2;1 + OST1 injected oocytes were not significantly different to water injected controls (Figure 4.1b).

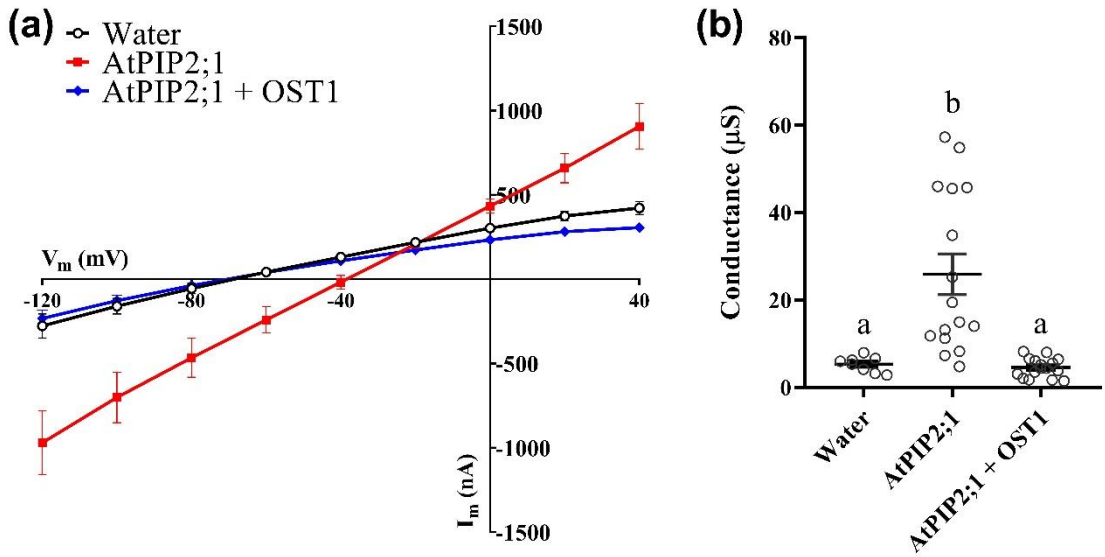

Figure 4.1: Ionic conductance of oocytes co-injected with plant kinase OST1 and AtPIP2;1. Oocytes were either injected with water, AtPIP2;l cRNA, or AtPIP2;1 and OST1 cRNA (1:2) and incubated for 24-30 h in Low Na^+ ringers solution. TEVC was performed in the Na100 solution. **(a)** IV curve of one representative oocyte batch. **(b)** Ionic conductance compiled from two independent oocyte batches where TEVC from one batch was performed in collaboration with Dr. Jiaen Qiu. Data points represent individual oocytes and data is presented as mean ± SEM. Significant differences ($p < 0.05$) are indicated by different letters using a one-way ANOVA, Fishers post-test.

Co-expression with OST1 also influenced osmotic permeability in AtPIP2;1 injected oocytes. Oocytes were acclimated in the isotonic swelling solution and transferred to the hypotonic swelling solution during photometric swelling assays. AtPIP2;1 expressed alone had greater osmotic permeability than that of water injected controls (Figure 4.2). AtPIP2;1 co-injected with OST1 had reduced osmotic permeability compared to AtPIP2;1 alone, but still significantly greater than that of water injected control oocytes (Figure 4.2).

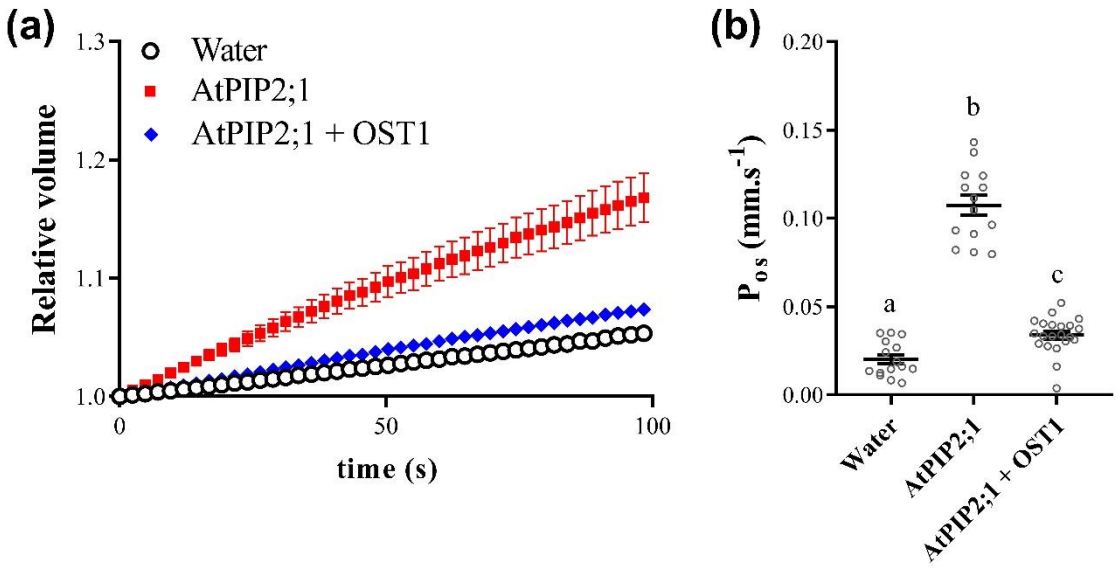

Figure 4.2: Co-expression of AtPIP2;1 with plant kinase OST1 influences AtPIP2;1 osmotic permeability. Oocytes were injected with water or AtPIP2;1 cRNA or AtPIP2;1 and OST1 cRNA and incubated in Low Na^+ Ringers solution for 24-30 h. Oocytes were pre-incubated in the isotonic swelling solution for approximately 1 h before being transferred to the hypotonic swelling solution for the assay **(a)** Relative changes in oocyte volume over 100 s. Data from one representative oocyte batch **(b)** Osmotic permeability (P_{os}) of oocytes injected with water, AtPIP2;1 cRNA or AtPIP2;1 and OST1 cRNA. Data is from two independent oocyte batches and is shown as mean ± SEM where each data point represents an individual oocyte. Different letters indicate statistical significance ($p < 0.05$) by one-way ANOVA, Fishers post-test.

The OST1 consensus motif has been identified as R-X-X-S/T (Shinozawa *et al.*, 2019). This consensus motif is found on AtPIP2;1 (Appendix 9.4: Figure S2) where the S121 site in loop B is proposed to be phosphorylated by OST1 (Grondin *et al.*, 2015). Furthermore, this consensus motif in loop B is conserved across all Arabidopsis PIP proteins, with the exception of AtPIP2;6 where the arginine (R) is a serine (S) (Appendix 9.4: Figure S2). AtPIP2;2, a close homolog to AtPIP2;1 with 92% protein sequence similarity, is also a dual water and ion permeable aquaporin (Kourghi *et al.*, 2017). AtPIP2;2 was co-expressed with OST1 in *X. laevis* oocytes to investigate whether OST1 would have a similar effect on AtPIP2;2 mediated water and ionic conductance. When expressed alone in oocytes AtPIP2;2 increased ionic conductance and when co-expressed with OST1 conductance was reduced as seen for AtPIP2;1 (Figure 4.3). This indicates that OST1 is influencing the ion channel function of both AtPIP2;1 and AtPIP2;2 through the same mechanism.

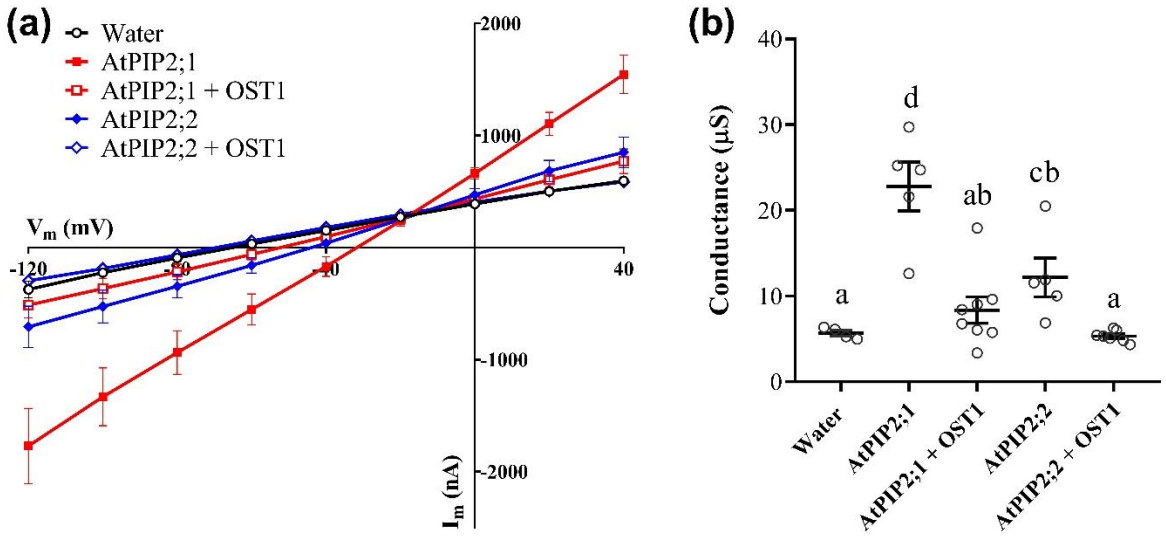

Figure 4.3: Ionic conductance of oocytes co-injected with AtPIP2;2 and OST1. Oocytes were injected with water or AtPIP2;1, AtPIP2;2 cRNA or co-injected (1:2) with AtPIP2;1 and OST1 or AtPIP2;2 and OST1 cRNA. Oocytes incubated in Ringers solution for 24-30 h and TEVC was performed in Na50 **(a)** IV curve **(b)** Ionic conductance of water and gene injected oocytes. TEVC was performed in collaboration with Dr. Jiaen Qiu. Each data point represents an individual oocyte. Data is shown as mean ± SEM. Different letters indicates statistical significance ($p < 0.05$) by one-way ANOVA, Fishers post-test.

4.2.2 Cytoplasmic loop B residue S121 influences AtPIP2;1 channel function

The phosphorylation state of the loop B residue S121 (or equivalent sites) has been implicated in the gating of the monomeric pore of plant aquaporins through interactions with other cytosolic facing loops and the N- and C-termini (Tornroth-Horsefield *et al.,* 2006). Specifically, phosphorylation of S121 is proposed to promote an open state of the monomeric pore allowing water permeation, while unphosphorylated S121 stabilises a closed state preventing water permeation. A previous study reported that an AtPIP2;1 S121 dephosphorylation mutant (S121A) did not have altered water permeability (Grondin *et al.,* 2015). To investigate whether the phosphorylation state of S121 may influence ionic conductance through AtPIP2;1, phospho-mimic (AtPIP2;1 S121D) and phospho-deficient (AtPIP2;1 S121A) versions were expressed in *X. laevis* oocytes and TEVC was performed. The effect of these mutations on AtPIP2;1 water permeability was also tested by photometric swelling assays.

When expressed in *X. laevis* oocytes, both AtPIP2;1 S121A and AtPIP2;1 S121D had significantly higher ionic conductance than the water injected controls but less than the wild-type AtPIP2;1 (Figure 4.4). There was no difference in ionic conductance observed between the S121A and S121D AtPIP2;1 mutants.

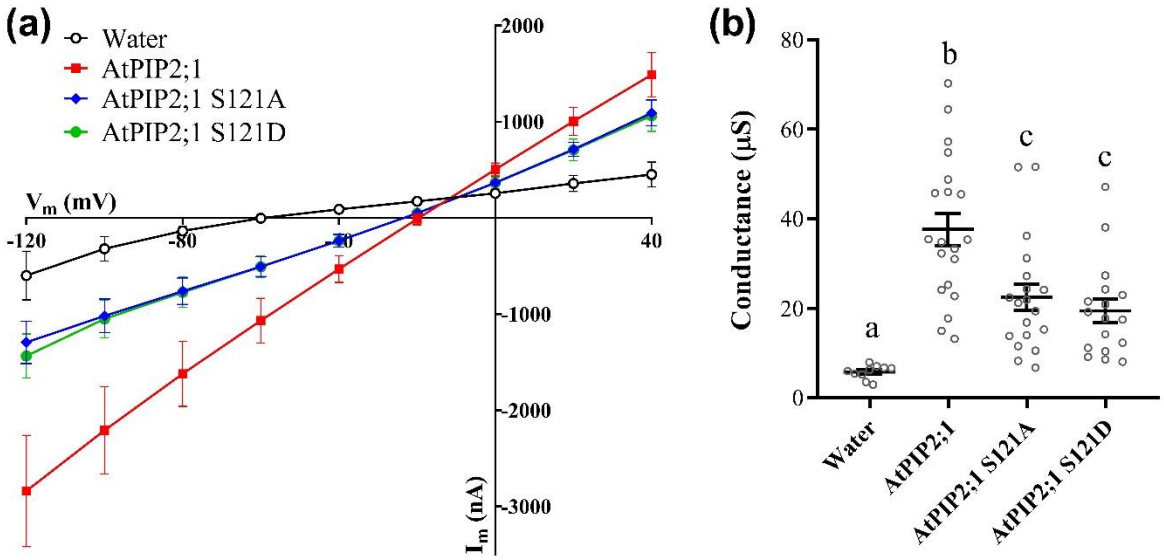

Figure 4.4: AtPIP2;1 S121 phospho-mimic and deficient mutants decrease ionic conductance. Oocytes were injected with either water or AtPIP2,1, AtPIP2;1 S121A or AtPIP2;1 S121D cRNA and incubated in Low Na^+ Ringers for 24-30 h. TEVC was performed in Na100. **(a)** IV curve of one representative oocyte batch **(b)** Ionic conductance of oocytes. Data is compiled from three independent oocyte batches where TEVC from one batch was performed in collaboration with Dr. Jiaen Qiu. Data is represented as mean ± SEM. Different letters indicate statistical significance ($p < 0.05$) by one-way ANOVA, Fishers post-test.

As with ionic conductance, the AtPIP2;1 S121 phospho-mimic (S121D) and deficient (S121A) mutants had altered osmotic permeability when expressed in *X. laevis* oocytes (Figure 4.5). AtPIP2;1 S121A and AtPIP2;1 S121D had significantly greater osmotic permeability than the water control oocytes but less than that of AtPIP2;1 (Figure 4.5). The osmotic permeability of the AtPIP2;1 S121 phospho-mutants were not different to each other.

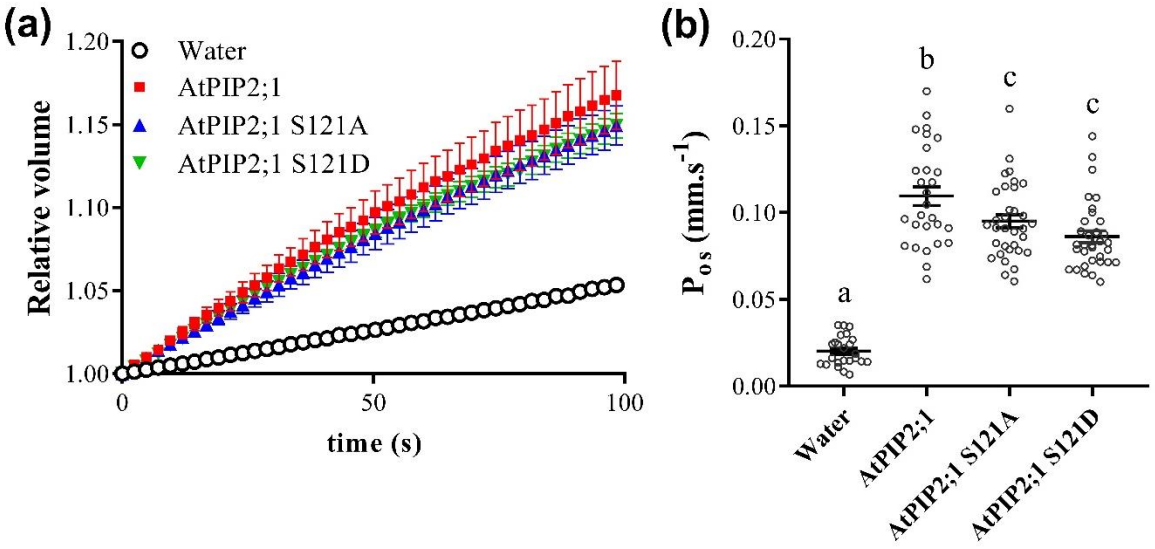

Figure 4.5: AtPIP2;1 S121 phosho-mimic and deficient mutants alter osmotic permeability. Oocytes were injected with either water or AtPIP2,1, AtPIP2;1 S121A or AtPIP2;1 S121D cRNA and incubated in Low Na^+ Ringers for 24-30 h. Oocytes were pre-incubated in the isotonic swelling solution for 1 h and then transferred to hypotonic swelling solution for the photometric swelling assay. **(a)** Relative volume increase over time of one representative oocyte batch. **(b)** Osmotic permeability (P_{os}) of injected oocytes. Data is compiled from two independent oocyte batches and represented as mean ± SEM. Different letters indicate statistical significance ($p < 0.05$) by one-way ANOVA, Fishers post-test.

To investigate whether OST1 was likely to be targeting the S121 site to influence ionic conductance in the same capacity as water permeability, OST1 was co-expressed with both AtPIP2;1 S121 phospho-mimic (AtPIP2;1 S121D) and phospho-deficient (AtPIP2;1 S121A) versions and TEVC was performed. Osmotic permeability was also assessed by photometric swelling assay. Co-expression with OST1 did not influence the ionic conductance or osmotic permeability of either of the AtPIP2;1 S121 phospho-mutants (Figure 4.6). While the AtPIP2;1 S121A and AtPIP2;1 S121D phospho-mutants had reduced ionic conductance (Figure 4.4) and osmotic permeability (Figure 4.5) compared with AtPIP2;1, there was no significant difference in water or ion transport when AtPIP2;1 S121A and S121D were expressed alone or when co-expressed with OST1 respectively (Figure 4.6). This is in stark contrast to the large reduction in ionic conductance and osmotic permeability when AtPIP2;1 was co-expressed with OST1 indicating that OST1 may be acting on AtPIP2;1 at the S121 residue.

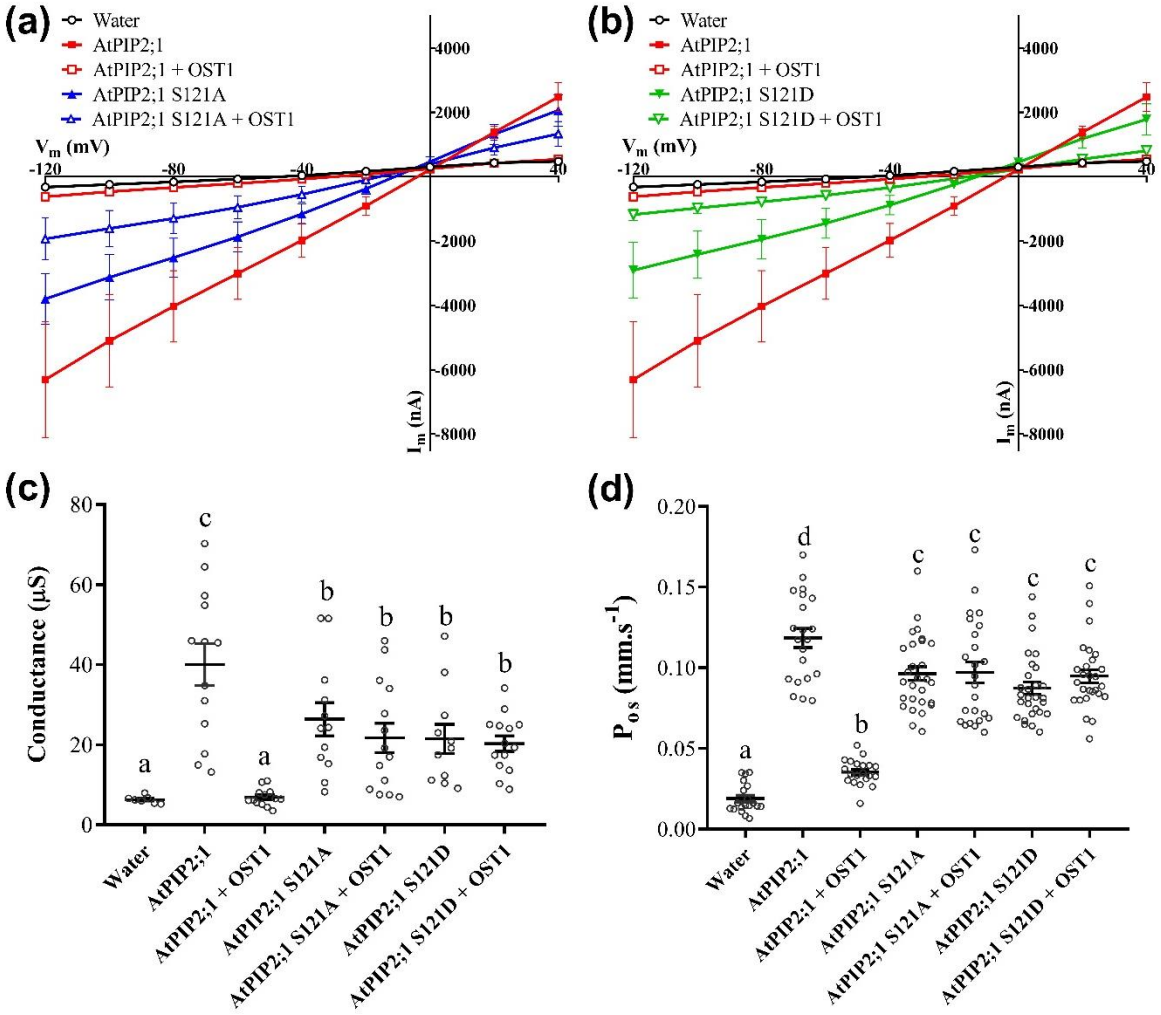

Figure 4.6: Co-expression with OST1 does not influence ionic conductance or osmotic permeability of AtPIP2;1 S121 phospho-mimic and deficient mutants. Oocytes were injected with water or AtPIP2;1, AtPIP2;1 S121A or AtPIP2;1 S121D cRNA or co-injected with OST1 cRNA (1:2). Oocytes were incubated in a Low Na^+ ringers for 24-30 h. TEVC was performed in Na100. **(a)** IV curves of oocytes from one representative batch expressing AtPIP2;1 or AtPIP2;1 S121A alone or co-expressed with OST1 **(b)** IV curves of oocytes from one representative batch expressing AtPIP2;1 or AtPIP2;1 S121A alone or co-expressed with OST1 **(c)** Ionic conductance of AtPIP2;1 S121 mutants co-expressed with OST1. Data is compiled from two independent oocyte batches where TEVC from 1 batch was performed in collaboration with Dr. Jiaen Qiu. Each data point represents an individual oocyte. Data from one batch graphed here has been shown previously in Figure 4.1 and Figure 4.4 respectively. **(d)** Osmotic permeability (P_{os}) of oocytes AtPIP2;1 S121 mutants co-expressed with OST1. Data is compiled from three independent oocytes batches where each data point represents individual oocytes. Data from one batch graphed here has been shown previously in Figure 4.2 and Figure 4.5 respectively. For panels (c) and (d) data is shown as mean ± SEM. Different letters indicate statistical significance ($p < 0.05$) by one-way ANOVA, Fishers post-test.

4.2.3 Cytoplasmic loop D residue S194 influences AtPIP2;1 channel function

The phosphorylation of the residue S194 located on the cytoplasmic loop D has been proposed to be involved in PIP channel gating by molecular modelling and by single-point mutagenesis studies (Nyblom *et al.,* 2009). Similar to the gating mechanism involving the phosphorylation of S121, phosphorylation of S194 may promote an open state of the monomeric pore allowing water permeation, while unphosphorylated S194 stabilises a closed state of the monomeric pore preventing water permeation. To investigate the role of phosphorylation of the loop D residue S194 in plant aquaporin pore gating, phosphorylation mutants of AtPIP2;1 S194 were generated: two phospho-mimic mutants (S194E and S194D) and a phospho-deficient mutant (S194A). As with other phosphorylation mutants examined in this thesis, the effects of these mutations on ionic conductance and osmotic permeability were investigated by TEVC and photometric swelling assays respectively.

Both the phospho-mimic mutants, AtPIP2;1 S194D and AtPIP2;1 S194E, had ionic conductance similar to that of AtPIP2;1 WT (Figure 4.7a, b). The phospho-deficient mutant AtPIP2;1 S194A had significantly greater ionic conductance compared to either AtPIP2;1 WT or either of the phospho-mimic mutants (Figure 4.7a, b). As was observed for AtPIP2;1 C-terminal mutants which elicit large currents (see Chapter 3), the osmotic permeability of AtPIP2;1 S194A was lower than that of AtPIP2;1 WT and the phospho-mimic mutants AtPIP2;1 S194E and AtPIP2;1 S194D but still greater than water injected controls (Figure 4.7c,d). The osmotic permeability of the phospho-mimic mutants AtPIP2;1 S194E and S194D did not differ from AtPIP2;1 WT or each other (Figure 4.7c, d).

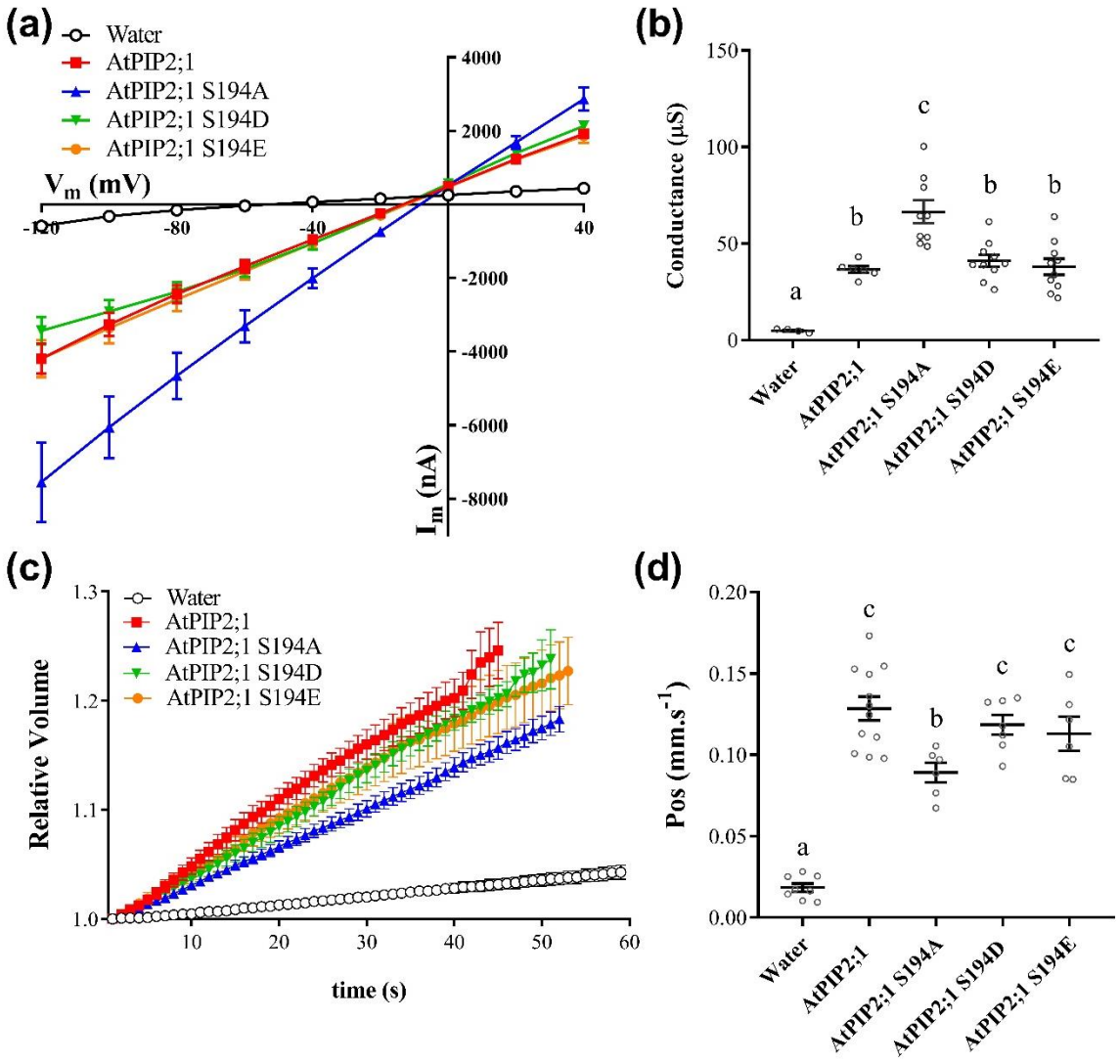

Figure 4.7: AtPIP2;1 S194 phospho-mimic and deficient mutants influence ionic conductance. Oocytes were injected with either water or AtPIP2,1, AtPIP2;1 S194A, AtPIP2;1 S194E or AtPIP2;1 S194D cRNA and incubated in Low Na^+ Ringers for 24-30 h. (a)-(b) TEVC was performed in Na100 (c)-(d) Oocytes were pre-incubated the isotonic swelling solution for 1 h and then transferred to the hypotonic swelling solution for the photometric swelling assay. **(a)** IV curve of one representative oocyte batch **(b)** Ionic conductance of oocytes from one representative oocyte batch. **(c)** Relative volume increase over time of one representative oocyte batch. **(d)** Osmotic permeability (P_{os}) of injected oocytes from one representative batch. Data in (b) and (d) is shown as mean ± SEM where each data point represents an individual oocyte. Different letters indicate statistical significance ($p < 0.05$) by one-way ANOVA, Fishers post-test.

4.2.4 CDPKs influence AtPIP2;1 water and ion channel function

Calcium-dependent protein kinases (CDPKs) constitute a large protein family in plants that have roles in many different plant processes. The effect of two CDPKs, CPK3 and CPK21, on AtPIP2;1 facilitated ion and water transport were investigated by their co-expression in *X. laevis* oocytes.

Co-expression of AtPIP2;1 with CPK21 did not influence ionic conductance but completely abolished water permeability. Oocytes that co-expressed AtPIP2;1 with CPK21 had greater ionic conductance than the water injected controls and were comparable to the ionic conductance of oocytes expressing AtPIP2;1 alone (Figure 4.8a, b). In contrast, oocytes with AtPIP2;1 co-expressed with CPK21 had no appreciable osmotic permeability with no significant difference between AtPIP2;1 + CPK21 and water injected control oocytes (Figure 4.8c).

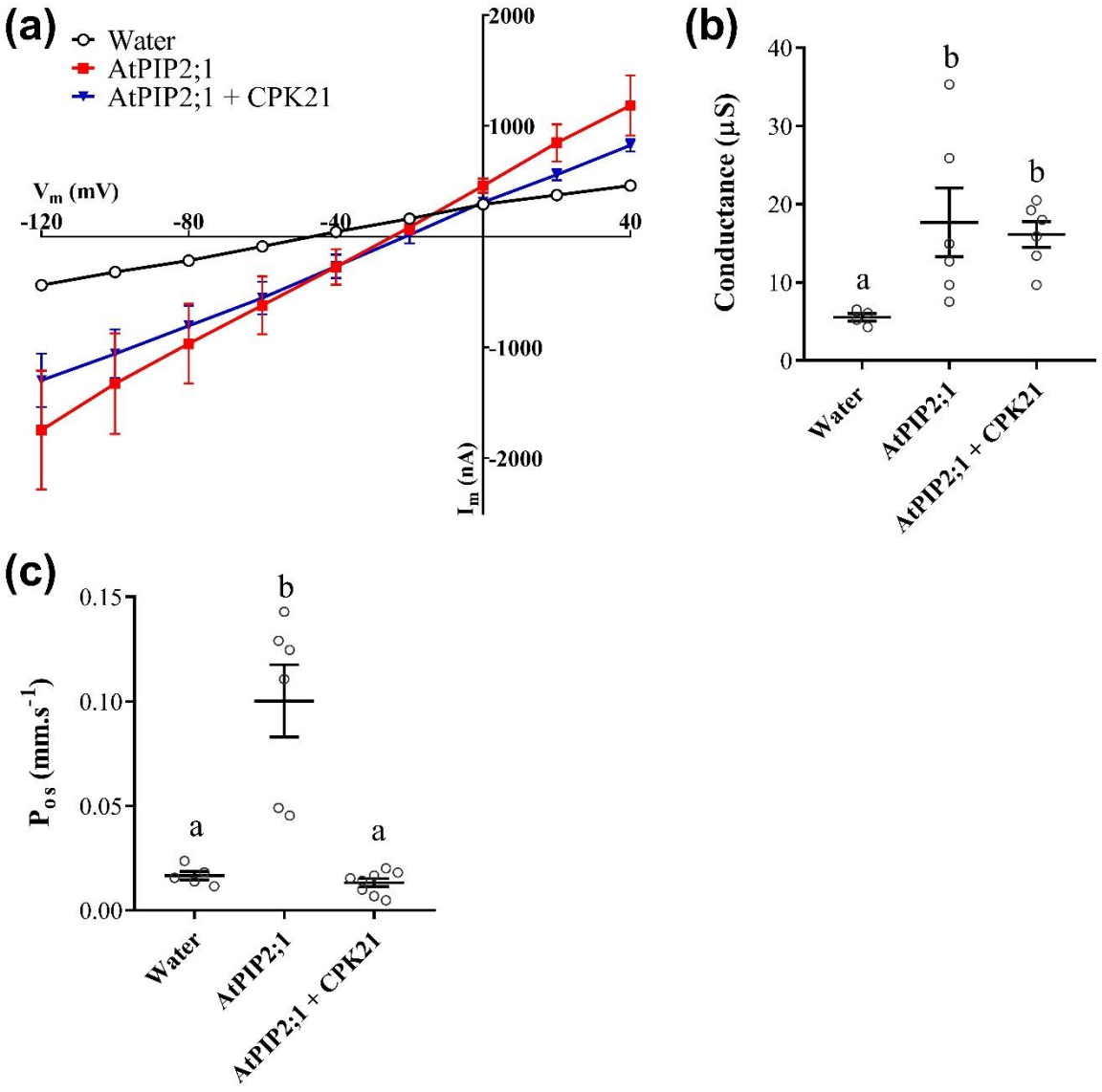

Figure 4.8: Co-expression of AtPIP2;1 with CPK21 influences AtPIP2;1 water and ion channel function. Oocytes were injected with water, AtPIP2;1 cRNA or AtPIP2;1 and CPK21 cRNA (1:2) and incubated in Low Na^+ Ringers for 24-30 h. **(a)** IV curve of water, AtPIP2;1, and AtPIP2;1 + CPK21 injected oocytes. TEVC was performed in Na100. Data is from one representative batch. **(b)** Conductance of injected oocytes. **(c)** Osmotic permeability (P_{os}) of injected oocytes. Data in (b) and (c) is shown as mean ± SEM where each data point represents an individual oocyte. Different letters indicate statistical significance ($p < 0.05$) by one-way ANOVA, Fishers post-test.

Co-expression of AtPIP2;1 with the CDPK CPK3 in oocytes abolished both ionic conductance and water permeability. When co-expressed with CPK3 the ionic conductance of AtPIP2;1 expressing oocytes is comparable to that of water injected controls, where AtPIP2;1 expressed alone is significantly higher than both control oocytes and AtPIP2;1 + CPK3 oocytes (Figure 4.9b). The osmotic permeability of oocytes co-expressing AtPIP2;1 and CPK3 was similarly reduced; oocytes that had AtPIP2;1 co-expressed with CPK3 had no appreciable osmotic permeability (Figure 4.9c).

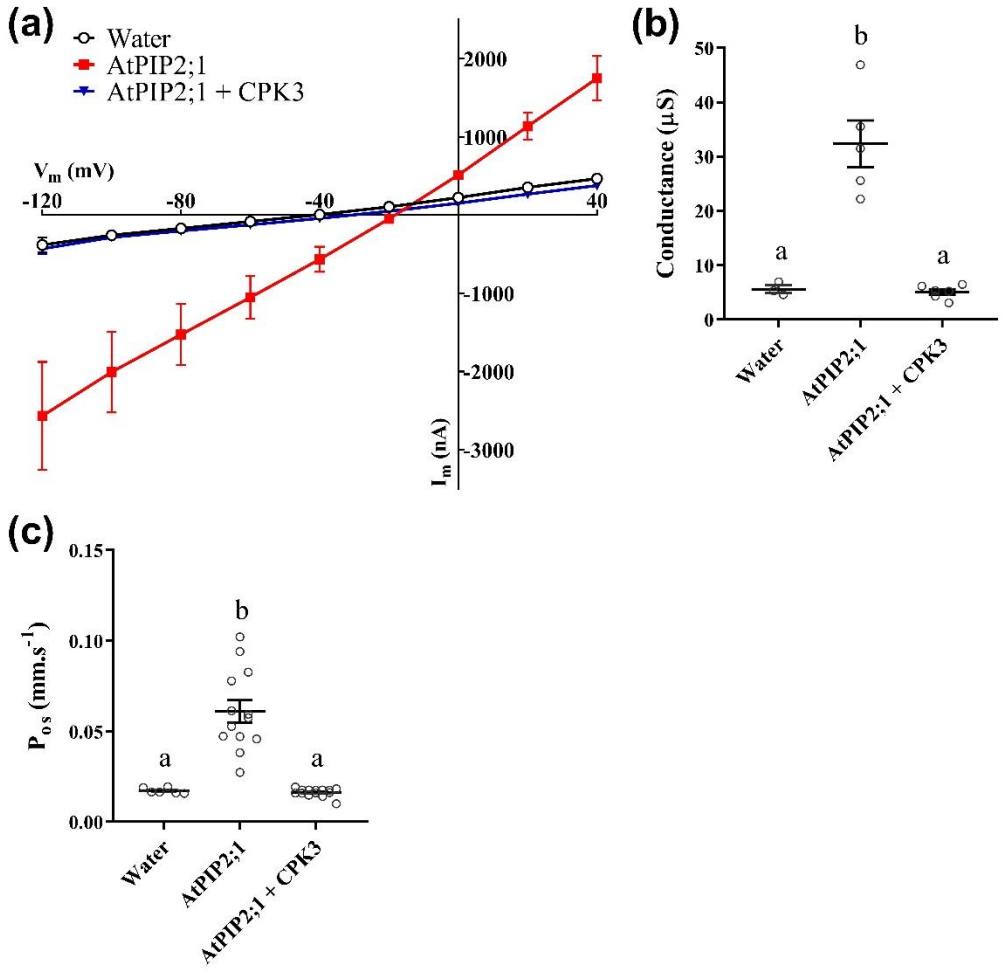

Figure 4.9 Co-expression of AtPIP2;1 with CPK3 abolishes both ionic conductance and water permeability through AtPIP2;1. Oocytes were injected with water, AtPIP2;1 cRNA or AtPIP2;1 and CPK3 cRNA (1:2) and incubated in Low Na^+ Ringers for 24-30 h. **(a)** IV curve of water, AtPIP2;1, and AtPIP2;1 + CPK3 injected oocytes. TEVC was performed in Na100. Data is from one representative batch. TEVC was performed in collaboration with Dr. Jiaen Qiu. **(b)** Conductance of injected oocytes. **(c)** Osmotic permeability (P_{os}) of injected oocytes. Data in (b) and (c) is shown as mean ± SEM where each data point represents an individual oocyte. Different letters indicate statistical significance ($p < 0.05$) by one-way ANOVA, Fishers post-test.

The minimal consensus motif for CDPK phosphorylation has been identified as R/K-X-X-S/T or R/X-K-X-S-X-X-R where X denotes any residue (Cheng *et al.*, 2002). Analysis of the AtPIP2;1 protein sequence found that two such CDPK consensus sequences are present (Figure 4.10). Both motifs are located on cytoplasmic facing aspects of the AtPIP2;1 protein where serine is the proposed phosphorylated residue; the first is located on the N-termini (S36) and the second on loop B (S121).

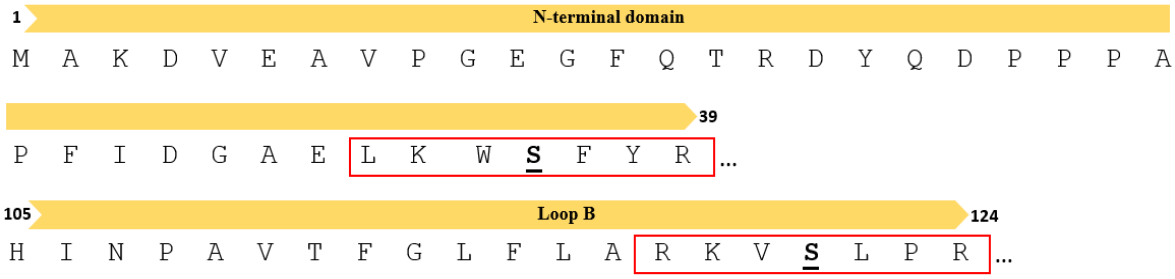

Figure 4.10: Possible CDPK consensus sites identified on cytosolic aspects of AtPIP2;1. The AtPIP2;1 protein sequence was analysed for the presence of possible CDPK consensus motifs (highlighted in red boxes) and may overlap with OST1 consensus sites. Two motifs on the cytosolic facing aspects of the protein were identified; one in the N-terminal domain and loop B where **S36** and **S121** are the phosphorylatable residues respectively. Ellipses indicates intervening sequence. There is another possible CDPK consensus site in the extracellular loop A where S66 would be the phosphorylated residue.

4.3 Discussion

The phosphorylation status of S121 and S194, located on the cytoplasmic facing loop B and loop D respectively, can influence AtPIP2;1 water and ion transport. Furthermore, co-expression of candidate plant kinases with the water-ion aquaporin AtPIP2;1 had profound effects on its water and ion channel function. The influence of these kinases on the combination of aquaporin facilitated water and ion conductances may have important implications for osmotic and ionic regulation *in planta*. In some cases in this chapter both the phospho-mimic and phospho-deficient mutants have water or ion channel activity different from the WT. Additionally, there are some instances where the phospho-mimic and phospho-deficient mutants do not have water or ion channel activity different to each other. Phosphomimic mutants do not always adequately simulate phosphoserine, which has a different charge and geometry compared to acidic amino acid side chains and, independent of phosphorylation, serine may have structural properties that are distinct from alanine, aspartic acid and glutamtic acid that could influence protein structure and activity. It should also be noted that PIP proteins may have in the order of 10-15 phosphorylation sites (Santoni, 2017) and the permutations of or relationships between these putative phosphorylation sites and their potential effects on function are mostly unknown.

4.3.1 Role of OST1 and phosphorylation of loop B S121 in gating of ion channel function

The plant kinase OST1 influences both the water and ion channel function of AtPIP2;1 *in vivo*. When OST1 was co-expressed with wild-type AtPIP2;1 in *X. laevis* oocytes, the AtPIP2;1 mediated water permeability and ionic conductance were significantly reduced (Figure 4.1 and 4.2). However, when co-expressed with either AtPIP2;1 S121 phospho-mimic or phospho-deficient single point mutants, OST1 did not have any affect (Figure 4.6).

The mechanism through which OST1 influences AtPIP2;1 activity was reported previously to be by phosphorylation of the loop B S121 residue (Grondin *et al.,* 2015). In the same study the co-expression of AtPIP2;1 with OST1 in *X. laevis* oocytes increased its osmotic permeability compared to AtPIP2;1 expressed alone. With a similar cRNA injection ratio between AtPIP2;1 and OST1 as described in Grondin *et al.,* (2015), co-expression with OST1 in *X. laevis* oocytes reduced both water permeability and ionic conductance mediated

by AtPIP2;1 (Figure 4.1 and 4.2). The decrease in AtPIP2;1 water channel function by co-expression with OST1 described in this chapter is different to the increase previously published (Grondin *et al.,* 2015). Both AtPIP2;1 S121A and S121D mutants had reduced osmotic permeability and ionic conductance when compared to wild-type AtPIP2;1 and were insensitive to co-expression with OST1 (Figure 4.4 - 4.6). In Grondin *et al.,* (2015), AtPIP2;1 S121A phospho-deficient mutant similarly had lower osmotic permeability than the wild-type AtPIP2;1 and was insensitive to OST1 co-expression. Furthermore, several studies have reported a reduction or total abolishment of water permeability for PIP2 S121A (or equivalent site) mutants (Amezcua-Romero *et al.,* 2010; Fischer and Kaldenhoff, 2008; Jang *et al.,* 2014; Johansson *et al.,* 1998; Van Wilder *et al.,* 2008). However, most studies do not include loop B phospho-mimic mutants with the exception of Van Wilder *et al.,* (2008) who observed reduction of osmotic permeability of oocytes expressing ZmPIP2;1 S126E and ZmPIP2;1 S126A. Localisation of YFP-tagged Strawberry (*Fragaria* × *ananassa*) PIP2;1 S121A using the line-scan confocal microscopy method at the oocyte cell edge found that FaPIP2;1 S121A was less effectively trafficked to the PM compared to the wild-type FaPIP2;1 (Yaneff *et al.,* 2016). Reduced PM localisation was also observed for GFP-tagged ZmPIP2;1 S126A and S126E (Van Wilder *et al.,* 2008). This suggests that while S121 is indeed likely the site of OST1 mediated phosphorylation, the influence of S121 phosphorylation on AtPIP2;1 water channel function may be associated with issues in protein-protein interaction with plasma-membrane trafficking chaperones, rather than by direct influence on protein structure (Yaneff *et al.,* 2016).

Phosphorylation of AtPIP2;1 by OST1 has been suggested to be involved in ABA-dependent stomatal closure (Grondin *et al.,* 2015). OST1 is known to be involved in the ABA signalling pathway that triggers stomatal closure by the rapid release of ions (predominately K^+ and anions) from guard cells in the osmotic stress response (for reviews see: Kim *et al.,* 2010; Roux and Leonhardt, 2018). Once OST1 is activated in the ABA signalling pathway it, in turn, activates by phosphorylation the guard cell anion channels SLAC1, SLAH1 and SLAH3 that mediate rapid ion efflux (Brandt *et al.,* 2012; Geiger *et al.,* 2011; Lee *et al.,* 2009). The phosphorylation of AtPIP2;1 by OST1 is proposed to be part of ABA-dependent stomatal regulation (Grondin *et al.,* 2015; Rodrigues *et al.,* 2017). AtPIP2;1 knock-out mutant plants had defects in their ABA-triggered stomatal closure response which were linked to ABA-dependent effects on guard cell osmotic permeability (did not increase with ABA treatment compared with Col-0) and ROS accumulation (did not accumulate in stomata with ABA treatment compared with Col-0) (Grondin *et al.,* 2015). AtPIP2;1 knock-out

mutant plants complemented with AtPIP2;1 S121A displayed the same defects in ABA-triggered stomatal closure to *pip2;1* plants whereas those complemented with AtPIP2;1 S121D had restored ABA-dependent stomatal closure responses (Grondin *et al.*, 2015).

AtPIP2;1 has been shown to facilitate H_2O_2 transport and it has been suggested that AtPIP2;1 mediates H_2O_2 movement in guard cell signalling and stomatal closure (Rodrigues *et al.*, 2017). The same complementation lines used in Grondin *et al.*, (2015) exhibited differences in guard cell H_2O_2 accumulation (Rodrigues *et al.*, 2017). Stomata of AtPIP2;1 S121A plants had lower H_2O_2 accumulation similar to that of Arabidopsis *pip2;1* plants whereas AtPIP2;1 S121D plants had higher H_2O_2 accumulation similar to that of Col-0 (Rodrigues *et al.*, 2017). The H_2O_2 sensitivity of ZmPIP2;5 expressing yeast was abolished for the ZmPIP2;5 S121A although its PM localisation was not altered (Bienert *et al.*, 2014). Interestingly, the H_2O_2 sensitivity of HvPIP2;5 expressing yeast was abolished by both S126A and S126D mutations (where S126 is the S121 equivalent site) but only the HvPIP2;5 S126D had reduced water permeability when expressed in oocytes (Rhee *et al.*, 2017). Although these studies indicate phosphorylation is important to PIP roles in H_2O_2 transport and signalling, further work is needed to dissect the possible relationship between water, ion and H_2O_2 transport. A recent paper investigating the influence of 14-3-3 protein interaction on AtPIP2;1 function identified the phosphorylated S121 as a potential 14-3-3 binding site (Prado *et al.*, 2019). Therefore, the guard cell and stomata phenotypes as described for AtPIP2;1 S121 mutant lines could involve many other regulatory mechanisms and processes, including H_2O_2 or ion permeability, in addition to or other than direct influences on AtPIP2;1 water channel activity.

OST1 (also SnRK2.6) is a member of the SnRK2 protein kinase family. Phylogenetically the SnRK2 family has three classes; those in class 2 and 3, where OST1 is a member of class 2, are activated by ABA and phosphorylate Ser/Thr residues in the consensus motif R-X-X-S/T (Vlad *et al.*, 2008). All Arabidopsis PIPs, with the exception of AtPIP2;6, contain this consensus motif in their cytoplasmic facing loop B where S121 (or threonine in the case of AtPIP2;5) is the phosphorylatable residue (Appendix 9.4, Figure S2). When AtPIP2;2 was co-expressed with OST1 in *X. laevis* oocytes its ionic conductance was decreased compared with oocytes where AtPIP2;2 was expressed alone, similar to what was observed for AtPIP2;1 (Figure 4.3). It is likely that (i) other AtPIP proteins may be phosphorylated by OST1 and (ii) other SnRKs may phosphorylate AtPIP2;1 and other AtPIP proteins. In Arabidopsis and rice, 9 and 10 members, respectively, of the 10 member SnRK2 protein family were found to be activated by hyper-osmotic stress, from either mannitol or NaCl

treatments (Boudsocq *et al.,* 2004; Kobayashi *et al.,* 2004). This suggests that while the role of SnRK2s in stomatal function has been most intensively studied in response to osmotic stress, there are likely to be many other osmotic stress related processes that this kinase family is involved in throughout whole plants.

Furthermore, through sequence analysis of Arabidopsis PIPs, another SnRK consensus motif may exist on the N-terminal domain (Figure 4.10). However, the N-terminal domain was not included in *in vitro* tests investigating OST1 phosphorylation of AtPIP2;1 (Grondin *et al.,* 2015).

4.3.2 Role of phosphorylation of loop D S194 in gating of ion channel function

The phosphorylation state of AtPIP2;1 loop D residue S194 influences the gating of its water and ion channel function. Phospho-deficient and phospho-mimetic versions of AtPIP2;1 S194 were generated; a serine to alanine (S194A) to mimic a dephosphorylated state and a serine to aspartic acid (S194D) and serine to glutamic acid (S194E) to mimic a phosphorylated state. When expressed in *X. laevis* oocytes the AtPIP2;1 S194D and S194E mutants had osmotic water permeability and ionic conductance comparable to that of wild-type AtPIP2;1, whereas oocytes expressing AtPIP2;1 S194A had greater ionic conductance but lower osmotic permeability in comparison to AtPIP2;1 WT (Figure 4.7).

The movement of the cytosolic loop D and its interactions with other cytosolic facing residues (i.e. N-terminal and loop B) is proposed to be the primary mechanism responsible for gating of the aquaporin monomeric pore (Hedfalk *et al.,* 2006; Nyblom *et al.,* 2009; Törnroth-Horsefield *et al.,* 2006). From the resolved crystal structure of the spinach (*Spinacia oleracea*) PIP2;1 (SoPIP2;1), molecular dynamics simulation modelling has indicated that the position of the loop D determines whether the aquaporin pore is in an open or closed state (Törnroth-Horsefield *et al.,* 2006). In these simulations, a closed conformation loop D is linked to the N-terminal domain (NTD) and loop B through hydrogen bonds and ionic interactions (Törnroth-Horsefield *et al.,* 2006). These closed conformation interactions can be stabilised by divalent cation binding (Cd^{2+} in the solved crystal structure but suggested to be Ca^{2+} *in planta*) anchoring loop D to the NTD, and by protonation of loop D H199 (on AtPIP2;1). Meanwhile, phosphorylation of the SoPIP2;1 loop D residue S188 (equivalent to AtPIP2;1 S194) promotes channel opening by disruption of these bonds (Frick

et al., 2013; Nyblom *et al.,* 2009; Törnroth-Horsefield *et al.,* 2006). A phospho-deficient mutant of the loop D serine ZmPIP2;1 S203A had reduced water permeability when expressed in *X. laevis* oocytes (no perturbation in PM localisation efficiency was observed) (Van Wilder *et al.,* 2008), and a phospho-mimic mutant SoPIP2;1 S188E increased water permeability of liposomes (Nyblom *et al.,* 2009). Further molecular dynamics simulations revealed that phosphorylation of S188 in loop D aided interactions with the CTD and promoting an open confirmation of the monomeric pore (Nyblom *et al.,* 2009). AtPIP2;1 S194A similarly had reduced water permeability (Figure 4.7d), and also had increased ion permeability (Figure 4.7.c). Although the ion permeation pathway through ion permeable PIPs is still unknown the water and ion channel function of AtPIP2;1 loop D phosphorylation mutants expressed in *X. laevis* oocytes indicate that the S194 phosphorylation state could be involved in gating of ion channel function. If the monomeric pore becomes more ion conducting influenced by changes in phosphorylation state of some residues, this could exclude water permeation and account for the inverse relationship between water and ion permeation observed the AtPIP2;1 S194A and described in Chapter 3, Figure 3.

Loop D has been shown to influence the ion and water channel activity of several mammalian aquaporins (for review see: Nesverova and Törnroth-Horsefield, 2019). Gating of HsAQP1 ion channel activity is linked to loop D; two arginine residues in AQP1 are required for cGMP binding and subsequent ion channel activation (Campbell *et al.,* 2012; Yu *et al.,* 2006). The water channel function of AQP4 is influenced by the phosphorylation state of its loop D. Phosphorylation of AQP4 loop D residue S180 by protein kinase C decreases its water permeability (Zelenina *et al.,* 2002). The phosphorylation of AQP4 S180 is proposed to promote loop D interaction with the CTD to partially block the cytoplasmic monomeric pore entrance (Hiroaki *et al.,* 2006). Phosphorylation of AQP5 S156 increases its trafficking and PM localisation but the functional effects have not been probed (Kitchen *et al.,* 2015).

4.3.3 The calcium dependent protein kinases CPK21 and CPK3 regulate AtPIP2;1 function and are involved in abiotic stress pathways

The ion and water channel function of AtPIP2;1 were both strongly influenced *in vivo* by two Arabidopsis calcium-dependent protein kinase (CDPK) isoforms CPK3 and CPK21. Co-expression of CPK3 with AtPIP2;1 in *X. laevis* oocytes abolished both the water and ion

channel function of AtPIP2;1 (Figure 4.9), whereas the co-expression of CPK21 with AtPIP2;1 did not affect ion channel function but abolished water permeability (Figure 4.8). Calcium is an important second messenger in several signal transduction pathways in plants and a known regulator of plant aquaporin function where it binds directly to aquaporin monomers via interactions with the cytoplasmically facing NTD and loops B and D to physically block the monomeric pore (Törnroth-Horsefield *et al.,* 2006; Verdoucq *et al.,* 2008). Calcium may exert another level of regulation on aquaporin function through the activation of kinases like CDPKs to influence plant aquaporins by phosphorylation events. The first reported plant ion channel NOD-26 was also found to be phosphorylated by a CDPK (Weaver and Roberts, 1992). Phosphorylation of NOD-26 regulated its water and ion transport activity and was linked to osmotic signals (Guenther *et al.,* 2003; Lee *et al.,* 1995; Weaver *et al.,* 1994).

Both CPK3 and CPK21 are from the same CDPK phylogenetic group (Group II) and are involved in signal transduction in the ABA signalling pathway in response to osmotic stress (for review see: Asano *et al.,* 2012; Hamel *et al.,* 2014; Schulz *et al.,* 2013). CPK3 was reported to be constitutively active in both root and leaf tissue but had increased protein kinase activity after several stress treatments, including salt and H_2O_2 (Mehlmer *et al.,* 2010). Under salt stress treatments (150 mM NaCl) *Cpk3* mutants had decreased germination rates while the germination rate of CPK3 over-expressers was increased (Mehlmer *et al.,* 2010). *Cpk3* mutants also exhibit defects in stomatal closure, likely associated with impairments identified with the ABA and Ca^{2+}-dependent activation of slow-type anion channels and Ca^{2+} channels (Mori *et al.,* 2006). CPK3 has been reported to phosphorylate TPK1, a two pore K^+ channel, which enabled binding of a 14-3-3 protein and subsequent channel activation (Latz *et al.,* 2013). Several 14-3-3 proteins have recently been proposed to influence AtPIP2;1 water permeation (Prado *et al.,* 2019). The influence of CPK3 on AtPIP2;1 water and ion permeation (Figure 4.9) may be via direct protein structural changes resulting from phosphorylation events or via the recruitment of other proteins to influence PIP function. CPK21 has also been linked to ABA signalling and the osmotic stress response in plants. Arabidopsis seedlings with loss of function CPK21 had increased tolerance to hyperosmotic stress (300 mM Mannitol) but *cpk21* mutants had similar salt tolerance levels to wild-type plants (Franz *et al.,* 2011). Under osmotic stress, either from drought or salt, the transcript abundance of *CPK21* increased (Valmonte *et al.,* 2014). CPK21 regulates several plant ion channels by phosphorylation with those channels involved in stomatal function being the most well characterised. When CPK21 was co-expressed in *X. laevis* oocytes with

the guard cell anion channel SLAC1, CPK21 was reported to control SLAC1 channel activation independently of and in response to Ca^{2+} levels (Geiger *et al.*, 2010). CPK21 is associated with microdomains in the plant cell PM and has been shown to *in vivo* phosphorylate another anion channel involved in stomatal closure, SLAH3 (Demir *et al.*, 2013). AtPIP2;1 is also involved in stomatal closure as demonstrated by *pip2;1* Arabidopsis plants that exhibited stomatal closure defects (Grondin *et al.*, 2015). The ion channel function of AtPIP2;1, in addition to its regulation by CDPKs also known to regulate stomatal closure particularly as part of the osmotic stress response, put the role AtPIP2;1 may have in these processes in a new context that should be explored further.

Both CPK3 and CPK21 have been implicated in regulation of K^+ transport pathways in addition to the osmotic stress response (for recent review see: Chérel and Gaillard, 2019). For example CPK3 has been shown to regulate by phosphorylation many K^+ transporters in guard cells (Mori *et al.*, 2006) and the C-terminus of outwardly-rectifying K^+ channel GORK, involved in stomatal closure and K^+-homeostasis in Arabidopsis roots, is phosphorylated by CPK21 (van Kleeff *et al.*, 2018). In addition to Na^+ AtPIP2;1 was shown to facilitate K^+ transport in *X. laevis* oocytes (Chapter 3). Influence on AtPIP2;1 Na^+ transport function by co-expression with CPK3 and CPK21 (Figures 4.8 and 4.9) may similarly effect K^+ transport. In roots for instance, CPK3 may regulate AtPIP2;1 under salt stress to minimise water and K^+ efflux from cells, and limit Na^+ influx (Figure 4.11). CPK21 may be regulating AtPIP2;1 to increase its ion transport capacity and generate localised osmotic gradients to drive water uptake that might not otherwise occur (Figure 4.11).

Two CDPK consensus motifs were found to be present on the cytosolic facing N-termini and loop B in the AtPIP2;1 protein sequence (Figure 4.10). Serine would be the target residue for phosphorylation; the first located on the N-termini (S36) and the second on loop B (S121). Both S36 and S121 have been proposed to be involved in PIP gating; bonds formed with S36 and S121 help to stabilise loop D to occlude the monomeric pore (Frick *et al.*, 2013). The existence of two motifs suggest that it is possible that different CDPK isoforms could target different sites. This is further supported by the divergent effects of CPK3 and CPK21 co-expression with AtPIP2;1 on AtPIP2;1 water and ion permeation; co-expression with CPK3 abolished AtPIP2;1 mediated water permeability and ionic conductance (Figure 4.9), while co-expression with CPK21 abolished AtPIP2;1 water permeability but had no effect on ionic conductance (Figure 4.8). Considering that the known phosphorylation site of OST1 is S121, and that co-expression OST1 abolished both the water and ion channel function of AtPIP2;1 (Figure 4.1 and 4.2), CPK3 may similarly be targeting S121.

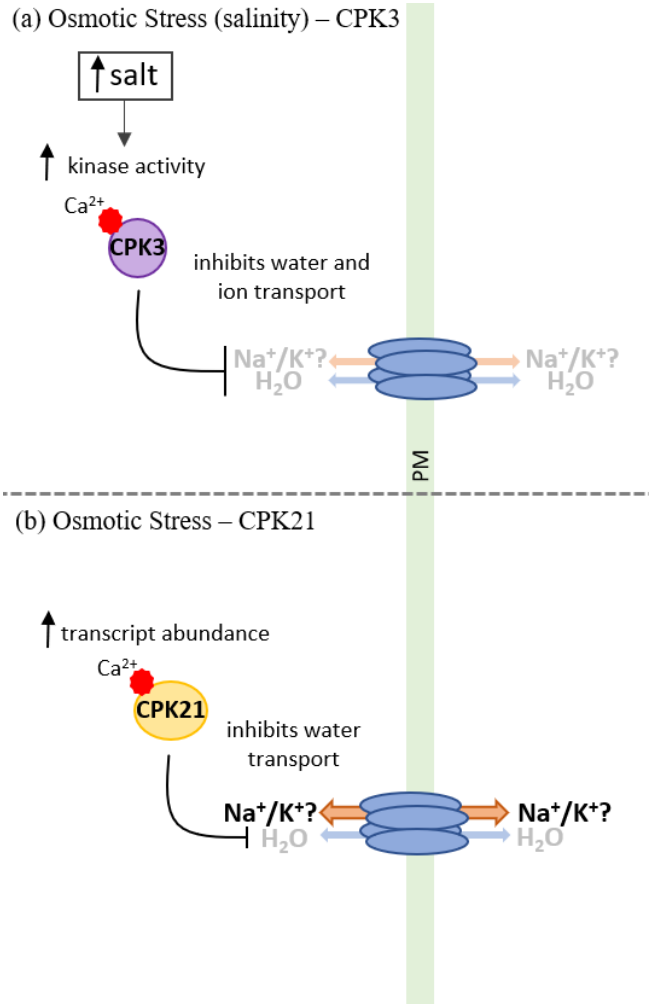

Figure 4.11: Potential regulation of AtPIP2;1 function by CPK3 and CPK21. (a) Under osmotic stress, specifically salinity, CPK3 kinase activity increased (Mehlmer *et al.*, 2010). Increased CPK3 activity may directly or indirectly regulate AtPIP2;1 function by inhibiting both water and ion transport. This could help reduce water loss and limit Na^+ influx in saline conditions. **(b)** Under osmotic stress, both drought and salt treatments, the transcript abundance of *CPK21* increased (Valmonte *et al.*, 2014). Greater transcript abundance and therefore possible protein abundance of CPK21 could regulate AtPIP2;1 function by inhibition of water transport only. AtPIP2;1 facilitated Na^+ transport could generate local Na^+ gradients to drive water influx possibly through another aquaporin isoform.

Chapter 5: Preliminary functional characterisation of cereal plasma membrane aquaporins

5.1 Introduction:

Setaria is a C_4 grass genus in the panicoideae clade and is closely related to many of the major grasses used globally for food, feed, and biofuel including maize, sugarcane, and sorghum. Both *Setaria italica* and *Setaria viridis* species are used as models for C_4 grasses, and they have many advantageous characteristics including small sequenced genomes (~515 Mb), rapid life-cycle, simple growth requirements and amenability to transformation (Bennetzen *et al.*, 2012; Li and Brutnell, 2011).

S. italica and *S. viridis* are both used as model genetic systems, particularly for investigating traits related to using grasses for biofuel production and for studying C_4 photosynthesis. These species differ in size, with *S. italica* at approx. 1 m tall and *S. viridis* around 30 cm, so the smaller *S. viridis* is particularly convenient to work with in the laboratory (Brutnell *et al.*, 2010; Doust *et al.*, 2009). The *Setaria* spp. have 41 aquaporin encoding genes (Azad *et al.*, 2016; McGaughey *et al.*, 2016; Figure 5.1) similar to the other grasses, such as rice, sorghum and maize, which have 33, 41 and 36 aquaporins identified in their genomes respectively (Chaumont *et al.*, 2001; Reddy *et al.*, 2015; Sakurai *et al.*, 2005). As a still emerging model there is limited information on *Setaria* aquaporins, particularly in comparison with the wealth of studies on aquaporins from Arabidopsis as the model dicot. Evolutionary divergence between dicots and monocots occurred between 140-170 million years ago (Bell *et al.*, 2010; Chaw *et al.*, 2004; Smith *et al.*, 2010), allowing time for aquaporin function and regulation in monocots to diverge from those in shared ancestors. Therefore, monocot aquaporin functional characteristics could be significantly different to the characteristics of the homologous dicot aquaporins (David *et al.*, 2019).

Aquaporins have key roles in many plant growth and development processes, but also in plant responses to abiotic stresses. In addition to salt and drought, aquaporins have been implicated as being involved in plant response to micronutrient deprivation and mineral toxicity (for reviews see: Bienert and Bienert, 2017; Sade and Moshelion, 2017). Currently, some plant aquaporin isoforms have been found to facilitate the transport of a range of neutral solutes (for example urea, glycerol, silicic acid and CO_2), including the signalling

molecule hydrogen peroxide (H_2O_2) and the micronutrient boric acid (Dynowski *et al.*, 2008a; Rodrigues *et al.*, 2017; Tanaka *et al.*, 2008).

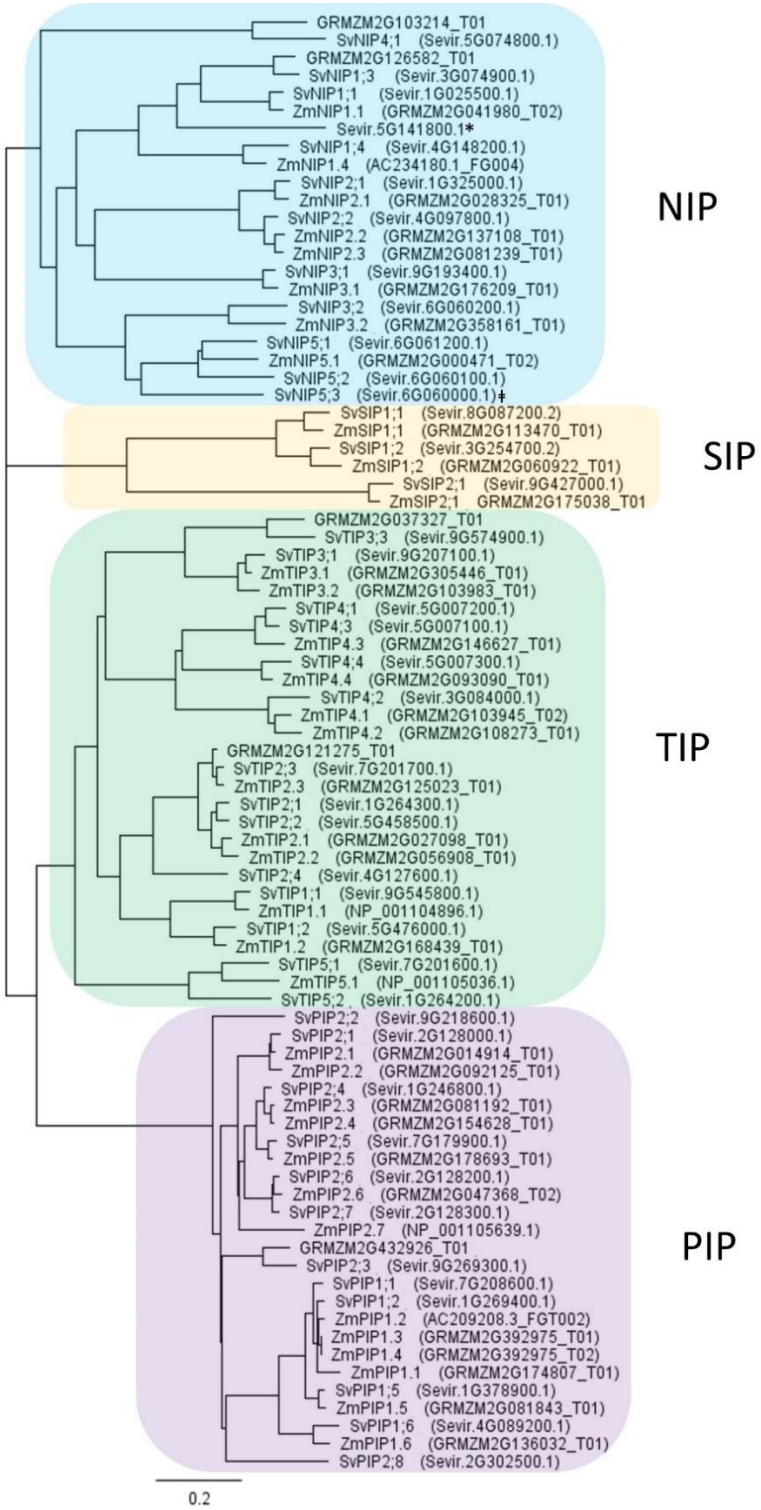

Figure 5.1: Phylogenetic analysis of *Setaria viridis* aquaporins. Protein sequences for putative *S. viridis* aquaporins were identified by a HMMER search using the protein sequences of aquaporins from Arabidopsis, barley (*Hordeum vulgare*), maize (*Zea mays*), and rice (*Oryza sativa*). A phylogenetic tree of *S. viridis* aquaporins was made using the protein sequences of *S. viridis* and maize aquaporins. Figure from McGaughey *et al.*, (2016).

Aquaporins from both plant and animal kingdoms have been found to facilitate H_2O_2 transport (for review see: Bienert and Chaumont, 2014). In plants, H_2O_2 is present at low concentrations (in the nanomolar range) and functions as both an intracellular and intercellular signalling molecule involved in many developmental and physiological processes including seed germination, cell death and senescence, stomatal movement, flowering, and root development (Barba-Espín *et al.,* 2011; Neill *et al.,* 2001; Petrov and Van Breusegem, 2012). H_2O_2 is also linked to plant response to abiotic stresses including drought and salinity (Bose *et al.,* 2014; Miller *et al.,* 2010; Noctor *et al.,* 2014) and to the regulation of aquaporins (Figure 5.2). Treatment of Arabidopsis roots with either H_2O_2 or salt (NaCl), resulted in the internalisation of AtPIP2;1 from the plasma membrane of root epidermal cells into small vesicular structures (Boursiac *et al.,* 2008) and increased the abundance of diphosphorylated AtPIP2;1 at the CTD sites S280 and S283 (Prak *et al.,* 2008). It was reported that the expression of Arabidopsis PIPs was differentially regulated in response to H_2O_2, drought and salt treatments, including those AtPIP isoforms found to be permeable to H_2O_2 (Hooijmaijers *et al.,* 2012; Jang *et al.,* 2004; Jang *et al.,* 2012), suggesting integration between aquaporin function and regulation, H_2O_2 signalling, and plant response to drought and salinity. Therefore, it is important to determine which monocot aquaporins mediate H_2O_2 transport towards understanding how aquaporin H_2O_2 transport could contribute to H_2O_2 signalling pathways and down-stream processes in cereal crops.

Boron, or boric acid as it primarily exists in soil, is an uncharged essential micronutrient required for plant growth and development particularly as a component of plant cell walls and in nucleic acid synthesis (O'Neill *et al.,* 2001; for review see also Camacho-cristóbal *et al.,* 2008). Both boron (B) deficient and B toxic soils limit plant growth and yield, and are widespread problems affecting soils worldwide (Nable *et al.,* 1997; Schnurbusch *et al.,* 2010a). In Australia, improvements to wheat yield (~14-16% yield advantage) have been achieved through use of B toxicity tolerant genotypes, and use of B-tolerant crops is being considered as an alternative to soil amelioration practices (Hrmova and Gilliham, 2018; McDonald *et al.,* 2012; Reid, 2010). Therefore, both B influx and efflux mechanisms in plants are of physiological importance. So far plant aquaporins from both the NIP, TIP and PIP sub-families have been shown to be involved in B transport processes where the altered expression of some isoforms has been shown to improve plant growth in both B limited and toxic conditions (Table 5.1).

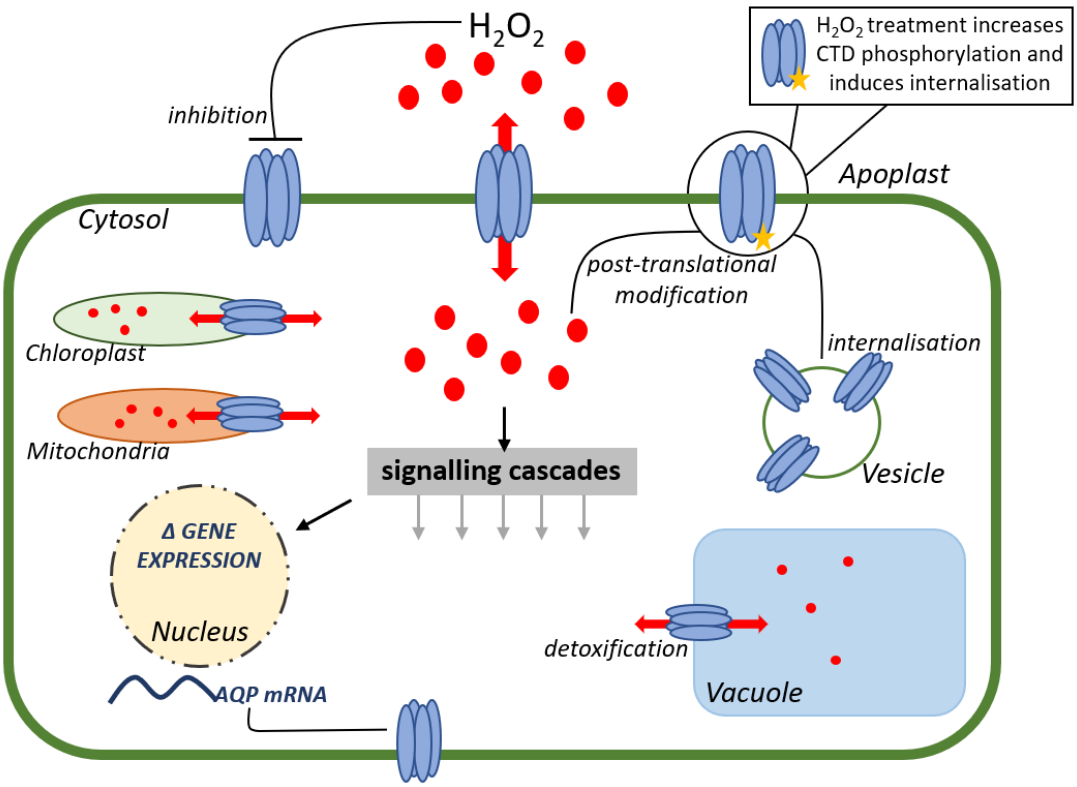

Figure 5.2: Overview of interaction and regulation of plant aquaporins by hydrogen peroxide (H_2O_2). H_2O_2 (red molecules) from the apoplast can be transported to the cytoplasm via aquaporins (shown in blue) where it is involved in various signalling pathways within the cell. H_2O_2 transport across many organelle membranes is suggested to be facilitated by aquaporins. H_2O_2 is also thought to be a regulator of aquaporin expression and has been demonstrated to alter aquaporin post-translation modifications (e.g. CTD phosphorylation) and trigger aquaporin internalisation from the PM into intracellular vesicles. Figure adapted from Bienert and Chaumont, (2014).

Given the wide range in physiological roles that aquaporins have been shown to be involved in, it is important to investigate their functional characteristics. However, there are many aquaporin isoforms yet to be functionally characterised. In this chapter, the permeability of SvPIPs to a range of solutes are investigated by their expression in the heterologous expression systems yeast (*Saccharomyces cerevisiae*) and *Xenopus laevis* oocytes. Permeability screens in yeast were performed for two neutral substrates of interest, H_2O_2 and boric acid (H_3BO_3). A freeze-thaw assay in yeast was also performed to compare the water permeability of the SvPIPs. SvPIP water permeability was also investigated in oocytes alongside permeability to the monovalent cation sodium (Na^+). In collaboration with Professors Maki Katsuhara and Keitaro Tanoi and Associate Professors Tomoaki Horie and Natsuko Kobayashi from Okayama University (M.K), Shinshu University (T.H) and

University of Tokyo (K.T and N.K), candidate PIPs from barley (*Hordeum vulgare*; HvPIPs) were also tested for ion transport function.

Table 5.1: Examples of aquaporin isoforms influencing plant growth in boron (B) toxic and deficient conditions. OE: over-expression; ↑: increase; Os: *Oryza sativa*; At: *Arabidopsis thaliana*.

Gene	Expression Type	Expression System	Boric Acid Treatment	Growth Effect	Ref
OsPIP1;3	OE	Arabidopsis	2.5 mM (B toxicity)	↑ tolerance to B toxicity	(Mosa *et al.*, 2016)
OsPIP2;6				↑ tolerance to B toxicity	
AtTIP5;1	OE	Arabidopsis	3 mM (B toxicity)	↑ tolerance to B toxicity	(Pang *et al.*, 2010)
AtNIP5;1	knock-down	Arabidopsis	3 µM (B deficiency)	↑ sensitivity to B deficiency	(Takano *et al.*, 2006)
AtNIP6;1	knock-down	Arabidopsis	0.1 µM (B deficiency)	↑ sensitivity to B deficiency	(Tanaka *et al.*, 2008)
OsPIP2;4	OE	Arabidopsis	2 mM (B toxicity)	↑ tolerance to B toxicity	(Kumar *et al.*, 2014)
OsPIP2;7					
OsNIP3;1	knock-down (RNAi)	Rice (*O.sativa*)	B deficient (hydroponics with no added B)	↑ sensitivity to B deficiency	(Hanaoka *et al.*, 2014)

5.2 Results:

5.2.1 Sequence similarity of *Setaria italica* and *Setaria viridis* PIPs

The two grass species of the same genus *Setaria italica* and *Setaria viridis* are close relatives and in evolutionary terms only very recently diverged (~8000 years; Bettinger *et al.*, 2010). Due to this recent divergence high sequence similarity between gene families in these species is expected. Both *Setaria* spp. are used as model organisms, and if aquaporin sequences are conserved, then functional characteristics determined for SiPIPs could reflect SvPIP function and *vice versa*. Protein sequence comparison of PIPs from *S. viridis* and *S. italica*

revealed that all, with the exception of PIP2;4, shared 100% protein sequence similarity (Figure 5.3). PIP2;4 in the two *Setaria* spp. has 99.3% similarity, with two amino acid differences. SvPIP2;4 has a Valine (V) and an Aspartic Acid (D) at positions 134 and 167 respectively whereas SiPIP2;4 has an Isoleucine (I) and an Alanine (A). For simplicity, the proteins will be referred to as SvPIPs throughout the remainder of this chapter although most functional data would also be applicable to SiPIPs.

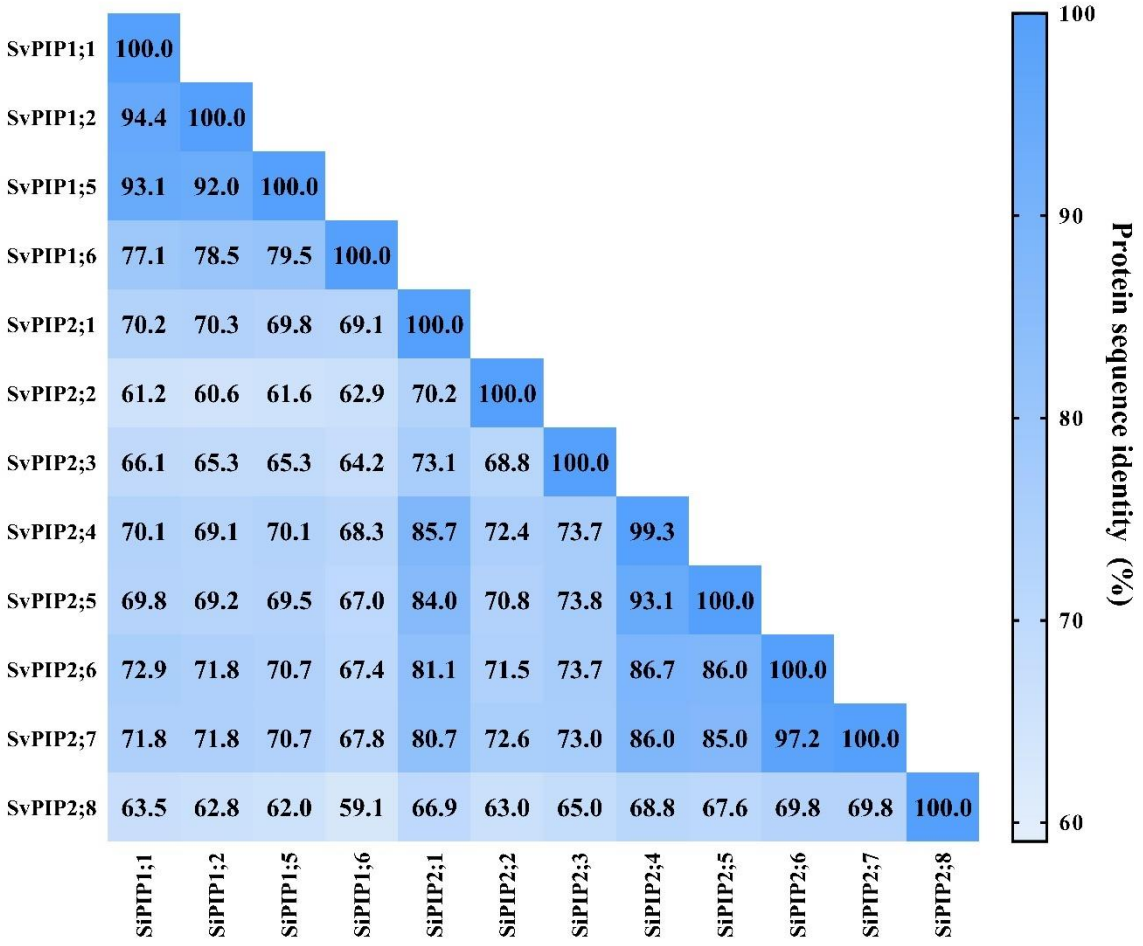

Figure 5.3: Percent identity matrix for *Setaria viridis* and *Setaria italica* PIP protein sequences. The amino acid sequence identity percentage is shown between the full-length protein sequences of *S. viridis* and *S. italica* PIPs. The *S. viridis* and *S. italica* protein sequences were obtained from Phytozome (https://phytozome.jgi.doe.gov; last accessed August 2019). Percent identity was calculated using the EMBL-EBI MUSCLE (3.8) online multiple sequence alignment tool (Madeira *et al.*, 2019). Sequence similarity is shown as a colour gradient where the darker blue is greater percent similarity. Accession numbers for *S. viridis* and *S. italica* PIPs are located in Appendix 9.3.

5.2.2 *Setaria viridis* PIP water permeability

SvPIP water permeability was investigated using yeast and *X. laevis* oocyte expression systems. In yeast, SvPIPs were expressed under a constitutive promoter in the double aquaporin knockout yeast strain, *aqy1/aqy2*. A freeze-thaw (FT) assay was performed to determine the osmotic tolerance of the SvPIP expressing yeast (Figure 5.4). Cycles of freeze (submersion in liquid nitrogen for 30 s) and thaw (submersion in 30ºC water bath for 20 min) causes rapid water flux across the yeast cell membrane. Yeast cells that have greater water permeability, for example via the expression of aquaporins with efficient water channel function, have an enhanced capacity to osmotically adjust and survive FT (Tanghe *et al.,* 2002; Tanghe *et al.,* 2004; Tanghe *et al.,* 2005). The *aqy1/aqy2* knockout strain is ideal for FT assays as it is extremely compromised in osmotic adjustment and has minimal (< 5%) FT survivorship (Figure 5.4; see empty vector control).

Yeast expressing the SvPIP1;2, 1;5, 1;6, 2;2 and 2;8 had very low FT survivorship similar to the empty vector control (Figure 5.4). SvPIP1;1, 2;1, 2;3, 2;5 and 2;6 all had higher FT survivorship than the empty vector control, implying higher water permeability, with SvPIP1;1 and the PIP2 sub-family isoforms having ~10% and > 40% FT survivorship, respectively (Figure 5.4).

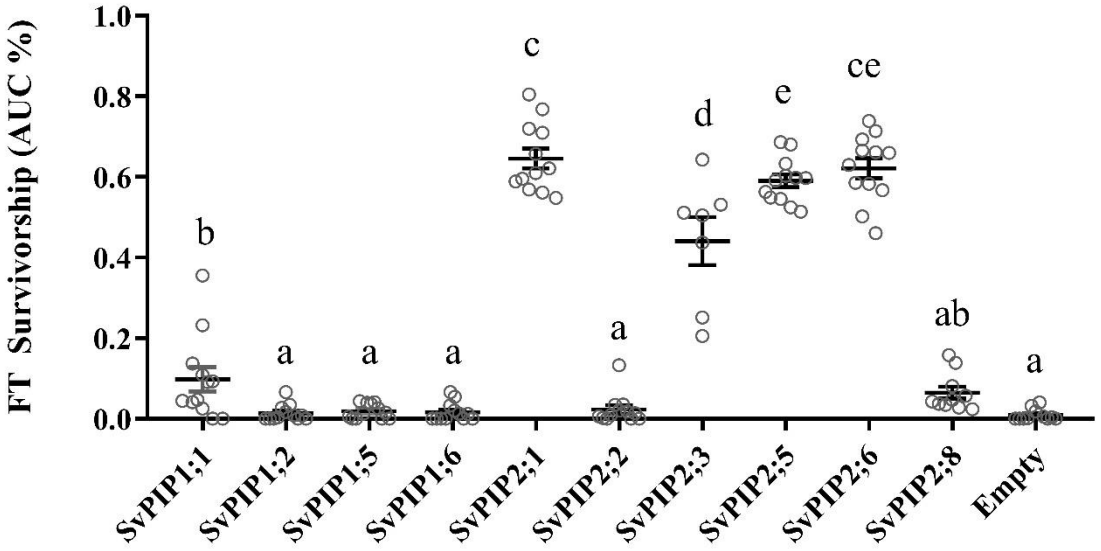

Figure 5.4: Freeze-thaw susceptibility of SvPIP expressing yeast. A freeze-thaw (FT) assay was performed to determine the osmotic tolerance of yeast expressing different SvPIP isoforms. Each yeast sample was subjected to three FT cycles. Each data point represents a biological replicate collected across three independent experimental replicates. Data is shown as mean ± SEM yeast cell survivorship (area under the curve (AUC) after three FT cycles relative to zero FT cycles). Statistical significance ($p < 0.05$) as indicated by different letters determined by one-way ANOVA (Fishers post-test).

Osmotic water permeability of the SvPIPs inferred from their expression in *X. laevis* oocytes was determined by a photometric swelling assay (Figure 5.5), described previously in Chapters 3 and 4. Oocytes expressing the SvPIP1 subfamily isoforms and SvPIP2;2 did not induce a higher osmotic water permeability than water injected control oocytes (Figure 5.5). Oocytes expressing all other SvPIP2 sub-family isoforms (SvPIP2;1, 2;3, 2;4, 2;5, 2;6, 2;7 and 2;8) had significantly greater osmotic permeability than the water injected control oocytes (Figure 5.5).

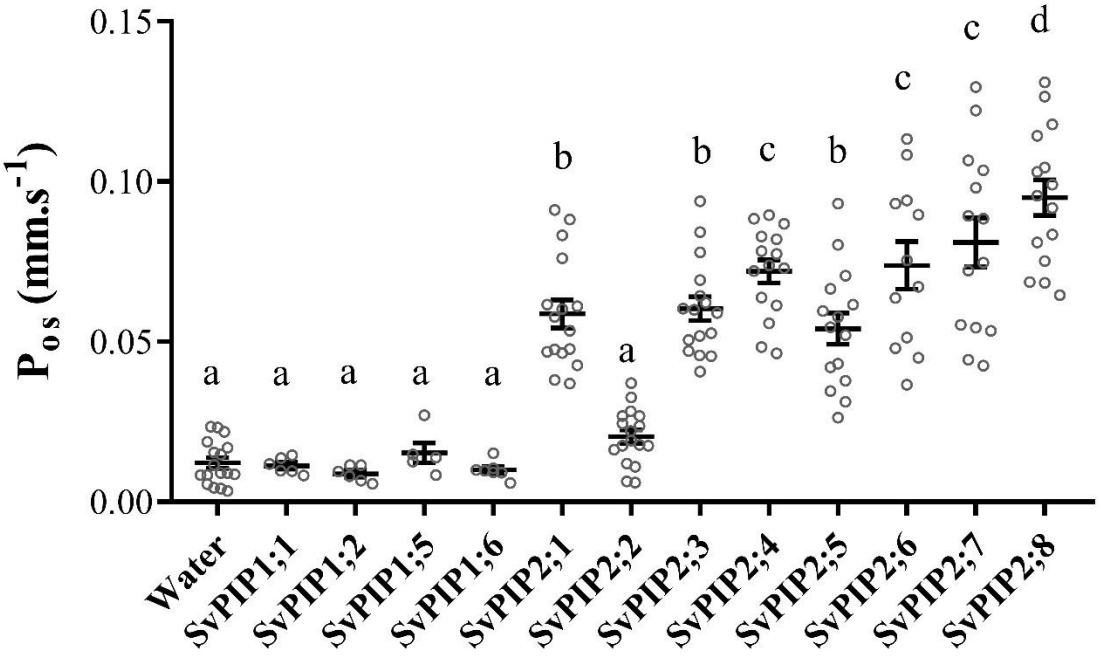

Figure 5.5: Osmotic water permeability of SvPIP expressing *X. laevis* oocytes. Oocytes were injected with 46 nL of water or 46 nL of water containing cRNA encoding SvPIP isoforms and incubated in Low Na^+ Ringers for 24-30 h post-injection. Osmotic permeability (P_{os}) was determined via photometric swelling where oocytes were pre-incubated in the isotonic swelling solution before being transferred to the hypotonic swelling solution for the assay. Each data point represents an individual oocyte. Data was compiled from two independent oocyte batches and is shown as mean ± SEM. Statistical significance ($p < 0.05$) as shown by different letters was determined by one-way ANOVA (Fishers post-test).

5.2.3 Hydrogen peroxide and boric acid transport facilitated by *Setaria viridis* PIPs

Some plant aquaporins have been shown to facilitate the transport of the neutral substrates boric acid (BA) and hydrogen peroxide (H_2O_2). Using yeast, the SvPIPs were screened for their capacity to facilitate both BA and H_2O_2 transport. The SvPIPs were expressed in the double aquaporin knock-out yeast strain *aqy1/aqy2* and the reactive oxygen species (ROS) sensitive yeast strain *snk7* and used for the BA and H_2O_2 assays, respectively. Accumulation of both BA and H_2O_2 in these yeast strains results in growth reduction (see negative control: empty vector). Yeast cells expressing an SvPIP capable of facilitating BA or H_2O_2 transport will have increased permeability to these substrates, which manifests as greater growth inhibition (shown as percent Area Under the Curve (AUC %) relative to non-treated). Lipid bilayers do exhibit some permeability to BA and H_2O_2 and the overexpression of plasma membrane localised proteins like aquaporins may change its inherent permeability to these substrates. However, many SvPIP transformants exhibit the same growth inhibition as empty vector (Figure 5.6-5.7).

Only yeast expressing SvPIP2;1 had reduced growth under increasing BA treatments compared to empty vector (Figure 5.6). In comparison to BA, many more SvPIP isoforms increased yeast susceptibility to H_2O_2 indicating their ability to facilitate H_2O_2 transport (Figure 5.7). Yeast expressing SvPIP1;1, 2;1, 2;5 and 2;6 had significantly reduced growth under increasing H_2O_2 treatment (Figure 5.7). Interestingly, expression of SvPIP2;2 appears to provide ROS susceptible yeast with a growth advantage when exposed to external H_2O_2 (Figure 5.7).

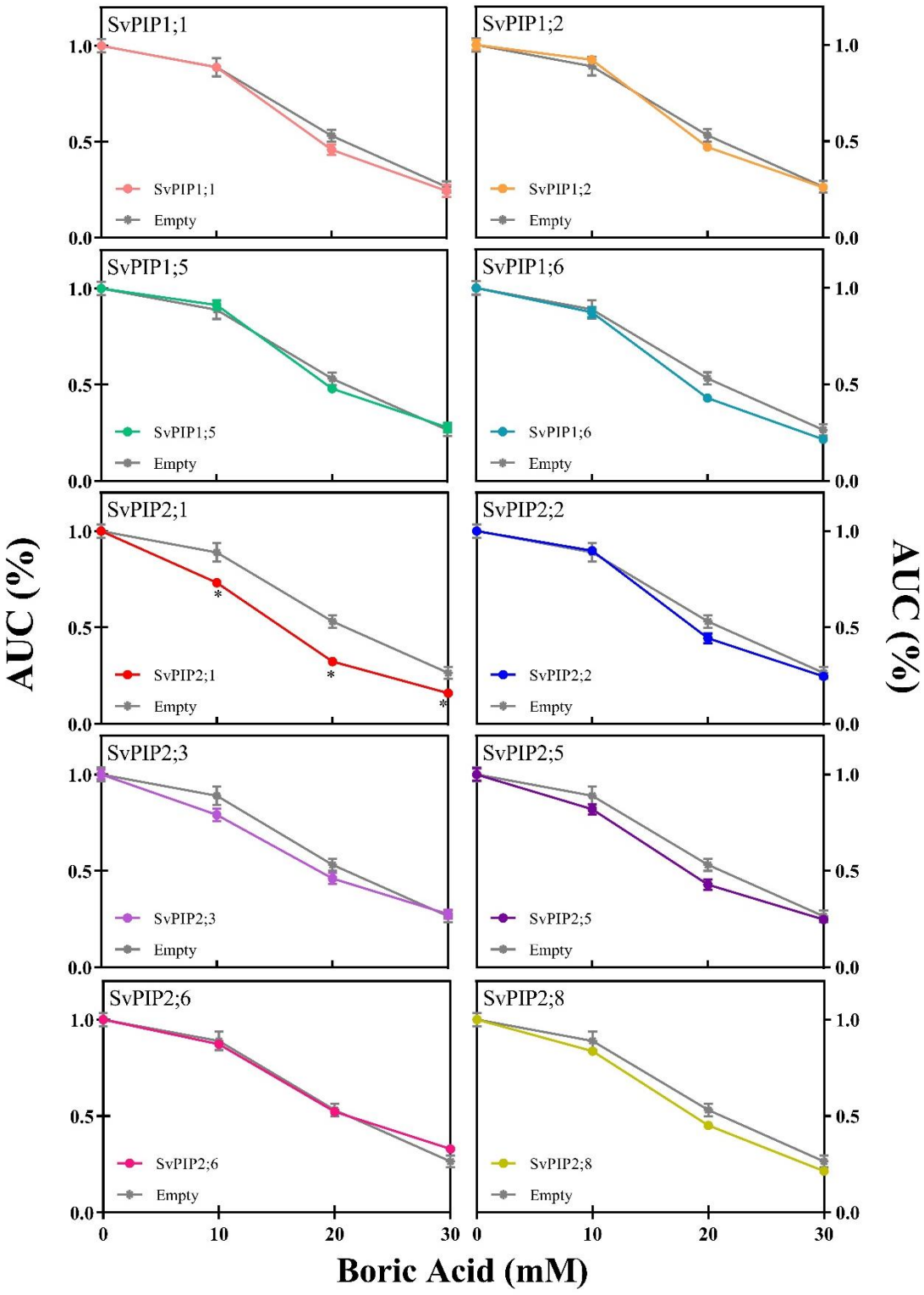

Figure 5.6: Boric acid susceptibility of yeast expressing SvPIP isoforms. Growth based assays were performed to determine the relative tolerance or susceptibility of yeast expressing different SvPIP isoforms to increasing boric acid (BA) treatment. Increased BA transport capacity is indicated by reduction of growth as compared to the empty vector. Data is shown as mean ± SEM area under the curve relative to 0 mM BA treatment (AUC%) where total n = 8-12 biological replicates from 4-5 independent experimental replicates. Statistical significance ($p < 0.05$) is indicated by an asterisk (*) as determined by one-way ANOVA for each treatment.

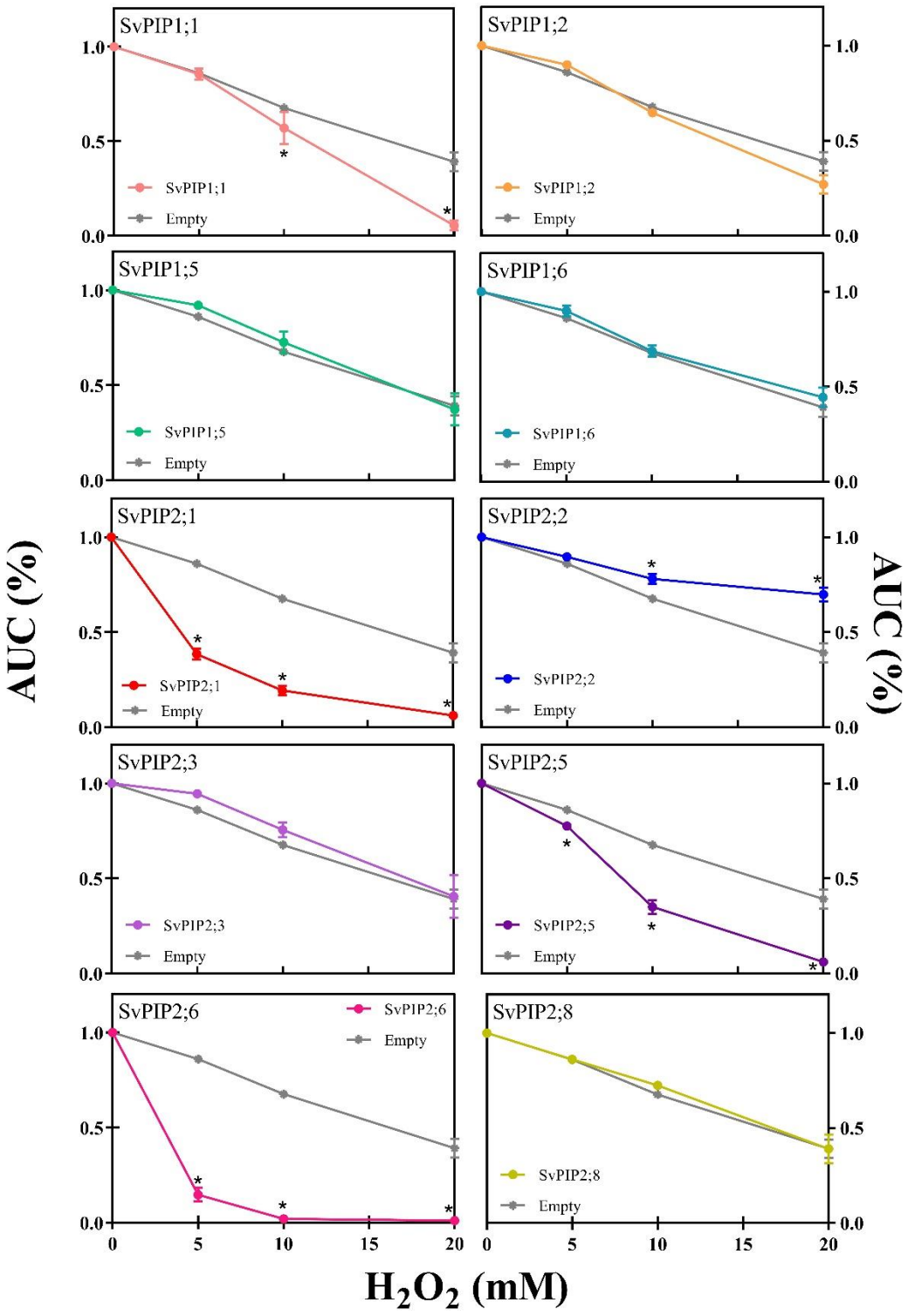

Figure 5.7: Hydrogen peroxide (H_2O_2) susceptibility in yeast expressing SvPIP isoforms. Growth based assays were performed to determine the relative tolerance or susceptibility of *skn7* yeast expressing different SvPIP isoforms to increasing hydrogen peroxide (H_2O_2) treatment. Increased H_2O_2 transport capacity is indicated by reduction of growth as compared to the empty vector. Data is shown as mean ± SEM area under the curve relative to 0 mM H_2O_2 treatment (AUC%) where total n = 8-12 biological replicates from 4-5 independent experimental replicates. Statistical significance ($p < 0.05$) is indicated by an asterisk (*) as determined by one-way ANOVA for each treatment concentration.

5.2.4 *Setaria viridis* and barley monocot PIP isoforms facilitate transport of the monovalent cation sodium (Na^+)

To investigate whether any SvPIP isoforms were capable of facilitating ion transport, the SvPIPs were expressed in *X. laevis* oocytes and TEVC was performed in Na100. The conductance of SvPIP expressing oocytes, calculated by taking the slope of a regression of the linear region across the reversal potential (–60 mV to +40 mV), was normalised to that of water injected controls to correct for batch variation (Figure 5.8). Representative IV curves and the raw conductance values for each batch are shown in Appendix 9.5.

From the SvPIP1 subfamily, two isoforms may facilitate ion transport when expressed in *X. laevis* oocytes (Figure 5.8a). SvPIP1;1 and SvPIP1;6 expressing oocytes had significantly greater relative conductance compared to that of water injected controls whereas SvPIP1;2 and SvPIP1;5 did not (Figure 5.8a). The SvPIP2 isoforms SvPIP2;1, 2;2, 2;6 and 2;8 may also facilitate ion transport when expressed in *X. laevis* oocytes (Figure 5.8b). Oocytes expressing these isoforms had greater relative conductance than that of the water injected control oocytes. The conductance of SvPIP2;3, 2;4, 2;5 and 2;7 expressing oocytes did not differ from controls (Figure 5.8b). However, there was variation in conductance between oocyte batches (Appendix 9.5, Figure S5) which may be indicative of regulatory differences within each batch.

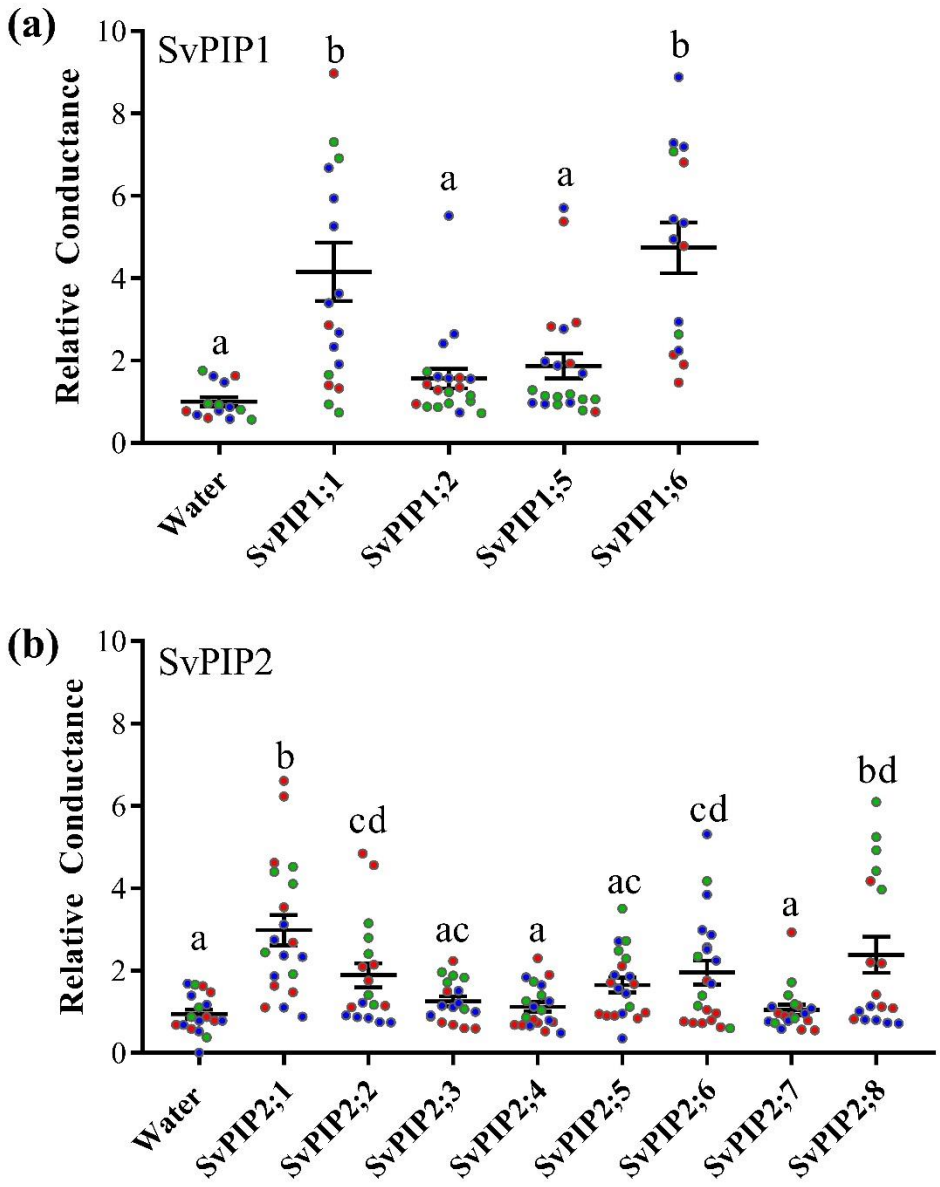

Figure 5.8: Relative ionic conductance of oocytes expressing SvPIPs. Oocytes were injected with 46 nL water or 46 nL water containing SvPIP cRNA. Post-injection oocytes were stored in Low Na^+ ringers for 24-30 h. TEVC was performed in Na100 solution. Conductance of **(a)** SvPIP1 and **(b)** SvPIP2 expressing oocytes was normalised to the conductance of water injected control oocytes within each batch. Data in each panel is shown as mean relative conductance ± SEM with each data point representing an individual oocyte. Data is each panel was compiled from three independent oocyte batches where TEVC from one batch was performed in collaboration with Dr. Jiaen Qiu. Statistical significance ($p < 0.05$) by one-way ANOVA (Fishers post-test) is indicated by different letters.

Candidate barley PIP2s (HvPIP2s), where HvPIP2 clones were provided by collaborators in the oocyte expression vector pXGB-ev1, were expressed in oocytes to investigate their ion transport function (Figure 5.9). Oocytes expressing HvPIP2;1 and HvPIP2;8 had significantly greater ionic conductance in Na100 compared to water injected controls. These results were consistent with data obtained in other oocyte batches and generated by other project collaborators (pers. comm. Professor Maki Katsuhara).

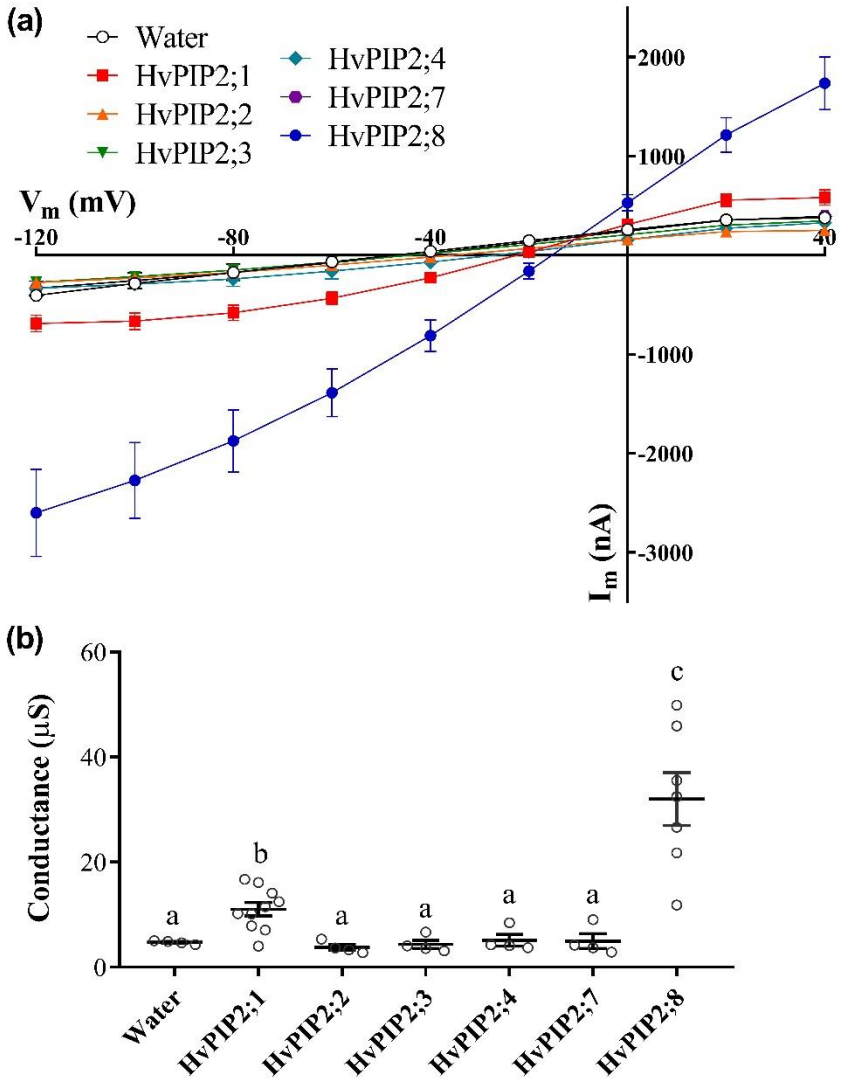

Figure 5.9: IV curves and ionic conductance for HvPIP2 expressing oocytes. Oocytes were injected with 46 nL of water or 46 nL of water containing HvPIP2 cRNA. Post-injection oocytes were stored in Low Na^+ ringers for 24-30 h. TEVC was performed in Na100. **(a)** IV curves of oocytes expressing HvPIP2s. **(b)** Ionic conductance of HvPIP2 expressing oocytes. Data is from one oocyte batch and is shown as mean ± SEM where each data point represents an individual oocyte. Statistical significance ($p < 0.05$) by one-way ANOVA (Fishers post-test) is indicated by different letters.

5.2.5 *Setaria viridis PIP* gene expression analysis

Transcriptome data for the *S. viridis* and *S. italica* spp. is publicly available through Phytomine (Phytozome etc). This data includes expression values of *S. viridis* and *S. italica* transcripts in different tissue types, growth conditions, and treatments (Figure 5.10). The transcriptome data was mined for *SvPIPs* and *SiPIPs* where red and blue colouring indicate high and low expression, respectively. The abundance of *SvPIP1;1*, *SvPIP1;2*, *SvPIP1;5*, *SvPIP2;1*, *SvPIP2;4* and *SvPIP2;6* transcripts were relatively high in all tissue types, growth conditions and treatments examined (Figure 5.10). Comparatively, *SvPIP1;6* and *SvPIP2;2* transcripts were only found in low abundance in roots and were not expressed at all in most other tissue types. *SvPIP2;5* transcripts were highly expressed in roots only, whereas *SvPIP2;8* transcripts were highly expressed in leaves only (Figure 5.10). The *SiPIPs* were similarly expressed in the same tissue types and treatments (Figure 5.10b)

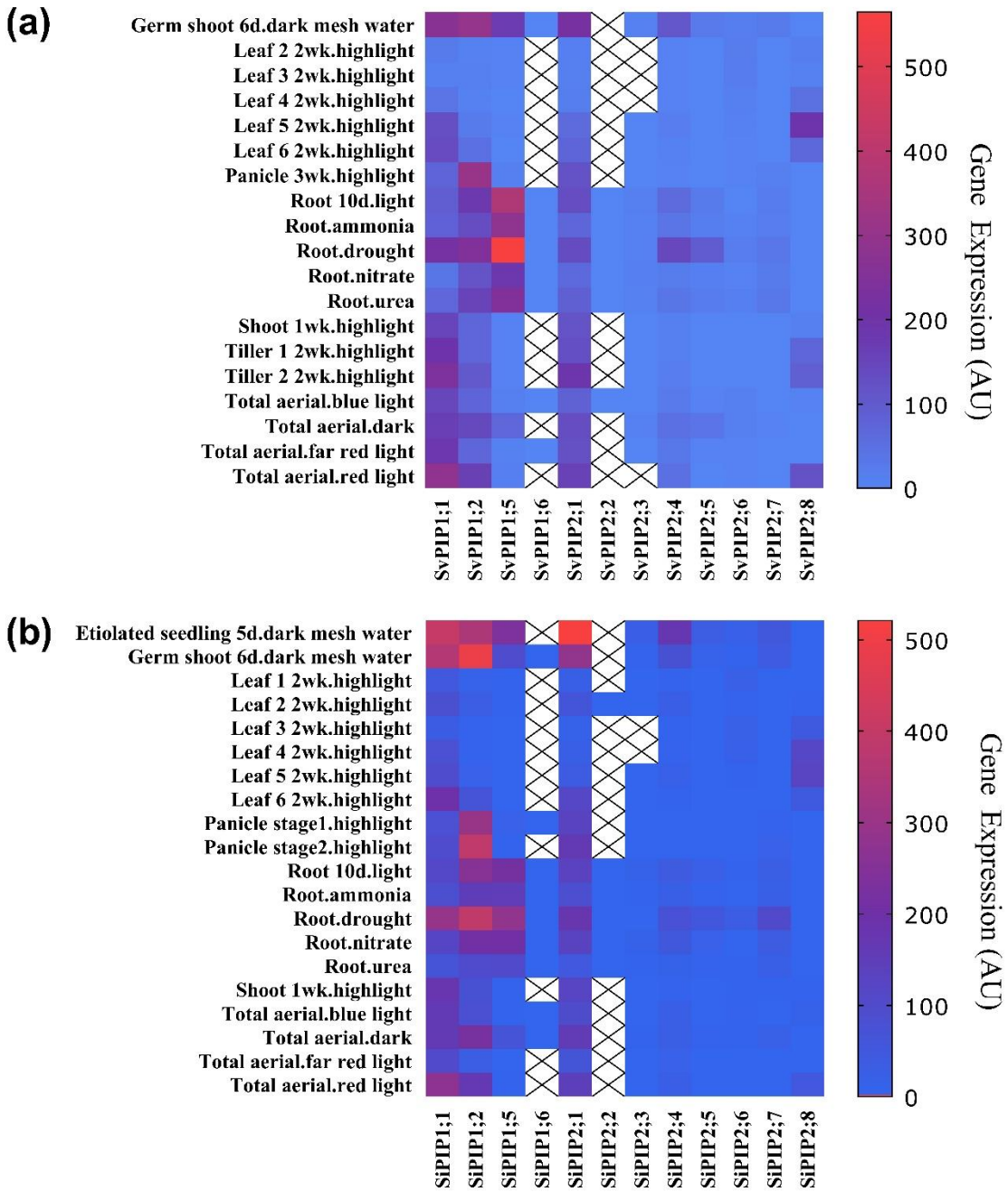

Figure 5.10: Expression data of *S. viridis* and *S. italica* PIPs. RNA-seq expression data was downloaded from the publicly available Phytomine database (last accessed July 2019; Phytozome etc) where next-generation sequencing reads were aligned to reference genomes, and gene- and transcript-level expression values are determined using Cufflinks. Expression data (Arbitrary Units; AU) for **(a)** *S. viridis* and **(b)** *S. italica* on Phytomine is reported for several tissue types, growth conditions and treatments. Different colours indicate expression level where red is high expression and blue is low expression. An X indicates no expression detected.

5.3 Discussion:

The SvPIPs were screened to compare their transport of water, boric acid, H_2O_2 and test their relative ionic conductance using the heterologous expression systems yeast and *X. laevis* oocytes. Several SvPIP isoforms facilitated the transport of water, ions and H_2O_2 but only one, SvPIP2;1, facilitated boric acid transport (Table 5.2). In general, aquaporin facilitated ion and H_2O_2 transport was observed for different SvPIP isoforms (Table 5.2). Two HvPIP isoforms were also found to facilitate ion transport when expressed in *X. laevis* oocytes.

Analysis of the SiPIP and SvPIP protein sequences revealed that all SiPIPs and SvPIPs were identical at the protein level, with the exception of PIP2;4 (Figure 5.3). SiPIP2;4 and SvPIP2;4 have two amino acid differences; an I to V change at position 131 and an A to D change at position 167. The I134V difference occurs in the transmembrane helix 3 but this position is not associated with any of the known selectivity filters (for review see Luang and Hrmova, 2017). Additionally, V and I have very similar structures and other properties (non-polar, aliphatic residues), it is therefore unlikely that this substitution would notably effect function. The second amino acid difference A167D occurs in the extracellular loop C. Due to the charge difference between A and D (where A is neutral and D is negatively charged and a common phosphorylation mimic substitute) it is conceivable that this could influence loop C gating through interaction and/or bond formation with residues of the other extracellular loop E. Further characterisation and comparison of the SvPIP2;4 and SiPIP2;4, or mutagenesis studies would be required to determine if these differences impact function. In general, the functional characteristics of SvPIPs proteins in heterologous systems are likely to match those for SiPIPs. This is supported by gene expression data which suggests that the *SvPIPs* and *SiPIPs* are similarly expressed (Figure 5.10). Although protein regulation and therefore function could still differ *in planta*.

Table 5.2: Summary of which SvPIPs can facilitate the transport of the substrates water, ions, H_2O_2 and BA when expressed in heterologous systems *X. laevis* oocytes and yeast. SvPIPs were expressed in yeast and oocytes and their capacity to facilitate the transport of water, ions (predominately Na^+), H_2O_2 and BA were tested in this chapter (Figures 5.4-5.8). +: transport of substrate indicated; -: no transport indicated; X: not tested; ?: other/unexplained phenotype observed.

Gene	Substrate			
	Water	Ions	H_2O_2	BA
SvPIP1;1	+	+	+	-
SvPIP1;2	-	-	-	-
SvPIP1;5	-	-	-	-
SvPIP1;6	-	+	-	-
SvPIP2;1	++	+	+	+
SvPIP2;2	-	+	?	-
SvPIP2;3	++	-	-	-
SvPIP2;4	++	-	X	X
SvPIP2;5	++	-	+	-
SvPIP2;6	++	+	+	-
SvPIP2;7	++	-	X	X
SvPIP2;8	+	+	-	-

5.3.1 Functional characteristics of the SvPIP1 subfamily

PIP1 subfamily members typically do not display any water permeability when expressed in heterologous systems although permeability to other substrates has been measured. A review of PIP1 expression in *X. laevis* oocytes reported that the vast majority of PIP1s did not increase oocyte osmotic permeability (Yaneff *et al.*, 2015). Absence of significant water transport has often been interpreted as failure of PIP1 proteins to efficiently reach the PM (for example: Fetter *et al.*, 2004). Several motifs (DxE and LxxxA) on PIP2 proteins have been identified as being required for successful ER export (Chevalier *et al.*, 2014; Zelazny *et al.*, 2009), although individual domain swaps of these motifs with PIP1s failed to alter PIP1 ER retention. When expressed in *X. laevis* oocytes the SvPIP1s did not increase oocyte osmotic permeability (Figure 5.5). The absence of SvPIP1 contribution to osmotic permeability could mean that the SvPIP1 proteins did not reach the PM; however, expression of both SvPIP1;1 and SvPIP1;6 in oocytes increased oocyte ionic conductance (Figure 5.8). This could be consistent with PIP localisation on the PM but should be confirmed by a

protein localisation study. SvPIP1;1 increased yeast FT survivability (from ~1% for empty vector to ~10%) when expressed in an aquaporin deficient yeast strain (Figure 5.4), but did not contribute to osmotic permeability when expressed in oocytes (Figure 5.5). When the PIP1;1 from the lycophyte *Selaginella moellendorffii* (SmPIP1;1) was expressed in oocytes, a small increase in oocyte osmotic permeability (though this was not statistically different to water injected controls) and weak localisation to the oocyte PM were observed (Bienert *et al.,* 2018). Minimal localisation to the oocyte PM, while not sufficient to alter oocyte water permeability if PIP1s are not efficient water channels, could account for the increased ionic conductance of SvPIP1;1 and SvPIP1;6 if they are efficient Na^+ channels. Alternatively, accumulation of SvPIP1 protein in the ER may have altered the trafficking and targeting of native oocyte channels or the yeast and oocyte systems are differentially phosphorylating SvPIPs to influence their function. Determination of SvPIP localisation in oocytes (particularly of SvPIP1s) is needed but the quarantine facilities required to achieve this were not available.

Of the four SvPIP1s only one, SvPIP1;1, reduced yeast growth in the *skn7* yeast strain when exposed to H_2O_2 (Figure 5.7). There are examples of H_2O_2 permeable and impermeable PIP1s in the literature. For example the AtPIP1;4 facilitates H_2O_2 transport in yeast (Tian *et al.,* 2016), whereas the ZmPIP1;2 does not (Bienert *et al.,* 2014). If the apparent transport capacity of SvPIP1;1 (Figure 5.7) is considered in context with its low abundance in the PM of these heterologous expression systems then it may be that the protein itself is an efficient transporter. To overcome PIP1 localisation issues they are often co-expressed with PIP2s which generally exhibit strong PM localisation. When expressed alone the *Fragaria x ananassa* PIP1;1 (FaPIP1;1) did not increase oocyte osmotic permeability but when co-expressed with the FaPIP2;1 the oocyte water permeability was even greater than that of FaPIP2;1 by itself (Yaneff *et al.,* 2014). Co-expression of FaPIP1;1 with FaPIP2;1 resulted in FaPIP1;1 localisation on the oocyte plasma membrane. Several studies similarly report on PIP1 relocalisation events facilitated by PIP2 co-expression, for example for maize and grapevine aquaporins in oocytes (Fetter *et al.,* 2004; Vandeleur *et al.,* 2009) and maize protoplasts (Zelazny *et al.,* 2007). However, in these cases PIP1 function in the context of water permeability could be perturbed by PIP2 function. Even if the PIP1s were co-expressed with a PIP2 known to be impermeable to the substrate of interest, ratios of homo- and hetero-tetramer formation could also influence apparent substrate permeability. The study of PIP1 function remains problematic, and it is difficult with the currently available

methods to determine if most PIP1s are truly not permeable to a particular substrate or whether the apparent lack of permeability is an artefact of insufficient protein in the PM.

The expression of *SvPIP1s* in various tissue types, treatments and growth conditions was investigated through the publicly available Phytomine dataset (Figure 5.10). *SvPIP1;1* was found to be relatively highly expressed throughout all tissue types, treatments and growth conditions examined (Figure 5.10). *SvPIP1;2* and *SvPIP1;5* were similarly highly expressed but more so in roots. Expression of *SvPIP1;6* on the other hand was either very low or not-detectable (Figure 5.10); the maize *PIP1;6* (*ZmPIP1;6*) was also found to be very lowly expressed in maize leaf tissue (Hachez *et al.,* 2008). This low expression may indicate that it has cell-specific expression and function that has not yet been determined, or that it is functionally redundant and therefore not used by the plant. It is not possible with the data collected in this chapter to infer physiological roles of SvPIP1s based on transcript information.

5.3.2 Functional characteristics of the SvPIP2 subfamily

PIP2 subfamily proteins are generally associated with efficient water channel function and their protein abundance *in planta* has been correlated to root hydraulic conductivity (di Pietro *et al.,* 2013). All SvPIPs with the exception of SvPIP2;2 facilitated water permeability when expressed in the heterologous systems *X. laevis* oocytes and the aquaporin deficient yeast strain *aqy1/aqy2* (Figures 5.4 and 5.5). Expression of SvPIP2;2 did not increase oocyte osmotic permeability or yeast FT survivorship; this may be due to its apparent lack of water transport capacity or due to low PM localisation efficiency. When expressed in oocytes the *Selaginella moellendorffii* PIP2;2 (SmPIP2;2) did not increase oocyte water permeability and was also found to be very lowly expressed in the oocyte PM (Bienert *et al.,* 2018). A previous localisation study of SiPIPs in yeast using a different expression vector found that SiPIP2;2 showed very weak PM localisation and a diffuse intracellular signal predominates (Osborn, 2017). All SvPIP2 proteins contain the TM3 LxxxA motif identified as aiding PM localisation and most possess an NTD DxE ER export motif including SvPIP2;2, although SvPIP2;2 also has an extended NTD (~8-10aa) at the 5' end which could perturb this signal (Chevalier *et al.,* 2014; Zelazny *et al.,* 2009). Interestingly, SvPIP2;8 exhibits water permeability when expressed in oocytes but not yeast (Figures 5.4 and 5.5) where SvPIP2;8 was also previously found to have low PM localisation in yeast (Osborn, 2017).

In addition to transporting water in yeast, SvPIPs also influenced yeast mutant growth in the presence of boric acid (BA) and H_2O_2 indicative of facilitated transport of these neutral substrates (Figures 5.6 and 5.7). One isoform, the SvPIP2;1, slightly increased yeast susceptibility to the BA treatment (Figure 5.6). Several PIPs from other species, including the rice PIP1;3, PIP2;4, PIP2;5 and PIP2;7 and the barley PIP1;3 and PIP1;4, have been shown to transport BA when expressed in yeast (Fitzpatrick and Reid, 2009; Kumar *et al.*, 2014; Mosa *et al.*, 2016). However, BA transport is more typically a feature of NIPs, and to a lesser extent TIPs, where the NIP Ar/R selectivity filters are essential for their high transport capacity for boron as well as the other metalloids such as silicon and arsenic (Mitani-Ueno *et al.*, 2011; see also: Durbak *et al.*, 2014; Hanaoka *et al.*, 2014; Kato *et al.*, 2009; Pang *et al.*, 2010; Schnurbusch *et al.*, 2010b; Takano *et al.*, 2006; Tanaka *et al.*, 2008). In barley, BA transport mechanisms at the root epidermis are currently thought to primarily involve two transporters: NIP2;1 (influxer) carrying the neutral BA, and BOT1 (effluxer) that transports the anionic form of BA (Schnurbusch *et al.*, 2010b; Sutton *et al.*, 2007; see also Hrmova and Gilliham, 2018). A similar NIP protein in Arabidopsis, AtNIP5;1, has been identified as the protein responsible for B uptake in Arabidopsis roots (Fujiwara *et al.*, 2010; Kato *et al.*, 2009; Takano *et al.*, 2006). B-toxicity tolerance mechanisms may involve down-regulation of NIP2;1 to reduce BA uptake whereas up-regulation of BOT1 would increase BA efflux (Hrmova and Gilliham, 2018). However, other aquaporins capable of mediating BA transport may be involved in BA influx and efflux. The bi-directional transport activity of OsPIP1;3 and OsPIP2;6 expressed in a boron sensitive yeast strain was different; OsPIP1;3 increased B influx and accumulation and OsPIP2;6 mediated rapid B efflux (Mosa *et al.*, 2016). The sidedness of aquaporin gating, as seen for the divalent cation block of Na^+ transport for AtPIP2;1 and AtPIP2;2 where outward rectification only was induced (Kourghi *et al.*, 2017), may influence whether an aquaporin is involved in BA influx or efflux. Another point of interest is that the boron permeable NbXIP1;1α is phosphorylated on its N-terminus and it has been suggested that the NTD is involved in gating of the channel linked to phosphorylation status (Ampah-Korsah *et al.*, 2016).

Plant aquaporin facilitated H_2O_2 transport, using yeast as the assay system, has been reported for members of the PIP, NIP and TIP sub-families across a number of different plant species (including Arabidopsis, maize, tobacco (*Nicotiana tabacum*), tomato (*Solanum lycopersicum*), potato (*Solanum tuberosum*) and tulip (*Tulipa gesneriana*); and aquaporin H_2O_2 transport is likely to be involved in a range of signalling or detoxification processes (for review see: Bienert and Chaumont, 2014). In addition to SvPIP1;1, several SvPIP2s

(PIP2;1, 2;5 and 2;6) increase *skn7* yeast susceptibility to H_2O_2 treatment (Figure 5.7). PIP2s from Arabidopsis (AtPIP2;1, 2;2, 2;4, 2;5 and 2;7) and Maize (ZmPIP2;5) also increased toxicity of H_2O_2 when expressed in yeast (Bienert *et al.,* 2014; Dynowski *et al.,* 2008a; Hooijmaijers *et al.,* 2012). Quite surprisingly, expression of the SvPIP2;2 appeared to enhance tolerance of yeast to increasing H_2O_2 treatment (Figure 5.7). The exact mechanism by which this occurs remains unknown and requires further investigation but SvPIP2;2 could be involved in a H_2O_2 efflux or sequestration mechanism. The overexpression of the H_2O_2 permeable TIP1;2 from *T. salsuginea* was found to enhance tolerance to multiple stresses (drought, salinity, oxidative stress) and hypothetically this may be related to increased capacity for H_2O_2 accumulation in the vacuole thereby reducing its concentration and effects in the cytosol (Wang *et al.,* 2014).

The root hydraulic conductivity of plants has been shown to decrease in response to H_2O_2 (Boursiac *et al.,* 2008; Martinez-Ballesta *et al.,* 2006; Ye and Steudle, 2006) and it is likely that this is linked to H_2O_2 influencing plant aquaporins. H_2O_2 has been reported to regulate aquaporin function directly through an oxidative gating mechanism (Henzler *et al.,* 2004; Ye and Steudle, 2006) and can also trigger the internalisation of aquaporins from the plasma membranes of root cells (Boursiac *et al.,* 2008). H_2O_2 is also an important signalling molecule in stomatal regulation, and several H_2O_2 permeable aquaporins (for example the AtPIP2;1) are expressed in guard cells and could be involved in H_2O_2 transport and signal transduction (Rodrigues *et al.,* 2017). Since H_2O_2 shares many structural and electrochemical similarities to water (H_2O), the permeation pathway of H_2O_2 through plant aquaporins is likely to be via the monomeric or water transporting pore (Bienert *et al.,* 2006); by the mutation of H199 (H199K) in AtPIP2;1 that was previously reported to influence its water selectivity and gating, H_2O_2 sensitivity was also abolished in yeast expressing the mutant AtPIP2;1 relative to wild type (Dynowski *et al.,* 2008a). However, as astutely observed by Bienert and Chaumont (2014), water permeability does not necessarily imply H_2O_2 permeability and *vice versa*, and does not appear to be linked to aquaporin selectivity filters. For example, the XIP aquaporins from the *Solanaceae* spp. have no appreciable water permeability but significantly increased H_2O_2 sensitivity when expressed in yeast (Bienert *et al.,* 2011). All PIP2s in Arabidopsis function as efficient water channels and have identical Ar/R selectivity filters but only 5 out of 8 PIP2 isoforms appear to be permeable to H_2O_2 (Bienert and Chaumont, 2014; Hooijmaijers *et al.,* 2012). SvPIP2 members similarly have identical selectivity filters (Azad *et al.,* 2016) and water transport capacity (with the exception of SvPIP2;2; Figure5.4-5.5) but not all result in increased H_2O_2 sensitivity when

expressed in yeast (Figure 5.7). These data and observations suggest that there is much more to substrate permeation and selectivity than is currently known, and that assuming exclusion of a particular substrate from being transported by aquaporins on the basis of these filters may be premature.

Several SvPIP2 proteins increased ionic conductance when expressed in *X. laevis* oocytes (Figure 5.8). Compared to water injected controls, the SvPIP2;1, 2;2, 2;6 and 2;8 had significantly greater relative ionic conductance (Figure 5.8). Due to variation in current magnitude across independent oocyte harvests, conductance was normalised within harvest to that of water injected controls, and data from several harvests were compiled. Although the mean of SvPIP2;2, 2;6 and 2;8 across four replicates indicate ionic conductance, this is only seen in some individual batches for these isoforms whereas SvPIP2;1 consistently exhibits ionic conductance (see Appendix 9.5, Figure S5). Given the influence of phosphorylation described previously in this thesis (Chapters 3 and 4), it is possible that endogenous kinase activity varies in these batches and therefore protein phosphorylation state may not be equivalent in each experimental replicate. Furthermore, some isoforms capable of facilitating ion transport may be more sensitive to PTM regulation than others; the coefficient of variation for SvPIP2;2, 2;6 and 2;8 is much greater compared to other SvPIPs indicating that ion transport function for these isoforms may be under greater regulatory control (Appendix 9.5, Table S5). Under the specific conditions tested here SvPIP2;1 facilitates ion transport, and SvPIP2;2, 2;6 and 2;8 may facilitate ion transport.

The expression of *SvPIP2s* in various tissue types, treatments and growth conditions was investigated through mining the publicly available Phytomine dataset (Figure 5.10). *SvPIP2;1*, *2;4* and *2;6* were expressed in all tissues and treatment types and at higher levels than the other *PIPs* (Figure 5.10). *SvPIP2;3*, *2;5*, and were more highly expressed in root tissues whereas *SvPIP2;8* was more highly expressed in the shoots and aerial parts of the plant (Figure 5.10). *SvPIP2;2* was found to be lowly expressed in roots only, as its transcripts were otherwise not detectable. The low expression of *SvPIP2;2* may be related to its limited permeability to many substrates including water (Table 5.10). A transcriptome study of a drought tolerant and drought sensitive *Setaria italica* cultivar found that 13 aquaporins, including five PIPs were differentially regulated in both varieties in response to drought stress treatment, although the authors did not indicate which particular PIP isoforms (Tang *et al.*, 2017); this study also notes that there was higher ROS accumulation in the sensitive variety.

The results in this chapter provide preliminary functional characterisation of SvPIPs, which in the future could be put together with protein regulation and abundance data to assess aquaporin physiological roles (for review see McGaughey *et al.,* 2018 - Chapter 1). To further resolve aquaporin physiological roles additional studies testing protein abundance, states of post-translational modification and gating in different tissues, stages of development, and in varying stress conditions, for each of the *Setaria* aquaporins of interest, is needed.

5.3.3 Some aquaporin isoforms from the agricultural crop barley facilitate ion transport

Several barley PIP2 (HvPIP2) isoforms were tested for ion transport function in collaboration with Professors Maki Katsuhara and Keitaro Tanoi and Associate Professors Tomoaki Horie and Natsuko Kobayashi from Okayama University (M.K), Shinshu University (T.H) and University of Tokyo (K.T and N.K), who kindly provided the HvPIP2 clones in an *X. laevis* oocyte expression vector. Of the candidate HvPIP2s examined two isoforms, HvPIP2;1 and HvPIP2;8, were found to facilitate ion transport when expressed in oocytes (Figure 5.9). HvPIP2 proteins were previously reported to be functional water channels (Horie *et al.,* 2011). HvPIP2;1 specifically has been linked to salt response in barley; *HvPIP2;1* transcripts are significantly down-regulated in roots under salt treatment (100 and 200 mM NaCl) (Katsuhara *et al.,* 2002; Ligaba *et al.,* 2011) but up-regulated in shoots (Katsuhara *et al.,* 2002). Transgenic rice plants over-expressing HvPIP2;1 had increased root hydraulic conductivity and shoot:root biomass but showed greater growth inhibition to 100 mM NaCl treatment compared to wild-type plants (Katsuhara *et al.,* 2003). Furthermore, the root hydraulic conductivity (L_{pr}) of barley was significantly decreased when treated with the kinase inhibitor staurosporine indicating that regulation of L_{pr} was likely to be phosphorylation-dependent (Horie *et al.,* 2011). The HvPIPs that facilitate ion transport could similarly be regulated by phosphorylation as described for AtPIP2;1 (Chapter 3).

Aquaporins facilitating ion transport have now been identified in an agriculturally significant crop and the potential roles of these proteins in osmotic stress tolerance mechanisms should be investigated further. This may be achieved by generating phosphomimetic versions of candidate HvPIPs for testing in heterologous systems. Towards probing function *in planta*,

HvPIP phospho-mutant transgenics could be tested for changes in root hydraulic conductivity and response to salt treatments.

Chapter 6: TIPs as ion permeable aquaporins in plants

6.1 Introduction

Most plant cells possess large vacuoles that can account for as much as 90% of their volume. Vacuoles have many complex and distinct roles within the cell which can depend on cell type and developmental stage, as well as tissue or organ type (Martinoia *et al.*, 2006; Marty, 1999). In general, vacuoles are responsible for turgor generation (through water and solute sequestration); storage of nutrients, secondary metabolites and proteins; and functioning as a compartment for protein degradation (Frigerio *et al.*, 2008; Isayenkov *et al.*, 2010; Zhang *et al.*, 2014). A primary role of vacuoles is to balance the osmotic pressure of the cytosol, mainly with ions, so that the cell can generate and maintain turgor (Sablowski, 2016; Zhang *et al.*, 2014). However, nutrient storage in vacuoles is necessary to allow plants to adapt to fluctuations in nutrient supply (for review see Martinoia *et al.*, 2006). Vacuoles are also used as the main storage site for toxic compounds that are removed from the cytoplasm to prevent disturbance of essential biochemical processes (Becker, 2007; Yamaguchi and Blumwald, 2005). Among the diversity of essential functions performed by plant vacuoles, they all commonly require the controlled flow of water and other solutes across the vacuolar membrane (tonoplast).

Tonoplast-intrinsic proteins (TIPs) are a sub-family of plant aquaporins notable for localisation on the tonoplast, although TIPs have also been found to localise to the plasma membrane (Gattolin *et al.*, 2011) or even the symbiosome membrane in rhizobia infected legume root nodules (Gavrin *et al.*, 2014). Similar to PIPs, TIPs are typically efficient water channels, where some TIP isoforms also have selectivity for a range of other solutes including urea, ammonia, H_2O_2 and glycerol (Barzana *et al.*, 2014; Bienert *et al.*, 2007; Gerbeau *et al.*, 1999; Jahn *et al.*, 2004; Loqué *et al.*, 2005). TIPs are proposed to primarily function as mediators in the exchange of water and other solutes between vacuolar compartments and the cytosol (Maurel *et al.*, 2015). TIPs have crucial roles in water balance between cytosol and vacuole, particularly during plant growth and changes in external osmotic pressure (Fricke and Chaumont, 2006; Fricke and Knipfer, 2017; Ludevid *et al.*, 1992; Okubo-Kurihara *et al.*, 2009; Tyerman *et al.*, 1999), and in solute transport allowing for the storage or release of nutrients and/or signalling molecules in the vacuole (for reviews see Maurel, 2007; Maurel *et al.*, 2008). TIPs are involved in osmotic stress responses, as

they are intrinsically involved in the maintenance of cellular and whole plant water balance, but some TIP isoforms have also been implicated in biotic stress responses.

Biotic stress in plants is caused by damage due to interaction with other organisms. Other organisms can deprive plants of nutrients or otherwise compete for nutrients and resources leading to reduced plant vigour and often resulting in decreases to yield quantity and quality. Plant pathogens, whether they be viruses, bacteria, fungi or nematodes, rely on their host plants as their nutrient source (Wirthmueller *et al.,* 2013). Several TIPs have been associated with the plant response to pathogen infection. Upon infection of sweet orange citrus plants (*Citrus sinensis*) by the proteobacterium *Candidatus liberibacter*, *CsTIP1;2*, *CsTIP2;1* and *CsTIP2;2* were down-regulated (Aritua *et al.,* 2013; De Paula Santos Martins *et al.,* 2015). In Arabidopsis two TIP isoforms were found to directly interact with a cucumber mosaic virus (CMV) replication protein, CMV1a, and it was suggested that this interaction may influence CMV replication that is associated with the host cell tonoplast (Kim *et al.,* 2006). As a result of root knot nematode infection the expression of the tobacco TIP TobRB7 was induced (Opperman *et al.,* 1994). This induction was specific to the giant root cells that differentiate due to the nematode infection. Transcripts encoding aquaporins homologous to TobRB7 in parsley and Medicago (*Medicago truncatula*) were also found to be highly abundant in roots that were infected by symbiotic arbuscular mycorrhizae (Krajinski *et al.,* 2000; Roussel *et al.,* 1997). There may be roles for TIPs in response to biotic stressors, like pathogen infection, because vacuolar localised channels TIPs are involved in the transport of water, nutrients and stress-induced signalling molecule (e.g. H_2O_2; Bienert *et al.,* 2007). For example, during Rhizobia infection in Medicago the TIP1g is retargeted from the tonoplast to the symbiosome membrane (Gavrin *et al.,* 2014). The symbiosomes of *Tip1g:RNAi* plants were also found to be unable to fully develop. As both symbionts and pathogens rely on their host organism for nutrients, enhanced or otherwise altered plant transport capacity for water and/or other solutes could be required to assist with symbiont establishment or adapt to pathogen invasion.

Cereal cyst nematode (CCN) *Heterodera avenae* is an obligate soil-borne parasite that infects the roots of cereal crops such as barley, wheat and oat. CCN infection can result in significant yield losses. Genetic variation for CCN resistance exists among the plant species that are hosts for CCN infection (for review see Van Gansbeke *et al.,* 2019). In dicot species several genes associated with CCN resistance have been identified (Liu *et al.,* 2012; Liu *et al.,* 2017; Paal *et al.,* 2004). For some monocot species, namely barley and wheat, resistance loci have been mapped (for review see Jayatilake *et al.,* 2015; Van Gansbeke *et al.,* 2019).

Through cereal breeding and use of CCN resistant cereal cultivars, yield loss from CCN infection has been reduced (Murray and Brennan, 2010). In barley, research into CCN resistance had identified 4 resistance loci: *Rha1, Rha2, Rha3* and *Rha4* (Andersen and Andersen, 1973; Barr *et al.*, 1998; Cotten and Hayes, 1969; Kretschmer *et al.*, 1997). A recent report investigating CCN resistance genes in barley has mapped the CCN resistance locus *Rha2* to a 978 kbp region on chromosome 2H (Van Gansbeke *et al.*, 2019). Within this region several single nucleotide polymorphisms (SNPs) were identified between CCN resistant barley cultivar, SloopSA, and its CCN susceptible ancestor, Sloop. One gene containing a SNP was predicted to encode HvTIP2;2 (Van Gansbeke *et al.*, 2019) where HvTIP2;2 alleles in the Sloop and SloopSA cultivars differ by a single amino acid in the third transmembrane helix. The authors suggest that if HvTIP2;2 Sloop SA has an enhanced transport capacity, of either water or other solutes such as NH_3, this may be related to the enlarged vacuoles observed in the syncytia (multi-nucleated cell formed by fusion of multiple cells induced by nematode infection) of CCN infected resistant plants (Van Gansbeke *et al.*, 2019).

Given that some PIP aquaporins were found to facilitate ion transport (Chapters 3-5), it is possible the difference in CCN resistance between Sloop and SloopSA cultivars may be related to differences in water or ion transport capacity of the two HvTIP2;2 alleles. Using *X. laevis* oocytes as an expression system the water and ion transport function of the Sloop and SloopSA HvTIP2;2 alleles were tested. Gene sequences for HvTIP2;2 Sloop and HvTIP2;2 SloopSA were kindly provided by Professor Diane Mather (UoA).

6.2 Results

6.2.1 HvTIP2;2 is a functional water channel

Previously characterised TIPs have displayed significant water permeability, although some can also facilitate the transport of other solutes (Barzana *et al.*, 2014; Bienert *et al.*, 2007; Gerbeau *et al.*, 1999; Jahn *et al.*, 2004; Loqué *et al.*, 2005). A single nucleotide polymorphism (SNP) was identified between the TIP2;2 alleles of the Sloop SA and Sloop barley. The single amino acid difference occurs in the third transmembrane domain where

SloopSA TIP2;2 has a F at site 117 (HvTIP2;2-F117) and Sloop TIP2;2 has an L (HvTIP2;2-L117).

Towards determining if this SNP would result in protein functional differences that could be linked to the SloopSA CCN resistant phenotype the water permeability of both HvTIP2;2-L117 and HvTIP2;2-F117 were examined by their expression in *X. laevis* oocytes (Figure 6.1). HvTIP2;2 injected oocytes were first pre-incubated in Na100 before being transferred to a 1 in 5 dilution of the same solution (osmolarity: 45 mOsm.kg^{-1}) for a photometric swelling assay.

Oocytes expressing either of the HvTIP2;2 alleles had greater water permeability than the water injected control oocytes (Figure 6.1). The allele associated with CCN resistance, HvTIP2;2-F117, had higher water permeability than the HvTIP2;2-L117 (Figure 6.1).

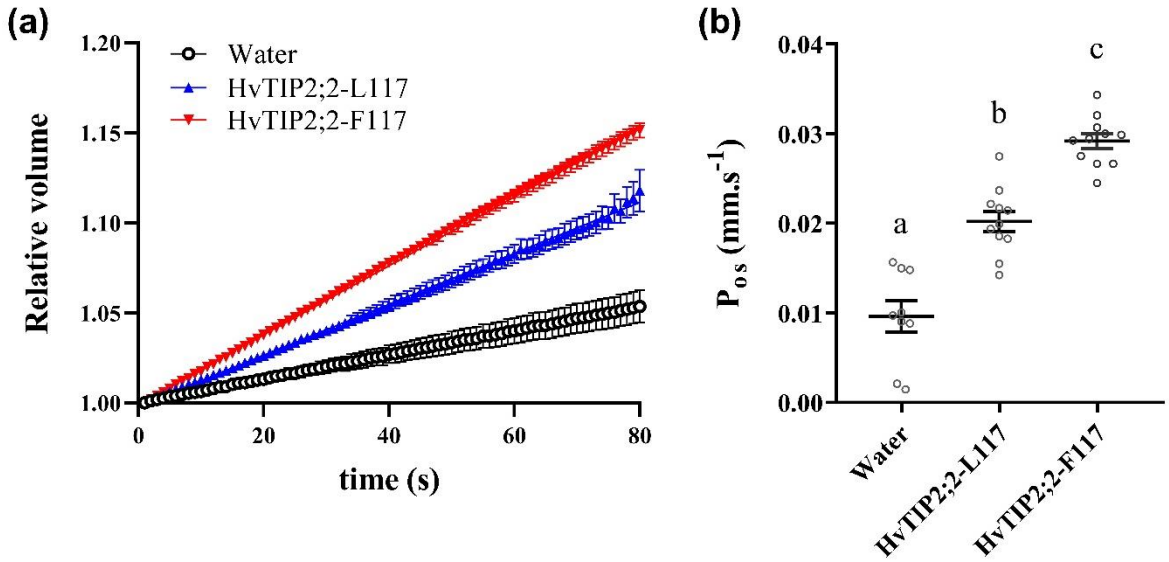

Figure 6.1: HvTIP2;2 is a functional water channel when expressed in *X. laevis* oocytes. Oocytes were injected with either water or water containing HvTIP2;2-L117 or HvTIP2;2-F117 cRNA and stored in Low Na^+ Ringers solution for 48 h prior to swelling. Oocytes were pre-incubated in Na100 for 1 h prior to being transferred to a 1:5 dilution of the same solution for the assay. **(a)** Relative volume increases over time for water-injected control and HvTIP2;2 expressing oocytes. **(b)** Osmotic permeability (P_{os}) of water control and HvTIP2;2 expressing oocytes. Data was compiled from three independent oocyte batches and is shown as mean ± SEM where each data point represents an individual oocyte. Letters indicate statistically significant differences ($p < 0.5$) by one-way ANOVA, Fishers post-test.

6.2.2 HvTIP2;2 has ion channel function

Members from the PIP and NIP plant aquaporin sub-families have demonstrated ion channel function (Byrt *et al.,* 2017; Kourghi *et al.,* 2017; Weaver *et al.,* 1994); members of the TIP sub-family may also have this function. If HvTIP2;2 has ion channel function, there may be differences between HvTIP2;2-L117 and HvTIP2;2-F117 similar to what was observed for water permeability (Figure 6.1). To investigate this, the ion transport activity of the two HvTIP2;2 alleles was tested in *X. laevis* oocytes by TEVC.

Both HvTIP2;2-L117 and HvTIP2;2-F117 have ion channel function when expressed in *X. laevis* oocytes; however, only HvTIP2;2-F117 conductance was significantly greater than that of water injected controls (Figure 6.2 and 6.3). The voltage characteristics of the HvTIP2;2s are very different to those observed for PIPs (see AtPIP2;1 as an example; Figure 6.2 and 6.3); AtPIP2;1 mediated currents are voltage- and time-independent whereas the HvTIP2;2-F117, and to a lesser extent HvTIP2;2-L117, displayed time-dependent deactivation at the more negative voltages tested (Figure 6.2 and 6.3). Interestingly, HvTIP2;2-F117 exhibited greater ionic conductance as well as greater water permeability compared to HvTIP2;2-L117 (Figure 6.1 and 6.3).

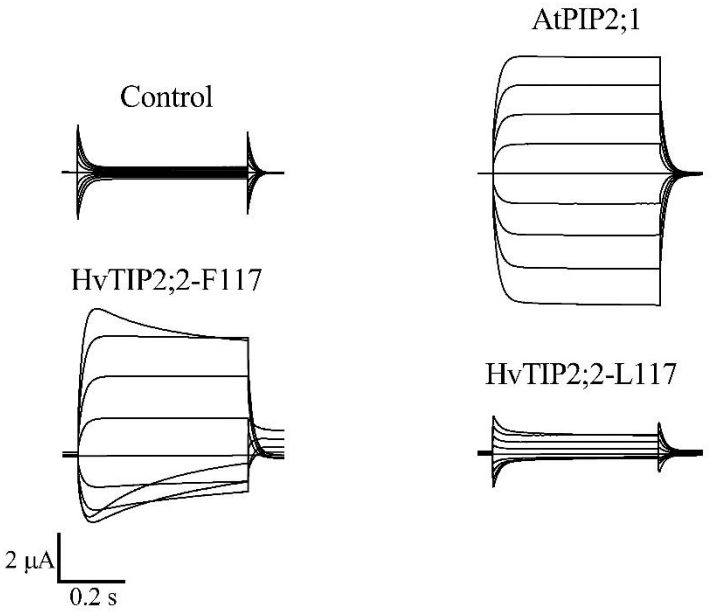

Figure 6.2: Examples of current traces of AtPIP2;1, HvTIP2;2-F117 and HvTIP2;2-L117. Oocytes were injected with either water (control) or water containing AtPIP2;1, HvTIP2;2-L117 or HvTIP2;2-F117 cRNA. Injected oocytes were stored in Low Na^+ Ringers solution for 48 h. Currents are shown as a function of time measured by TEVC (steps from 40 mV to −120 mV from a holding potential of −40 mV) in Na100.

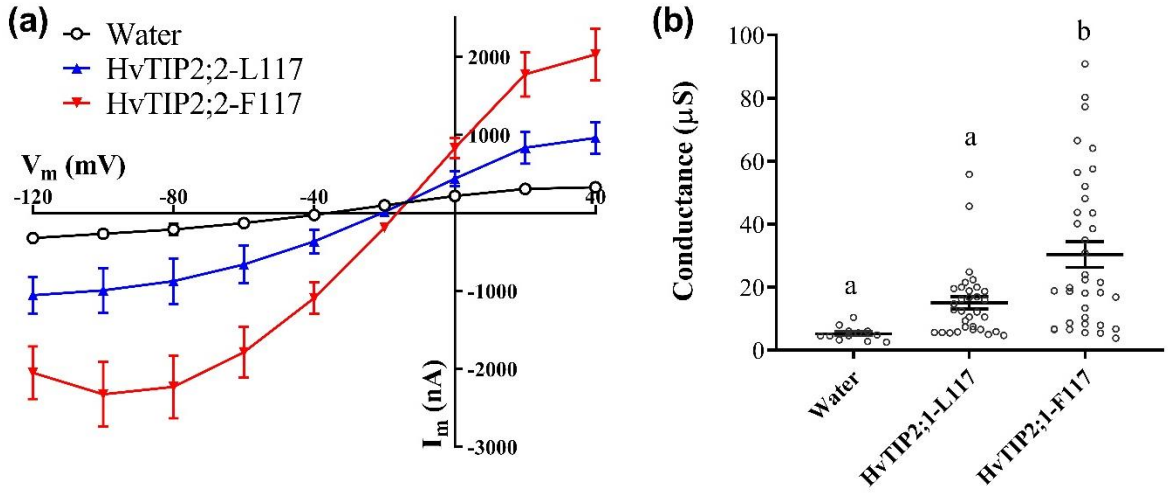

Figure 6.3: Ion channel function of HvTIP2;2-L117 and HvTIP2;2-F117 variants expressed in *X. laevis* oocytes. Oocytes were injected with either water or water containing HvTIP2;2-L117 or HvTIP2;2-F117 cRNA. Injected oocytes were stored in Low Na^+ Ringers solution for 48 h prior to TEVC. TEVC was performed in Na100. **(a)** IV curve of one representative batch. **(b)** Conductance of HvTIP2;2 injected oocytes. Data is compiled from three independent oocyte batches and is shown as mean ± SEM where each data point represents an individual oocyte. Statistical significance ($p < 0.05$) was determined by one-way ANOVA (Fishers post-test) and indicated by different letters.

6.3 Discussion

In addition to PIPs, TIPs may also facilitate ion transport. Both HvTIP2;2-L117 and HvTIP2;2-F117 were functional water and ion channels (Figure 6.1; Figure 6.3). The ion conductance properties of the HvTIP2;2s were also very different to those exhibited by the ion transporting AtPIP2;1 (Figure 6.2). Furthermore, the HvTIP2;2 allele from the CCN-resistant cultivar, HvTIP2;2-F117, had greater water permeability and ionic conductance than that of HvTIP2;2 allele from its CCN resistant ancestor, HvTIP2;2-L117 (Figure 6.1; Figure 6.3). The HvTIP2;2 alleles were discovered by fine mapping the CCN resistance loci *Rha2*; the greater water and ion channel function of HvTIP2;2-F117 may be associated with the CCN resistance of the SloopSA cultivar but further research is needed to test this hypothesis *in planta*. This may include gene editing the TIP2;2 of CCN susceptible barley cultivars to the CCN-resistant TIP2;2 and testing CCN-resistance of gene edited plants.

Vacuolar transporters and channels, such as TIPs, facilitate the movement of molecules across the tonoplast. As HvTIP2;2 has demonstrated water and ion channel function when expressed in the heterologous expression system *X. laevis* oocytes (Figure 6.1 and 6.3) it may be contributing to tonoplast water and ion flux. Similar to NSCCs in plant cell plasma membranes, there are channels that contribute to non-selective ion currents across the tonoplast whose molecular identity are still unknown (for review see Pottosin & Dobrovinskaya, 2014). Patch-clamp of plant cell vacuoles determined the existence of two types of NSCCs on the tonoplast; slow vacuolar (SV) channels, and fast vacuolar (FV) channels (for review see Demidchik and Maathuis, 2007; Chapter 1 Table 1.1). SV channels have been reported to be active on the tonoplast in all tissue types of terrestrial plants (for review see Hedrich and Marten, 2011) and a gene encoding for an SV channel has been identified in Arabidopsis as AtTPC1 (Peiter *et al.,* 2005). However there is no conclusive candidate for FV channels, which are predominately active in root and leaf cell vacuoles (for reviews see Pottosin and Dobrovinskaya, 2014; Ward *et al.,* 2009). FV channels are inhibited by the divalent cations Ca^{2+} and Mg^{2+} (Brüggemann *et al.,* 1999a; Tikhonova *et al.,* 1997) and show bi-phasic voltage dependence where they are gated open at large positive or negative voltages (Pottosin *et al.,* 2003; Tikhonova *et al.,* 1997). FV channels show greatest permeability for NH_4^+ (< 25%) than other monovalent cations (Brüggemann *et al.,* 1999b). To further investigate HvTIP2;2 as a candidate for vacuolar NSCC, response to divalent cations (e.g. Ca^{2+} and Mg^{2+}) and the relative permeability to other monovalent cations (e.g. K^+ and particularly NH_4^+) would need to be established.

HvTIP2;2 is the first TIP aquaporin that has been identified as having ion channel function. However there is some sort of a precedence for ion transport for TIP isoforms in the literature. Resolution of AtTIP2;1 crystal structure revealed a novel water-filled side pore that extends from the monomeric pore to the vacuole facing vestibule (Kirscht *et al.,* 2016). It was suggested that this side pore functions to deprotonate ammonium ions as they move through the AtTIP2;1 monomeric pore from the cytosol, or alternatively, to protonate ammonia as it moves from the cytosol to the vacuole (Kirscht *et al.,* 2016). The latter could be a mechanism to maintain the ammonium 'acid trap' in the vacuole (Loqué *et al.,* 2005; Wood *et al.,* 2006). This means that there is not only a (side) pore through which H^+ moves, but ammonium ions may also travel part of the way through the AtTIP2;1 pore although modelling of AtTIP2;1 predicted no ammonium permeation through the monomeric pore due to electrostatic repulsion and desolvation effects (Kirscht *et al.,* 2016).

The greater water permeability and ionic conductance of HvTIP2;2-F117 may be associated with the CCN resistance of the SloopSA barley cultivar. The authors who identified HvTIP2;2 as a candidate gene in the *Rha2* CCN resistance loci speculated that increased permeation of water and other solutes across the tonoplast could cause the enlarged vacuoles observed in the syncytia formed in CCN infected roots of CCN resistant SloopSA plants (Van Gansbeke *et al.,* 2019). While the exact mechanism(s) that confer CCN resistance are at present unknown, it could be that the increased water and solute movement through HvTIP2;2-F117 aids in the formation of these large vacuoles. Enlarged vacuoles may confer resistance through restriction of cytosolic space for the CCN to occupy and/or by reducing nutrient availability by enhanced solute movement into the vacuole. The greater outward rectification of HvTIP2;2-F117 indicates that it may facilitate greater flux into rather than out of the vacuole (Figure 6.2 and 6.3). The tendency for HvTIP2;2-F117 to close at more negative membrane potentials (i.e. when the tonoplast becomes more negative) may prevent solute leakage from the vacuole to the cytosol (Figure 6.2 and 6.3). In future research it will be particularly prudent to examine HvTIP2;2-F117 for permeability to other solutes such as NH_4^+ or K^+ which may be more physiologically valuable, both for the plant to sequester into the vacuole and for the CCN to appropriate.

Observation of ion permeability for HvTIP2;2 leads us to the hypothesis that aquaporins with water and ion channel functions may be present in multiple aquaporin sub-families, not just within the PIPs or indeed NIPs (Weaver *et al.,* 1994). The ion channel function may be inextricably linked to the diverse and crucial roles aquaporins have in all aspects of plant growth, development, reproduction, and abiotic and biotic stress responses.

Chapter 7: Investigating the evolutionary origins and permeability characteristics of ion permeable aquaporins

7.1 Introduction

Ion channel function for aquaporins is a feature common across the plant and animal kingdoms (Byrt *et al.,* 2017; Liu *et al.,* 2005; Weaver *et al.,* 1994; Yanochko and Yool, 2002; Yool *et al.,* 1996). This suggests that there could be early evolutionary origin for aquaporin ion channel function, although of course it is possible that ion permeation evolved independently in plants and animals after their evolutionary divergence, which is estimated to have occurred approximately one billion years ago (Doolittle *et al.,* 1996). Plants exhibit the greatest aquaporin diversification with a high multiplicity of isoforms. In Arabidopsis 35 aquaporins have been identified (Johanson *et al.,* 2001) and in the grasses rice (*Oryza sativa*), maize (*Zea mays*) and sorghum (*Sorghum bicolor*), 33, 36 and 41 aquaporin encoding genes have been identified, respectively (Chaumont *et al.,* 2001; Reddy *et al.,* 2015; Sakurai *et al.,* 2005).

Based on sequence homology and subcellular localisation patterns plant aquaporins form several subfamilies; plasma membrane intrinsic proteins (PIPs), tonoplast intrinsic proteins (TIPs), nodulin-26 intrinsic proteins (NIPs), small basic intrinsic proteins (SIPs) and X-intrinsic proteins (XIPs; not present in monocots). Other MIP subfamilies, such as the hybrid intrinsic proteins (HIPs) and GlpF-like intrinsic proteins (GIPs) are found only in mosses and were lost during the evolution of higher land plants (Figure 7.1b; Anderberg *et al.,* 2011; Danielson and Johanson, 2008; Li *et al.,* 2014). Identification of several aquaporins in dicots and monocots capable of facilitating ion transport (see Chapters 3-5) at least indicates that a common land plant ancestor, such as terrestrial algae, may have possessed an aquaporin with both water and ion transport function.

Klebsormidium nitens is a charophytic filamentous terrestrial alga generally considered to be closely related to the common ancestor of the first land plants (Figure 7.1a; Leliaert *et al.,* 2012; Lewis and McCourt, 2004). Furthermore, the *K. nitens* genome has been sequenced (Hori *et al.,* 2014) providing opportunity to investigate whether the aquaporins of early plant ancestors may have ion channel function (Figure 7.1b).

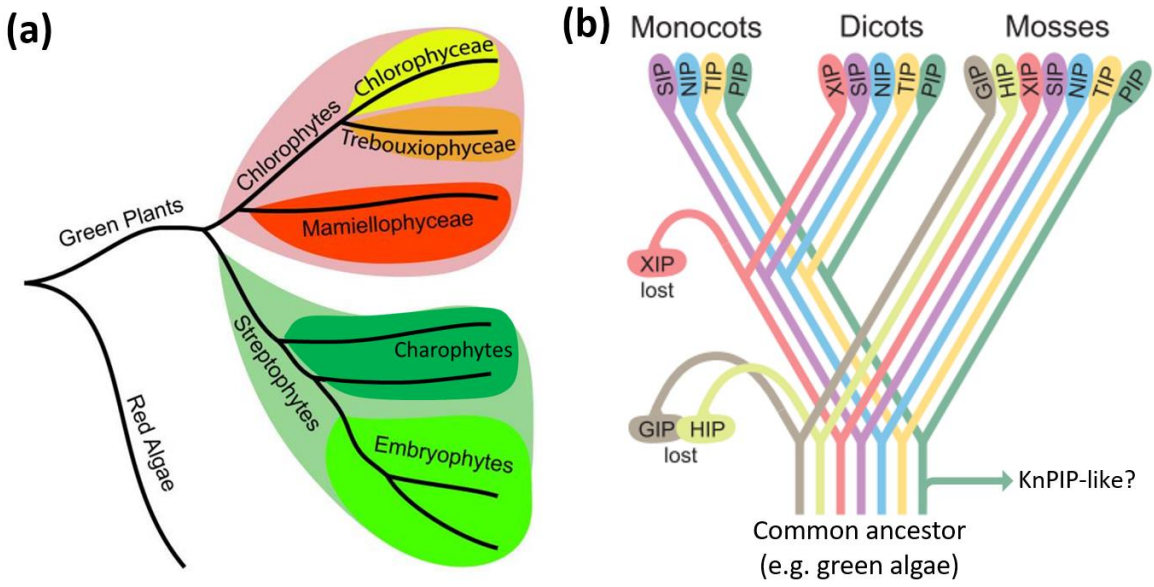

Figure 7.1: Evolution of green plants and the MIP protein family in land plants. (a) Basic phylogeny of green plants. Green plants consist of two phyla; the chlorophytes which include a number of classes of green algae, and the streptophytes which include charophytic green algae and land plants (embryophytes). Figure adapted from Anderberg *et al.,* (2011). **(b)** During the evolution of higher land plants, both GIPs and HIPs subfamilies were lost; and subsequently, during the divergence of monocots from dicots the XIPs were lost in monocots. An early PIP-like aquaporin in a green alga such as *K. nitens* (KnPIP-like) may possess the functional characteristics of water and ion transport, also found in some land plant PIPs, suggesting an early evolutionary origin of these features. Figure adapted from Danielson and Johanson (2008).

Arabidopsis PIP2;1 and PIP2;2 (AtPIP2;1 and AtPIP2;2) are molecular candidates proposed to contribute to the non-selective cation channel (NSCC) ionic conductance previously measured *in planta* (Byrt *et al.,* 2017; Essah *et al.,* 2003; McGaughey *et al.,* 2018; see also Chapter 1 Table 1). NSCCs are a group of transmembrane channel proteins that are permeable to a wide range of cations (see Chapter 1.2). However, the molecular identity of many of the channels conferring NSC currents have not been determined. Towards assessing whether AtPIP2;1 could account for NSCC conductances in Arabidopsis roots the scaled magnitudes for AtPIP2;1 water permeability and ionic conductance in *X. laevis* oocytes reported in (Byrt *et al.,* 2017), and the measured water permeabilities and NSCC conductances of Arabidopsis root protoplasts were compared (see McGaughey *et al.,* 2018). This comparison of the scaled magnitude for AtPIP2;1 conductance indicated that AtPIP2;1 hypothetically could quantitatively account for the NSCC conductance measured *in planta*, in Arabidopsis roots (McGaughey *et al.,* 2018). If ion permeable aquaporins are contributing to NSCC currents that have been identified *in planta* then they would be expected to exhibit

permeability to a range of monovalent cations *in vivo*. AtPIP2;1 was previously shown to be permeable to Na^+ (Byrt *et al.,* 2017) and in Chapter 3 it was demonstrated that AtPIP2;1 is also permeable to K^+ when expressed in *X. laevis* oocytes. AtPIP2;1 permeability to other monovalent cations including Rubidium (Rb^+), Cesium (Cs^+), and Ammonium (NH_4^+) remain to be tested.

Aquaporins have also been proposed to be osmo-sensors and some isoforms show mechano-sensitive properties (for reviews see Hill and Shachar-Hill, 2015; Ozu *et al.,* 2018). The perception of osmotic stress initiates a range of adaptive responses including signal transduction, transcriptional regulation and post-translational modification of proteins (Johansson *et al.,* 2000). However, the mechanisms and molecular identity of proteins involved in how plant cells perceive changes in osmotic pressure have not been comprehensively revealed (Nongpiur *et al.,* 2019). Changes in membrane tension has been proposed as a regulatory mechanism for several aquaporins across the taxonomic kingdoms of life including in the plant species maize, red beet (*Beta vulgaris*) and grapevine (*Vitis vinifera*) (Goldman *et al.,* 2017; Leitão *et al.,* 2014; Ozu *et al.,* 2011; Ozu *et al.,* 2013; Soveral *et al.,* 2008; Wan *et al.,* 2004; Ye *et al.,* 2004). Regulation of aquaporin function by changes in osmotic pressure or membrane tension is hypothesised to be an adaptive response to hyper- and hypo-osmotic stress (Hill and Shachar-Hill, 2015). When osmotic pressure was increased, the osmotic permeability of wheat root cell tonoplast enriched vesicles decreased (Niemietz and Tyerman, 1997). A similar, but even more dramatic, response was observed for NOD-26 enriched symbiosome vesicles (Vandeleur *et al.,* 2005). *Beta vulgaris* TIP1;2 (BvTIP1;2) and VvTIP2;1 when expressed in *X. laevis* oocytes and yeast respectively, were gated from an open to closed state in a membrane-tension dependent manner (Goldman *et al.,* 2017; Leitão *et al.,* 2014). Mechano-sensitive ion channels have also been described in plants (for review see Hamilton *et al.,* 2014). Mechano-sensitive ion channels function in osmotic shock protection and generally mediate the release of metabolites or ions in response to hypo-osmotic stress (Booth and Blount, 2012; Haswell *et al.,* 2011). Changes to AtPIP2;1 localisation and function have previously been associated with osmotic stress (Boursiac *et al.,* 2005; Li *et al.,* 2011; Prak *et al.,* 2008, see also Chapter 1). As a dual water and ion permeable aquaporin, the ion channel function of AtPIP2;1 may be influenced by membrane tension changes.

This chapter investigates whether AtPIP2;1 is permeable to the monovalent cations Rb^+ and Cs^+, and whether AtPIP2;1 ion channel function is influenced by changes in osmotic pressure. As described in previous chapters (see Chapter 3) AtPIP2;1 phospho-mutants were

identified that carry large Na^+ currents that are more consistently observed than that of the wild-type AtPIP2;1. Therefore, these mutants were used alongside wild-type AtPIP2;1 in experiments directed at assessing the permeability of AtPIP2;1 to other cations and the response to changes in osmotic pressure and oocyte membrane tension. The water and ion permeability characteristics of a PIP-like aquaporin from *K. nitens* is also tested.

7.2 Results

7.2.1 AtPIP2;1 is permeable to the monovalent cations Rb^+ and Cs^+

AtPIP2;1 has been proposed as a molecular candidate that could contribute to *in planta* currents associated with NSCCs. Previously, AtPIP2;1 was shown to be permeable to the monovalent cations Na^+ and K^+ (Byrt *et al.,* 2017; Kourghi *et al.,* 2017; Chapter 3). AtPIP2;l, and in some cases AtPIP2;1 S283D, were expressed in *X. laevis* oocytes and TEVC performed to investigate AtPIP2;1 permeability to the monovalent cations Rb^+ and Cs^+. AtPIP2;1 can facilitate Rb^+ transport when expressed in *X. laevis* oocytes (Figure 7.2a-b). In a Rb50 solution, AtPIP2;1 expressing oocytes had higher ionic conductance than that of water controls (Figure 7.2b). AtPIP2;1 permeability to Cs^+ was investigated in a Cs100 solution. Oocytes expressing AtPIP2;1 or the phospho-mimic mutant AtPIP2;1 S283D had greater ionic conductance than water injected controls (Figure 7.2c-d). This is consistent with observations for Na^+ or K^+ associated conductance mediated by the AtPIP2;1 phospho-mimic S283D reported in Chapter 3. Similarly, oocytes expressing AtPIP2;1 S283D had significantly greater ionic conductance than oocytes expressing wild type AtPIP2;1 when assayed in solutions containing Cs^+ (Figure 7.2d).

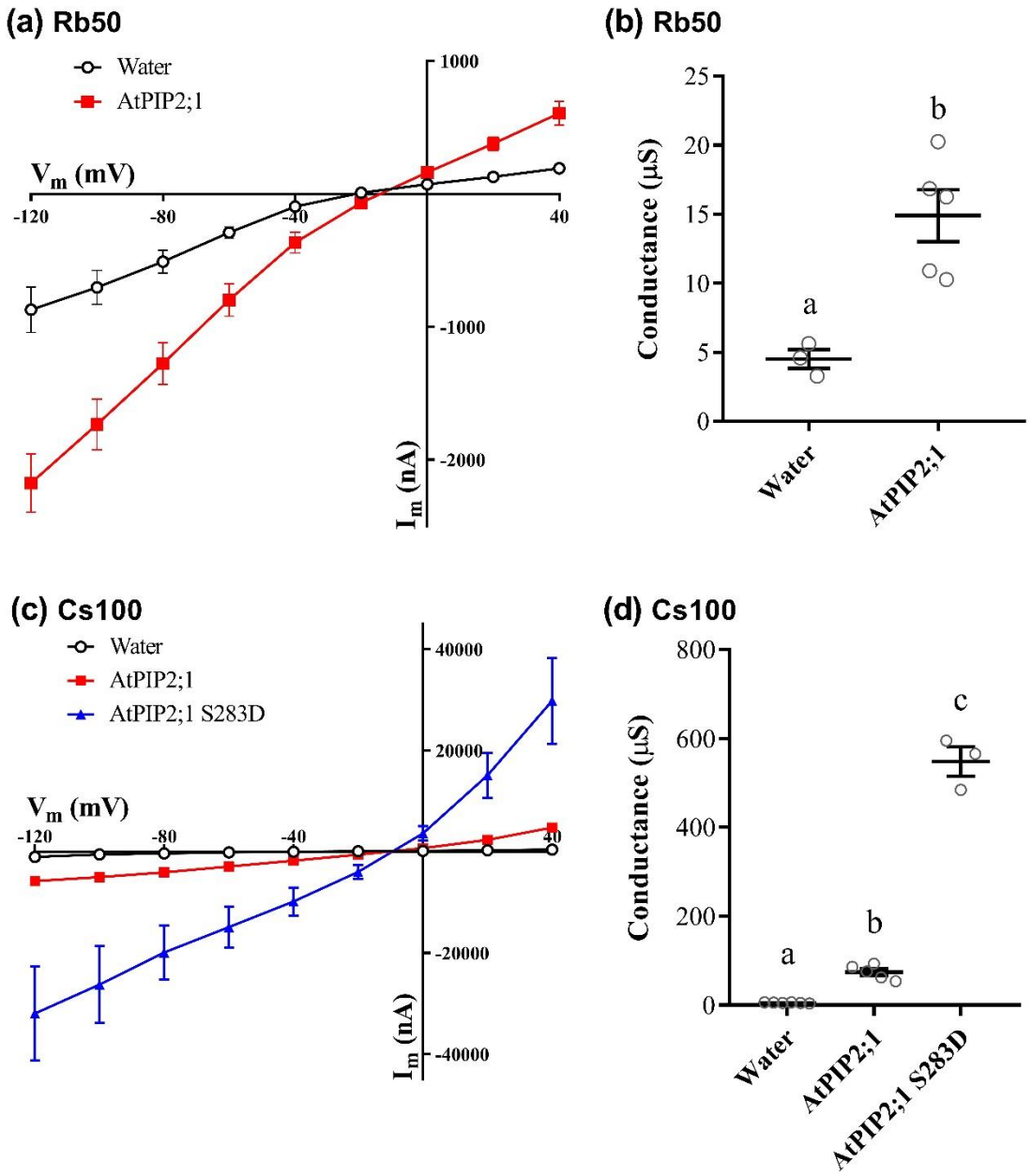

Figure 7.2: AtPIP2;1 facilitates the transport of the monovalent cations Rb^+ and Cs^+. Oocytes were injected with either 46 nL water or 46 nL water containing AtPIP2;1 or AtPIP2;1 S283D cRNA and incubated in Low Na^+ Ringers for 24-30 h. TEVC was performed in Rb50 and Cs100. **(a)** IV curve of injected oocytes in Rb50. **(b)** Ionic conductance of injected oocytes in Rb50. Data is shown as mean ± SEM where each data point represents an individual oocyte. **(c)** IV curve of injected oocytes in Cs100. TEVC was performed in collaboration with Dr Jiaen Qiu. **(d)** Ionic conductance of injected oocytes in Cs100. Data is shown as mean ± SEM where each data point represents an individual oocyte. Different letters indicate statistical significance ($p < 0.05$) by (b) two-tailed t-test and (d) one-way ANOVA.

7.2.2 AtPIP2;1 induced currents in response to changes in osmotic pressure

There has been speculation that aquaporins may have a role as osmo-sensors and the water channel activity of some plant aquaporins have been demonstrated to be mechano-sensitive (Goldman *et al.*, 2017; Hill *et al.*, 2004; Leitão *et al.*, 2014). Whether AtPIP2;1 ion channel function may be influenced by alterations in osmotic pressure, indicating a potential role in osmo-sensing, or a stretch-activated functional component was investigated here. AtPIP2;1 and the AtPIP2;1 S283D phopho-mimic mutant, which elicits currents of a greater magnitude, were expressed in *X. laevis* oocytes and exposed sequentially to Na50 solutions with identical ionic concentrations but differing osmolarity. Oocytes were first exposed to an isotonic solution and then a hypotonic solution; the hypotonic solution had an osmolarity of 170 $mOsm.kg^{-1}$ and the isotonic solution was adjusted with mannitol to have an osmolarity of 240 $mOsm.kg^{-1}$. The difference in osmolarity between the hypo- and iso-tonic solutions used in this experiment was limited to prevent excessive swelling of the oocyte while clamped by the two electrodes, because this would cause physical damage to the oocyte.

It should be noted that due to the solution composition and design of the experiment, the influence of three effects on AtPIP2;1 ion channel function were being measured simultaneously. During the experiment there would have been inward water flow from the change in solution osmolarity. This would in turn cause some oocyte swelling and increase membrane tension. Water flow would be also be in the opposing direction to the ion current imposed by some voltage clamp steps. Therefore, this experiment can only give an indication on whether AtPIP2;1 ion transport is likely to be osmo-sensing or stretch activated.

There was no statistically significant differences between ionic conductance of water control oocytes, or those expressing AtPIP2;1 and AtPIP2;1 phospho-mimic mutants in either the isotonic or hypotonic solutions (Figure 7.3).

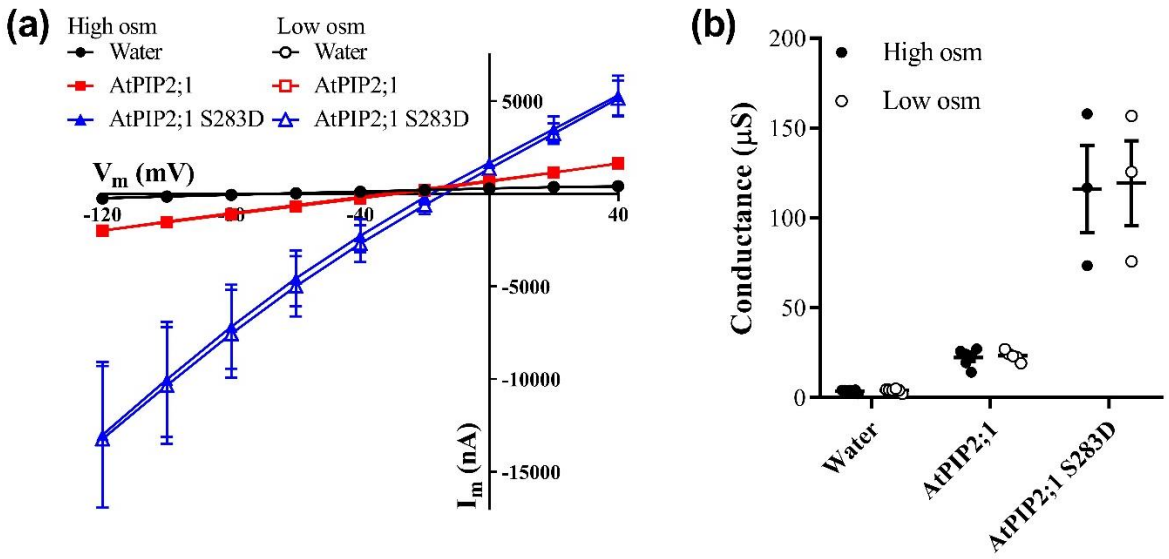

Figure 7.3: Ion channel function of AtPIP2;1 wild-type and the AtPIP2;1 S283D phospho-mutant in solutions with different external osmolarity. Oocytes were injected with either 46 nL water or 46 nL water containing wild-type AtPIP2;1 or AtPIP2;1 S283D cRNA and incubated in Low Na^+ Ringers for 24-30 h. TEVC was performed Na50 with either an osmolarity of 240 $mOsm.kg^{-1}$ adjusted with D-mannitol (high osm), or an otherwise identical solution with an osmolarity of 170 $mOsm.kg^{-1}$ adjusted with D-mannitol (low osm). Data was obtained from the same oocytes that were sequentially exposed to both solutions (high then low). **(a)** IV curve of injected oocytes in the high (solid shapes) and low (unfilled shapes) osmolarity solutions. Where IV data points are obscured for low osm treatments they are identical to high osm. **(b)** Ionic conductance of injected oocytes in the high osm and low osm solutions. Data is shown as mean ± SEM where each data point represents an individual oocyte.

7.2.3 Ion and water channel function of *Klebsormidium nitens* PIP-like aquaporin

The genome of the charophytic filamentous green algae *K. nitens* (previously identified as *K. flaccidum*) was recently sequenced and made publicly available enabling the identification of MIP encoding genes. MIP protein sequences from several algal species along with MIPs from the moss *Physcomitrella patens* and the higher plant and model dicot Arabidopsis (Anderberg *et al.,* 2011; Danielson and Johanson, 2008; Johanson *et al.,* 2001) were used to BLAST search the *K. nitens* genome and 14 possible MIP orthologs were identified (Figure 7.4). Of these, eight may be classified as full-length MIPs consisting of six predicted transmembrane helices and two NPA motifs (or in the case of kfl00057_0120 an NPA and NPV motif) (Figure 7.4a). Phylogenetic analyses of the putative *K. nitens* MIPs was performed using protein sequences of the 22 algal MIPs identified in Anderberg *et al.,* (2011) and *P. patens* MIPs identified in Danielson and Johanson, (2008). The N- and C-termini of the MIPs were excluded from this analysis due to their high sequence divergence (Anderberg *et al.,* 2011). Phylogenetic analysis of *K. nitens* MIPs revealed that it possesses representative orthologs of each algal specific sub-family (MIPA-E) and the sub-families present in land plants (Figure 7.4b). The *K. nitens* MIP kfl00044_0280 was selected for further characterisation and investigation because it was the only full-length KnMIP that clustered with the PIP sub-family (Figure 7.4b) and will be referred to as KnPIP-like.

(a)

Accession number	Protein length	TMHMM prediction and NPA location
kfl00044_0280	332	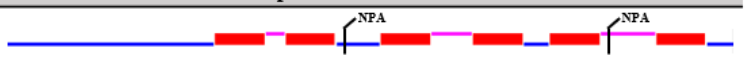
kfl00259_0180	211	
kfl00089_0120	260	
kfl01697_0010	256	
kfl00620_0140	314	
kfl00056_0210	257	
kfl01013_0040	182	
kfl00019_0540	279	
kfl00068_0250	318	
kfl00064_0100	221	
kfl00068_0230	267	
kfl00111_0030	212	
kfl00002_0390	387	
kfl00057_0120	246	

(b)

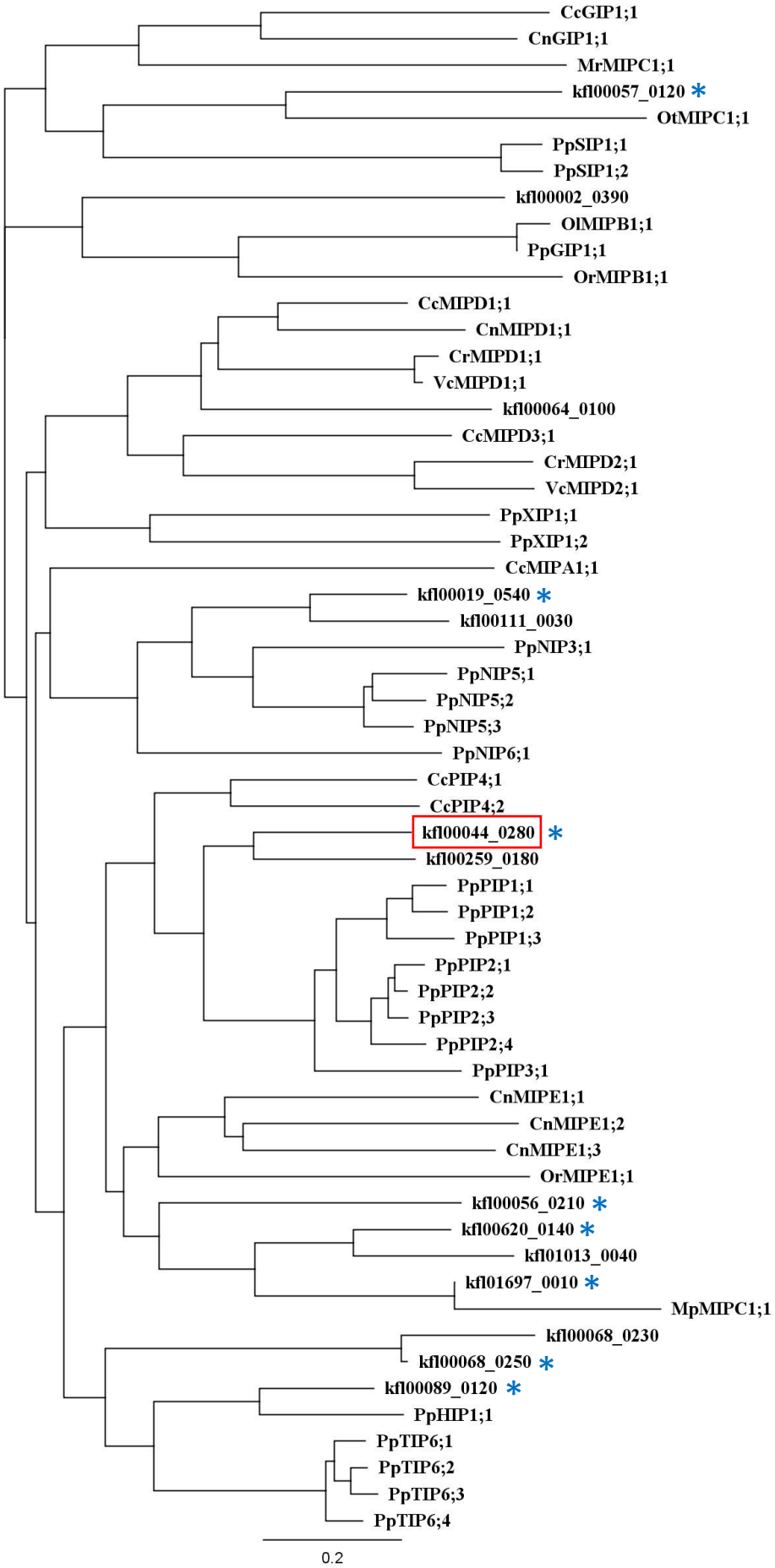
CcGIP1;1
CnGIP1;1
MrMIPC1;1
kfl00057_0120 *
OtMIPC1;1
PpSIP1;1
PpSIP1;2
kfl00002_0390
OlMIPB1;1
PpGIP1;1
OrMIPB1;1
CcMIPD1;1
CnMIPD1;1
CrMIPD1;1
VcMIPD1;1
kfl00064_0100
CcMIPD3;1
CrMIPD2;1
VcMIPD2;1
PpXIP1;1
PpXIP1;2
CcMIPA1;1
kfl00019_0540 *
kfl00111_0030
PpNIP3;1
PpNIP5;1
PpNIP5;2
PpNIP5;3
PpNIP6;1
CcPIP4;1
CcPIP4;2
kfl00044_0280 *
kfl00259_0180
PpPIP1;1
PpPIP1;2
PpPIP1;3
PpPIP2;1
PpPIP2;2
PpPIP2;3
PpPIP2;4
PpPIP3;1
CnMIPE1;1
CnMIPE1;2
CnMIPE1;3
OrMIPE1;1
kfl00056_0210 *
kfl00620_0140 *
kfl01013_0040
kfl01697_0010 *
MpMIPC1;1
kfl00068_0230
kfl00068_0250 *
kfl00089_0120 *
PpHIP1;1
PpTIP6;1
PpTIP6;2
PpTIP6;3
PpTIP6;4
0.2

Figure 7.4: Putative MIP orthologs identified in *K. nitens* genome and phylogenetic analysis. The publicly available *K. nitens* genome (http://www.plantmorphogenesis.bio.titech.ac.jp/~algae_genome_project/klebsormidium/index.html; last accessed September 2019) was mined for MIPs via BLAST of algal MIPs identified in Anderberg *et al.*, (2011) and MIPs from *P. patens* and Arabidopsis. **(a)** Accession numbers and protein sequence length (number of amino acids) of closest hits from BLAST search. The TMHMM predicted transmembrane helices (TMHMMv2.0: http://www.cbs.dtu.dk/services/TMHMM/) are shown as thick red bars, inside/cytosolic facing regions shown as thin blue bars and outside/extracellular facing regions shown as thin pink bars. Approximate NPA motif locations are indicated by black markers. **(b)** Phylogenetic analysis of putative MIPs from *K. nitens*. MIP protein sequences, excluding the N- and C-termini, from the algal species *K. nitens* (kfl), *Chlamydomonas reinhardtii* (Cr), *Volvox carteri* (Vc), *Coccomyxa C-169*[g] (Cc), *Chlorella NC64A* (Cn), *Ostreococcus lucimarinus* (Ol), *Ostreococcus RCC809* (Or), *Ostreococcus tauri* (Ot), *Micromonas pusilla CCMP1545* (Mp), *Micromonas RCC299* (Mr), and the moss *P. patens* (Pp) were used. Protein sequences for the MIPs used in the phylogenetic analysis excepting *K. nitens* were obtained from the supplementary materials of Anderberg *et al.*, (2011). The candidate KnMIP selected for further characterisation (Kfl00044_0280; KnPIP-like) is outlined in red. The full length KnPIP-like has 44.9% protein sequence similarity to AtPIP2;1. Blue asterisks indicate a full-length MIP possessing two NPA motifs. The phylogenetic tree was generated using Geneious Tree Builder (Jukes-Cantor and Neighnour-Joining method) (Geneious 8.1.3; https://www.geneious.com).

To investigate the water and ion channel function of KnPIP-like it was expressed in *X. laevis* oocytes and photometric swelling assays and TEVC were performed, respectively (Figure 7.5). Oocytes expressing KnPIP-like had greater ionic conductance and osmotic permeability (P_{os}) than water injected controls. However, KnPIP-like expressing oocytes had significantly lower (unpaired t-test: $p < 0.005$) P_{os} and ionic conductance than that of AtPIP2;1 with an average (± SEM) P_{os} of 0.0205 ± 0.0016 $mm.s^{-1}$ and conductance of 20.43 ± 3.1 µS compared to 0.0772 ± 0.0036 $mm.s^{-1}$ and 41.07 ± 5.99 µS respectively (AtPIP2;1 data from Chapter 3). The large variation in ionic conductance for KnPIP-like may be linked to variable phosphorylation between oocytes.

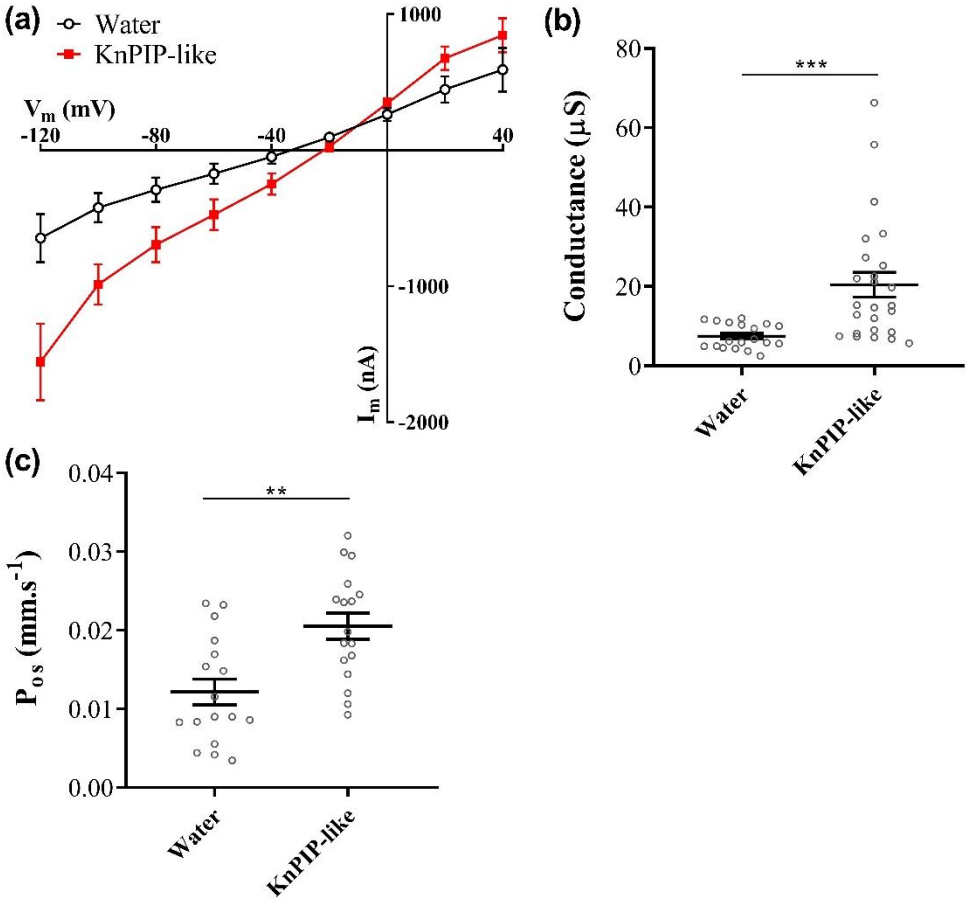

Figure 7.5: Ionic conductance and osmotic permeability of oocytes expressing the *K. nitens* PIP-like aquaporin. Oocyte were either injected with water or water containing KnPIP-like cRNA and incubated for 24-30 h post-injection in Low Na^+ Ringers. **(a)** IV curves of water and KnPIP-like injected oocytes from one representative batch. TEVC was performed in Na100. **(b)** Ionic conductance of water and KnPIP-like injected oocytes compiled from TEVC data across four independent oocyte batches. **(c)** Osmotic permeability (P_{os}) of water and KnPIP-like injected oocytes. Data is compiled from two independent oocytes batches. Data in (b) and (c) is shown as mean ± SEM where each data point represents an individual oocyte. Statistical significance determined by unpaired t-test (**: $p < 0.005$, ***: $p < 0.001$).

7.3 Discussion

7.3.1 AtPIP2;1 facilitates Rb^+ and Cs^+ transport and its ion channel function is not dependent on an hypoosmotic gradient

AtPIP2;1 is permeable to the monovalent cations Na^+ (Byrt *et al.,* 2017), K^+, Rb^+ and Cs^+ *in vivo* (Chapter 3 and Figure 7.2), which is consistent with the hypothesis that AtPIP2;1 may contribute to NSC conductance in plants. Reducing the external osmotic pressure did not influence, by either activation or inhibition, AtPIP2;1 mediated ionic conductance when expressed in *X. laevis* oocytes (Figure 7.3). Considering the direction of water flow into the oocyte during TEVC measurements, it might be expected that the inward current would be enhanced (ions carried by water) and the outward current to be reduced, but neither was observed (Figure 7.3). This indicates that AtPIP2;1 ion channel function is not stretch activated and it may not be acting as an osmo-sensor that would influence the activity of other channels and transporters.

The current-voltage characteristics of the AtPIP2;1 as an ion channel shares similarities with those previously reported for voltage-independent NSCCs (VI-NSCC). VI-NSCCs are permeable to monovalent cations with a weak selectivity profile of $K^+ > NH_4^+ > Rb^+ \sim Cs^+ \sim Na^+ > Li^+ >$ tetraethylammonium (TEA^+) (see Chapter 1, Table 1.1). AtPIP2;1 induces a conductance that carries Na^+, K^+, Rb^+ and Cs^+ *in vivo* (Byrt *et al.,* 2017; Chapter 3; Figure 7.2). Given these observations, it is likely AtPIP2;1 would be able to conduct other monovalent cations described in the selectivity profile for VI-NSCCs. However, further experiments are required to determine the order of the relative selectivity of AtPIP2;1 to each of the different monovalent cations. Determining NH_4^+ permeability of ion permeable aquaporins by TEVC could be difficult due to the acid-base properties of ammonia and the pH inhibition of aquaporins. This is because in the high pH conditions which would be required to prevent pH gating of aquaporins (for example pH 8.5 has been typically used throughout this thesis), ammonia would predominate, rather than ammonium ions. Therefore, other methods to investigate NH_4^+ permeability need to be considered as transport of NH_4^+ by ion permeable aquaporins may have important implications for nutrient acquisition. In addition to the suggested commonalities in monovalent cation permeation for NSCCs and AtPIP2;1, they also share similar regulatory properties. Both NSCCs and

AtPIP2;1 are regulated by pH, intracellular Ca^{2+} levels and cGMP (Chapter 3; Byrt *et al.,* 2017; Essah *et al.,* 2003; Kourghi *et al.,* 2017; Rubio *et al.,* 2003).

The ionic conductance of AtPIP2;1 wild-type, and the AtPIP2;1 283D phospho-mimic mutant, was not influenced by treatments designed to reduce the external osmotic pressure and cause an increase in membrane tension (Figure 7.3). A recent study investigated the osmotic response of *X. laevis* oocytes expressing either BvPIP2;1 or BvTIP1;2 when exposed to different osmotic and mechanical conditions (Goldman *et al.,* 2017). BvPIP2;1 water channel function was not mechano-sensitive; oocytes expressing BvPIP2;1 maintained the same osmotic permeability coefficient (P_f) throughout all osmotic conditions tested (Goldman *et al.,* 2017). Data reported here suggests that the ion channel function of AtPIP2;1 is not likely to be osmo-sensitive (Figure 7.3). Comparatively, BvTIP1;2 was mechano-sensitive as the P_f of oocytes expressing BvTIP1;2 decreased significantly as osmotic pressure and membrane tension increased (Goldman *et al.,* 2017). Another tonoplast localised aquaporin VvTIP2;1 was also demonstrated to be mechano-sensitive. When expressed in yeast (*S. cerevisiae*) VvTIP2;1 was gated in a similar turgor-dependent manner as was observed for BvTIP1;2 (Leitão *et al.,* 2014). The mechano-sensitivity of tonoplast localised plant aquaporins may be a mechanism enabling the osmotic adjustment of the vacuole with respect to the cytoplasm by gating TIP water transport when the cell experiences hypo-osmotic conditions (Goldman *et al.,* 2017). A study of red beet vacuoles identified an osmotic pressure activated channel that may transport both cations and water (Alexandre and Lassalles, 1991). In Chapter 5, HvTIP2;2 was shown to induce a distinctive ion conductance with properties distinct from PIP2;1. At the time of investigating the effect of osmotic pressure on AtPIP2;1, the ion permeability of the candidate TIP isoform had not been discovered. To further investigate whether aquaporins that induce ion currents respond to osmotic pressure or stretch activation it would be of interest to test whether or not TIP2;2 is osmo-sensitive.

7.3.2 Water and ion channel activities associated with a PIP-like aquaporin from the alga *K. nitens*

The transition from aquatic to terrestrial environments required algae to evolve a suite of adaptive mechanisms to overcome unpredictable and often harsh environmental conditions. These transitions eventually led to the existence of land plants as we know them today

(Hoffmann, 1989; Rensing *et al.,* 2008). Extant charophyte algae, such as the *Klebsormidium* spp., are closely related to the common ancestor of land plants (Lewis and McCourt, 2004). The *Klebsormidium* spp. are widely distributed and survive in a range of environments including those prone to drought, extreme heat or extreme cold; indeed some *Klebsormidium* spp. have exhibited tolerance to the common terrestrial abiotic stresses drought and freezing (Holzinger and Karsten, 2013; Holzinger *et al.,* 2011; Karsten and Holzinger, 2014). Tolerance to these stresses in land plants have previously been linked to the function of aquaporins (for example: Aroca *et al.,* 2005; Li *et al.,* 2016).

Phylogenetic analysis of 22 MIPs identified across 9 species of chlorophytic algal had previously revealed the presence of 5 MIP subfamilies (MIPA-E) unique to algae (Anderberg *et al.,* 2011). Some alga also encoded isoforms from the PIP and GIP subfamilies more typically associated with land plant MIPs indicating the early evolution of these MIP types in green plants (Anderberg *et al.,* 2011). A BLAST search found 14 possible MIP orthologs in the *K. nitens* genomes, although only 8 are likely to be functional MIPs as determined by the presence of the classical six transmembrane helices and two NPA motifs (Table 7.2.1). Phylogenetic analysis of all 14 KnMIPs revealed that *K. nitens* possesses MIP isoforms from all algal specific subfamilies (MIPA-E) as well as isoforms that clustered in subfamilies previously identified only in land plants (Figure 7.4). This is indicative of its evolutionary position as an intermediary between chlorophytic algae and the first land plants (Figure 7.1a).

The KnPIP-like aquaporin was a functional water and ion channel when expressed in *X. laevis* oocytes (Figure 7.5). However, KnPIP-like apparent water permeability and ionic conductance were observed to be smaller in magnitude than that of AtPIP2;1 (Figure 7.5 and Chapter 3). It is possible KnPIP-like did not target as efficiently to the PM as AtPIP2;1 and this difference in protein density resulted in lower apparent water and ion channel function. It is also possible that for *K. nitens*, limiting the KnPIP-like water and ion permeability is advantageous. Restricting passive flux of water and ions across the cell membrane could be beneficial for alga living in terrestrial habitats that may experience rapid changes in water availability, temperature changes (e.g. freezing) and desiccation.

Chapter 8: General Discussion

8.1 A historical context for aquaporin facilitated ion transport

The first report of ion channel function for a plant aquaporin was by Weaver *et al.,* in 1994. Reconstitution of soybean (*Glycine max*) NOD-26 into planar lipid bilayers revealed voltage sensitive ion channel activity and it was found to facilitate both cation and anion transport, though it was weakly selective for anions (Weaver *et al.,* 1994). A year later a follow up study on GmNOD-26 reported that the phosphorylation state of the CTD residue S262 regulated its voltage-sensitivity (Lee *et al.,* 1995). Around this time, animal aquaporin research was following a similar trajectory with several isoforms being investigated for ion channel function leading to the identification of the ion-permeable AQP0 (Ehring *et al.,* 1990; Modesto *et al.,* 1996; Zampighi *et al.,* 1985), AQP1 (Anthony *et al.,* 2000; Saparov *et al.,* 2001; Yool *et al.,* 1996), AQP6 (Yasui *et al.,* 1999b) and BIB (Yanochko and Yool, 2002). Research into the ion channel function of animal aquaporins continued, and progressed into testing of their regulation and roles in physiological processes and human diseases (De Ieso and Yool, 2018; Soveral *et al.,* 2018), whereas there were no further reports on plant aquaporin ion channels in the intervening 20 years prior to reports by Byrt *et al.,* (2017) and Kourghi *et al.,* (2017), which describe Na^+ associated ionic conductances induced by Arabidopsis PIP2;1 and PIP2;2 when expressed in *X. laevis* oocytes.

8.2 Ion transporting aquaporins as candidates for non-selective cation channels

Since their "re-discovery" by Byrt *et al.,* (2017), ion transporting plant aquaporins have been put forward as molecular candidates for the elusive proteins contributing to non-selective cation currents observed *in planta* (McGaughey *et al.,* 2018; Munns *et al.,* 2019). This initial hypothesis was based on voltage characteristics and regulatory similarities (i.e. responses to changes in pH and Ca^{2+}) that AtPIP2;1 shares with NSCCs reported for root epidermal cells (Byrt *et al.,* 2017; Demidchik and Tester, 2002; Roberts and Tester, 1997). cGMP signalling is also involved in NSCC regulation whereby salinity and osmotic stress cause intracellular cGMP concentrations to increase rapidly and treatment with cGMP reduces NSCC mediated root Na^+ influx in a number of species (Donaldson *et al.,* 2004; Essah *et al.,* 2003; Maathuis

and Sanders, 2001; Rubio *et al.,* 2003). A similar inhibition of AtPIP2;1 Na^+ associated currents in oocytes by exogenous cGMP application is described in Chapter 3 although the mechanism for this is unknown. AtPIP2;1 expression in oocytes also increases permeability to a range of monovalent cations, such as Na^+, K^+, Rb^+ and Cs^+, consistent with a non-selective cation channel function (Chapters 3 and 7). Determination of the relative selectivity of AtPIP2;1 to these substrates is required to compare to that of candidate NSCCs (see Chapter 1; Table 1.1).

A recent review commented that the Na^+ flux through AtPIP2;1 would not be physiologically relevant *in planta* based on AtPIP2;1 associated conductance measurements from *X. laevis* oocytes (Isayenkov and Maathuis, 2019); however for this comparison the authors neglected to scale ion conductance in oocytes relative to water permeability reported for roots. Byrt *et al.,* (2017) showed a linear relationship between ion conductance and water permeability for AtPIP2;1 in oocytes. Therefore, calculations reported by McGaughey *et al.,* (2018) scale ion conductance reported for AtPIP2;1 in oocytes to the water permeability of root protoplasts. This revealed that AtPIP2;1 could quantitatively account for NSCC conductances in Arabidopsis roots. Data in this thesis (Chapters 3 and 7) further supports the hypothesis that ion permeable PIPs could function as NSCCs *in planta*, particularly in the context that phosphorylation of AtPIP2;1 CTD induces even greater conductances.

8.3 The connexin connection: PIP interaction with other ion channels that could account for induction of ion currents.

PIP interaction with other plant proteins has been the topic of several studies (Chen *et al.,* 2012; Dreze *et al.,* 2011; Jones *et al.,* 2014) with the most recent interactome identifying 388 proteins as putative interactants with AtPIP2;1 (Bellati *et al.,* 2016). The apparent promiscuity of PIP interactions and aquaporin conservation through evolution prompts us to consider that plant aquaporin expression in *X. laevis* oocytes may be activating native ion channels or transporters and these proteins could account for the observed conductances. In *X. laevis* oocytes, similar to plants, non-selective cation channels constitute a large, varied and mostly molecularly unidentified group of ion channels (Sobczak *et al.,* 2010; Weber, 1999). When expressed in oocytes AtPIP2;1 exhibits characteristics consistent with NSCCs and hence comparisons between endogenous oocyte NSCCs reported in the literature and

AtPIP2;1 associated currents is required towards exploring whether AtPIP2;1 is activating an endogenous protein in oocytes.

For instance; high levels of membrane protein expression (injection of 50 ng cRNA) in *X. laevis* oocytes may induce a hyper-polarisation activated NSCC 4-7 days post-injection that is also inhibited (~40% current reduction) by pH increase from 6.5 to 8.2 (Tzounopoulos *et al.,* 1995). Additionally, a hyper-polarisation and acid activated NSCC and a stretch-activated or mechano-sensitive NSCC that is weakly selective for monovalent cations but also permeable to Ca^{2+} have also been described in oocytes (Kuruma *et al.,* 2000; Yang and Sachs, 1990).

The ion channel characteristics of AtPIP2;1 when expressed in oocytes cannot be attributed to the above NSCC types. AtPIP2;1 induced currents are not hyper-polarisation activated (e.g. Chapter 3 and 6) or inhibited by increases in pH (actually the opposite where low pH gates AtPIP2;1 water and ion transport, see Byrt *et al.,* 2017). AtPIP2;1 ion channel function is not stretch activated (see Chapter 7), and it is not permeable to Ca^{2+} (it is instead regulated by Ca^{2+} and other divalent cations, see Kourghi *et al.,* 2017).

Another endogenous oocyte NSCC, whose molecular identity was proposed to be Connexin38, does share some similar features with AtPIP2;1 induced currents (Arellano *et al.,* 1995; Ebihara, 1996; Zhang *et al.,* 1998). It carried monovalent cation conductances that were reversibly blocked by the divalent cations Ca^{2+} and Mg^{2+} and was inhibited by niflumic acid as has been similarly reported for AtPIP2;1 induced currents in oocytes (Kourghi *et al.,* 2017; Manchun, 2013). In similar solutions the NSCC/Connexin38 (115 mM NaCl, 50 µM Ca^{2+}, pH 7.0) was reported to have a conductance of 28 µS (Arellano *et al.,* 1995) and for AtPIP2;1 (100 mM NaCl, 50 µM $CaCl_2$, pH 8.5) a conductance of 41.07 ± 5.99 µS was reported (Chapter 3). The NSCC/Connexin38 and AtPIP2;1 also share similar inhibitory responses to concentrations of Ca^{2+} and Mg^{2+} of around ~100 µM and > 1000 µM respectively (Arellano *et al.,* 1995; Kourghi *et al.,* 2017). Interaction between aquaporins and connexins has been reported previously; for example in animals, the water-ion aquaporin AQP0 was shown to directly interact with two connexin isoforms via its CTD (Yu and Jiang, 2004; Yu *et al.,* 2005). Therefore, AtPIP2;1 interaction with a connexin could potentially result in the detection of AtPIP2;1-associated ionic conductance.

While the possibility that plant aquaporins could be interacting with endogenous ion channels including connexins to account for the observed ion transport cannot be excluded, the following observations suggest this may not be the case. The steady-state currents

observed via the NSCC/Connexin38 exhibited rectification at very positive (+30mV) and negative (-100 mV) membrane potentials (Zhang *et al.,* 1998), and this is not typically observed for PIP2 expressing oocytes (but time-dependent outward rectification is observed for the HvTIP2;2, see Chapter 6). Furthermore AtPIP2;2, another candidate ion-transporting plant aquaporin, displayed significantly different sensitivity to divalent cations compared to AtPIP2;1 (Kourghi *et al.,* 2017), and these characteristics were not consistent with those reported for the NSCC/Connexin38 (Arellano *et al.,* 1995). The CTD of PIPs are highly conserved, but not all PIPs facilitate ion transport in the oocyte system; AtPIP2;7 expression in oocytes does not induce ionic conductances (Kourghi *et al.,* 2017) and only a few SvPIP2 and HvPIP2 isoforms do (Chapter 5). Other phosphorylation sites (i.e. loop D) have not been linked to Connexin interactions, yet these sites can influence PIP mediated ionic conductance (see Chapter 4).

Several questions remain about the role of PIP interaction with other channels in the oocyte system. Is PIP expression and potential interaction causing the re-localisation and activation of endogenous ion channels that would not otherwise contribute to measurable ionic conductance? Are all the different plant aquaporins that facilitate ion transport interacting with different Connexins and/or other endogenous channels? What could possibly be the mechanism of discrimination between which connexins or transporters each aquaporin may interact with considering the high protein similarity between the aquaporins tested? How is this protein interaction increasing ion conductance but reducing water permeability that would account for the inverse relationship of water and ion transport shown for some phosphorylation mutants? Finally, ion channel activity of the mammalian AQP0 and AQP1 and plant GmNOD-26 has been demonstrated in 'clean' lipid bilayer systems, where no endogenous proteins could account for the ionic conductance, indicating that at least some aquaporins function as ion channels (Ehring *et al.,* 1990; Modesto *et al.,* 1996; Saparov *et al.,* 2001; Weaver *et al.,* 1994).

The ionic conductance observed for aquaporins of interest could be solely contributed by the aquaporin candidate, or it could be a combination of flux through ion-permeable aquaporins and flux through an unknown interactant(s), or it could be solely the result of aquaporin regulation of the ion permeability of other interacting channels or transporters. Regardless of which possibility is correct the ion transport associated with plant aquaporin function is a mechanism with significant physiological implications, which should be investigated further.

8.4 Phosphorylation as a regulatory mechanism for PIP2 water and ion transport

Phosphorylation has been shown to influence aquaporin channel gating, localisation and trafficking in both plants and animals (Chapter 3; Table 1). The regulatory intersection of aquaporin function, localisation and trafficking by reversible phosphorylation events can enable adjustment of membrane permeability in response to changes in water potential, and contribute to cell solute homeostasis. For example, salinity treatments were reported to trigger enhanced location-cycling of AtPIP2;1 in Arabidopsis root cells (Li *et al.,* 2011; Luu *et al.,* 2012; Martinière *et al.,* 2012). Changes in the abundances of particular AtPIP2;1 phospho-peptides were also reported in response to salt stress; in particular, the abundance of diphosphorylated AtPIP2;1 at S280 and S283 decreased (Hsu *et al.,* 2009; Prak *et al.,* 2008; Vialaret *et al.,* 2014). When expressed in oocytes the disphosphorylated AtPIP2;1 mutant (AtPIP2;1 S280D/S283D) had increased ion transport, and changes in phosphorylation at other sites also influenced AtPIP2;1 ionic conductance (Chapters 3 and 4). Hence, the salt-induced phosphorylation-dependent internalisation of AtPIP2;1 from the PM (Boursiac *et al.,* 2005; Prak *et al.,* 2008; Ueda *et al.,* 2016) could be a mechanism used by plants to co-ordinately adjust water and Na^+ or K^+ flux into or out of the cell under stress conditions. Under normal conditions AtPIP2;1 may provide another pathway for other important cations like K^+ (Chapter 3) or possibly even NH_4^+.

A recent paper investigating the influence of aquaporin phosphorylation events on the circadian regulation of leaf hydraulics described AtPIP2;1 interaction with several 14-3-3 proteins (also known as General Regulatory Factors (GRFs)) (Prado *et al.,* 2019). GRF4 and 10 directly and preferentially interacted with AtPIP2;1 when CTD sites S280 and S283 were phosphorylated and this interaction increased AtPIP2;1 water channel function in *X. laevis* oocytes by approximately 1.2-1.5 fold. In addition to gating and other changes in protein conformation, this indicates phosphorylation may influence PIP function by acting as a regulator of protein-protein interactions. Whether or not GRFs additionally influence AtPIP2;1 ion channel function in a phosphorylation-dependent manner is of particular interest because several plant ion channels have been shown to be directly and indirectly (e.g. through activation of upstream kinases) activated or inhibited by GRFs (Duby *et al.,* 2009; Ormancey *et al.,* 2017; Thiel *et al.,* 2006; van Kleeff *et al.,* 2018).

8.5 Potential roles of dual water and ion permeable aquaporins *in planta* and their significance

8.5.1 Salinity stress tolerance

The mechanisms plants use to cope with salt stress can be described as osmotic, ionic, or tissue tolerance mechanisms, depending on whether they help the plant to: (i) conserve water, (ii) reduce NaCl influx into roots and control its subsequent translocation or partitioning throughout the plant, or (iii) compartmentalise NaCl into vacuoles to prevent cytotoxic effects, respectively (Munns and Tester, 2008; Roy *et al.,* 2014). Ion permeable aquaporins could conceivably have roles in all three of these tolerance mechanisms.

(i) Conservation of water: in response to osmotic stress plants close stomata to reduce water loss via transpiration. Stomatal closure is mediated by rapid water-ion efflux in guard cells (Kollist *et al.,* 2014). Aquaporins are known to mediate water transport in stomatal closure processes (Hachez *et al.*, 2017), and water-ion channel aquaporins could also be included in the suite of ion channels and transporters involved in the ion flux component of this process (although for the most part aquaporins are not included at all in guard cell transport models, e.g. Jezek and Blatt, 2017). In roots, water-ion channel aquaporins could generate local osmotic gradients via altering Na^+ transport to restrict the effects of the driving force for water loss that occurs with an increase in soil salinity. A similar mechanism for generating local osmotic gradients is described for HsAQP1 in animal cells – see section 8.4.2.

(ii) Controlling Na^+ influx and translocation: under salt stress NSCCs are the primary mechanism for Na^+ influx, and this influx results in a significant membrane depolarisation (reported to be by 60-80mV for a 100 mM NaCl treatment) increasing K^+ leakage (Apse and Blumwald, 2007; Demidchik, 2014). Salt stress results in decreased abundance of diphosphorylated AtPIP2;1 at S280 and S283 (Hsu *et al.,* 2009; Prak *et al.,* 2008; Vialaret *et al.,* 2014) and has also been shown to induce AtPIP2;1 internalisation into intracellular vesicles (Boursiac *et al.,* 2005; Prak *et al.,* 2008). Diphosphorylated AtPIP2;1 (S280D/S283D) has increased ion channel function whereas dephosphorylated AtPIP2;1 (S280A/S283A) has increased water channel function (Chapter 3). Reduction of diphosphorylated (i.e. ion channel activated) AtPIP2;1 abundance or its removal

from the PM could be part of a process to slow the Na^+ induced depolarisation of the PM and reduce Na^+ influx while also reducing K^+ and water efflux. A similar mechanism of internalisation of ion channels in response to salt stress was proposed by Baral *et al.,* (2015).

(iii) Compartmentalisation of Na^+: AtPIP2;1 internalised into intracellular bodies induced by salt stress may by trafficked to and from the vacuole (Boursiac *et al.,* 2005; Prak *et al.,* 2008; Ueda *et al.,* 2016). Transport of Na^+ via PM originated intracellular vesicles to the vacuole under salt stress was shown in tobacco BY2 cells (Garcia de la Garma *et al.,* 2015; see also Chapter 1.2, Figure 3; located in published review in appendix 9.1). This vesicular transport process was quantitatively reviewed recently by Flowers *et al.,* (2018) as a putative salt tolerance mechanism.

8.5.2 Ion and water transport energetics

The "osmotic engine model" is a term that has been coined in cancer research, and describes the actin- and myosin-independent mechanism of cell migration based on polar water and ion transport (Stroka *et al.,* 2014). The establishment of 'micro-environment' osmotic gradients through polarised distribution and co-localisation of water and ion channels allows for rapid changes in cell volume at the leading (net influx) and trailing (net efflux) edges of cancer cells resulting in cell movement or migration (De Ieso and Yool, 2018). The role of aquaporins in this mechanism, as water channels, is well described and there are many studies reporting on aquaporin involvement in cancer metastasis by facilitating water flux (Hu and Verkman, 2006; McCoy and Sontheimer, 2007; McCoy *et al.*, 2010; Papadopoulos *et al.,* 2008). More recently, pharmacological studies targeting HsAQP1 identified two bumetanide derivatives that selectively blocked HsAQP1 ion channel activity and impaired cancer cell migration (Kourghi *et al.,* 2015), indicating that dual water and ion transport through HsAQP1 significantly contributes to the "osmotic engine" of migrating cancer cells.

In general, plant cells have no requirement for migration (with the exception of pollen tubes; for review see: Johnson and Preuss, 2002). But some plant cells and organs can move with respect to other parts of the plant, for example how sunflowers track the sun east to west (Briggs, 2016), and a similar "osmotic engine" mechanism could be used to energise plant cell movement through polar water and/or ion transport. Several recent reviews have discussed the energetics of water and ion transport in plants (Fricke, 2017; Munns *et al.,*

2019; Wegner and Shabala, 2019). Classical interpretations of membrane transport in plant cells refer to water movement as being driven exclusively by water potential gradients; however, there is experimental evidence that water can appear to be transported 'energetically uphill' against substantial osmotic gradients (Knipfer and Fricke, 2010; Oertli, 1966; Pickard, 2003; for reviews see also Nardini *et al.,* 2011; Wegner, 2014; Zimmermann *et al.,* 2004). 'Active' water transport is an established phenomenon in mammalian systems and is proposed to occur via the coupling or co-transport of water and ions or water and sugar molecules (Zeuthen, 2010). The presence of similar co-transport mechanisms and their physiological relevance are beginning to be explored in plants and algae (Fricke, 2015; Fricke, 2017; Raven and Doblin, 2014; Wegner, 2015).

Before the existence of proteinaceous channels and transporters was known, Dainty, (1963) proposed there were two pore types in plant cell membranes that mediate water flux; an exclusive water pore (a role which many plant aquaporin isoforms may fulfil) and pores that are capable of both water and solute transport (in this case water and ions mediated by dual water-ion aquaporins) such that water transport may drive solute flux and vice versa. The latter could allow water and ions to be transported under conditions where favourable water potential or electro-chemical gradients are not respectively present. Further to this, Wegner, (2014) postulated that exclusive water pores (orthodox aquaporins) and pores facilitating solute-water co-transport must be inversely regulated to sustain water or ion flux against their gradients. These theories surmise two distinct protein types fulfilling two distinct reciprocal functions; interestingly this inverse regulation between water and ion channel activity appears to occur for AtPIP2;1 influenced by its phosphorylation status (Chapter 3).

Typical transport properties described in Zeuthen and Macaulay, (2012) used to distinguish between other co-transport mechanisms and unstirred layer effects may not be easily applicable to dual water and ion permeable aquaporins. This concept assumes that low water permeability of the ion channel or transporter in question and high passive water permeability of the membrane, such as facilitated by aquaporins, increase efficiency of the effects of unstirred layers (Zeuthen and Macaulay, 2012).

The energetic feasibility of the 'active' or 'energetically uphill' transport of water in plants remains a matter of some debate; Fricke (2017) suggests that such transport would be unsustainable. By comparison, 'downhill' water flow (i.e. water transport with its osmotic gradient) to effectively 'drag' solutes against an electro-chemical potential via "molecular turbines" (e.g. water-ion aquaporins) could be used to generate chemical energy by altering

membrane potential (Fricke, 2015). The reversal potential of excised membrane patches of the multicellular alga *Chara* exposed to symmetrical KCl solution differing in osmolarity shifted from 0 mV to +10 mV indicating K^+ was transported with the water flow (Homblé and Véry, 1992). A 'rechargeable K^+ battery' has been described as a sucrose loading mechanism in phloem under conditions where H^+-ATPase activity is limited; cycling of K^+ in phloem and surrounding cells via the K^+ channel ATK2 can generate electro-chemical gradients to energise the PM for other transport processes (Dreyer *et al.,* 2017; Gajdanowicz *et al.,* 2011). How dual ion-water transport through ion permeable aquaporins could be utilised by the cell to influence membrane energetics and drive the 'work' of other membrane transport processes is a fascinating topic for future research.

8.6 Limitations and areas for further research

8.6.1 Limitations

With the advantage of hindsight I have identified several limitations of experiments reported in this study.

In this research, the primary investigative tool used was *X. laevis* oocytes. Oocytes are a popular and generally powerful system used for the characterisation of transport protein function (Miller and Zhou, 2000). While many properties of expressed channels and transporters can be easily studied in oocytes, they are still living biological systems that possess many endogenous ion channels and transporters (Sobczak *et al.,* 2010). Furthermore, as living cells oocytes are also capable of influencing the function of the expressed proteins, including by PTM; for example, the phosphorylation state of plant aquaporins can be altered by endogenous oocyte kinases and phosphatases (Johansson *et al.,* 1998; Van Wilder *et al.,* 2008). Variation in the localisation of proteins in oocytes is another limitation of this system and this study, particularly considering the proposed role of CTD phosphorylation in PIP trafficking and localisation *in planta* (Prak *et al.,* 2008). The cell size and opacity of *X. laevis* oocytes prevents accurate localisation of proteins in intact cells; basically, only the external edge of the oocyte can be visualised which, depending on the plane of focus, can influence how a tagged protein appears to be localised. Other techniques may be used to overcome some of these pitfalls such as fixing and sectioning (Van Wilder *et al.,* 2008) or use of tetramethylrhodamine (TMR) dextran (an unconjugated nonspecific fluorochrome marker),

along with a line-scan analysis approach, to delineate the oocyte interior and scrutinise the location of putatively PM localised proteins (Yaneff *et al.,* 2014). However, access to the necessary equipment and facilities to achieve this was unavailable at the time of this research due to quarantine restrictions on oocyte transport. As an alternative, observation of the localisation of phospho-mutant aquaporins in yeast was investigated, and this approach may provide an indication of the relationship between aquaporin phosphorylation state and localisation changes. Quantification of total protein expressed in each oocyte, particularly the phosphorylation mutants, would also have been beneficial in order to investigate whether certain mutations affected protein translation efficiency. However, the relationship between water and ion transport shown in Chapter 3, Figure 3 cannot be explained by differences in protein abundance on the PM.

A further limitation was the use of TEVC. From the TEVC experiments performed within this thesis it cannot be exclusively determined which ions are being conducted (even if one ionic species is hugely predominant over others). Future TEVC studies could include a solution series of different concentrations of the ion of interest to observe shifts in the membrane reversal potential. Additionally, experiments using radio-isotopes or ion specific probes could be done.

8.6.2 Further research: Answering the next big questions

Early reports that some animal aquaporins could function as ion channels were met with scepticism; some healthy debate in the plant aquaporin field is similarly expected. Therefore, to unequivocally demonstrate whether or not there is ion permeation through the plant aquaporin isoforms described within this thesis, their ion channel function needs to be tested in a lipid bilayer or lipid vesicle system free of potential interacting partners. The phosphorylation-mutants should also be examined in a bilayer system to address whether differences in apparent transport capacity is related to phosphorylation-dependent protein abundance or protein conformation changes.

The exact physiological roles and significance of water-ion plant aquaporins remains to be determined. *In planta* regulatory processes and phosphorylation influencing the function and protein localisaiton of water-ion plant aquaporins may be different to that observed when function and localisation is investigated in heterologous systems and with protein phosphorylation mutants. Therefore, to progress our understanding of *in planta* function and

regulation, several knock-out, over-expresser and complementation lines of water-ion aquaporin candidates are currently being generated for future research. These resources will be used to explore differences in ion flux at the root, and response to osmotic stresses.

Tobacco BY2 cells may also provide a useful tool for investigating the transport properties of PIPs and their regulation by phosphorylation *in planta*. BY2 cells are transformable and can produce stable cell lines that are often used as a less complex system to investigate biological properties of plant cells. BY2 cells would allow the study of the intersection of ion transporting PIP protein function, trafficking and localisation in response to salinity, and whether these features are coordinated to contribute to osmotic stress tolerance mechanisms in plant cells.

Chapter 9: Appendices

9.1 Review: Regulating root aquaporin function in response to changes in salinity

Statement of Authorship

Title of Paper	Regulating root aquaporin function in response to changes in salinity
Publication Status	[X] Published [ ] Accepted for Publication [ ] Unpublished and Unsubmitted work written in manuscript style [ ] Submitted for Publication
Publication Details	McGaughey, S. A., Qiu, J., Tyerman, S. D. and Byrt, C. S. (2018). Regulating Root Aquaporin Function in Response to Changes in Salinity. Annual Plant Reviews. 1, 1–36. DOI: 10.1002/9781119312994.APR0626

Principal Author

Name of Principal Author (Candidate)	Samantha McGaughey		
Contribution to the Paper	Drafted and revised the manuscript, including data mining and figure design.		
Overall percentage (%)	70 %		
Certification:	This paper reports on original research I conducted during the period of my Higher Degree by Research candidature and is not subject to any obligations or contractual agreements with a third party that would constrain its inclusion in this thesis. I am the primary author of this paper.		
Signature		Date	24-10-2019

Co-Author Contributions

By signing the Statement of Authorship, each author certifies that:

i. the candidate's stated contribution to the publication is accurate (as detailed above);

ii. permission is granted for the candidate in include the publication in the thesis; and

iii. the sum of all co-author contributions is equal to 100% less the candidate's stated contribution.

Name of Co-Author	Jiaen Qiu		
Contribution to the Paper	Contributed on ABA regulation section.		
Signature		Date	28-10-2019

Name of Co-Author	Stephen Tyerman		
Contribution to the Paper	Contributed to manuscript conception and revision.		
Signature		Date	28/10/2019

Name of Co-Author	Caitlin Byrt		
Contribution to the Paper	Contributed to manuscript conception and revision.		
Signature		Date	25/10/2019

9.2 Supplementary information for Chapter 1

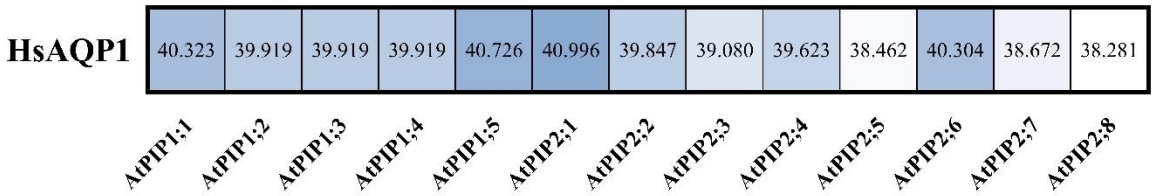

Figure S1: Protein sequence similarity between HsAQP1 and AtPIPs. AtPIP2;1 has highest sequence similarity to HsAQP1. Other AtMIPs had < 38% sequence similarity (data not shown).

9.3 Supplementary information for Chapter 2

Table S1: List of constructs generated for use in the *X. laevis* oocyte expression system. Constructs were generated in the pGEMHE-DEST vector (ampicillin resistance).

Construct Name	Experimental use
pGEMHE::AtPIP2;1	TEVC/swelling
pGEMHE::AtPIP2;1 S280A	TEVC/swelling
pGEMHE::AtPIP2;1 S280D	TEVC/swelling
pGEMHE::AtPIP2;1 S283A	TEVC/swelling
pGEMHE::AtPIP2;1 S283D	TEVC/swelling
pGEMHE::AtPIP2;1 S280A/S283A	TEVC/swelling
pGEMHE::AtPIP2;1 S280D/S283A	TEVC/swelling
pGEMHE::AtPIP2;1 S280A/S283D	TEVC/swelling
pGEMHE::AtPIP2;1 S280D/S283D	TEVC/swelling
pGEMHE::AtPIP2;1 S121A	TEVC/swelling
pGEMHE::AtPIP2;1 S121D	TEVC/swelling
pGEMHE::AtPIP2;1 S194A	TEVC/swelling
pGEMHE::AtPIP2;1 S194D	TEVC/swelling
pGEMHE::AtPIP2;1 S194E	TEVC/swelling
pGEMHE::SvPIP1;1	TEVC/swelling
pGEMHE::SvPIP1;2	TEVC/swelling
pGEMHE::SvPIP1;5	TEVC/swelling
pGEMHE::SvPIP1;6	TEVC/swelling
pGEMHE::SvPIP2;1	TEVC/swelling
pGEMHE::SvPIP2;2	TEVC/swelling
pGEMHE::SvPIP2;3	TEVC/swelling
pGEMHE::SvPIP2;4	TEVC/swelling
pGEMHE::SvPIP2;5	TEVC/swelling
pGEMHE::SvPIP2;6	TEVC/swelling
pGEMHE::SvPIP2;7	TEVC/swelling
pGEMHE::SvPIP2;8	TEVC/swelling
pGEMHE::KnPIP-like	TEVC/swelling
pGEMHE::HvTIP2;2-F117	TEVC/swelling
pGEMHE::HvTIP2;2-L117	TEVC/swelling

Table S2: List of constructs generated for use in yeast expression system and yeast transformants made .

Construct Name	Selection	Yeast strain	Experimental use
pRS423::SvPIP1;1	HIS	*aqy1/aqy2, skn7*	FT, H_2O_2 and BA assays
pRS423::SvPIP1;2	HIS	*aqy1/aqy2, skn7*	FT, H_2O_2 and BA assays
pRS423::SvPIP1;5	HIS	*aqy1/aqy2, skn7*	FT, H_2O_2 and BA assays
pRS423::SvPIP1;6	HIS	*aqy1/aqy2, skn7*	FT, H_2O_2 and BA assays
pRS423::SvPIP2;1	HIS	*aqy1/aqy2, skn7*	FT, H_2O_2 and BA assays
pRS423::SvPIP2;2	HIS	*aqy1/aqy2, skn7*	FT, H_2O_2 and BA assays
pRS423::SvPIP2;3	HIS	*aqy1/aqy2, skn7*	FT, H_2O_2 and BA assays
pRS423::SvPIP2;5	HIS	*aqy1/aqy2, skn7*	FT, H_2O_2 and BA assays
pRS423::SvPIP2;6	HIS	*aqy1/aqy2, skn7*	FT, H_2O_2 and BA assays
pRS423::SvPIP2;8	HIS	*aqy1/aqy2, skn7*	FT, H_2O_2 and BA assays

Table S3: Accession numbers for *Setaria italica* and *Setaria viridis* PIPs.

Setaria italica		***Setaria viridis***	
Gene name	**Accession number**	**Gene name**	**Accession number**
SiPIP1;1	Seita.7G196700.1	SvPIP1;1	Sevir.7G208600.1
SiPIP1;2	Seita.1G264900.1	SvPIP1;2	Sevir.1G269400.1
SiPIP1;5	Seita.1G372300.1	SvPIP1;5	Sevir.1G378900.1
SiPIP1;6	Seita.4G089800.1	SvPIP1;6	Sevir.4G089200.1
SiPIP2;1	Seita.2G123000.1	SvPIP2;1	Sevir.2G128000.1
SiPIP2;2	Seita.9G219400.1	SvPIP2;2	Sevir.9G218600.1
SiPIP2;3	Seita.9G268100.1	SvPIP2;3	Sevir.9G269300.1
SiPIP2;4	Seita.1G241900.1	SvPIP2;4	Sevir.1G246800.1
SiPIP2;5	Seita.7G170200.1	SvPIP2;5	Sevir.7G179900.1
SiPIP2;6	Seita.2G123200.1	SvPIP2;6	Sevir.2G128200.1
SiPIP2;7	Seita.2G123300.1	SvPIP2;7	Sevir.2G128300.1
SiPIP2;8	Seita.2G291500.1	SvPIP2;8	Sevir.2G302500.1

9.4 Supplementary information for Chapter 4

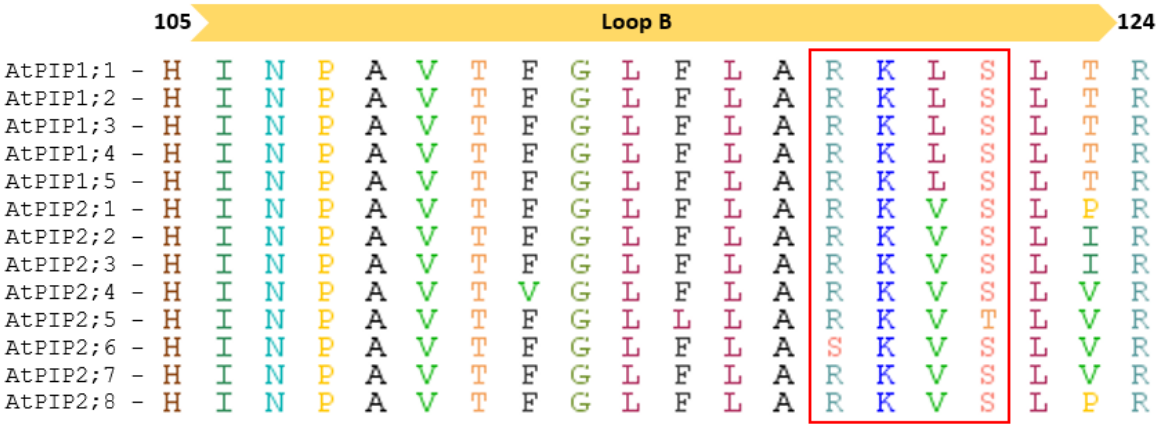

Figure S2: OST1 consensus motif identified in loop B of AtPIP protein sequences.

9.5 Supplementary information for Chapter 5

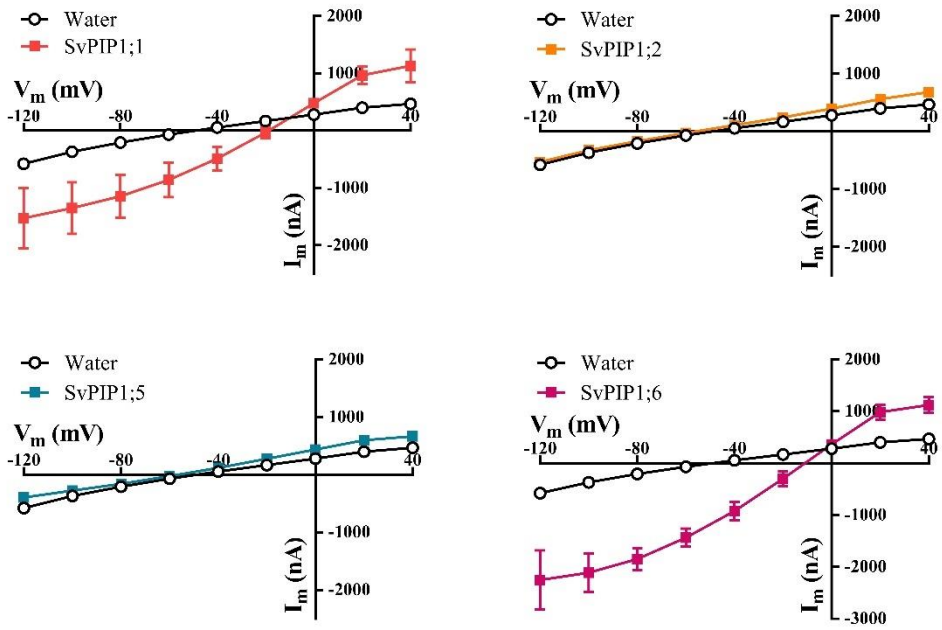

Figure S3: Example IV curves of oocytes expressing SvPIP1s. Oocytes were injected with either water or water containing SvPIP1 cRNA. Post-injection oocytes were incubated in Low Na^+ Ringers for 24-36 h. TEVC was performed in Na100 solution.

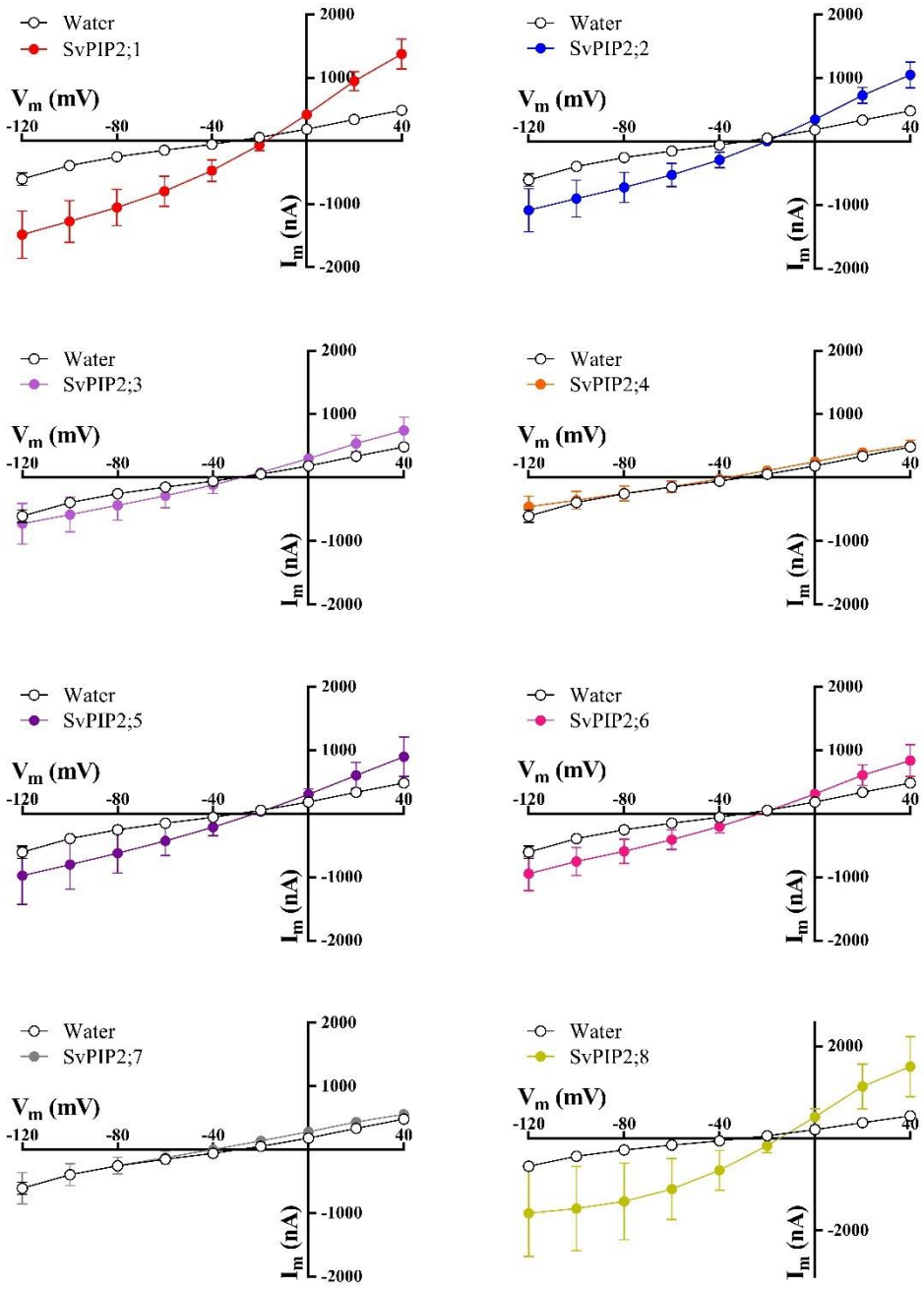

Figure S4: Example IV curves of oocytes expressing SvPIP2s. Oocytes were injected with either water or water containing SvPIP2 cRNA. Post-injection oocytes were incubated in Low Na^+ Ringers for 24-36 h. TEVC was performed in Na100 solution.

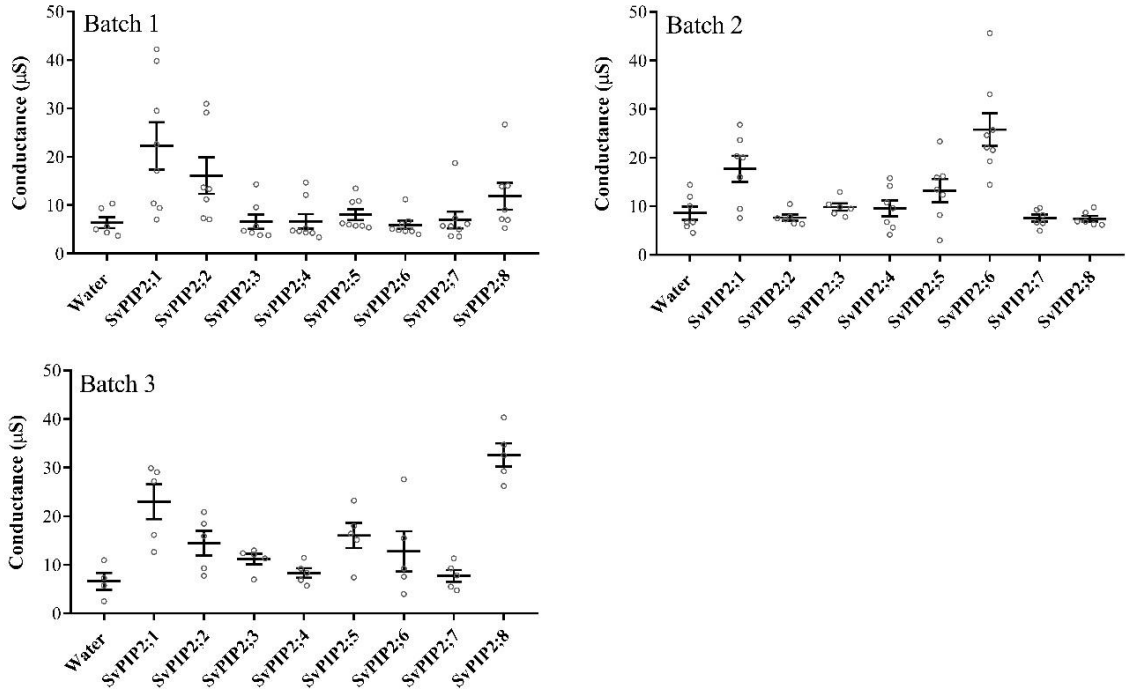

Figure S5: Ionic conductances of SvPIP2 injected oocytes graphed for each oocyte batch. Data is shown as mean ± SEM where each data point represents an individual oocyte.

Table S5: Coefficient of variation for relative conductance of SvPIP2 expressing oocytes. Coefficient of variation (CV) was calculated for data shown in Figure 5.8b.

Gene injected	CV (%)
Water control	50
SvPIP2;1	55.2
SvPIP2;2	66.6
SvPIP2;3	40.6
SvPIP2;4	46.7
SvPIP2;5	49
SvPIP2;6	67.5
SvPIP2;7	51.8
SvPIP2;8	78.3

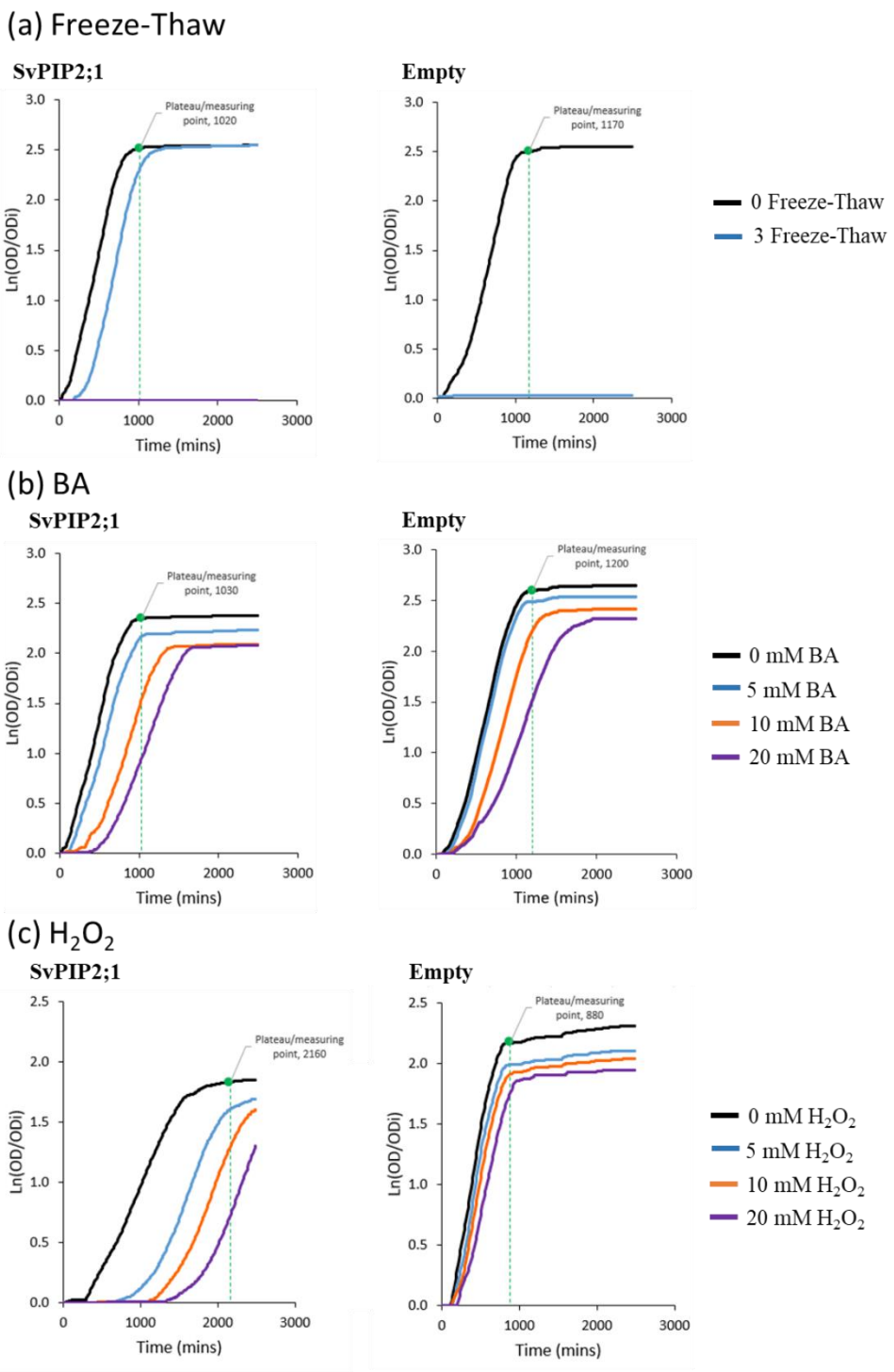

Figure S6: Example yeast growth curves. Examples of the yeast growth curves generated to calculate AUC % for **(a)** Freeze-Thaw, **(b)** BA and **(c)** H_2O_2 assays. AUC for each treatment was calculated relative to its untreated control (0 Freeze thaw, 0 mM BA or 0 mM H_2O_2) from time zero up until the untreated control culture reached stationary phase (plateau/measuring point).

Chapter 10: References

Ahmad, I. and Maathuis, F. J. M. (2014). Cellular and tissue distribution of potassium: Physiological relevance, mechanisms and regulation. *J. Plant Physiol.* **171**, 708–714.

Alberti, S., Gitler, A. D. and Lindquist, S. (2007). A suite of Gateway® cloning vectors for high-throughput genetic analysis in *Saccharomyces cerevisiae*. *Yeast* **24**, 913–919.

Alexandre, J. and Lassalles, J. P. (1991). Hydrostatic and osmotic pressure activated channel in plant vacuole. *Biophys. J.* **60**, 1326–1336.

Allen, G. J. and Sanders, D. (1997). Vacuolar ion channels of higher plants. *Adv. Bot. Res.* **25**, 217–252.

Alleva, K., Niemietz, C. M., Sutka, M., Maurel, C., Parisi, M., Tyerman, S. D. and Amodeo, G. (2006). Plasma membrane of *Beta vulgaris* storage root shows high water channel activity regulated by cytoplasmic pH and a dual range of calcium concentrations. *J. Exp. Bot.* **57**, 609–621.

Almadanim, M. C., Alexandre, B. M., Rosa, M. T. G., Sapeta, H., Leitão, A. E., Ramalho, J. C., Lam, T. K. T., Negrão, S., Abreu, I. A. and Oliveira, M. M. (2017). Rice calcium-dependent protein kinase OsCPK17 targets plasma membrane intrinsic protein and sucrose-phosphate synthase and is required for a proper cold stress response. *Plant Cell Environ.* **40**, 1197–1213.

Amezcua-Romero, J. C., Pantoja, O. and Vera-Estrella, R. (2010). Ser123 is essential for the water channel activity of McPIP2;1 from *Mesembryanthemum crystallinum*. *J. Biol. Chem.* **285**, 16739–16747.

Ampah-Korsah, H., Anderberg, H. I., Engfors, A., Kirscht, A., Nordén, K., Kjellström, S., Kjellbom, P. and Johanson, U. (2016). The aquaporin splice variant NbXIP1;1α is permeable to boric acid and is phosphorylated in the N-terminal domain. *Front. Plant Sci.* **7**,.

Anderberg, H. I., Danielson, J. A. H. Å. H. and Johanson, U. (2011). Algal MIPs, high diversity and conserved motifs. *Bmc Evol. Biol.* **11**,.

Andersen, A. and Andersen, K. (1973). Linkage between marker genes on barley chromosome 2 and a gene for resistance to *Heterodera avenae*. *Hereditas* **73**, 271–276.

Anschütz, U., Becker, D. and Shabala, S. (2014). Going beyond nutrition: Regulation of potassium homoeostasis as a common denominator of plant adaptive responses to environment. *J. Plant Physiol.* **171**, 670–687.

Anthony, T. L., Brooks, H. L., Boassa, D., Leonov, S., Yanochko, G. M., Regan, J. W. and Yool, A. J. (2000). Cloned human aquaporin-1 Is a cyclic GMP-gated ion channel. *Mol. Pharmacol.* **57**, 576–588.

Apse, M. P. and Blumwald, E. (2007). Na^+ transport in plants. *FEBS Lett.* **581**, 2247–2254.

Arellano, R. O., Woodward, R. M. and Miledi, R. (1995). A monovalent cationic conductance that is blocked by extracellular divalent cations in *Xenopus* oocytes. *J.*

Physiol. **484**, 593–604.

Aritua, V., Achor, D., Gmitter, F. G., Albrigo, G. and Wang, N. (2013). Transcriptional and microscopic analyses of Citrus stem and root responses to *Candidatus Liberibacter asiaticus* infection. *PLoS One* **8**, 4–8.

Aroca, R., Amodeo, G., Fernandez-Illescas, S., Herman, E. M., Chaumont, F. and Chrispeels, M. J. (2005). The role of aquaporins and membrane damage in chilling and hydrogen peroxide induced changes in the hydraulic conductance of maize roots. *Plant Physiol.* **137**, 341–353.

Asano, T., Hayashi, N., Kikuchi, S. and Ohsugi, R. (2012). CDPK-mediated abiotic stress signaling. *Plant Signal. Behav.* **7**, 817–821.

Azad, A. K., Katsuhara, M., Sawa, Y., Ishikawa, T. and Shibata, H. (2008). Characterization of four plasma membrane aquaporins in tulip petals: A putative homolog is regulated by phosphorylation. *Plant Cell Physiol.* **49**, 1196–1208.

Azad, A. K., Ahmed, J., Alum, A., Hasan, M., Ishikawa, T., Sawa, Y. and Katsuhara, M. (2016). Genome-wide characterization of major intrinsic proteins in four grass plants and their non-aqua transport selectivity profiles with comparative perspective. *PLoS One* **11**, e0157735.

Balagué, C., Lin, B., Alcon, C., Flottes, G., Malmström, S., Köhler, C., Neuhaus, G., Pelletier, G., Gaymard, F. and Roby, D. (2003). HLM1, an essential signaling component in the hypersensitive response, is a member of the cyclic nucleotide-gates channel ion channel family. *Plant Cell* **15**, 365–379.

Baral, A., Shruthi, K. S. and Mathew, M. K. (2015). Vesicular trafficking and salinity responses in plants. *IUBMB Life* **67**, 677–686.

Barba-Espín, G., Diaz-Vivancos, P., Job, D., Belghazi, M., Job, C. and Hernández, J. A. (2011). Understanding the role of H_2O_2 during pea seed germination: A combined proteomic and hormone profiling approach. *Plant, Cell Environ.* **34**, 1907–1919.

Barr, A. R., Chalmers, K. J., Karakousis, A., Kretschmer, J. M., Manning, S., Lance, R. C. M., Lewis, J., Jeffries, S. P. and Langridge, P. (1998). RFLP mapping of a new cereal cyst nematode resistance locus in barley. *Plant Breed.* **117**, 185–187.

Bartels, D. and Sunkar, R. (2005). Drought and salt tolerance in plants. *CRC. Crit. Rev. Plant Sci.* **24**, 23–58.

Barzana, G., Aroca, R., Bienert, G. P., Chaumont, F. and Ruiz-Lozano, J. M. (2014). New insights into the regulation of aquaporins by the arbuscular mycorrhizal symbiosis in maize plants under drought stress and possible implications for plant performance. *Mol. Plant-Microbe Interact.* **27**, 349–363.

Becker, B. (2007). Function and evolution of the vacuolar compartment in green algae and land plants (*Viridiplantae*). *Int. Rev. Cytol.* **264**, 1–24.

Bedford, J. J., Leader, J. P. and Walker, R. J. (2003). Aquaporin expression in normal human kidney and in renal disease. *J. Am. Soc. Nephrol.* **14**, 2581–2587.

Behera, S., Xu, Z., Luoni, L., Bonza, M. C., Doccula, F. G., De Michelis, M. I., Morris, R. J., Schwarzländer, M. and Costa, A. (2018). Cellular Ca^{2+} signals generate defined pH signatures in plants. *Plant Cell* **30**, 2704–2719.

Bell, C. D., Soltis, D. E. and Soltis, P. S. (2010). The age and diversification of the angiosperms re-revisited. *Am. J. Bot.* **97**, 1296–1303.

Bellati, J., Champeyroux, C., Hem, S., Rofidal, V., Krouk, G., Maurel, C. and Santoni, V. (2016). Novel aquaporin regulatory mechanisms revealed by interactomics. *Mol. Cell. Proteomics* **15**, 3473–3487.

Benito, B., Haro, R., Amtmann, A., Cuin, T. A. and Dreyer, I. (2014). The twins K^+ and Na^+ in plants. *J. Plant Physiol.* **171**, 723–731.

Bennetzen, J. L., Schmutz, J., Wang, H., Percifield, R., Hawkins, J., Pontaroli, A. C., Estep, M., Feng, L., Vaughn, J. N., Grimwood, J., et al. (2012). Reference genome sequence of the model plant *Setaria*. *Nat. Biotechnol.* **30**, 555–564.

Bethke, P. C. and Jones, R. L. (1997). Reversible protein phosphorylation regulates the activity of the slow-vacuolar ion channel. *Plant J.* **11**, 1227–1235.

Bettinger, R. L., Barton, L. and Morgan, C. (2010). The origins of food production in north China: A different kind of agricultural revolution. *Evol. Anthropol.* **19**, 9–21.

Bienert, M. D. and Bienert, G. P. (2017). Plant Aquaporins and Metalloids. In *Plant Aquaporins*, pp. 297–332. Springer.

Bienert, G. P. and Chaumont, F. (2014). Aquaporin-facilitated transmembrane diffusion of hydrogen peroxide. *Biochim. Biophys. Acta - Gen. Subj.* **1840**, 1596–1604.

Bienert, G. P., Schjoerring, J. K. and Jahn, T. P. (2006). Membrane transport of hydrogen peroxide. *Biochim. Biophys. Acta-Biomembranes* **1758**, 994–1003.

Bienert, G. P., Moller, A. L. B., Kristiansen, K. A., Schulz, A., Moller, I. M., Schjoerring, J. K. and Jahn, T. P. (2007). Specific aquaporins facilitate the diffusion of hydrogen peroxide across membranes. *J. Biol. Chem.* **282**, 1183–1192.

Bienert, G. P., Bienert, M. D., Jahn, T. P., Boutry, M. and Chaumont, F. (2011). *Solanaceae* XIPs are plasma membrane aquaporins that facilitate the transport of many uncharged substrates. *Plant J.* **66**, 306–317.

Bienert, G. P., Heinen, R. B., Berny, M. C. and Chaumont, F. (2014). Maize plasma membrane aquaporin ZmPIP2;5, but not ZmPIP1;2, facilitates transmembrane diffusion of hydrogen peroxide. *Biochim. Biophys. Acta-Biomembranes* **1838**, 216–222.

Bienert, M. D., Diehn, T. A., Richet, N., Chaumont, F. and Bienert, G. P. (2018). Heterotetramerization of plant PIP1 and PIP2 aquaporins is an evolutionary ancient feature to guide PIP1 plasma membrane localization and function. *Front. Plant Sci.* **9**,.

Booth, I. R. and Blount, P. (2012). The MscS and MscL families of mechanosensitive channels act as microbial emergency release valves. *J. Bacteriol.* **194**, 4802–4809.

Bose, J., Rodrigo-Moreno, A. and Shabala, S. (2014). ROS homeostasis in halophytes in the context of salinity stress tolerance. *J. Exp. Bot.* **65**, 1241–1257.

Bose, J., Munns, R., Shabala, S., Gilliham, M., Pogson, B. and Tyerman, S. D. (2017). Chloroplast function and ion regulation in plants growing on saline soils: Lessons from halophytes. *J. Exp. Bot.* **68**, 3129–3143.

Boudsocq, M., Barbier-Brygoo, H. and Laurière, C. (2004). Identification of nine sucrose nonfermenting 1-related protein kinases 2 activated by hyperosmotic and saline stresses in *Arabidopsis thaliana*. *J. Biol. Chem.* **279**, 41758–41766.

Boursiac, Y., Chen, S., Luu, D.-T. T., Sorieul, M., van den Dries, N. and Maurel, C. (2005). Early effects of salinity on water transport in *Arabidopsis* roots. Molecular and cellular features of aquaporin expression. *Plant Physiol.* **139**, 790–805.

Boursiac, Y., Boudet, J., Postaire, O., Luu, D.-T. T., Tournaire-Roux, C. and Maurel, C. (2008). Stimulus-induced downregulation of root water transport involves reactive oxygen species-activated cell signalling and plasma membrane intrinsic protein internalization. *Plant J.* **56**, 207–218.

Brandt, B., Brodsky, D. E., Xue, S., Negi, J., Iba, K., Kangasjärvi, J., Ghassemian, M., Stephan, A. B., Hu, H. and Schroeder, J. I. (2012). Reconstitution of abscisic acid activation of SLAC1 anion channel by CPK6 and OST1 kinases and branched ABI1 PP2C phosphatase action. *Proc. Natl. Acad. Sci. U. S. A.* **109**, 10593–10598.

Briggs, W. R. (2016). How do sunflowers follow the Sun - And to what end? *Science (80-.).* **353**, 541–542.

Britto, D. T. and Kronzucker, H. J. (2008). Cellular mechanisms of potassium transport in plants. *Physiol. Plant.* **133**, 637–650.

Brüggemann, L. I., Pottosin, I. I. and Schönknecht, G. (1999a). Cytoplasmic magnesium regulates the fast activating vacuolar cation channel. *J. Exp. Bot.* **50**, 1547–1552.

Brüggemann, L. I., Pottosin, I. I. and Schönknecht, G. (1999b). Selectivity of the fast activating vacuolar cation channel. *J. Exp. Bot.* **50**, 873–876.

Brutnell, T. P., Wang, L., Swartwood, K., Goldschmidt, A., Jackson, D., Zhu, X.-G., Kellogg, E. and Eck, J. Van (2010). *Setaria viridis*: A model for C_4 photosynthesis. *Plant Cell* **22**, 2537–2544.

Byrt, C. S., Zhao, M., Kourghi, M., Bose, J., Henderson, S. W., Qiu, J., Gilliham, M., Schultz, C., Schwarz, M., Ramesh, S. A., et al. (2017). Non-selective cation channel activity of aquaporin AtPIP2;1 regulated by Ca^{2+} and pH. *Plant Cell Environ.* **40**, 802–815.

Camacho-cristóbal, J. J., Rexach, J. and González-Fontes, A. (2008). Boron in plants: Deficiency and toxicity. *J. Integr. Plant Biol.* **50**, 1247–1255.

Campbell, E. M., Birdsell, D. N. and Yool, A. J. (2012). The activity of human aquaporin 1 as a cGMP-gated cation channel is regulated by tyrosine phosphorylation in the carboxyl-terminal domain. *Mol. Pharmacol.* **81**, 97–105.

Cerana, R. and Colombo, R. (1992). K^+ and Cl^- conductance of *Arabidopsis thaliana* plasma membrane at depolarized voltages. *Bot. Acta* **105**, 273–277.

Chandy, G., Zampighi, G. A., Kreman, M. and Hall, J. E. (1997). Comparison of the water transporting properties of MIP and AQP1. *J. Membr. Biol.* **159**, 29–39.

Chaumont, F. and Tyerman, S. D. (2014). Aquaporins: Highly regulated channels controlling plant water relations. *Plant Physiol.* **164**, 1600–1618.

Chaumont, F., Barrieu, F., Wojcik, E., Chrispeels, M. J. and Jung, R. (2001). Aquaporins constitute a large and highly divergent protein family in Maize. *Plant Physiol.* **125**, 1206–1215.

Chaves, M. M., Flexas, J. and Pinheiro, C. (2009). Photosynthesis under drought and salt stress: Regulation mechanisms from whole plant to cell. *Ann. Bot.* **103**, 551–560.

Chaw, S. M., Chang, C. C., Chen, H. L. and Li, W. H. (2004). Dating the monocot-dicot divergence and the origin of core eudicots using whole chloroplast genomes. *J. Mol. Evol.* **58**, 424–441.

Che-Othman, M. H., Millar, A. H. and Taylor, N. L. (2017). Connecting salt stress signalling pathways with salinity-induced changes in mitochondrial metabolic processes in C_3 plants. *Plant Cell Environ.* **40**, 2875–2905.

Chen, J., Lalonde, S., Obrdlik, P., Vatani, A. N., Parsa, S. A., Vilarino, C., Revuelta, J. L., Frommer, W. B. and Rhee, S. Y. (2012). Uncovering Arabidopsis membrane protein interactome enriched in transporters using mating-based split ubiquitin assays and classification models. *Front. Plant Sci.* **3**,.

Cheng, S., Willmann, M. R., Chen, H. and Sheen, J. (2002). Calcium signaling through protein kinases . The Arabidopsis Calcium-Dependent Protein Kinase gene family. *Plant Physiol.* **129**, 469–485.

Chérel, I. and Gaillard, I. (2019). The complex fine-tuning of K^+ fluxes in plants in relation to osmotic and ionic abiotic stresses. *Int. J. Mol. Sci.* **20**,.

Chevalier, A. S., Bienert, G. P. and Chaumont, F. (2014). A new LxxxA motif in the transmembrane helix3 of maize aquaporins belonging to the plasma membrane intrinsic protein PIP2 group is required for their trafficking to the plasma membrane. *Plant Physiol.* **166**, 125–138.

Clark, G. B. and Roux, S. J. (1995). Annexins of plant cells. *Plant Physiol.* **109**, 1133–1139.

Clough, S. J., Fengler, K. A., Yu, I. C., Lippok, B., Smith, R. K. and Bent, A. F. (2000). The *Arabidopsis* dnd1 "defense, no death" gene encodes a mutated cyclic nucleotide-gated ion channel. *PNAS* **97**, 9323–9328.

Conti, M., Hsieh, M., Musa Zamah, A. and Oh, J. S. (2012). Novel signaling mechanisms in the ovary during oocyte maturation and ovulation. *Mol. Cell. Endocrinol.* **356**, 65–73.

Corratgé-Faillie, C., Ronzier, E., Sanchez, F., Prado, K., Kim, J. H., Lanciano, S., Leonhardt, N., Lacombe, B. and Xiong, T. C. (2017). The Arabidopsis guard cell outward potassium channel GORK is regulated by CPK33. *FEBS Lett.* **591**, 1982–1992.

Cosgrove, D. J. and Hedrich, R. (1991). Stretch-activated chloride, potassium, and calcium channels coexisting in plasma membranes of guard cells of *Vicia faba* L. *Planta* **186**, 143–153.

Cotten, J. and Hayes, J. D. (1969). Genetic resistance to the cereal cyst nematode. *Heredity (Edinb).* **24**, 593–600.

Dai, A. (2013). Increasing drought under global warming in observations and models. *Nat.*

Clim. Chang. **3**, 52–58.

Dainty, J. (1963). Water Relations of Plant Cells. *Adv. Bot. Res.* **1**, 279–326.

Danielson, J. Å. A. H. and Johanson, U. (2008). Unexpected complexity of the aquaporin gene family in the moss *Physcomitrella patens*. *BMC Plant Biol.* **8**, 1–15.

Davenport, R. (2002). Glutamate receptors in plants. *Ann. Bot.* **90**, 549–557.

Davenport, R. J. and Tester, M. (2000a). A weakly voltage-dependent, nonselective cation channel mediates toxic sodium influx in wheat. *Plant Physiol.* **122**, 823–34.

Davenport, R. J. and Tester, M. (2000b). A weakly voltage-dependent, nonselective cation channel mediates toxic sodium influx in wheat. *Plant Physiol.* **122**, 823–834.

David, R., Byrt, C. S., Tyerman, S. D., Gilliham, M. and Wege, S. (2019). Roles of membrane transporters: connecting the dots from sequence to phenotype. *Ann. Bot.* **124**, 201–208.

de Boer, A. H. and Wegner, L. H. (1997). Regulatory mechanisms of ion channels in xylem parenchyma cells. *J. Exp. Bot.* **48**, 441–449.

De Ieso, M. L. and Yool, A. J. (2018). Mechanisms of aquaporin-facilitated cancer invasion and metastasis. *Front. Chem.* **6**,.

De Paula Santos Martins, C., Pedrosa, A. M., Du, D., Gonçalves, L. P., Yu, Q., Gmitter, F. G. and Costa, M. G. C. (2015). Genome-wide characterization and expression analysis of major intrinsic proteins during abiotic and biotic stresses in sweet orange (*Citrus sinensis* L. Osb.). *PLoS One* **10**, 1–17.

Demidchik, V. (2014). Mechanisms and physiological roles of K^+ efflux from root cells. *J. Plant Physiol.* **171**, 696–707.

Demidchik, V. and Maathuis, F. J. M. M. (2007). Physiological roles of nonselective cation channels in plants: From salt stress to signalling and development. *New Phytol.* **175**, 387–404.

Demidchik, V. and Tester, M. (2002). Sodium fluxes through nonselective cation channels in the plasma membrane of protoplasts from Arabidopsis roots. *Plant Physiol.* **128**, 379–387.

Demidchik, V., Sokolik, A. and Yurin, V. (1997). The effect of Cu^{2+} on ion transport systems of the plant. *Plant Physiol.* **114**, 1313–1325.

Demidchik, V., Davenport, R. J. and Tester, M. (2002a). Nonselective cation channels in plants. *Annu. Rev. Plant Biol.* **53**, 67–107.

Demidchik, V., Bowen, H. C., Maathuis, F. J. M., Shabala, S. N., Tester, M. A., White, P. J. and Davies, J. M. (2002b). *Arabidopsis thaliana* root non-selective cation channels mediate calcium uptake and are involved in growth. *Plant J.* **32**, 799–808.

Demidchik, V., Shabala, S., Coutts, K., Tester, M. and Davies, J. (2003). Free oxygen radicals regulate plasma membrane Ca^{2+}- and K^+-permeable channels in plant root cells. *J. Cell Sci.* **116**, 81–88.

Demidchik, V., Essah, P. A. and Tester, M. (2004). Glutamate activates cation currents in the plasma membrane of *Arabidopsis* root cells. *Planta* **219**, 167–175.

Demidchik, V., Shabala, S. N. and Davies, J. M. (2007). Spatial variation in H_2O_2 response of Arabidopsis thaliana root epidermal Ca^{2+} flux and plasma membrane Ca^{2+} channels. *Plant J.* **49**, 377–386.

Demir, F., Horntrich, C., Blachutzik, J. O., Scherzer, S., Reinders, Y., Kierszniowska, S., Schulze, W. X., Harms, G. S., Hedrich, R., Geiger, D., et al. (2013). Arabidopsis nanodomain-delimited ABA signaling pathway regulates the anion channel SLAH3. *PNAS* **110**, 8296–8301.

Dennison, K. L. and Spalding, E. P. (2000). Glutamate-gated calcium fluxes in *Arabidopsis*. *Plant Physiol.* **124**, 1511–1514.

di Pietro, M., Vialaret, J., Li, G.-W., Hem, S., Prado, K., Rossignol, M., Maurel, C. and Santoni, V. (2013). Coordinated post-translational responses of aquaporins to abiotic and nutritional stimuli in Arabidopsis roots. *Mol. Cell. Proteomics* **12**, 3886–3897.

Donaldson, L., Ludidi, N., Knight, M. R., Gehring, C. and Denby, K. (2004). Salt and osmotic stress cause rapid increases in *Arabidopsis thaliana* cGMP levels. *FEBS Lett.* **569**, 317–320.

Doolittle, R. F., Feng, D.-F., Tsang, S., Cho, G. and Little, E. (1996). Determining divergence times of the major kingdoms of living organisms with a protein clock. *Science (80-.).* **271**, 470–477.

Doust, A. N., Kellogg, E. A., Devos, K. M. and Bennetzen, J. L. (2009). Foxtail Millet: A sequence-driven grass model system. *Plant Physiol.* **149**, 137–141.

Dreyer, I., Gomez-Porras, J. L. and Riedelsberger, J. (2017). The potassium battery: a mobile energy source for transport processes in plant vascular tissues. *New Phytol.* **216**, 1049–1053.

Dreze, M., Carvunis, A.-R., Charloteaux, B., Galli, M., Pevzner, S. J., Tasan, M., Ahn, Y.-Y., Balumuri, P., Barabasi, A.-L., Bautista, V., et al. (2011). Evidence for network evolution in an Arabidopsis interactome map. *Science (80-.).* **333**, 601–607.

Dubos, C., Huggins, D., Grant, G. H., Knight, M. R. and Campbell, M. M. (2003). A role for glycine in the gating of plant NMDA-like receptors. *Plant J.* **35**, 800–810.

Duby, G., Poreba, W., Piotrowiak, D., Bobik, K., Derua, R., Waelkens, E. and Boutry, M. (2009). Activation of plant plasma membrane H^+-ATPase by 14-3-3 proteins is negatively controlled by two phosphorylation sites within the H^+-ATPase C-terminal region. *J. Biol. Chem.* **284**, 4213–4221.

Durbak, A. R., Phillips, K. A., Pike, S., O'Neill, M. A., Mares, J., Gallavotti, A., Malcomber, S. T., Gassmann, W., McSteen, P., Open, C. W., et al. (2014). Transport of boron by the tassel-less1 aquaporin is critical for vegetative and reproductive development in Maize. *Plant Cell* **26**, 2978–2995.

Dutta, R. and Robinson, K. R. (2004). Identification and characterisation of stretch-activated ion channels in pollen protoplasts. *Plant Physiol.* **135**, 1398–1406.

Dynowski, M., Schaaf, G., Loque, D., Moran, O. and Ludewig, U. (2008a). Plant plasma membrane water channels conduct the signalling molecule H_2O_2. *Biochem. J.* **414**, 53–61.

Dynowski, M., Mayer, M., Moran, O. and Ludewig, U. (2008b). Molecular determinants of ammonia and urea conductance in plant aquaporin homologs. *Febs Lett.* **582**, 2458–2462.

Ebihara, L. (1996). *Xenopus* connexin38 forms hemi-gap-junctional channels in the nonjunctional plasma membrane of *Xenopus* oocytes. *Biophys. J.* **71**, 742–748.

Ehring, G. R., Zampighi, G., Horwitz, J., Bok, D. and Hall, J. E. (1990). Properties of channels reconstituted from the major intrinsic protein of lens fiber membranes. *J Gen Physiol* **96**, 631–664.

Elzenga, J. T. M. and Van Volkenburgh, E. (1994). Characterization of ion channels in the plasma membrane of epidermal cells of expanding pea (*Pisum sativum* arg) leaves. *J. Membr. Biol.* **137**, 227–235.

Essah, P. A., Davenport, R. and Tester, M. (2003). Sodium influx and accumulation in Arabidopsis. *Plant Physiol.* **133**, 307–318.

Estacion, M., Sinkins, W. G., Jones, S. W., Applegate, M. A. B. and Schilling, W. P. (2006). Human TRPC6 expressed in HEK 293 cells forms non-selective cation channels with limited Ca^{2+} permeability. *J. Physiol.* **572**, 359–377.

Eto, K., Noda, Y., Horikawa, S., Uchida, S. and Sasaki, S. (2010). Phosphorylation of aquaporin-2 regulates its water permeability. *J. Biol. Chem.* **285**, 40777–40784.

Farooq, M., Wahid, A., Kobayashi, N., Fujita, D. and Basra, S. M. . M. A. (2009). Plant drought stress: effects, mechanisms and management. *Agron. Sustain. Dev.* **29**, 185–212.

Farooq, M., Hussain, M., Wahid, A. and Siddique, K. H. . (2012). Drought stress in plants: An overview. In *Plant Responses to Drought Stress* (ed. R. Aroca), pp. 1–33. Springer-Berlin.

Fenton, R. A., Moeller, H. B., Hoffert, J. D., Yu, M.-J., Nielsen, S. and Knepper, M. A. (2008). Acute regulation of aquaporin-2 phosphorylation at Ser-264 by vasopressin. *Proc. Natl. Acad. Sci. U. S. A.* **105**, 3134–3139.

Fetter, K., Van Wilder, V., Moshelion, M. and Chaumont, F. (2004). Interactions between plasma membrane aquaporins modulate their water channel activity. *Plant Cell* **16**, 215–228.

Fischer, M. and Kaldenhoff, R. (2008). On the pH regulation of plant aquaporins. *J. Biol. Chem.* **283**, 33889–33892.

Fischer, G., Kosinska-Eriksson, U., Aponte-Santamaría, C., Palmgren, M., Geijer, C., Hedfalk, K., Hohmann, S., De Groot, B. L., Neutze, R. and Lindkvist-Petersson, K. (2009). Crystal structure of a yeast aquaporin at 1.15 Å reveals a novel gating mechanism. *PLoS Biol.* **7**,.

Fitzpatrick, K. L. and Reid, R. J. (2009). The involvement of aquaglyceroporins in transport of boron in barley roots. *Plant, Cell Environ.* **32**, 1357–1365.

Flowers, T. J., Glenn, E. P. and Volkov, V. (2018). Could vesicular transport of Na^+ and Cl^- be a feature of salt tolerance in halophytes? *Ann. Bot.* **123**, 1–18.

Foreman, J., Demidchik, V., Bothwell, J. H. F., Mylona, P., Miedema, H., Angel

Torres, M., Linstead, P., Costa, S., Brownlee, C., Jones, J. D. G., et al. (2003). Reactive oxygen species produced by NADPH oxidase regulate plant cell growth. *Nature* **422**, 442–446.

Franz, S., Ehlert, B., Liese, A., Kurth, J., Cazalé, A. C. and Romeis, T. (2011). Calcium-dependent protein kinase CPK21 functions in abiotic stress response in *Arabidopsis thaliana*. *Mol. Plant* **4**, 83–96.

Frick, A., Järvå, M., Törnroth-Horsefield, S., Jarva, M., Tornroth-Horsefield, S., Järvå, M. and Törnroth-Horsefield, S. (2013). Structural basis for pH gating of plant aquaporins. *FEBS Lett.* **587**, 989–993.

Fricke, W. (2015). The significance of water co-transport for sustaining transpirational water flow in plants: a quantitative approach. *J. Exp. Bot.* **66**, 731–739.

Fricke, W. (2017). Water transport and energy. *Plant Cell Environ.* **40**, 977–994.

Fricke, W. and Chaumont, F. (2006). Solute and water relations of growing plant cells. In *The Expanding Cell*, pp. 7–31. Springer.

Fricke, W. and Knipfer, T. (2017). Plant Aquaporins and Cell Elongation. In *Plant Aquaporins*, pp. 107–131. Springer International Publishing.

Frigerio, L., Hinz, G. and Robinson, D. G. (2008). Multiple vacuoles in plant cells: Rule or exception? *Traffic* **9**, 1564–1570.

Fujiwara, T., Miwa, K., Tanaka, M. and Kamiya, T. (2010). Molecular mechanisms of boron transport in plants: Involvement of Arabidopsis NIP5;1 and NIP6;1. In *MIPs and their Role in the Exchange of Metalloids*, pp. 83–96. Springer.

Gajdanowicz, P., Michard, E., Sandmann, M., Rocha, M., Corrêa, L. G. G., Ramírez-Aguilar, S. J., Gomez-Porras, J. L., González, W., Thibaud, J. B., Van Dongen, J. T., et al. (2011). Potassium (K^+) gradients serve as a mobile energy source in plant vascular tissues. *Proc. Natl. Acad. Sci. U. S. A.* **108**, 864–869.

Gambetta, G. A., Knipfer, T., Fricke, W. and McElrone, A. J. (2017). Aquaporins and root water uptake. In *Plant Aquaporins*, pp. 133–153. Springer.

Garcia de la Garma, J., Fernandez-Garcia, N., Bardisi, E., Pallol, B., Asensio-Rubio, J. S., Bru, R. and Olmos, E. (2015). New insights into plant salt acclimation: The roles of vesicle trafficking and reactive oxygen species signalling in mitochondria and the endomembrane system. *New Phytol.* **205**, 216–239.

Gattolin, S., Sorieul, M. and Frigerio, L. (2011). Mapping of tonoplast intrinsic proteins in maturing and germinating *Arabidopsis* seeds reveals dual localization of embryonic TIPs to the tonoplast and plasma membrane. *Mol. Plant* **4**, 180–189.

Gavrin, A., Kaiser, B. N., Geiger, D., Tyerman, S. D., Wen, Z. Y., Bisseling, T., Fedorova, E. E. and Fedorov, E. V. (2014). Adjustment of host cells for accommodation of symbiotic bacteria: Vacuole defunctionalization, HOPS suppression, and TIP1g retargeting in *Medicago*. *Plant Cell* **26**, 3809–3822.

Geiger, D., Scherzer, S., Mumm, P., Marten, I., Ache, P., Matschi, S., Liese, A., Wellmann, C., Al-Rasheid, K. A. S. S., Grill, E., et al. (2010). Guard cell anion channel SLAC1 is regulated by CDPK protein kinases with distinct Ca^{2+} affinities. *Proc. Natl. Acad. Sci.* **107**, 8023–8028.

Geiger, D., Maierhofer, T., AL-Rasheid, K. A. S., Scherzer, S., Mumm, P., Liese, A., Ache, P., Wellmann, C., Marten, I., Grill, E., et al. (2011). Stomatal closure by fast abscisic acid signaling is mediated by the guard cell anion channel SLAH3 and the receptor RCAR1. *Sci. Signal.* **4**, 1–13.

Gelli, A. and Blumwald, E. (1997). Hyperpolarization-activated Ca^{2+}-permeable channels in the plasma membrane of Tomato cells. *J. Membr. Biol.* **155**, 35–45.

Gerbeau, P., Guclu, J., Ripoche, P. and Maurel, C. (1999). Aquaporin Nt-TIPα can account for the high permeability of tobacco cell vacuolar membrane to small neutral solutes. *Plant J.* **18**, 577–587.

Glass, D. . and Krebs, E. . (1980). Protein phosphorylation catalyzed by cyclic AMP-dependent and cyclic GMP-dependent protein kinases. *Annu. Rev. Pharmacol. Toxicol.* **20**, 363–388.

Gobert, A., Park, G., Amtmann, A., Sanders, D. and Maathuis, F. J. M. (2006). *Arabidopsis thaliana* Cyclic Nucleotide Gated Channel 3 forms a non-selective ion transporter involved in germination and cation transport. *J. Exp. Bot.* **57**, 791–800.

Goldman, R. P., Jozefkowicz, C., Canessa Fortuna, A., Sutka, M., Alleva, K. and Ozu, M. (2017). Tonoplast (BvTIP1;2) and plasma membrane (BvPIP2;1) aquaporins show different mechanosensitive properties. *FEBS Lett.* **591**, 1555–1565.

Greenway, H. and Munns, R. (1980). Mechanisms of salt tolerance in nonhalophytes. *Annu. Rev. Plant Physiol.* **31**, 149–190.

Grondin, A., Rodrigues, O., Verdoucq, L., Merlot, S., Leonhardt, N. and Maurel, C. (2015). Aquaporins contribute to ABA-triggered stomatal closure through OST1-mediated phosphorylation. *Plant Cell* **27**, 1945–1954.

Groszmann, M., Osborn, H. L. and Evans, J. R. (2017). Carbon dioxide and water transport through plant aquaporins. *Plant. Cell Environ.* **40**, 938–961.

Guenther, J. F., Chanmanivone, N., Galetovic, M. P., Wallace, I. S., Cobb, J. A. and Roberts, D. M. (2003). Phosphorylation of soybean nodulin 26 on serine 262 enhances water permeability and is regulated developmentally and by osmotic signals. *Plant Cell* **15**, 981–991.

Guinamard, R., Demion, M., Chatelier, A. and Bois, P. (2006). Calcium-activated nonselective cation channels in mammalian cardiomyocytes. *Trends Cardiovasc. Med.* **16**, 245–250.

Gunnarson, E., Axehult, G., Baturina, G., Zelenin, S., Zelenina, M. and Aperia, A. (2005). Lead induces increased water permeability in astrocytes expressing aquaporin 4. *Neuroscience* **136**, 105–114.

Hachez, C., Heinen, R. B., Draye, X. and Chaumont, F. (2008). The expression pattern of plasma membrane aquaporins in maize leaf highlights their role in hydraulic regulation. *Plant Mol. Biol.* **68**, 337–353.

Hachez, C., Milhiet, T., Heinen, R. B. and Chaumont, F. (2017). Roles of Aquaporins in Stomata. In *Plant Aquaporins*, pp. 167–183. Springer.

Hamel, L.-P., Sheen, J. and Séguin, A. (2014). Ancient signals: comparative genomics of green plant CDPKs. **154**, 2262–2265.

Hamilton, D. W. A., Hills, A., Köhler, B. and Blatt, M. R. (2000). Ca^{2+} channels at the plasma membrane of stomatal guard cells are activated by hyperpolarization and abscisic acid. *PNAS* **97**, 4967–4972.

Hamilton, E. S., Schlegel, A. M. and Haswell, E. S. (2014). United in diversity: Mechanosensitive ion channels in plants. *Annu. Rev. Plant Biol.* **66**, 113–137.

Han, Z. and Patil, R. V. (2000). Protein kinase A-dependent phosphorylation of aquaporin-1. *Biochem. Biophys. Res. Commun.* **273**, 328–332.

Hanaoka, H., Uraguchi, S., Takano, J., Tanaka, M. and Fujiwara, T. (2014). OsNIP3;1, a rice boric acid channel, regulates boron distribution and is essential for growth under boron-deficient conditions. *Plant J.* **78**, 890–902.

Haswell, E. S. and Meyerowitz, E. M. (2006). MscS-like proteins control plastid size and shape in *Arabidopsis thaliana*. *Curr. Biol.* **16**, 1–11.

Haswell, E. S., Rob, P. and Rees, D. C. (2011). Mechanosenstitve channels:what they can do and how do they do it? *Structure* **19**, 1356–1369.

Hazama, A., Kozono, D., Guggino, W. B., Agre, P. and Yasui, M. (2002). Ion permeation of AQP6 water channel protein. Single channel recordings after Hg^{2+} activation. *J. Biol. Chem.* **277**, 29224–30.

Hedfalk, K., Tornroth-Horsefield, S., Nyblom, M., Johanson, U., Kjellbom, P. and Neutze, R. (2006). Aquaporin gating. *Curr. Opin. Struct. Biol.* **16**, 447–456.

Hedrich, R. and Marten, I. (2011). TPC1 - SV channels gain shape. *Mol. Plant* **4**, 428–441.

Hedrich, R. and Neher, E. (1987). Cytoplasmic calcium regulates voltage-dependent ion channels in plant vacuoles. *Nature* **329**, 833–836.

Hedrich, R. and Roelfsema, M. R. G. (2001). Plant ion transport. *Life Sci.*

Henzler, T., Ye, Q. and Steudle, E. (2004). Oxidative gating of water channels (aquaporins) in *Chara* by hydroxyl radicals. *Plant Cell Environ.* **27**, 1184–1195.

Higinbotham, N. (1973). Electro potentials of plant cells. *Ann. Rev. Plant Physiol* **46**, 25–46.

Hill, A. E. and Shachar-Hill, Y. (2015). Are aquaporins the missing transmembrane osmosensors? *J. Membr. Biol.* **248**, 753–765.

Hill, A. E., Shachar-Hill, B. and Shachar-Hill, Y. (2004). What are aquaporins for? *J. Membr. Biol.* **197**, 1–32.

Hiroaki, Y., Tani, K., Kamegawa, A., Gyobu, N., Nishikawa, K., Suzuki, H., Walz, T., Sasaki, S., Mitsuoka, K., Kimura, K., et al. (2006). Implications of the aquaporin-4 structure on array formation and cell adhesion. *J. Mol. Biol.* **355**, 628–639.

Hoffert, J. D., Pisitkun, T., Wang, G., Shen, R.-F. and Knepper, M. A. (2006). Quantitative phosphoproteomics of vasopressin-sensitive renal cells: Regulation of aquaporin-2 phosphorylation at two sites. *Proc. Natl. Acad. Sci.* **103**, 7159–7164.

Hoffert, J. D., Fenton, R. A., Moeller, H. B., Simons, B., Tchapyjnikov, D., McDill, B. W., Yu, M. J., Pisitkun, T., Chen, F. and Knepper, M. A. (2008). Vasopressin-

stimulated increase in phosphorylation at Ser269 potentiates plasma membrane retention of aquaporin-2. *J. Biol. Chem.* **283**, 24617–24627.

Hoffmann, L. (1989). Algae of terrestrial habitats. *Bot. Rev.* **55**, 77–105.

Holzinger, A. and Karsten, U. (2013). Desiccation stress and tolerance in green algae: Consequences for ultrastructure, physiological, and molecular mechanisms. *Front. Plant Sci.* **4**,.

Holzinger, A., Lütz, C. and Karsten, U. (2011). Desiccation stress causes structural and ultrastructural alterations in the aeroterrestrial green alga *Klebsormidium crenulatum* (Klebsormidiophyceae, Streptophyta) isolated from an alpine soil crust. *J. Phycol.* **47**, 591–602.

Homblé, F. and Véry, A. A. (1992). Coupling of water and potassium ions in K^+ channels of the tonoplast of *Chara*. *Biophys. J.* **63**, 996–999.

Hooijmaijers, C., Rhee, J. Y., Kwak, K. J., Chung, G. C., Horie, T., Katsuhara, M. and Kang, H. (2012). Hydrogen peroxide permeability of plasma membrane aquaporins of *Arabidopsis thaliana*. *J. Plant Res.* **125**, 147–153.

Hori, K., Maruyama, F., Fujisawa, T., Togashi, T., Yamamoto, N., Seo, M., Sato, S., Yamada, T., Mori, H., Tajima, N., et al. (2014). *Klebsormidium flaccidum* genome reveals primary factors for plant terrestrial adaptation. *Nat. Commun.* **5**, 3978.

Horie, T., Kaneko, T., Sugimoto, G., Sasano, S., Panda, S. K., Shibasaka, M. and Katsuhara, M. (2011). Mechanisms of water transport mediated by PIP aquaporins and their regulation via phosphorylation events under salinity stress in Barley roots. *Plant Cell Physiol.* **52**, 663–675.

Hrabak, E. M., Chan, C. W. M., Gribskov, M., Harper, J. F., Choi, J. H., Halford, N., Kudla, J., Luan, S., Nimmo, H. G., Sussman, M. R., et al. (2003). The Arabidopsis CDPK-SnRK superfamily of protein kinases. *Plant Physiol.* **132**, 666–680.

Hrmova, M. and Gilliham, M. (2018). Plants fighting back: to transport or not to transport, this is a structural question. *Curr. Opin. Plant Biol.* **46**, 68–76.

Hsu, J.-L., Wang, L.-Y., Wang, S.-Y., Lin, C.-H., Ho, K.-C., Shi, F.-K. and Chang, I.-F. (2009). Functional phosphoproteomic profiling of phosphorylation sites in membrane fractions of salt-stressed *Arabidopsis thaliana*. *Proteome Sci.* **7**, 42.

Hu, J. and Verkman, A. S. (2006). Increased migration and metastatic potential of tumor cells expressing aquaporin water channels. *FASEB J.* **20**,.

Hua, B. G., Mercier, R. W., Leng, Q. and Berkowitz, G. A. (2003). Plants do it differently. A new basis for potassium/sodium selectivity in the pore of an ion channel. *Plant Physiol.* **132**, 1353–1361.

Ikeda, M., Beitz, E., Kozono, D., Guggino, W. B., Agre, P. and Yasui, M. (2002). Characterization of aquaporin-6 as a nitrate channel in mammalian cells. Requirement of pore-lining residue threonine 63. *J. Biol. Chem.* **277**, 39873–39879.

Isayenkov, S. V. and Maathuis, F. J. M. (2019). Plant salinity stress: Many unanswered questions remain. *Front. Plant Sci.* **10**,.

Isayenkov, S., Isner, J. C. and Maathuis, F. J. M. (2010). Vacuolar ion channels: Roles

in plant nutrition and signalling. *FEBS Lett.* **584**, 1982–1988.

Jahn, T. P., Møller, A. L. B., Zeuthen, T., Holm, L. M., Klærke, D. A., Mohsin, B., Kühlbrandt, W. and Schjoerring, J. K. (2004). Aquaporin homologues in plants and mammals transport ammonia. *FEBS Lett.* **574**, 31–36.

James, R. A., Blake, C., Zwart, A. B., Hare, R. A., Rathjen, A. J. and Munns, R. (2012). Impact of ancestral wheat sodium exclusion genes Nax1 and Nax2 on grain yield of durum wheat on saline soils. *Funct. Plant Biol.* **39**, 609–618.

Jang, J. Y., Kim, D. G., Kim, Y. O., Kim, J. S. and Kang, H. S. (2004). An expression analysis of a gene family encoding plasma membrane aquaporins in response to abiotic stresses in *Arabidopsis thaliana*. *Plant Mol. Biol.* **54**, 713–725.

Jang, J. Y., Rhee, J. Y., Chung, G. C. and Kang, H. (2012). Aquaporin as a membrane transporter of hydrogen peroxide in plant response to stresses. *Plant Signal. Behav.* **7**, 1180–1181.

Jang, H. Y., Rhee, J., Carlson, J. E. and Ahn, S. J. (2014). The Camelina aquaporin CsPIP2;1 is regulated by phosphorylation at Ser273, but not at Ser277, of the C-terminus and is involved in salt- and drought-stress responses. *J. Plant Physiol.* **171**, 1401–1412.

Jayatilake, D. V., Tucker, E. J., Brueggemann, J., Lewis, J., Garcia, M., Dreisigacker, S., Hayden, M. J., Chalmers, K. and Mather, D. E. (2015). Genetic mapping of the Cre8 locus for resistance against cereal cyst nematode (*Heterodera avenae* Woll.) in wheat. *Mol. Breed.* **35**,.

Jezek, M. and Blatt, M. R. (2017). The membrane transport system of the guard cell and its integration for stomatal dynamics. *Plant Physiol.* **174**, 487–519.

Johanson, U., Karlsson, M., Johansson, I., Gustavsson, S., Sjö, S., Fraysse, L., Weig, A. R. and Kjellbom, P. (2001). The complete set of genes encoding Major Intrinsic Proteins in Arabidopsis provides a framework for a new nomenclature for Major Intrinsic Proteins in plants. *Plant Physiol.* **126**, 1358–1369.

Johansson, I., Karlsson, M., Shukla, V. K., Chrispeels, M. J., Larsson, C. and Kjellbom, P. (1998). Water transport activity of the plasma membrane aquaporin PM28A is regulated by phosphorylation. *Plant Cell* **10**, 451–459.

Johansson, I., Karlsson, M., Johanson, U., Larsson, C. and Kjellbom, P. (2000). The role of aquaporins in cellular and whole plant water balance. *Biochim. Biophys. Acta-Biomembranes* **1465**, 324–342.

Johnson, M. A. and Preuss, D. (2002). Plotting a course: Multiple signals guide pollen tubes to their targets. *Dev. Cell* **2**, 273–281.

Jones, A. M., Xuan, Y., Xu, M., Wang, R.-S., Ho, C.-H., Lalonde, S., You, C. H., Sardi, M. I., Parsa, S. A., Smith-Valle, E., et al. (2014). Border Control—A membrane-linked interactome of *Arabidopsis*. *Science (80-.).* **344**, 711–716.

Karsten, U. and Holzinger, A. (2014). Green algae in alpine biological soil crust communities: Acclimation strategies against ultraviolet radiation and dehydration. *Biodivers. Conserv.* **23**, 1845–1858.

Kato, Y., Miwa, K., Takano, J., Wada, M. and Fujiwara, T. (2009). Highly boron

deficiency-tolerant plants generated by enhanced expression of NIP5;1, a boric acid channel. *Plant Cell Physiol.* **50**, 58–66.

Katsuhara, M., Akiyama, Y., Koshio, K., Shibasaka, M. and Kasamo, K. (2002). Functional analysis of water channels in barley roots. *Plant Cell Physiol.* **43**, 885–893.

Katsuhara, M., Koshio, K., Shibasaka, M., Hayashi, Y., Hayakawa, T. and Kasamo, K. (2003). Over-expression of a barley aquaporin increased the shoot/root ratio and raised salt sensitivity in transgenic rice plants. *Plant Cell Physiol.* **44**, 1378–1383.

Kiegle, E., Gilliham, M., Haseloff, J. and Tester, M. (2000). Hyperpolarisation-activated calcium currents found only in cells from the elongation zone of *Arabidopsis thaliana* roots. *Plant J.* **21**, 225–229.

Kim, M. J., Kim, H. R. and Paek, K. H. (2006). Arabidopsis tonoplast proteins TIP1 and TIP2 interact with the cucumber mosaic virus 1a replication protein. *J. Gen. Virol.* **87**, 3425–3431.

Kim, T.-H. H., Böhmer, M., Hu, H. H., Nishimura, N., Schroeder, J. I., Bohmer, M., Hu, H. H., Nishimura, N. and Schroeder, J. I. (2010). Guard cell signal transduction network: Advances in understanding abscisic acid, CO_2, and Ca^{2+} signaling. *Annu. Rev. Plant Biol. Vol 61* **61**, 561–591.

Kirscht, A., Kaptan, S. S., Bienert, G. P., Chaumont, F., Nissen, P., De Groot, B. L., Kjellbom, P., Gourdon 5¤, P. and Johanson, U. (2016). Crystal structure of an ammonia-permeable aquaporin. *PLOS Biol.* **14**, e1002411.

Kitchen, P., Öberg, F., Sjöhamn, J., Hedfalk, K., Bill, R. M., Conner, A. C., Conner, M. T. and Törnroth-Horsefield, S. (2015). Plasma membrane abundance of human aquaporin 5 is dynamically regulated by multiple pathways. *PLoS One* **10**,.

Knipfer, T. and Fricke, W. (2010). Root pressure and a solute reflection coefficient close to unity exclude a purely apoplastic pathway of radial water transport in barley (*Hordeum vulgare*). *Source New Phytol.* **187**, 159–170.

Kobayashi, Y., Yamamoto, S., Minami, H., Kagaya, Y. and Hattori, T. (2004). Differential activation of the rice sucrose nonfermenting1-related protein kinase2 family by hyperosmotic stress and abscisic acid. *Plant Cell* **16**, 1163–1177.

Kollist, H., Nuhkat, M. and Roelfsema, M. R. G. (2014). Closing gaps: Linking elements that control stomatal movement. *New Phytol.* **203**, 44–62.

Kourghi, M., Pei, J. V., De Ieso, M. L., Flynn, G. and Yool, A. J. (2015). Bumetanide derivatives AqB007 and AqB011 selectively block the Aquaporin-1 ion channel conductance and slow cancer cell migration. *Mol. Pharmacol.* **89**, 133–140.

Kourghi, M., Nourmohammadi, S., Pei, J., Qiu, J., McGaughey, S., Tyerman, S., Byrt, C. and Yool, A. (2017). Divalent cations regulate the ion conductance properties of diverse classes of aquaporins. *Int. J. Mol. Sci.* **18**,.

Kourghi, M., Pei, J. V., De Ieso, M. L., Nourmohammadi, S., Chow, P. H. and Yool, A. J. (2018). Fundamental structural and functional properties of Aquaporin ion channels found across the kingdoms of life. *Clin. Exp. Pharmacol. Physiol.* **45**, 401–409.

Krajinski, F., Biela, A., Schubert, D., Gianinazzi-Pearson, V., Kaldenhoff, R. and Franken, P. (2000). Arbuscular mycorrhiza development regulates the mRNA abundance of Mtaqp1 encoding a mercury-insensitive aquaporin of *Medicago truncatula*. *Planta* **211**, 85–90.

Kretschmer, J. M., Chalmers, K. J., Manning, S., Karakousis, A., Barr, A. R., Islam, A. K. M. R., Logue, S. J., Choe, Y. W., Barker, S. J., Lance, R. C. M., et al. (1997). RFLP mapping of the *Ha2* cereal cyst nematode resistance gene in barley. *Theor. Appl. Genet.* **94**, 1060–1064.

Kronzucker, H. J. and Britto, D. T. (2011). Sodium transport in plants: A critical review. *New Phytol.* **189**, 54–81.

Kulik, A., Wawer, I., Krzywińska, E., Bucholc, M. and Dobrowolska, G. (2011). SnRK2 protein kinases--key regulators of plant response to abiotic stresses. *OMICS* **15**, 859–72.

Kumar, K., Mosa, K. A., Chhikara, S., Musante, C., White, J. C. and Dhankher, O. P. (2014). Two rice plasma membrane intrinsic proteins, OsPIP2;4 and OsPIP2;7, are involved in transport and providing tolerance to boron toxicity. *Planta* **239**, 187–198.

Kumari, S. S., Ghandi, J., Mustehan, M. H., Eren, S. and Varadaraj, K. (2013). Functional characterisation of an AQP0 missense mutation, R33C, that causes dominat congenital lens cataract, reveals impaired cell-to-cell adhesion. *Exp. Eye Res.* **116**, 1–38.

Kuruma, A., Hirayama, Y. and Hartzell, H. C. (2000). A hyperpolarization- and acid-activated nonselective cation current in *Xenopus* oocytes. *Am. J. Physiol. Physiol.* **279**, C1401–C1413.

Kushmerick, C., Rice, S. J., Baldo, G. J., Haspel, H. C. and Mathias, R. T. (1995). Ion, water and neutral solute transport in *Xenopus* oocytes expressing frog lens MIP. *Exp. Eye Res.* **61**, 351–362.

Kuwahara, M., Fushimi, K., Terada, Y., Liqun, B., Marumo, F. and Sasaki, S. (1995). cAMP-dependent Phosphorylation Stimulates Water Permeability of Aquaporin-collecting Duct Water Channel Protein Expressed in *Xenopus* Oocytes. *J. Biol. Chem.* **270**, 10384–10387.

Lam, H. M., Chiu, J., Hsieh, M. H., Meisel, L., Oliveira, I. C., Shin, M. and Coruzzi, G. (1998). Glutamate-receptor genes in plants. *Nature* **396**, 125–126.

Latz, A., Mehlmer, N., Zapf, S., Mueller, T. D., Wurzinger, B., Pfister, B., Csaszar, E., Hedrich, R., Teige, M. and Becker, D. (2013). Salt stress triggers phosphorylation of the arabidopsis vacuolar K^+ channel TPK1 by calcium-dependent protein kinases (CDPKs). *Mol. Plant* **6**, 1274–1289.

Lee, J. W., Zhang, Y., Weaver, C. D., Shomer, N. H., Louis, C. F. and Roberts, D. M. (1995). Phosphorylation of Nodulin 26 on Serine 262 affects its voltage-sensitive channel activity in planar lipid bilayers. *J. Biol. Chem.* **270**, 27051–27057.

Lee, S. C., Lan, W., Buchanan, B. B. and Luan, S. (2009). A protein kinase-phosphatase pair interacts with an ion channel to regulate ABA signaling in plant guard cells. *Proc. Natl. Acad. Sci. U. S. A.* **106**, 21419–21424.

Leitão, L., Prista, C., Loureiro-Dias, M. C., Moura, T. F. and Soveral, G. (2014). The

grapevine tonoplast aquaporin TIP2;1 is a pressure gated water channel. *Biochem. Biophys. Res. Commun.* **450**, 289–294.

Leliaert, F., Smith, D. R., Moreau, H., Herron, M. D., Verbruggen, H., Delwiche, C. F. and De Clerck, O. (2012). Phylogeny and molecular evolution of the green algae. *CRC. Crit. Rev. Plant Sci.* **31**, 1–46.

Leng, Q., Mercier, R. W., Hua, B. G., Fromm, H. and Berkowitz, G. A. (2002). Electrophysiological analysis of cloned cyclic nucleotide-gated ion channels. *Plant Physiol.* **128**, 400–410.

Lewis, L. A. and McCourt, R. M. (2004). Green algae and the origin of land plants. *Am. J. Bot.* **91**, 1535–1556.

Li, P. and Brutnell, T. P. (2011). *Setaria viridis* and *Setaria italica*, model genetic systems for the Panicoid grasses. *J. Exp. Bot.* 2–7.

Li, X., Borsics, T., Harrington, H. M. and Christopher, D. A. (2005). Arabidopsis AtCNGC10 rescues potassium channel mutants of *E. coli*, yeast and Arabidopsis and is regulated by calcium/calmodulin and cyclic GMP in *E. coli*. *Funct. Plant Biol.* **32**, 643–653.

Li, R. Y., Ago, Y., Liu, W. J., Mitani, N., Feldmann, J., McGrath, S. P., Ma, J. F. and Zhao, F. J. (2009). The rice aquaporin Lsi1 mediates uptake of methylated arsenic species. *Plant Physiol.* **150**, 2071–2080.

Li, X., Wang, X., Yang, Y., Li, R., He, Q., Fang, X., Luu, D.-T., Maurel, C. and Lin, J. (2011). Single-molecule analysis of PIP2;1 dynamics and partitioning reveals multiple modes of *Arabidopsis* plasma membrane aquaporin regulation. *Plant Cell* **23**, 3780–3797.

Li, G., Santoni, V. and Maurel, C. (2014). Plant aquaporins: Roles in plant physiology. *Biochim. Biophys. Acta - Gen. Subj.* **1840**, 1574–1582.

Li, R., Wang, J., Li, S., Zhang, L., Qi, C., Weeda, S., Zhao, B., Ren, S., Guo, Y.-D., Toenniessen, G. H., et al. (2016). Plasma membrane intrinsic proteins SlPIP2;1, SlPIP2;7 and SlPIP2;5 conferring enhanced drought stress tolerance in tomato. *Sci. Rep.* **6**, 31814.

Ligaba, A., Katsuhara, M., Shibasaka, M. and Djira, G. (2011). Abiotic stresses modulate expression of major intrinsic proteins in barley (*Hordeum vulgare*). *Comptes Rendus - Biol.* **334**, 127–139.

Liu, K., Kozono, D., Kato, Y., Agre, P., Hazama, A. and Yasui, M. (2005). Conversion of aquaporin 6 from an anion channel to a water-selective channel by a single amino acid substitution. *Proc. Natl. Acad. Sci. U. S. A.* **102**, 2192–7.

Liu, S., Kandoth, P. K., Warren, S. D., Yeckel, G., Heinz, R., Alden, J., Yang, C., Jamai, A., El-Mellouki, T., Juvale, P. S., et al. (2012). A soybean cyst nematode resistance gene points to a new mechanism of plant resistance to pathogens. *Nature* **492**, 256–260.

Liu, S., Kandoth, P. K., Lakhssassi, N., Kang, J., Colantonio, V., Heinz, R., Yeckel, G., Zhou, Z., Bekal, S., Dapprich, J., et al. (2017). The soybean GmSNAP18 gene underlies two types of resistance to soybean cyst nematode. *Nat. Commun.* **8**, 1–11.

Loqué, D., Ludewig, U., Yuan, L. and von Wirén, N. (2005). Tonoplast intrinsic proteins AtTIP2;1 and AtTIP2;3 facilitate NH_3 transport into the vacuole. *Plant Physiol.* **137**, 671–680.

Lu, H. J., Matsuzaki, T., Bouley, R., Hasler, U., Qin, Q. H. and Brown, D. (2008). The phosphorylation state of serine 256 is dominant over that of serine 261 in the regulation of AQP2 trafficking in renal epithelial cells. *Am J Physiol Ren. Physiol* **295**, F290-4.

Luang, S. and Hrmova, M. (2017). Structural Basis of the Permeation Function of Plant Aquaporins. In *Plant Aquaporins*, pp. 1–28. Springer.

Ludevid, D., Höfte, H., Himelblau, E. and Chrispeels, M. J. (1992). The expression pattern of the tonoplast intrinsic protein γ-TIP in Arabidopsis thaliana is correlated with cell enlargement. *Plant Physiol.* **100**, 1633–9.

Luu, D. T., Martiniãre, A., Sorieul, M., Runions, J., Maurel, C., Martiniere, A., Sorieul, M., Runions, J. and Maurel, C. (2012). Fluorescence recovery after photobleaching reveals high cycling dynamics of plasma membrane aquaporins in Arabidopsis roots under salt stress. *Plant J.* **69**, 894–905.

Ma, J. F., Tamai, K., Yamaji, N., Mitani, N., Konishi, S., Katsuhara, M., Ishiguro, M., Murata, Y. and Yano, M. (2006). A silicon transporter in rice. *Nature* **440**, 688–691.

Maathuis, F. J. M. (2006). cGMP modulates gene transcription and cation transport in *Arabidopsis* roots. *Plant J.* **45**, 700–711.

Maathuis, F. J. and Sanders, D. (2001). Sodium uptake in *Arabidopsis* roots is regulated by cyclic nucleotides. *Plant Physiol.* **127**, 1617–25.

Madeira, F., Park, Y. mi, Lee, J., Buso, N., Gur, T., Madhusoodanan, N., Basutkar, P., Tivey, A. R. N., Potter, S. C., Finn, R. D., et al. (2019). The EMBL-EBI search and sequence analysis tools APIs in 2019. *Nucleic Acids Res.* **47**, W636–W641.

Manchun, Z. (2013). CO_2 and ion transport via plant aquaporins.

Martinez-Ballesta, M. D. C., Silva, C., Lopez-Berenguer, C., Cabanero, F. J. and Carvajal, M. (2006). Plant aquaporins: New perspectives on water and nutrient uptake in saline environment. *Plant Biol.* **8**, 535–546.

Martinière, A., Li, X., Runions, J., Lin, J., Maurel, C. and Luu, D.-T. (2012). Salt stress triggers enhanced cycling of *Arabidopsis* root plasma-membrane aquaporins. *Plant Signal. Behav.* **7**, 529–32.

Martinoia, E., Maeshima, M. and Neuhaus, H. E. (2006). Vacuolar transporters and their essential role in plant metabolism. *J. Exp. Bot.* **58**, 83–102.

Marty, F. (1999). Plant Vacuoles. *Plant Cell Online* **11**, 587–600.

Maser, P., Thomine, S., Schroeder, J. I., Ward, J. M., Hirschi, K., Sze, H., Talke, I. N., Amtmann, A., Maathuis, F. J. M., Sanders, D., et al. (2001). Phylogenetic relationships within cation transporter families of *Arabidopsis*. *Plant Physiol.* **126**, 1646–1667.

Maurel, C. (2007). Plant aquaporins: novel functions and regulation properties. *Febs Lett.* **581**, 2227–2236.

Maurel, C., Kado, R. T., Guern, J. and Chrispeels, M. J. (1995). Phosphorylation Regulates the Water Channel Activity of the Seed-Specific Aquaporin Alpha-Tip. *Embo J.* **14**, 3028–3035.

Maurel, C., Verdoucq, L., Luu, D.-T. T. and Santoni, V. (2008). Plant aquaporins: Membrane channels with multiple integrated functions. *Annu. Rev. Plant Biol* **59**, 595–624.

Maurel, C., Boursiac, Y., Luu, D. D.-T. T., Santoni, V., Shahzad, Z. and Verdoucq, L. (2015). Aquaporins in plants. *Physiol. Rev.* **95**, 1321–1358.

McCoy, E. and Sontheimer, H. (2007). Expression and function of water channels (aquaporins) in migrating malignant astrocytes. *Glia* **55**, 1034–1043.

McCoy, E. S., Haas, B. R. and Sontheimer, H. (2010). Water permeability through aquaporin-4 is regulated by protein kinase C and becomes rate-limiting for glioma invasion. *Neuroscience* **168**, 971–981.

McDonald, G. K., Taylor, J. D., Verbyla, A. and Kuchel, H. (2012). Assessing the importance of subsoil constraints to yield of wheat and its implications for yield improvement. *Crop Pasture Sci.* **63**, 1043–1065.

McGaughey, S. A., Osborn, H. L., Chen, L., Pegler, J. L., Tyerman, S. D., Furbank, R. T., Byrt, C. S. and Grof, C. P. L. (2016). Roles of aquaporins in *Setaria viridis* stem development and sugar storage. *Front. Plant Sci.* **7**,.

McGaughey, S. A., Qiu, J., Tyerman, S. D. and Byrt, C. S. (2018). Regulating root Aquaporin function in response to changes in salinity. *Annu. Plant Rev.* **1**, 1–36.

Mehlmer, N., Wurzinger, B., Stael, S., Hofmann-Rodrigues, D., Csaszar, E., Pfister, B., Bayer, R. and Teige, M. (2010). The Ca^{2+}-dependent protein kinase CPK3 is required for MAPK-independent salt-stress acclimation in *Arabidopsis*. *Plant J.* **63**, 484–498.

Metzger, M. B., Maurer, M. J., Dancy, B. M. and Michaelis, S. (2008). Degradation of a cytosolic protein requires endoplasmic reticulum-associated degradation machinery. *J. Biol. Chem.* **283**, 32302–32316.

Miller, A. J. and Zhou, J. J. (2000). *Xenopus* oocytes as an expression system for plant transporters. *Biochim. Biophys. Acta - Biomembr.* **1465**, 343–358.

Miller, G., Suzuki, N., Ciftci-Yilmaz, S. and Mittler, R. (2010). Reactive oxygen species homeostasis and signalling during drought and salinity stresses. *Plant, Cell Environ.* **33**, 453–467.

Mitani-Ueno, N., Yamaji, N., Zhao, F.-J. J. and Ma, J. F. (2011). The aromatic/arginine selectivity filter of NIP aquaporins plays a critical role in substrate selectivity for silicon, boron, and arsenic. *J. Exp. Bot.* **62**, 4391–4398.

Modesto, E., Lampe, P. D., Ribeiro, M. C., Spray, D. C. and Campos De Carvalho, A. C. (1996). Properties of chicken lens MIP channels reconstituted into planar lipid bilayers. *J. Membr. Biol.* **154**, 239–249.

Moeller, H. B., Praetorius, J., Rutzler, M. R. and Fenton, R. A. (2010). Phosphorylation of aquaporin-2 regulates its endocytosis and protein-protein interactions. *Proc. Natl. Acad. Sci.* **107**, 424–429.

Mori, I. C., Murata, Y., Yang, Y., Munemasa, S., Wang, Y. F., Andreoli, S., Tiriac, H., Alonso, J. M., Harper, J. F., Ecker, J. R., et al. (2006). CDPKs CPK6 and CPK3 function in ABA regulation of guard cell S-type anion- and Ca^{2+}- permeable channels and stomatal closure. *PLoS Biol.* **4**, 1749–1762.

Mosa, K. A., Kumar, K., Chhikara, S., Musante, C., White, J. C. and Dhankher, O. P. (2016). Enhanced boron tolerance in plants mediated by bidirectional transport through plasma membrane intrinsic proteins. *Sci. Rep.* **6**,.

Munns, R. (2002). Comparative physiology of salt and water stress. *Plant. Cell Environ.* **25**, 239–250.

Munns, R. and Tester, M. (2008). Mechanisms of salinity tolerance. *Annu. Rev. Plant Biol* **59**, 651–81.

Munns, R., James, R. A., Xu, B., Athman, A., Conn, S. J., Jordans, C., Byrt, C. S., Hare, R. A., Tyerman, S. D., Tester, M., et al. (2012). Wheat grain yield on saline soils is improved by an ancestral Na^+ transporter gene. *Nat. Biotechnol.* **30**, 360–364.

Munns, R., Day, D. A., Fricke, W., Watt, M., Arsova, B., Barkla, B. J., Bose, J., Byrt, C. S., Chen, Z., Foster, K. J., et al. (2019). Energy costs of salt tolerance in crop plants. *New Phytol.*

Murray, G. M. and Brennan, J. P. (2010). Estimating disease losses to the Australian wheat industry. *Australas. Plant Pathol.* 558–570.

Nable, R. O., Bañuelos, G. S. and Paull, J. G. (1997). Boron toxicity. *Plant Soil* **193**, 181–198.

Nardini, A., Salleo, S. and Jansen, S. (2011). More than just a vulnerable pipeline: Xylem physiology in the light of ion-mediated regulation of plant water transport. *J. Exp. Bot.* **62**, 4701–4718.

Neill, S. J., Desikan, R., Clarke, A., Hurst, R. D. and Hancock, J. T. (2001). Hydrogen peroxide and nitric oxide as signalling molecules in plants. *J. Exp. Bot.* **53**, 1237–1247.

Németh-Cahalan, K. L. and Hall, J. E. (2000). pH and calcium regulate the water permeability of aquaporin 0. *J. Biol. Chem.* **275**, 6777–6782.

Nesverova, V. and Törnroth-Horsefield, S. (2019). Phosphorylation-dependent regulation of mammalian aquaporins. *Cells* **8**, 1–21.

Niemietz, C. M. and Tyerman, S. D. (1997). Characterization of water channels in Wheat root membrane vesicles. *Plant Physiol.* **115**, 561–567.

Nilius, B. (1990). Permeation properties of a non-selective cation channel in human vascular endothelial cells. *Pflügers Arch. Eur. J. Physiol.* **416**, 609–611.

Noctor, G., Mhamdi, A. and Foyer, C. H. (2014). The roles of reactive oxygen metabolism in drought: Not so cut and dried. *Plant Physiol.* **164**, 1636–1648.

Nongpiur, R. C., Singla-Pareek, S. L., Pareek, A., Quinn, D. J., Mcferran, N. V, Nelson, J., Duprex, W. P. and Kingdom, U. (2019). The quest for 'osmosensors' in plants. *J. Exp. Bot.* 1–31.

Nyblom, M., Frick, A., Wang, Y., Ekvall, M., Hallgren, K., Hedfalk, K., Neutze, R., Tajkhorshid, E. and Törnroth-Horsefield, S. (2009). Structural and functional analysis of SoPIP2;1 mutants adds insight into plant aquaporin gating. *J. Mol. Biol.* **387**, 653–668.

O'Neill, M. A., Eberhard, S., Albersheim, P. and Darvill, A. G. (2001). Requirement of borate cross-linking of cell wall rhamnogalacturonan II for *Arabidopsis* growth. *Science (80-.).* **294**, 846–849.

Oertli, J. J. (1966). Active water transport in plants. *Physiol. Plant.* **19**, 809–817.

Okubo-Kurihara, E., Sano, T., Higaki, T., Kutsuna, N. and Hasezawa, S. (2009). Acceleration of vacuolar regeneration and cell growth by overexpression of an aquaporin NtTIP1;1in Tobacco BY-2 cells. *Plant Cell Physiol.* **50**, 151–160.

Opperman, C. H., Taylor, C. G. and Conkling, M. A. (1994). Root-knot nematode-directed expression of a plant root-specific gene. *Science (80-.).* **263**, 221–223.

Ormancey, M., Thuleau, P., Mazars, C. and Cotelle, V. (2017). CDPKs and 14-3-3 proteins: Emerging duo in signaling. *Trends Plant Sci.* **22**, 263–272.

Osakabe, Y., Osakabe, K., Shinozaki, K., Tran, L.-S. P. and Testerink, C. (2014). Response of plants to water stress. *Front. Plant Sci.* **5**, 1–8.

Osborn, H. L. (2017). Understanding CO_2 diffusion in C_4 plants: An investigation of CO_2 permeable aquaporins and carbonic anhydrase in the C_4 grass *Setaria viridis*.

Otto, B., Uehlein, N., Sdorra, S., Fischer, M., Ayaz, M., Belastegui-Macadam, X., Heckwolf, M., Lachnit, M., Pede, N., Priem, N., et al. (2010). Aquaporin tetramer composition modifies the function of Tobacco aquaporins. *J. Biol. Chem.* **285**, 31253–31260.

Ozu, M., Dorr, R. A., Teresa Politi, M., Parisi, M. and Toriano, R. (2011). Water flux through human aquaporin 1: Inhibition by intracellular furosemide and maximal response with high osmotic gradients. *Eur. Biophys. J.* **40**, 737–746.

Ozu, M., Dorr, R. A., Gutiérrez, F., Teresa Politi, M. and Toriano, R. (2013). Human AQP1 is a constitutively open channel that closes by a membrane-tension-mediated mechanism. *Biophys. J.* **104**, 85–95.

Ozu, M., Galizia, L., Acuña, C. and Amodeo, G. (2018). Aquaporins: More than functional monomers in a tetrameric arrangement. *Cells* **7**, 1–24.

Paal, J., Henselewski, H., Muth, J., Meksem, K., Menéndez, C. M., Salamini, F., Ballvora, A. and Gebhardt, C. (2004). Molecular cloning of the potato *Gro1-4* gene conferring resistance to pathotype Ro1 of the root cyst nematode *Globodera rostochiensis*, based on a candidate gene approach. *Plant J.* **38**, 285–297.

Pang, Y., Li, L., Ren, F., Lu, P., Wei, P., Cai, J., Xin, L., Zhang, J., Chen, J. and Wang, X. (2010). Overexpression of the tonoplast aquaporin AtTIP5;1 conferred tolerance to boron toxicity in Arabidopsis. *J. Genet. Genomics* **37**, 389–397.

Papadopoulos, M. C., Saadoun, S. and Verkman, A. S. (2008). Aquaporins and cell migration. *Pflugers Arch. Eur. J. Physiol.* **456**, 693–700.

Peiter, E., Maathuis, F. J. M., Mills, L. N., Knight, H., Pelloux, J., Hetherington, A.

M. and Sanders, D. (2005). The vacuolar Ca^{2+}-activated channel TPC1 regulates germination and stomatal movement. *Nature* **434**, 404.

Petrov, V. D. and Van Breusegem, F. (2012). Hydrogen peroxide-a central hub for information flow in plant cells. *AoB Plants* **12**,.

Pickard, W. F. (2003). The riddle of root pressure. II. Root exudation at extreme osmolalities. *Funct. Plant Biol.* **30**, 135–141.

Pickard, B. G. and Ding, J. P. (1993). The mechanosensory calcium-selective ion channel: Key component of a plasmalemmal control centre? *Aust. J. Plant Physiol.* **20**, 439–459.

Piñeros, M. A. and Kochian, L. V. (2003). Differences in whole-cell and single-channel ion currents across the plasma membrane of mesophyll cells from two closely related *Thlaspi* species. *Plant Physiol.* **131**, 583–594.

Pottosin, I. and Dobrovinskaya, O. (2014). Non-selective cation channels in plasma and vacuolar membranes and their contribution to K^+ transport. *J. Plant Physiol.* **171**, 732–742.

Pottosin, I. I. and Martínez-Estévez, M. (2003). Regulation of the fast vacuolar channel by cytosolic and vacuolar potassium. *Biophys. J.* **84**, 977–986.

Pottosin, I. I., Martínez-Estévez, M., Dobrovinskaya, O. R. and Muñiz, J. (2003). Potassium-selective channel in the red beet vacuolar membrane. *J. Exp. Bot.* **54**, 663–667.

Prado, K. and Maurel, C. (2013). Regulation of leaf hydraulics: from molecular to whole plant levels. *Front. Plant Sci.* **4**,.

Prado, K., Cotelle, V., Li, G., Bellati, J., Tang, N., Tournaire-Roux, C., Martiniere, A., Santoni, V., Maurel, C., Martiniere, A., et al. (2019). Oscillating aquaporin phosphorylations and 14-3-3 proteins mediate circadian regulation of leaf hydraulics. *Plant Cell* **4**, tpc.00804.2018.

Prak, S., Hem, S., Boudet, J., Viennois, G., Sommerer, N., Rossignol, M., Maurel, C. and Santoni, V. (2008). Multiple phosphorylations in the C-terminal tail of plant plasma membrane aquaporins. *Mol. Cell. Proteomics* **7**, 1019–1030.

Qi, Z., Kishigami, A., Nakagawa, Y., Iida, H. and Sokabe, M. (2004). A mechanosensitive anion channel in *Arabidopsis thaliana* mesophyll cells. *Plant Cell Physiol.* **45**, 1704–1708.

Qi, Z., Stephens, N. R. and Spalding, E. P. (2006). Calcium entry mediated by GLR3.3, an *Arabidopsis* glutamate receptor with a broad agonist profile. *Plant Physiol.* **142**, 963–971.

Qing, D., Yang, Z., Li, M., Wong, W. S., Guo, G., Liu, S., Guo, H. and Li, N. (2016). Quantitative and functional phosphoproteomic analysis reveals that ethylene regulates water transport via the C-terminal phosphorylation of aquaporin PIP2;1 in *Arabidopsis*. *Mol. Plant* **9**, 158–174.

Qiu, J., Henderson, S. W., Tester, M., Roy, S. J. and Gilliham, M. (2016). SLAH1, a homologue of the slow type anion channel SLAC1, modulates shoot Cl^- accumulation and salt tolerance in *Arabidopsis thaliana*. *J. Exp. Bot.* **67**, 4495–4505.

Raven, J. A. and Doblin, M. A. (2014). Active water transport in unicellular algae: Where, why, and how. *J. Exp. Bot.* **65**, 6279–6292.

Reddy, P. S., Rao, T. S. R. B., Sharma, K. K. and Vadez, V. (2015). Genome-wide identification and characterization of the aquaporin gene family in *Sorghum bicolor* (L.). *Plant Gene* **1**, 18–28.

Reid, R. (2010). Can we really increase yields by making crop plants tolerant to boron toxicity? *Plant Sci.* **178**, 9–11.

Rensing, S. A., Lang, D., Zimmer, A. D., Terry, A., Salamov, A., Shapiro, H., Nishiyama, T., Perroud, P. F., Lindquist, E. A., Kamisugi, Y., et al. (2008). The *Physcomitrella* genome reveals evolutionary insights into the conquest of land by plants. *Science (80-.).* **319**, 64–69.

Rhee, J., Horie, T., Sasano, S., Nakahara, Y. and Katsuhara, M. (2017). Identification of an H_2O_2 permeable PIP aquaporin in barley and a serine residue promoting H_2O_2 transport. *Physiol. Plant.* **159**, 120–128.

Ricanek, P., Lunde, L. K., Frye, S. A., Støen, M., Nygård, S., Morth, J. P., Rydning, A., Vatn, M. H., Amiry-Moghaddam, M. and Tønjum, T. (2015). Reduced expression of aquaporins in human intestinal mucosa in early stage inflammatory bowel disease. *Clin. Exp. Gastroenterol.* **8**, 49–67.

Roberts, S. K. and Tester, M. (1997). A patch clamp study of Na^+ transport in maize roots. *J. Exp. Bot.* **48**, 431–440.

Roberts, D. M. and Tyerman, S. D. (2002). Voltage-dependent cation channels permeable to NH_4^+, K^+, and Ca^{2+} in the symbiosome membrane of the model legume Lotus japonicus. *Plant Physiol.* **128**, 370–378.

Rodrigues, O., Reshetnyak, G., Grondin, A., Saijo, Y., Leonhardt, N., Maurel, C. and Verdoucq, L. (2017). Aquaporins facilitate hydrogen peroxide entry into guard cells to mediate ABA- and pathogen-triggered stomatal closure. *Proc. Natl. Acad. Sci.* **114**, 9200–9205.

Roussel, H., Bruns, S., Gianinazzi-pearson, V., Hahlbrock, K. and Franken, P. (1997). Induction of a membrane intrinsic protein encoding mRNA in AM elicitor-stimulated cell suspension cultures of parsley.pdf. *Plant Sci.* **126**, 203–210.

Roux, B. and Leonhardt, N. (2018). The Regulation of Ion Channels and Transporters in the Guard Cell. In *Advances in Botanical Research*, pp. 171–214. Academic Press Inc.

Roy, S. J., Negrão, S. and Tester, M. (2014). Salt resistant crop plants. *Curr. Opin. Biotechnol.* **26**, 115–124.

Rubio, F., Flores, P., Navarro, J. M. and Martínez, V. (2003). Effects of Ca^{2+}, K^+ and cGMP on Na^+ uptake in pepper plants. *Plant Sci.* **165**, 1043–1049.

Rubio, F., Alemán, F., Nieves-Cordones, M. and Martínez, V. (2010). Studies on Arabidopsis *athak5*, *atakt1* double mutants disclose the range of concentrations at which AtHAK5, AtAKT1 and unknown systems mediate K^+ uptake. *Physiol. Plant.* **139**, 220–228.

Sablowski, R. (2016). Coordination of plant cell growth and division: collective control or

mutual agreement? *Curr. Opin. Plant Biol.* **34**, 54–60.

Sade, N. and Moshelion, M. (2017). Plant aquaporins and abiotic stress. In *Plant Aquaporins*, pp. 185–206. Springer.

Sakurai, J., Ishikawa, F., Yamaguchi, T., Uemura, M. and Maeshima, M. (2005). Identification of 33 rice aquaporin genes and analysis of their expression and function. *Plant Cell Physiol.* **46**, 1568–1577.

Santoni, V. (2017). Plant Aquaporin Posttranslational Regulation. In *Plant Aquaporins*, pp. 83–105. Springer.

Saparov, S. M., Kozono, D., Rothe, U., Agre, P. and Pohl, P. (2001). Water and ion permeation of Aquaporin-1 in planar lipid bilayers. *J. Biol. Chem.* **276**, 31515–31520.

Sato, A., Gambale, F., Dreyer, I. and Uozumi, N. (2010). Modulation of the *Arabidopsis* KAT1 channel by an activator of protein kinase C in *Xenopus laevis* oocytes. *FEBS J.* **277**, 2318–2328.

Schnurbusch, T., Hayes, J. and Sutton, T. (2010a). Boron toxicity tolerance in wheat and barley: Australian perspectives. *Breed. Sci.* **60**, 297–304.

Schnurbusch, T., Hayes, J., Hrmova, M., Baumann, U., Ramesh, S. A., Tyerman, S. D., Langridge, P. and Sutton, T. (2010b). Boron toxicity tolerance in Barley through reduced expression of the multifunctional aquaporin HvNIP2;1. *Plant Physiol.* **153**, 1706–1715.

Schroeder, J. I., Delhaize, E., Frommer, W. B., Guerinot, M. Lou, Harrison, M. J., Herrera-Estrella, L., Horie, T., Kochian, L. V., Munns, R., Nishizawa, N. K., et al. (2013). Using membrane transporters to improve crops for sustainable food production. *Nature* **497**, 60–66.

Schulz, P., Herde, M. and Romeis, T. (2013). Calcium-Dependent Protein Kinases: Hubs in plant stress signaling and development. *Plant Physiol.* **163**, 523–530.

Shabala, S. and Shabala, L. (2011). Ion transport and osmotic adjustment in plants and bacteria. *Biomol. Concepts* **2**, 407–419.

Shabala, L., Cuin, T. A., Newman, I. A. and Shabala, S. (2005). Salinity-induced ion flux patterns from the excised roots of Arabidopsis *sos* mutants. *Planta* **222**, 1041–1050.

Shabala, S., Demidchik, V., Shabala, L., Cuin, T. a, Smith, S. J., Miller, A. J., Davies, J. M. and Newman, I. a (2006). Extracellular Ca^{2+} ameliorates NaCl-induced K^+ loss from Arabidopsis root and leaf cells by controlling plasma membrane K^+-permeable channels. *Plant Physiol.* **141**, 1653–1665.

Shabala, S., Cuin, T. A. and Pottosin, I. (2007). Polyamines prevent NaCl-induced K^+ efflux from pea mesophyll by blocking non-selective cation channels. *FEBS Lett.* **581**, 1993–1999.

Sharma, T., Dreyer, I. and Riedelsberger, J. (2013). The role of K^+ channels in uptake and redistribution of potassium in the model plant *Arabidopsis thaliana*. *Front. Plant Sci.* **4**, 1–16.

Shen, L., Shrager, P., Girsch, S. J., Donaldson, P. J. and Peracchia, C. (1991). Channel

reconstitution in liposomes and planar bilayers with HPLC-purified MIP26 of bovine lens. *J. Membr. Biol.* **124**, 21–32.

Shinozawa, A., Otake, R., Takezawa, D., Umezawa, T., Komatsu, K., Tanaka, K., Amagai, A., Ishikawa, S., Hara, Y., Kamisugi, Y., et al. (2019). SnRK2 protein kinases represent an ancient system in plants for adaptation to a terrestrial environment. *Commun. Biol.* **2**, 30.

Sjövall-Larsen, S., Alexandersson, E., Johansson, I., Karlsson, M., Johanson, U. and Kjellbom, P. (2006). Purification and characterization of two protein kinases acting on the aquaporin SoPIP2;1. *Biochim. Biophys. Acta - Biomembr.* **1758**, 1157–1164.

Smith, S. A., Beaulieu, J. M. and Donoghue, M. J. (2010). An uncorrelated relaxed-clock analysis suggests an earlier origin for flowering plants. *Proc. Natl. Acad. Sci.* **107**, 5897–5902.

Sobczak, K., Bangel-Ruland, N., Leier, G. and Weber, W. M. (2010). Endogenous transport systems in the *Xenopus laevis* oocyte plasma membrane. *Methods* **51**, 183–189.

Soveral, G., Madeira, A., Loureiro-Dias, M. C. and Moura, T. F. (2008). Membrane tension regulates water transport in yeast. *Biochim. Biophys. Acta - Biomembr.* **1778**, 2573–2579.

Soveral, G., Nielsen, S. and Casini, A. (2018). *Aquaporins in health and disease: new molecular targets for drug discovery*. CRC Press.

Spalding, E. P., Slayman, C. L., Goldsmith, M. H. M., Gradmann, D. and Bertl, A. (1992). Ion channels in *Arabidopsis* plasma membrane: Transport characteristics and involvement in light-induced voltage changes. *Plant Physiol.* **99**, 96–102.

Stoeckel, H. and Takeda, K. (1989). Calcium-activated, voltage dependent, non-selective cation currents in endosperm plasma membrane from higher plants. *Proc. R. Soc. London* **237**, 213–231.

Stroka, K. M., Jiang, H., Chen, S. H., Tong, Z., Wirtz, D., Sun, S. X. and Konstantopoulos, K. (2014). Water permeation drives tumor cell migration in confined microenvironments. *Cell* **157**, 611–623.

Sutton, T., Baumann, U., Hayes, J., Collins, N. C., Shi, B. J., Schnurbusch, T., Hay, A., Mayo, G., Pallotta, M., Tester, M., et al. (2007). Boron-toxicity tolerance in barley arising from efflux transporter amplification. *Science (80-.).* **318**, 1446–1449.

Takano, J., Wada, M., Ludewig, U., Schaaf, G., Von Wirén, N. and Fujiwara, T. (2006). The Arabidopsis major intrinsic protein NIP5;1 is essential for efficient boron uptake and plant development under boron limitation. *Plant Cell* **18**, 1498–1509.

Tanaka, M., Wallace, I. S., Takano, J., Roberts, D. M. and Fujiwara, T. (2008). NIP6;1 Is a boric acid channel for preferential transport of boron to growing shoot tissues in *Arabidopsis*. *Plant Cell* **20**, 2860–2875.

Tang, S., Li, L., Wang, Y., Chen, Q., Zhang, W., Jia, G., Zhi, H., Zhao, B. and Diao, X. (2017). Genotype-specific physiological and transcriptomic responses to drought stress in *Setaria italica* (an emerging model for Panicoideae grasses). *Sci. Rep.* **7**, 1–15.

Tanghe, A., Van Dijck, P., Dumortier, F., Teunissen, A., Hohmann, S. and Thevelein, J. M. (2002). Aquaporin expression correlates with freeze tolerance in baker's yeast, and overexpression improves freeze tolerance in industrial strains. *Appl. Environ. Microbiol.* **68**, 5981–5989.

Tanghe, A., Van Dijck, P., Colavizza, D. and Thevelein, J. M. (2004). Aquaporin-mediated improvement of freeze tolerance of *Saccharomyces cerevisiae* is restricted to rapid freezing conditions. *Appl. Environ. Microbiol.* **70**, 3377–3382.

Tanghe, A., Carbrey, J. M., Agre, P., Thevelein, J. M. and Van Dijck, P. (2005). Aquaporin expression and freeze tolerance in *Candida albicans*. *Appl. Environ. Microbiol.* **71**, 6434–6437.

Temmei, Y., Uchida, S., Hoshino, D., Kanzawa, N., Kuwahara, M., Sasaki, S. and Tsuchiya, T. (2005). Water channel activities of *Mimosa pudica* plasma membrane intrinsic proteins are regulated by direct interaction and phosphorylation. *Febs Lett.* **579**, 4417–4422.

Tester, M. and Davenport, R. (2003). Na^+ tolerance and Na^+ transport in higher plants. *Ann. Bot.* **91**, 503–527.

Thiel, G., Moroni, A., Orsi, S., Camoni, L., Visconti, S., Giacometti, S., Marra, M., Aducci, P., Olivari, C., Sottocornola, B., et al. (2006). The potassium channel KAT1 is activated by plant and animal 14-3-3 proteins. *J. Biol. Chem.* **281**, 35735–35741.

Tian, S., Wang, X., Li, P., Wang, H., Ji, H., Xie, J., Qiu, Q., Shen, D. and Dong, H. (2016). Plant aquaporin AtPIP1;4 links apoplastic H_2O_2 induction to disease immunity pathways. *Plant Physiol.* **171**, 1635–1650.

Tikhonova, L., Pottosin, I. I., Dietz, K. and Schonknecht, G. (1997). Fast-activating cation channel in barley mesophyll vacuoles. Inhibition by calcium. *Plant J.* **11**, 1059–1070.

Tornroth-Horsefield, S., Wang, Y., Hedfalk, K., Johanson, U., Karlsson, M., Tajkhorshid, E., Neutze, R. and Kjellbom, P. (2006). Structural mechanism of plant aquaporin gating. *Nature* **439**, 688–694.

Törnroth-Horsefield, S., Hedfalk, K., Fischer, G., Lindkvist-Petersson, K. and Neutze, R. (2010). Structural insights into eukaryotic aquaporin regulation. *FEBS Lett.* **584**, 2580–2588.

Tournaire-Roux, C., Sutka, M., Javot, H. H., Gout, E. E., Gerbeau, P., Luu, D.-T. T., Bligny, R. and Maurel, C. (2002). Cytosolic pH regulates root water transport during anoxic stress through gating of aquaporins. *Nature* **425**, 187–194.

Trenberth, K. E., Dai, A., van der Schrier, G., Jones, P. D., Barichivich, J., Briffa, K. R. and Sheffield, J. (2014). Global warming and changes in drought. *Nat. Clim. Chang.* **4**, 17–22.

Tyerman, S. D., Whitehead, L. F. and Day, D. A. (1995). A channel-like transporter for NH_4^+ on the symbiotic interface of N_2-fixing plants. *Nature* **378**, 629–632.

Tyerman, S. D., Skerrett, M., Garrill, A., Findlay, G. P. and Leigh, R. A. (1997). Pathways for the permeation of Na^+ and Cl^- into protoplasts derived from the cortex of wheat roots. *J. Exp. Bot.* **48**, 459–480.

Tyerman, S. D., Bohnert, H. J., Maurel, C., Steudle, E. and Smith, J. A. C. (1999). Plant aquaporins: their molecular biology, biophysics and significance for plant water relations. *J. Exp. Bot.* **50**, 1055–1071.

Tzounopoulos, T., Maylie, J. and Adelman, J. P. (1995). Induction of endogenous channels by high levels of heterologous membrane proteins in *Xenopus* oocytes. *Biophys. J.* **69**, 904–908.

Ueda, M., Tsutsumi, N. and Fujimoto, M. (2016). Salt stress induces internalization of plasma membrane aquaporin into the vacuole in *Arabidopsis thaliana*. *Biochem. Biophys. Res. Commun.* **474**, 742–746.

Uehlein, N., Lovisolo, C., Siefritz, F. and Kaldenhoff, R. (2003). The tobacco aquaporin NtAQP1 is a membrane CO_2 pore with physiological functions. *Nature* **425**, 734–737.

Valmonte, G. R., Arthur, K., Higgins, C. M. and Macdiarmid, R. M. (2014). Calcium-dependent protein kinases in plants : Evolution, expression and function. **55**, 551–569.

Van Balkom, B. W. M., Savelkoul, P. J. M., Markovich, D., Hofman, E., Nielsen, S., Van Der Sluijs, P. and Deen, P. M. T. (2002). The role of putative phosphorylation sites in the targeting and shuttling of the aquaporin-2 water channel. *J. Biol. Chem.* **277**, 41473–41479.

Van den Wijngaard, P. W. J., Bunney, T. D., Roobeek, I., Schönknecht, G. and De Boer, A. H. (2001). Slow vacuolar channels from barley mesophyll cells are regulated by 14-3-3 proteins. *FEBS Lett.* **488**, 100–104.

Van Gansbeke, B., Khoo, K. H. P., Lewis, J. G., Chalmers, K. J. and Mather, D. E. (2019). Fine mapping of Rha2 in barley reveals candidate genes for resistance against cereal cyst nematode. *Theor. Appl. Genet.* **132**, 1309–1320.

van Kleeff, P. J. M., Gao, J., Mol, S., Zwart, N., Zhang, H., Li, K. W. and de Boer, A. H. (2018). The Arabidopsis GORK K^+-channel is phosphorylated by calcium-dependent protein kinase 21 (CPK21), which in turn is activated by 14-3-3 proteins. *Plant Physiol. Biochem.* **125**, 219–231.

Van Wilder, V. V. V., Miecielica, U., Degand, H. H. H., Derua, R., Waelkens, E. and Chaumont, F. F. (2008). Maize plasma membrane aquaporins belonging to the PIP1 and PIP2 subgroups are in vivo phosphorylated. *Plant Cell Physiol.* **49**, 1364–1377.

Vandeleur, R., Niemietz, C., Tilbrook, J. and Tyerman, S. D. (2005). Roles of aquaporins in root responses to irrigation. *Plant Soil* **274**, 141–161.

Vandeleur, R. K., Mayo, G., Shelden, M. C., Gilliham, M., Kaiser, B. N. and Tyerman, S. D. (2009). The role of plasma membrane intrinsic protein aquaporins in water transport through roots: diurnal and drought stress responses reveal different strategies between isohydric and anisohydric cultivars of grapevine. *Plant Physiol.* **149**, 445–460.

Vandeleur, R. K., Sullivan, W., Athman, A., Jordans, C., Gilliham, M., Kaiser, B. N. and Tyerman, S. D. (2014). Rapid shoot-to-root signalling regulates root hydraulic conductance via aquaporins. *Plant, Cell Environ.* **37**, 520–538.

Velarde-Buendía, A. M., Shabala, S., Cvikrova, M., Dobrovinskaya, O. and Pottosin, I. (2012). Salt-sensitive and salt-tolerant barley varieties differ in the extent of potentiation of the ROS-induced K^+ efflux by polyamines. *Plant Physiol. Biochem.*

61, 18–23.

Verdoucq, L., Grondin, A. and Maurel, C. (2008). Structure–function analysis of plant aquaporin AtPIP2;1 gating by divalent cations and protons. *Biochem. J.* **415**, 409–416.

Very, A. A., Robinson, M. F., Mansfield, T. A. and Sanders, D. (1998). Guard cell cation channels are involved in Na^+-induced stomatal closure in a halophyte. *Plant J.* **14**, 509–521.

Véry, A. A. and Davies, J. M. (2000). Hyperpolarization-activated calcium channels at the tip of *Arabidopsis* root hairs. *PNAS* **97**, 9801–9806.

Véry, A. A. and Sentenac, H. (2002). Cation channels in the *Arabidopsis* plasma membrane. *Trends Plant Sci.* **7**, 168–175.

Vialaret, J., Di Pietro, M., Hem, S., Maurel, C., Rossignol, M. and Santoni, V. (2014). Phosphorylation dynamics of membrane proteins from Arabidopsis roots submitted to salt stress. *Proteomics* **14**, 1058–1070.

Vlad, F., Turk, B. E., Peynot, P., Leung, J. and Merlot, S. (2008). A versatile strategy to define the phosphorylation preferences of plant protein kinases and screen for putative substrates. *Plant J.* **55**, 104–117.

Volkov, V. and Amtmann, A. (2006). *Thellungiella halophila*, a salt-tolerant relative of *Arabidopsis thaliana*, has specific root ion-channel features supporting K^+/Na^+ homeostasis under salinity stress. *Plant J.* **48**, 342–353.

Volkov, V., Wang, B., Dominy, P. J., Fricke, W. and Amtmann, A. (2004). *Thellungiella halophila*, a salt-tolerant relative of *Arabidopsis thaliana*, possesses effective mechanisms to discriminate between potassium and sodium. *Plant, Cell Environ.* **27**, 1–14.

Wan, X. C., Steudle, E. and Hartung, W. (2004). Gating of water channels (aquaporins) in cortical cells of young corn roots by mechanical stimuli (pressure pulses): Effects of ABA and of $HgCl_2$. *J. Exp. Bot.* **55**, 411–422.

Wang, L.-L. L., Chen, A.-P. P., Zhong, N.-Q. Q., Liu, N., Wu, X.-M. M., Wang, F., Yang, C.-L. L., Romero, M. F. and Xia, G.-X. X. (2014). The *Thellungiella salsuginea* tonoplast aquaporin TsTIP1;2 functions in protection against multiple abiotic stresses. *Plant Cell Physiol.* **55**, 148–161.

Wang, C., Hu, H., Qin, X., Zeise, B., Xu, D., Rappel, W.-J. J., Boron, W. F. and Schroeder, J. I. (2016). Reconstitution of CO_2 regulation of SLAC1 anion channel and function of CO_2-permeable PIP2;1 aquaporin as CARBONIC ANHYDRASE4 interactor. *Plant Cell* **28**, 568–582.

Ward, J. M., Mäser, P. and Schroeder, J. I. (2009). Plant ion channels: Gene families, physiology, and functional genomics analyses. *Annu. Rev. Physiol.* **71**, 59–82.

Weaver, C. D. and Roberts, D. M. (1992). Determination of the site of phosphorylation of Nodulin 26 by the calcium-dependent protein kinase from Soybean nodules. *Biochemistry* **31**, 8954–8959.

Weaver, C. D., Shomer, N. H., Louis, C. F. and Roberts, D. M. (1994). Nodulin 26, a nodule-specific symbiosome membrane protein from Soybean, is an ion channel. *J.*

Biol. Chem. **269**, 17858–17862.

Weber, W.-M. (1999). Ion currents of *Xenopus laevis* oocytes: state of the art. *Biochim. Biophys. Acta (BBA)-Biomembranes* **1421**, 213–233.

Wegner, L. H. (2014). Root pressure and beyond: energetically uphill water transport into xylem vessels? *J. Exp. Bot.* **65**, 381–393.

Wegner, L. H. (2015). A thermodynamic analysis of the feasibility of water secretion into xylem vessels against a water potential gradient. *Funct. Plant Biol.* **42**, 828–835.

Wegner, L. H. and Raschke, K. (1994). Ion channels in the xylem parenchyma of barley roots. *Plant Physiol.* **105**, 799–813.

Wegner, L. H. and Shabala, S. (2019). Biochemical pH clamp: the forgotten resource in membrane bioenergetics. *New Phytol.* nph.16094.

White, P. J. (1997). Cation channels in the plasma membrane of rye roots. *J. Exp. Bot.* **48**, 499–514.

White, P. J. and Broadley, M. R. (2001). Chloride in soils and its uptake and movement within the plant: A review. *Ann. Bot.* **88**, 967–988.

White, P. J. and Davenport, R. J. (2002). The voltage-independent cation channel in the plasma membrane of wheat roots is permeable to divalent cations and may be involved in cytosolic Ca^{2+} homeostasis. *Plant Physiol.* **130**, 1386–1395.

White, P. J. and Tester, M. A. (1992). Potassium channels from the plasma membrane of rye roots characterised following incorporation into planar lipid bilayers. *Planta* **186**, 188–202.

Wirthmueller, L., Maqbool, A. and Banfield, M. J. (2013). On the front line: Structural insights into plant-pathogen interactions. *Nat. Rev. Microbiol.* **11**, 761–776.

Wood, C. C., Porée, F., Dreyer, I., Koehler, G. J. and Udvardi, M. K. (2006). Mechanisms of ammonium transport, accumulation, and retention in ooyctes and yeast cells expressing Arabidopsis AtAMT1;1. *FEBS Lett.* **580**, 3931–3936.

Wu, H., Shabala, L., Zhou, M. and Shabala, S. (2015). Chloroplast-generated ROS dominate NaCl- induced K^+ efflux in wheat leaf mesophyll. *Plant Signal. Behav.* **10**, 1–4.

Yamaguchi, T. and Blumwald, E. (2005). Developing salt-tolerant crop plants: challenges and opportunities. *Trends Plant Sci.* **10**, 615–620.

Yaneff, A., Sigaut, L., Marquez, M., Alleva, K., Pietrasanta, L. I., Amodeo, G., Pietrasanta, I. and Amodeo, G. (2014). Heteromerization of PIP aquaporins affects their intrinsic permeability. *Proc. Natl. Acad. Sci. U. S. A.* **111**, 231–236.

Yaneff, A., Vitali, V. and Amodeo, G. (2015). PIP1 aquaporins: Intrinsic water channels or PIP2 aquaporin modulators? *FEBS Lett.* **589**, 3508–3515.

Yaneff, A., Sigaut, L., Gómez, N., Aliaga Fandiño, C., Alleva, K., Pietrasanta, L. I. and Amodeo, G. (2016). Loop B serine of a plasma membrane aquaporin type PIP2 but not PIP1 plays a key role in pH sensing. *Biochim. Biophys. Acta - Biomembr.* **1858**, 2778–2787.

Yang, B. X. and Sachs, F. (1990). Characterization of stretch-activated ion channels in *Xenopus* oocytes. *J. Physiol.* **431**, 103–122.

Yanochko, G. M. and Yool, A. J. (2002). Regulated cationic channel function in *Xenopus* oocytes expressing *Drosophila* Big Brain. *J. Neurosci.* **22**, 2530–2540.

Yanochko, G. M. and Yool, A. J. (2004). Block by extracellular divalent cations of *Drosophila* Big Brain channels expressed in *Xenopus* oocytes. *Biophys. J.* **86**, 1470–1478.

Yanochko, G. M., Vaillancourt, R. R., Regan, J. W. and Yool, A. J. (2000). The MIP-related channel, big brain is regulated by tyrosine phosphorylation in *Xenopus* oocytes. *FASEB J.* **14**, 344.

Yasui, M., Kwon, T.-H., Knepper, M. A., Nielsen, S. and Agre, P. (1999a). Aquaporin-6: An intracellular vesicle water channel protein in renal epithelia. *Proc. Natl. Acad. Sci.* **96**, 5808–5813.

Yasui, M., Hazama, A., Kwon, T.-H. H., Nielsen, S., Guggino, W. B., Agre, P., Yasui, M., Hazama, A., Kwon, T.-H. H., Nielsen, S., et al. (1999b). Rapid gating and anion permeability of an intracellular aquaporin. *Nature* **402**, 184–187.

Ye, Q. and Steudle, E. (2006). Oxidative gating of water channels (aquaporins) in corn roots. *Plant, Cell Environ.* **29**, 459–470.

Ye, Q., Wiera, B. and Steudle, E. (2004). A cohesion/tension mechanism explains the gating of water channels (aquaporins) in *Chara* internodes by high concentration. *J. Exp. Bot.* **55**, 449–461.

Yool, A. J. (2006). Dominant-negative suppression of Big Brain ion channel activity by mutation of a conserved glutamate in the first transmembrane domain. *Gene Expr.* **13**, 329–337.

Yool, A. J., Stamer, W. D. and Regan, J. W. (1996). Forskolin stimulation of water and cation permeability in aquaporin1 water channels. *Science (80-.).* **273**, 1216–1218.

Yu, X. S. and Jiang, J. X. (2004). Interaction of major intrinsic protein (aquaporin-0) with fiber connexins in lens development. *J. Cell Sci.* **117**, 871–880.

Yu, X. S., Yin, X., Lafer, E. M. and Jiang, J. X. (2005). Developmental regulation of the direct interaction between the intracellular loop of connexin 45.6 and the C terminus of Major intrinsic protein (aquaporin-0). *J. Biol. Chem.* **280**, 22081–22090.

Yu, J., Yool, A. J., Schulten, K. and Tajkhorshid, E. (2006). Mechanism of gating and ion conductivity of a possible tetrameric pore in Aquaporin-1. *Structure* **14**, 1411–1423.

Zampighi, G. A., Hall, J. E. and Kreman, M. (1985). Purified lens junctional protein forms channels in planar lipid films. *Proc. Natl. Acad. Sci. U. S. A.* **82**, 8468–8472.

Zelazny, E., Borst, J. W., Muylaert, M., Batoko, H., Hemminga, M. A. and Chaumont, F. (2007). FRET imaging in living maize cells reveals that plasma membrane aquaporins interact to regulate their subcellular localization. **104**, 12359–12364.

Zelazny, E., Miecielica, U., Borst, J. W., Hemminga, M. A. and Chaumont, F. (2009).

An N-terminal diacidic motif is required for the trafficking of maize aquaporins ZmPIP2;4 and ZmPIP2;5 to the plasma membrane. *Plant J.* **57**, 346–355.

Zelenina, M., Zelenin, S., Bondar, A. A., Brismar, H. and Aperia, A. (2002). Water permeability of aquaporin-4 is decreased by protein kinase C and dopamine. *Am. J. Physiol. Physiol.* **283**, F309–F318.

Zeuthen, T. (2010). Water-transporting proteins. *J. Membr. Biol.* **234**, 57–73.

Zeuthen, T. and Macaulay, N. (2012). Transport of water against its concentration gradient: Fact or fiction? *Wiley Interdiscip. Rev. Membr. Transp. Signal.* **1**, 373–381.

Zhang, Y., McBride, D. W. and Hamill, O. P. (1998). The ion selectivity of a membrane conductance inactivated by extracellular calcium in *Xenopus* oocytes. *J. Physiol.* **508**, 763–776.

Zhang, W. H., Skerrett, M., Walker, N. A., Patrick, J. W. and Tyerman, S. D. (2002). Nonselective currents and channels in plasma membranes of protoplasts from coats of developing seeds of bean. *Plant Physiol.* **128**, 388–399.

Zhang, W. H., Walker, N. A., Patrick, J. W. and Tyerman, S. D. (2004). Calcium-dependent K current in plasma membranes of dermal cells of developing bean cotyledons. *Plant, Cell Environ.* **27**, 251–262.

Zhang, W., Zitron, E., Hö, M., Kihm, L., Morath, C., Scherer, D., Hegge, S., Thomas, D., Schmitt, C. P., Zeier, M., et al. (2007). Aquaporin-1 channel function is positively regulated by protein kinase C. *J. Biol. Chem.* **282**, 20933–20940.

Zhang, C., Hicks, G. R. and Raikhel, N. V (2014). Plant vacuole morphology and vacuolar trafficking. *Front. Plant Sci.* **5**, 476.

Zhao, F., Song, C. P., He, J. and Zhu, H. (2007). Polyamines improve K^+/Na^+ homeostasis in barley seedlings by regulating root ion channel activities. *Plant Physiol.* **145**, 1061–1072.

Zimmermann, U., Schneider, H., Wegner, L. H. and Haase, A. (2004). Water ascent in tall trees: Does evolution of land plants rely on a highly metastable state? *New Phytol.* **162**, 575–615.

Zwiazek, J. J., Xu, H., Tan, X., Navarro-Ródenas, A., Morte, A., Benga, G., Popescu, O., Pop, V. I., Holmes, R., Agre, P., et al. (2017). Significance of oxygen transport through aquaporins. *Sci. Rep.* **7**, 40411.